



DEPARTMENT OF PURE AND APPLIED CHEMISTRY

THE DESIGN AND SYNTHESIS OF MOLECULAR TOOLS
FOR PROBING BIOLOGICAL FUNCTION

KIRSTY MILNE

PHD

2019

THE DESIGN AND SYNTHESIS OF MOLECULAR TOOLS FOR PROBING BIOLOGICAL FUNCTION

Thesis submitted to the University of Strathclyde in fulfilment of the requirements
for the degree of Doctor of Philosophy

by

Kirsty Milne

2019

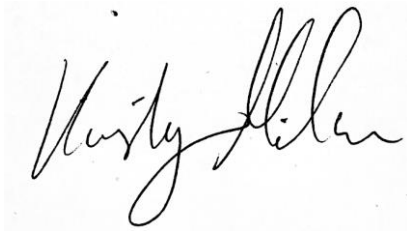
Date: 13/11/2019

Declaration of Copyright

This thesis is the result of the author's original research. It has been composed by the author and has not been previously submitted for examination which has led to the award of a degree.

The copyright of this thesis belongs to the author under the terms of the United Kingdom Copyright Acts as qualified by the University of Strathclyde Regulation 3.50. Due acknowledgement must always be made of the use of any materials contained in, or derived from, this thesis.

Signed:

A handwritten signature in black ink, appearing to read 'Kirsty Milne', written in a cursive style.

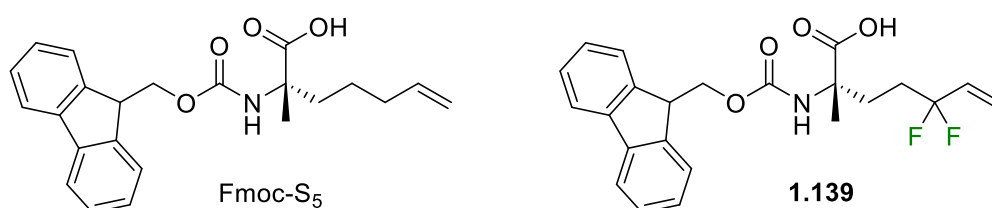
KIRSTY MILNE

Date: 13/11/2019

Abstract

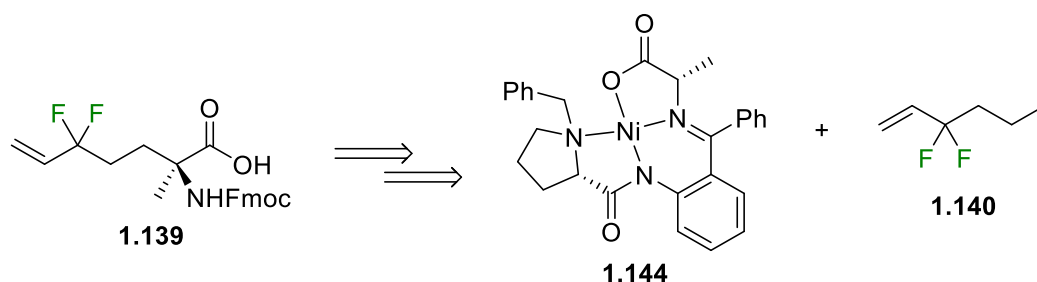
Chapter 1

With the pharmaceutical industry becoming more interested in exploiting protein-protein interactions, the technique of peptide stapling has become more common. Current strategies either exploit the reactivity of naturally occurring side chains such as glutamic acid, lysine and cysteine, or employ a ring-closing metathesis of either functionalised natural amino acids or unnatural, unsaturated hydrocarbon amino acid staples, such as Fmoc S₅, placed at strategic points in the sequence. However, functionalised hydrocarbon amino acid staples are essentially unknown, particularly those which are fluorinated.

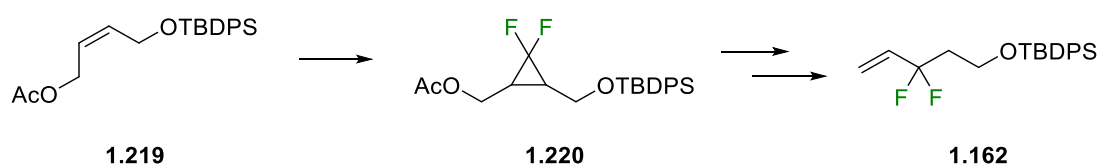


Fluorination is a commonly employed strategy for both small molecules and peptides. Thus, combining both peptide stapling, and fluorination could bring a valuable contribution to the world of peptide synthesis by potentially improving the strength of protein-protein interactions and providing a useful method of measuring interactions.

The first chapter of this thesis contains several routes for the synthesis of 3,3-difluoro-5-iodopent-1-ene (**1.140**), a key intermediate on the pathway to a fluorinated Fmoc S₅ analogue.



Three routes towards **1.140** are discussed within, with the most successful route involving a difluorocyclopropanation and radical induced ring-opening reaction as key steps.



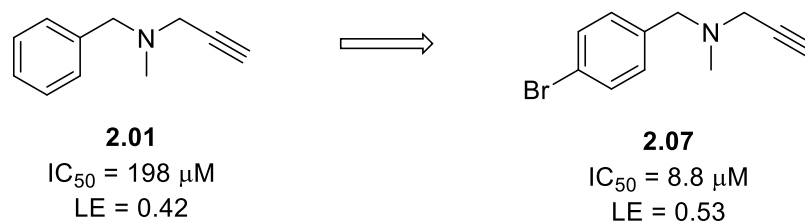
Once the desired building block was in hand, attempts at alkylating a nickel(II) alanine benzyl proline benzophenone (Ni-Ala-BPB) Schiff base complex were made. Efforts towards optimising this towards the preparation of **1.139** are described.

Chapter 2

A new potential therapeutic target, pyrroline-5-carboxylate reductase-1 (PYCR1), has been identified through reported genetic knockout studies *in vitro* and *in vivo*, with a reduction in proliferation of cancer cells and tumours reported. PYCR1 reduces pyrroline-5-carboxylate (P5C) to proline with the consumption of the reduced form of nicotinamide adenosine dinucleotide phosphate (NADPH). This process produces adenosine triphosphate (ATP) and nicotinamide adenosine dinucleotide phosphate (NADP⁺) which contribute to many cellular processes. In certain cancers PYCR1 is upregulated which exacerbates this effect and leads to increased cell survival.

A small molecule tool compound was sought to study the effect of inhibiting PYCR1 *in vitro*. A medium throughput screen of a library of pharmaceutical compounds (LOPAC) identified pargyline as a hit.

The second chapter of this thesis contains the synthesis of various pargyline analogues and a structure activity relationship study (SAR) on the inhibition of PYCR1. Compound **2.07** was found to be the most active, with a 20-fold increase in IC₅₀ in comparison to pargyline and had the best ligand efficiency.



2.07 was then taken forward as a lead compound into further pathway relevant cell-based assays and *in vivo* mouse models to further validate PYCR1 as an oncology target. *In vitro* cell assays identified a reduction in proline in two different cancer cell lines when incubated with compound **2.07**, which correlated with a reduction in cell proliferation observed. *In vivo* testing resulted in a statistically significant reduction in tumour size in a xenograft mouse model which was treated with compound **2.07**.

Acknowledgements

I would firstly like to thank my supervisor, Craig Jamieson, for giving me the opportunity to work on such a varied and interesting project and all his help and support for the duration of this project.

I would like to thank all the members of the Jamieson and Watson groups, past and present, for their support and input during my PhD and for making my working environment the best place to be.

I would also like to thank Conor Townsley and Jenna Mowat for their assistance during their fourth-year placements. Conor synthesised large batches of intermediates for the fluoroS₅ synthesis and Jenna assisted in the synthesis of some of the PYCR1 inhibitors.

A huge thanks go to our collaborators in the Agami group at the Netherlands Cancer Institute, who were responsible for all of the biological work carried out in the second chapter of this thesis. This project would not have gotten off the ground without their expertise and hard work.

I would like to thank all the support staff, past and present, for helping the department run smoothly, in particular: Craig Irving, in NMR for all his knowledge and dedication to keeping the instruments up and running; Gavin Bain, who assisted in the ozonolysis experiments and provided valuable training in key pieces of equipment; Pat Keating, in the mass spectrometry unit and finally our IT expert John Dunseath, who brought my PC back to life more times than I can count.

I would also want to thank my family for their unwavering support throughout the whole of my PhD. I would not have made it this far without them.

Finally, I would like to thank Barry M^cBride and Paul M^cCranor. This work would never have started without their enthusiastic approaches to teaching all those years ago in high school which inspired and introduced me to the beautiful, but complex, world of chemistry.

Abbreviations

3F-Tyr	3-fluorotyrosine
4F-Phe	4-fluorophenylalanine
5F-Leu	5-fluoroleucine
5-HT2A	5-hydroxytryptamine receptor 2A
6MP	mercaptopurine
6-PG	6-phosphogluconate
AIBN	azobisisobutyronitrile
Ala	alanine
Asn	asparagine
Asp	aspartic acid
ATP	adenosine triphosphate
BCL9	B-cell CLL/lymphoma 9
BCRA1	breast cancer type 1 susceptibility protein
BEMP	2-tert-butylimino-2-diethylamino-1,3-dimethylperhydro-1,3,2-diazaphosphorine
BPAP	benzyl proline aminoacetophenone
BPB	benzyl proline aminobenzophenone
BPBA	benzyl proline aminobenzaldehyde
BPin	pinacol boronate ester
Cat.	Catalytic
CD	circular dichroism
CDI	carbonyl diimidazole
CRISPR	clustered randomly interspaced short palindromic repeat
CuAAc	copper catalysed alkyne-azide cycloadditions
DAST	(diethylamino)sulfur trifluoride
DBU	1,8-Diazabicyclo[5.4.0]undec-7-ene
DCE	Dichloroethane

DCM	Dichloromethane
DEC	diethylcarbamyl
DHQA	dihydroquinidine acetate
DIBAL-H	diisobutylaluminium hydride
DIPEA	diisopropylethylamine
Diricore	differential ribosome codon reading
DMAP	<i>N,N</i> -dimethylaminopyridine
DMF	<i>N,N</i> -dimethylformamide
DMP	Dess-Martin periodinane
DMSO	dimethylsulfoxide
DNA	deoxyribonucleic acid
dppf	1,1'-bis(diphenylphosphino)ferrocene
E-4-P	Ethrose-4-phosphate
EDCI	1-Ethyl-3-(3-dimethylaminopropyl)carbodiimide
EDG	electron donating group
EDTA	ethylenediaminetetraacetic acid
<i>ee</i>	enantiomeric excess
EGFR	epidermal growth factor receptor
EWG	electron withdrawing group
F%	percentage bioavailability
F-6-P	fructose-6-phosphate
FAXS	fluorine chemical shift derived anisotropy and exchange for screening
Fmoc	fluorenylmethoxycarbonyl
FTIR	fourier transformed Infra-red spectroscopy
G-3-P	glyceraldehyde-3-phosphate
G5K	glutamate-5-kinase
G-6-P	glucose-6-phosphate

Gln	glutamine
Glu	glutamic acid
Gly	glycine
GMPS	guanosine monophosphate synthetase
Grubbs' G1	Grubb's first-generation catalyst
HA	heavy atoms
HATU	1-[Bis(dimethylamino)methylene]-1H-1,2,3-triazolo[4,5-b]pyridinium 3-oxid hexafluorophosphate
hDM2	human double minute 2
HER-2	human epidermal growth factor receptor-2
HGPRT	hypoxanthine guanine phosphoribosyl transferase
HIV	human immunodeficiency virus
HPLC	high performance liquid chromatography
HRP	horseradish peroxidase
Ile	isoleucine
IMPDH	inosine monophosphate dehydrogenase
K _i	inhibition constant
LCMS	liquid chromatography mass spectroscopy
L-CPL	left-handed circularly polarised light
LDA	lithium diisopropylamide
LE	ligand efficiency
Leu	leucine
LOPAC	library of pharmaceutical compounds
Lys	lysine
MAO-B	monoamine oxidase B
MDFA	methyl 2,2-(difluorosulfonyl)acetate
Met	methionine
MeTIMP	methyl-thioinosine monophosphate

MS	molecular sieves
Ms	methyl sulfonyl
MTBE	methyl tert-butyl ether
NaBDFA	sodium bromodifluoroacetate
NaCDFA	sodium chlorodifluoroacetate
NADP+	nicotinamide adenine dinucleotide phosphate
NADPH	nicotinamide adenine dinucleotide phosphate (reduced form)
NaHMDS	sodium hexamethyldisilazide
NFSI	<i>N</i> -Fluorobenzenesulfonimide
NKI	the Netherlands Cancer Institute
NMR	nuclear magnetic resonance spectroscopy
OAT	ornithine aminotransferase
Orn	ornithine
P5C	pyrroline-5-carboxylate
Phe	phenylalanine
PPAT	phosphoribosyl pyrophosphate amidotransferase
PPI	protein-protein interaction
ppm	parts per million
PRA	5-phosphoribosylamine
Pro	proline
PRODH	Proline dehydrogenase
PRPP	5-phosphor-D-ribose-1-pyrophosphate
PRPS1	phosphoribosyl pyrophosphate synthetase 1
PTSA	<i>para</i> -toluene sulfonic acid
PYCR1	pyrroline-5-carboxylate reductase-1
Quant.	Quantitative
R-5-P	ribose-5-phosphate
RCM	ring-closing metathesis

R-CPL	right-handed circularly polarised light
RNA	ribonucleic acid
RT	room temperature
Ru-5-P	ribulose-5-phosphate
S-7-P	Sedoheptulose-7-phosphate
SAR	structure activity relationship
Sat.	saturated
Ser	serine
SM	Suzuki-Miyaura
S _N Ar	nucleophilic aromatic substitution
SPPS	solid phase peptide synthesis
STAB	sodium triacetoxymethylborohydride
T _{1/2}	half-life
TBAF	tetrabutylammonium fluoride
TBAI	tetrabutylammonium iodide
TBAT	tetrabutylammonium triphenyldifluorosilicate
TBDPS	<i>tert</i> -butyldiphenylsilyl
TBS	<i>tert</i> -butyldimethylsilyl
^t BuOK	potassium <i>tert</i> -butoxide
TCDI	thiocarbonyldiimidazole
TdGTP	thiadeoxyguanosine triphosphate
TES	triethylsilyl
TFA	trifluoroacetic acid
TFDA	trimethylsilyl fluorosulfonyldifluoroacetate
Tfm-Phe	trifluoromethylphenylalanine
TGDP	thioguanosine diphosphate
TGMP	thioguanosine monophosphate
TGTP	thioguanosine triphosphate

THF	tetrahydrofuran
THFA	tetrahydro-2-furoic acid
THP	tertrahdropyran
Thr	threonine
TIMP	thioinosine monophosphate
TIPS	triisopropylsilyl
TLC	thin layer chromatography
TMS	trimethylsilyl
TPMT	thiopurine methyl transferase
TREAT-HF	Triethylamine trihydrofluoride
tRNA	transfer RNA
Trp	tryptophan
TXMP	thioxanthine monophosphate
UV	ultra-violet
Val	valine
VCPR	vinyl cyclopropane rearrangement
X-5-P	xyulose-5-phosphate
XtalFluor-E [®]	(Diethylamino)difluorosulfonium tetrafluoroborate
γ-GPR	γ-glutmayl phosphate reductase

Table of Contents

Abstract	iii
Acknowledgements.....	vi
Table of Contents	xiii
Table of Figures	xx
Table of Schemes	xxv
Table of Tables	xxx
1 Chapter 1: The Design and Synthesis of a Novel Fluorinated Amino Acid Hydrocarbon Staple.....	31
1.1 Introduction.....	31
1.1.1 Peptide Stapling	31
1.1.1.1 Proteins and α -Helix Formation.....	31
1.1.1.2 Methods of Helix Stabilisation.....	35
1.1.2 Amino Acid Synthesis	41
1.1.3 Fluorination	49
1.1.3.1 Fluorine in Medicinal Chemistry	49
1.1.3.2 Fluorine as a Nuclear Magnetic Resonance (NMR) Probe.....	51
1.1.3.3 Methods of Fluorination	52
1.2 Aims	67
1.3 Results and Discussion	68
1.3.1 Synthesis of Fmoc S ₅	68
1.3.2 Retrosynthetic Analysis of Fluorinated Fmoc S ₅	71
1.3.3 Synthesis of Key Fluorinated Building Block 1.140	71
1.3.3.1 Generation 1	71
1.3.3.2 Generation 2	76

1.3.3.3	Generation 3	82
1.3.4	Alkylation of nickel complex 1.144 with 1.140 and isolation of Fmoc amino acid 1.139.....	95
1.4	Conclusions.....	101
1.5	Future Work.....	102
2	Chapter 2: The Design and Synthesis of Molecular Tools to Study the Role of PYCR1 in Oncology	106
2.1	Introduction.....	106
2.1.1	Cancer in Society	106
2.1.2	PYCR1 and its Role in Cancer	113
2.2	Aims	127
2.3	Results and Discussion	128
2.3.1	Synthesis of Pargyline Analogues.....	128
2.3.2	Benzyl Group Substitutions.....	139
2.3.3	<i>N</i> -Methyl substitutions	145
2.3.4	Propargyl Group Substitutions.....	147
2.3.5	Further Biological Studies with Compound 2.07	150
2.4	Conclusion	158
2.5	Future work	159
3	Experimental.....	161
3.1	General	161
3.2	Chapter 1 – Experimental.....	163
3.2.1	Fmoc S ₅ Synthesis	163
3.2.1.1	Synthesis of <i>N</i> -Benzylproline Hydrochloride (1.142).....	163

3.2.1.2	Synthesis of <i>N</i> -Benzylproline Benzoacetophenone Schiff Base (BPB)	
(1.143)		164
3.2.1.3	Synthesis of (S) Ni-Ala-BPB Auxiliary (1.144)	164
3.2.1.4	Synthesis of 5-Iodopent-1-ene (1.145)	165
3.2.1.5	Synthesis of (S) Ni-S ₅ -BPB Auxiliary (1.146)	166
3.2.1.6	Synthesis of S ₅ Free Amino Acid (1.147)	167
3.2.1.7	Synthesis of Fmoc S ₅ (1.148)	168
3.2.2	Generation 1	168
3.2.2.1	Synthesis of Aldehyde 1.158	168
3.2.2.2	Synthesis of Alcohol 1.160	170
3.2.2.3	Synthesis of Mesylate 1.161a	171
3.2.2.4	Synthesis of Tosylate 1.161b	172
3.2.2.5	Attempted Synthesis of TBDPS protected alcohol 1.162	173
3.2.2.6	Synthesis of Xanthate 1.179	173
3.2.2.7	Attempted Synthesis of TBDPS Protected Alcohol 1.162	174
3.2.3	Generation 2	174
3.2.3.1	Synthesis of Benzyl 2,2-difluoroacetate (1.181)	174
3.2.3.2	Synthesis of THP Protected Bromoethanol (1.182a)	175
3.2.3.3	Synthesis of THP Protected Iodoethanol (1.182b)	176
3.2.3.4	Synthesis of 2,2-difluoro- <i>N</i> -methoxy- <i>N</i> -methylacetamide (1.196)	176
3.2.3.5	Attempted Synthesis of Ester 1.183 and Amide 1.197	177
3.2.4	Generation 3	178
3.2.4.1	Synthesis of Prop-2-yn-1-yl Acetate (1.209a)	178
3.2.4.2	Synthesis of Vinyl BPin 1.210a	179

3.2.4.3	Synthesis of Sodium 2-Bromo-2,2-Difluoro Acetate	180
3.2.4.4	Synthesis of TBS Protected Propargyl Alcohol 1.209b	180
3.2.4.5	Synthesis of Vinyl BPin 1.210b	181
3.2.4.6	Attempted Synthesis of Difluorocyclopropanes 1.211a and 1.211b 181	
3.2.4.7	Synthesis of TBDPS protected Butene Diol 1.218.....	182
3.2.4.8	Synthesis of TBDPS and Acetate Protected Butene Diol 1.219 ..	183
3.2.4.9	Synthesis of Difluorocyclopropane 1.220	183
3.2.4.10	Synthesis of Difluorocyclopropane 1.221	185
3.2.4.11	Synthesis of Thiocarbonylimidazolidine 1.222a	186
3.2.4.12	Synthesis of Xanthate 1.222b	187
3.2.4.13	Synthesis of Iodo Difluorocyclopropane 1.222c	188
3.2.4.14	Synthesis of TBDPS Protected Alcohol 1.162.....	189
3.2.4.15	Synthesis of 3,3-difluoropent-4-en-1-ol (1.163).....	190
3.2.4.16	Synthesis of TBDPS Protected Pentenol 1.223	192
3.2.4.17	Attempted Optimisation of the Acid Deprotection of 1.223	193
3.2.4.18	Synthesis of Tosylate 1.228	194
3.2.4.19	Synthesis of Key Building Block (1.140)	196
3.2.5	Synthesis of Fmoc Amino Acid (1.139).....	197
3.2.5.1	Synthesis of alkylated nickel complex (1.157)	197
3.2.5.2	Attempted Optimisation of the Alkylation Conditions.....	198
3.2.5.3	Synthesis of Fmoc Amino Acid (1.139)	200
3.3	Chapter 2 – Experimental.....	201
3.3.1	General Procedure A: alkylation with DIPEA	201
3.3.1.1	<i>N</i> -(4-fluorobenzyl)- <i>N</i> -methylprop-2-yn-1-amine (2.02)	201

3.3.1.2	<i>N</i> -methyl- <i>N</i> -(4-nitrobenzyl)prop-2-yn-1-amine (2.03)	202
3.3.1.3	4-((methyl(prop-2-yn-1-yl)amino)methyl)benzonitrile (2.04)....	202
3.3.1.4	<i>N</i> -(3,4-dichlorobenzyl)- <i>N</i> -methylprop-2-yn-1-amine (2.05).....	203
3.3.2	General Procedure B: alkylation with potassium carbonate	203
3.3.2.1	<i>N</i> -(4-chlorobenzyl)- <i>N</i> -methylprop-2-yn-1-amine (2.06).....	203
3.3.2.2	<i>N</i> -(4-bromobenzyl)- <i>N</i> -methylprop-2-yn-1-amine (2.07)	204
3.3.2.3	<i>N</i> -(4-iodobenzyl)- <i>N</i> -methylprop-2-yn-1-amine (2.08).....	204
3.3.2.4	<i>N</i> -(3-chlorobenzyl)- <i>N</i> -methylprop-2-yn-1-amine (2.09).....	205
3.3.2.5	<i>N</i> -(2-bromobenzyl)- <i>N</i> -methylprop-2-yn-1-amine (2.10)	205
3.3.2.6	<i>N</i> -(4-methoxybenzyl)- <i>N</i> -methylprop-2-yn-1-amine (2.11).....	206
3.3.2.7	<i>N</i> -methyl- <i>N</i> -(4-(trifluoromethyl)benzyl)prop-2-yn-1-amine (2.12)	206
3.3.2.8	1-(4-((methyl(prop-2-yn-1-yl)amino)methyl)phenyl)ethan-1-one	
(2.13)		207
3.3.2.9	<i>N</i> -(4-chloro-3-(trifluoromethyl)benzyl)- <i>N</i> -methylprop-2-yn-1-amine (2.14)	207
3.3.2.10	<i>N</i> -(2,4-dibromobenzyl)- <i>N</i> -methylprop-2-yn-1-amine (2.15)	208
3.3.2.11	<i>N</i> -methyl- <i>N</i> -(naphthalen-2-ylmethyl)prop-2-yn-1-amine (2.16)	209
3.3.2.12	<i>N</i> -methyl- <i>N</i> -((3-methylisoxazol-5-yl)methyl)prop-2-yn-1-amine	
(2.17)		209
3.3.2.13	<i>N</i> -(4-bromobenzyl)- <i>N</i> -propylprop-2-yn-1-amine (2.18)	210
3.3.2.14	<i>N</i> -(4-bromobenzyl)- <i>N</i> -(prop-2-yn-1-yl)but-3-en-1-amine (2.19)	210
3.3.2.15	<i>N</i> -(4-bromobenzyl)- <i>N</i> -(cyclopropylmethyl)prop-2-yn-1-amine	
(2.20)		211
3.3.2.16	<i>N</i> -(4-bromobenzyl)- <i>N</i> -((3-methylisoxazol-5-yl)methyl)prop-2-yn-1-amine (2.21)	211

3.3.2.17	<i>tert</i> -Butyl <i>N</i> -(4-bromobenzyl)- <i>N</i> -(prop-2-yn-1-yl)glycinate (2.22)	212
3.3.2.18	5-bromo-2-(prop-2-yn-1-yl)isoindoline (2.23)	212
3.3.2.19	6-bromo-2-(prop-2-yn-1-yl)-1,2,3,4-tetrahydroisoquinoline (2.24)	213
3.3.2.20	<i>N</i> -(4-bromobenzyl)- <i>N</i> -methylprop-2-en-1-amine (2.25)	213
3.3.2.21	<i>N</i> -(4-bromobenzyl)- <i>N</i> -methylpropan-1-amine (2.26)	214
3.3.2.22	<i>N</i> -(4-bromobenzyl)- <i>N</i> -methylbut-3-yn-1-amine (2.27)	214
3.3.2.23	<i>N</i> -benzyl-1-(4-bromophenyl)- <i>N</i> -methylmethanamine (2.28)	215
3.3.2.24	<i>N</i> -(4-bromobenzyl)- <i>N</i> -methylbut-2-yn-1-amine (2.29)	216
3.3.2.25	<i>N</i> -(4-bromobenzyl)- <i>N</i> -methylbut-3-yn-2-amine (2.30)	216
3.3.2.26	4-((methyl(prop-2-yn-1-yl)amino)methyl)benzamide (2.31)	217
3.3.3	Bespoke Alkylating Agent Synthesis	217
3.3.3.1	Attempted Synthesis of 2,4-dibromo-1-(bromomethyl)benzene (2.33)	217
3.3.3.2	Attempted Synthesis of 2,4-dibromobenzyl 4-methylbenzenesulfonate (2.35)	218
3.3.3.3	Synthesis of 2,4-dibromo-1-(bromomethyl)benzene (2.33)	218
3.3.3.4	But-3-yn-2-yl 4-methylbenzenesulfonate (2.37)	219
3.3.3.5	Synthesis of 4-(bromomethyl)benzamide (2.39)	220
3.3.4	General Procedure C: reductive amination	220
3.3.4.1	<i>N</i> -(3-bromobenzyl)- <i>N</i> -methylprop-2-yn-1-amine (2.40)	221
3.3.4.2	<i>N</i> -methyl- <i>N</i> -(4-methylbenzyl)prop-2-yn-1-amine (2.41)	221
3.3.4.3	<i>N</i> -(3,5-dichlorobenzyl)- <i>N</i> -methylprop-2-yn-1-amine (2.42)	222
3.3.4.4	<i>N</i> -(2,4-dimethylbenzyl)- <i>N</i> -methylprop-2-yn-1-amine (2.43)	222
3.3.4.5	<i>N</i> -(2,4-dimethoxybenzyl)- <i>N</i> -methylprop-2-yn-1-amine (2.44) ...	223

3.3.4.6	<i>N</i> -(4-bromo-2-methylbenzyl)- <i>N</i> -methylprop-2-yn-1-amine (2.45)	223
3.3.4.7	<i>N</i> -((4-bromothiophen-2-yl)methyl)- <i>N</i> -methylprop-2-yn-1-amine (2.46)	224
3.3.4.8	<i>N</i> -(4-bromo-2-chlorobenzyl)- <i>N</i> -methylprop-2-yn-1-amine (2.47)	224
3.3.4.9	<i>N</i> -(4-bromo-2-fluorobenzyl)- <i>N</i> -methylprop-2-yn-1-amine (2.48)	225
3.3.4.10	<i>N</i> -(2-bromo-4-fluorobenzyl)- <i>N</i> -methylprop-2-yn-1-amine (2.49)	226
3.3.4.11	<i>N</i> -(2-bromo-4-chlorobenzyl)- <i>N</i> -methylprop-2-yn-1-amine (2.50)	226
3.3.5	Compounds Synthesised Using Modified Reductive Amination Conditions	227
3.3.5.1	<i>N</i> -(4-bromobenzyl)- <i>N</i> -isopropylprop-2-yn-1-amine (2.51)	227
3.3.5.2	<i>N</i> -(4-bromobenzyl)prop-2-yn-1-amine (2.52)	228
3.3.5.3	<i>N</i> -(4-bromobenzyl)- <i>N</i> -ethylprop-2-yn-1-amine (2.53)	229
3.3.5.4	<i>N,N</i> -bis(4-bromobenzyl)prop-2-yn-1-amine (2.54)	229
3.3.6	Synthesis of <i>N</i> -((4'-fluoro-[1,1'-biphenyl]-4-yl)methyl)- <i>N</i> -methylprop-2-yn-1-amine (2.56)	230
3.3.7	Synthesis of <i>N</i> -(4-bromobenzyl)- <i>N</i> -(prop-2-yn-1-yl)acetamide (2.59)	231
3.3.8	<i>N</i> -(4-bromobenzyl)- <i>N</i> -(prop-2-yn-1-yl)methanesulfonamide (2.60) .	231
3.3.9	Synthesis of <i>N</i> -(4-bromobenzyl)- <i>N</i> -(2,2,2-trifluoroethyl)prop-2-yn-1-amine (2.61)	232
4	References	234

Appendix 1: Structures Names and Abbreviations of Sugars Involved in the Pentose Phosphate Pathway.....	A
Appendix 2: Topliss Decision Tree for Aromatic Systems (adapted from reference 218)	C

Table of Figures

Figure 1: structure of a typical α -helix residues 361-381 from R335W mutant of human Lamin (PDB 3V4Q) ⁵	32
Figure 2: typical CD spectra of protein secondary structures.....	33
Figure 3: Interaction of Ubb ⁺¹ (red) with α -helix 9 (green) of E2-25K (blue). Adapted from structure 3K9P from the RSCB PDB. ¹²	34
Figure 4: α -Helix stabilisation using glutamic acid and lysine at i, i+4. A salt bridge is illustrated on the left and a lactam bridge on the right.	35
Figure 5: Structure of the model substrate used to determine the presence of an absorbance maximum at 222 nm in a CD spectrum ²⁰	37
Figure 6: mismatched stereochemistry utilised by Kawamoto <i>et. al.</i> showing the helicity and binding constant for the single and double CuACC peptides on the left and right hand sides, respectively. ⁸	39
Figure 7: New amino acid staples developed by Verdine	40
Figure 8: different chiral ligands used in the synthesis of Ni(II) Schiff bases	43
Figure 9: Crystal structure of Ni(II)-Ala-BPBP showing the π -stacking interaction between the benzyl group and the aromatic ring ³²	44
Figure 10: Structure of the commercially available Marouka chiral phase transfer catalyst	48
Figure 11: A selection of fluorine-containing drug molecules	49
Figure 12: Effects of fluorine on bioavailability and half-life of selected 5-HT _{2A} receptor antagonists. ^a Calculated by ChemBioDraw	50
Figure 13: Structures of erythromycin and flurithromycin with hydroxy group which can be eliminated in acidic conditions highlighted in red	51
Figure 14: A selection of commonly used fluorinated amino acids.....	51

Figure 15: Outline of the changes in fluorine signal observed in a FAXS experiment. E is the enzyme, L is the fluorinated ligand, C is the fluorinated control and S is a non-fluorinated enzyme substrate. Top, changes in the ^{19}F signal of the ligand upon binding to the enzyme. Bottom, changes in the ^{19}F signal of the ligand upon displacement from the enzyme	52
Figure 16: A selection of electrophilic fluorination agents including the cost per mmol as sold by Sigma Aldrich ^{55–57}	53
Figure 17: A selection of nucleophilic fluorinating agents including the cost per mmol as sold by Sigma Aldrich ^{63–65}	56
Figure 18: Difluorocarbene sources with their associated costs from Sigma Aldrich unless otherwise stated. ^{83–85} ^a Sourced from Fluorochem, ⁸⁶ ^b Sourced from Apollo Scientific, ⁸⁷ ^c Sourced from Enamine, ⁸⁸ ^d Exchange rate USD-GBP 08/05/2019 ⁸⁹	64
Figure 19: Fluorinated analogue of Fmoc S ₅	67
Figure 20: Key intermediate 1.140	68
Figure 21: ^{19}F NMR of the Barton M ^c Combie reaction with 1.179 showing a complex mixture of fluorinated products.....	76
Figure 22: ^{19}F NMR of the crude reaction mixture used to prepare 1.155	79
Figure 23: Stabilised enolate of Weinreb amide 1.196.....	80
Figure 24: ^1H NMR of the crude reaction mixture, highlighting alkene species 1.198 (dd) and the presence of a CF ₂ H unit (t)	82
Figure 25: ^1H NMR of crude reaction mixture showing a 2:1 mixture of 1.220 to 1.219	86
Figure 26: ^{19}F NMR of crude reaction mixture for the deoxygenation and ring-opening of 1.222a	88
Figure 27: ^1H NMR spectrum of the alkene region of 1.163 after attempted Kugelrohr distillation. Two sets of alkene peaks are now visible, indicating the product was degrading under thermal conditions	92
Figure 28: HPLC trace of the base equivalent study showing a large peak of an unknown analyte, potentially related to starting material 1.144, at 5.5 minutes	98

Figure 29: ^1H NMR spectrum of 1.139 after purification, showing minor contamination potentially by Fmoc- β -alanine.....	101
Figure 30: Structure of Fmoc-Amox ¹²⁵	104
Figure 31: Cell cycle upon detection of DNA damage ¹²⁹	106
Figure 32: Commonly used chemotherapy drugs and their mechanisms of action. ^{140–143}	108
Figure 33: Structure of TIMP ¹⁴⁶	109
Figure 34: Metabolic fate and mechanism of action of 6MP. Pale blue boxes are metabolites of 6MP, blue boxes are materials required for <i>de novo</i> purine synthesis, green ovals are active enzymes, the pink enzyme is an inhibited enzyme, purple boxes are end products, red box and red cross are the effects of DNA and RNA incorporation and the effects of enzyme inhibition on purine synthesis ¹⁴⁵	109
Figure 35: Structure of paclitaxel bound to tubulin as generated by electron microscopy PDB: 3J6G ¹⁵³	111
Figure 36: Structure of imatinib and its mechanism of action ¹⁵⁷	112
Figure 37: Structures of gefitinib and erlotinib and their mechanism of action ^{159,160}	112
Figure 38: Simplified mechanism of ribosomal protein synthesis in the absence (top) and presence (bottom) of proline deficiency ¹⁷¹	114
Figure 39: Transfer RNA in the charged and uncharged state ¹⁷¹	114
Figure 40: Cell adaptations to low proline environments showing the increased expression of PYCR1 ¹⁶⁸	115
Figure 41: Biological assembly of PYCR1 showing the characteristic pentamer of dimers (PDB: 5UAV) ¹⁷²	115
Figure 42: Active site of PYCR1 showing the interaction of NADPH (blue) and P5C mimic THFA (green). Image generated from PDB: 5UAV ¹⁷²	117
Figure 43: 2D interaction map for NADPH (top left) and THFA (bottom right) generated in Discovery Studio 2017 using PDB: 5UAV ¹⁷²	118
Figure 44: The proline cycle and the pentose phosphate pathway. The structures of the sugars are outlined in Appendix 1	119

Figure 45: Format of the MTT assay showing the detectable product ¹⁸²	120
Figure 46: Cell proliferation data for both DU145 and PC-3 prostate cancer cell lines showing reduced cell proliferation was present in the cell lines where PYCR1 was knocked out ¹⁷⁸	121
Figure 47: Format of the WST-8 assay showing the detectable product ¹⁸³	121
Figure 48: Cell proliferation data for both SPC-A1 and H1703 lung cancer cell lines showing reduced cell proliferation was present in the cell lines where PYCR1 was knocked out ¹⁸¹	122
Figure 49: Data from the <i>in vivo</i> PYCR1 knock out tumour growth studies showing a reduction in tumour growth in the cells where PYCR1 was knocked out ¹⁶⁸	122
Figure 50: Structures and targets of some known tool compounds ^{188–190}	124
Figure 51: Assay conditions developed by NKI to study the effect of small molecule inhibitors of PYCR1.....	124
Figure 52: Structure of pargyline and its activity and ligand efficiency (LE) for both PYCR1 and MAO-B).....	125
Figure 53: Structure of rasagiline and its binding to the flavin cofactor found within MAO-B.....	127
Figure 54: Structure of pargyline showing the three main areas of interest: benzyl group (blue), <i>N</i> -methyl (red) and propargyl (green).....	128
Figure 55: Compounds synthesised by alkylation using DIPEA as a base.....	129
Figure 56: Compounds synthesised by alkylation using potassium carbonate as a base. ^a Isolated as the HCl salt, ^b synthesised using 10 mol% potassium iodide.....	130
Figure 57: ¹ H NMR of the resulting compounds of each set of reaction conditions (green, Appel; Red, tosylation; blue, bromination) between δ = 8-4.5 ppm.....	132
Figure 58: Pargyline analogues synthesised by reductive amination.....	134
Figure 59: ¹ H NMR of compound 2.59.....	137
Figure 60:UV trace from the LCMS analysis showing compound 2.59 at R_t = 7.1 mins.....	138
Figure 61: Activities and LE of single halogen substitution of the benzyl group. ^a Pargyline was used as the standard, IC_{50} = 372 ± 46 μ M; ^b pargyline was used as the	

standard, $IC_{50} = 198 \pm 29 \mu M$; ^c 2.07 was used as the standard, $IC_{50} = 9.2 \pm 1.0 \mu M$; ^d 2.07 was used as the standard, $IC_{50} = 23 \pm 6 \mu M$; ^e 2.07 was used as the standard, $IC_{50} = 8.6 \pm 2.4 \mu M$; ^f synthesised by another member of the laboratory ²⁰⁹	139
Figure 62: Activities and LE of single substitution of the benzyl group. ^a 2.07 was used as the standard, $IC_{50} = 8.3 \pm 1.2 \mu M$; ^b pargyline used as the standard, $IC_{50} = 198 \pm 30 \mu M$; ^c 2.07 was used as the standard, $IC_{50} = 10 \pm 2 \mu M$; ^d 2.07 was used as the standard, $IC_{50} = 9.7 \pm 1.0 \mu M$; ^e pargyline was used as the standard, $IC_{50} = 372 \pm 46 \mu M$, ^f synthesised by another member of the laboratory ²⁰⁹	141
Figure 63: Activities and LE of disubstitution of the benzyl group. ^a 2.07 was used as the standard, $IC_{50} = 9.2 \pm 1.0 \mu M$; ^b 2.07 was used as the standard, $IC_{50} = 30 \pm 6 \mu M$; ^c 2.07 was used as the standard, $IC_{50} = 23 \pm 6 \mu M$, ^d 2.07 was used as the standard, $IC_{50} = 26 \pm 3 \mu M$; ^e 2.07 was used as the standard, $IC_{50} = 8.6 \pm 2.4 \mu M$; ^f synthesised by another member of the laboratory ²⁰⁹	142
Figure 64: Activities and LE of modifications to the benzyl group. ^a 2.07 was used as the standard, $IC_{50} = 23 \pm 6 \mu M$; ^b 2.07 was used as the standard, $IC_{50} = 9.2 \pm 1.0 \mu M$; ^c 2.07 was used as the standard, $IC_{50} = 30 \pm 6 \mu M$; ^d synthesised by another member of the laboratory ²⁰⁹	144
Figure 65: Overlay of compounds 2.07 (blue) and 2.46 (red) generated in ChemBioDraw3D 17.1. Both structures were energy minimised using the MM2 energy minimisation calculation	145
Figure 66: Strategies attempted by Swett <i>et. al.</i> to attempt to increase the potency of pargyline towards MAO by altering the <i>N</i> -methyl group, all modifications resulted in reduced activity.....	146
Figure 67: Activities and LE of modifications to the <i>N</i> -methyl group. ^a 2.07 was used as the standard, $IC_{50} = 15 \pm 3 \mu M$; ^b 2.07 was used as the standard, $IC_{50} = 23 \pm 6 \mu M$; ^c 2.07 was used as the standard, $IC_{50} = 26 \pm 3 \mu M$	146
Figure 68: Strategies attempted by Swett <i>et. al.</i> to attempt to increase the potency of pargyline towards MAO by altering the propargylic group, all groups showed reduced activity.....	148

Figure 69: Activities and LE of modifications to the propargyl group. ^a 2.07 was used as the standard, IC ₅₀ = 15 ± 3 µM; ^b 2.07 was used as the standard, IC ₅₀ = 10 ± 2 µM; ^c 2.07 was used as the standard, IC ₅₀ = 8.6 ± 2 µM; ^d commercially available; ^e synthesised by another member of the laboratory ²⁰⁹	148
Figure 70: Summary of the SAR studies on the pargyline analogues showing the differences between the parent compound 2.1 and the lead compound 2.07	150
Figure 71: Assay format used in the determination of the inhibition of MAO-B	151
Figure 72: Effect of pargyline and compound 2.07 on the proline levels of the SUM-159-PT breast cancer cell line carried out by the Agami group at NKI	152
Figure 73: Effect of pargyline and compound 2.07 on the levels of essential amino acids in SUM-159-PT cells carried out by the Agami group at NKI	153
Figure 74: Results of the glutamine flux assay which show reduced incorporation of ¹³ C in cells treated with compound 2.07 (10 µM) carried out by the Berkers group at Utrecht University	154
Figure 75: Results of the <i>in vitro</i> cell proliferation study in both MDA-MB-231 and SUM-159-PT breast cancer cell lines as carried out by the Agami group at NKI	155
Figure 76: Metabolic fate of pargyline ²²⁰	156
Figure 77: Potential metabolic fate of compound 2.07	156
Figure 78: Results of the <i>in vivo</i> clearance studies as carried out by the Agami group at NKI	156
Figure 79: Results of the <i>in vivo</i> tumour growth studies in xenograft mouse models of MDA-MB-231 and SUM-159-PT cell lines as carried out by the Agami group at NKI	157
Figure 80: Some new analogues for testing in the PYCR1 assay. Top: heterocyclic incorporation into the benzyl region. Bottom: Other pargyline-related drugs.....	159

Table of Schemes

Scheme 1: Cross-linking strategy utilised by Phelan to link two Glu residues in the i, i+7 position. n = 1, 2 or 3.....	36
Scheme 2: Cross-linking of two cysteine residues in the i, i+11 positions.....	36
Scheme 3: Cross linking of two cysteine residues in the i, i+4 position ²⁰	37

Scheme 4: Scrima's conditions for helix stabilisation using CuAAC.....	38
Scheme 5: RCM peptide stapling as developed by Grubbs	39
Scheme 6: A. All-hydrocarbon stapling in the i, i+4 positions as developed by Verdine. B. All-hydrocarbon stapling in the i, i+7 positions as developed by Verdine	40
Scheme 7: Schöllkopf auxiliary method of amino acid synthesis	42
Scheme 8: General route to Ni(II)-Gly-BPBP Schiff base complex ³⁰	45
Scheme 9: Asymmetric alkylation of β -keto-esters with subsequent Schmidt rearrangement to form the protected amino acid	46
Scheme 10: Strecker multicomponent amino acid synthesis outlining the synthesis of alanine	46
Scheme 11: Asymmetric Strecker reaction using a chiral amino acid to set the stereochemistry	47
Scheme 12: α,α -disubstituted amino acid synthesis by Maruoka chiral phase transfer catalysis	48
Scheme 13: Synthesis of aryl fluorides from turbo Grignard reagents as developed by Knochel.....	54
Scheme 14: Fluorination of sp^3 centres using Selectfluor®	54
Scheme 15: Proposed mechanism of the reaction outlined in Scheme 4	54
Scheme 16: Synthetic route to solithromycin (1.53) ⁶¹	55
Scheme 17: Synthetic route to clevudine 1.63 ⁶²	56
Scheme 18: S_NAr using KF	57
Scheme 19: Reactions of oxygen-containing molecules with DAST	57
Scheme 20: Reactions of alcohols with XtalFluor-E	57
Scheme 21: Synthetic route to odanacatib (1.77) ⁶⁹	58
Scheme 22: Synthesis of key building block 1.81 ⁷⁰	59
Scheme 23: Synthetic route to Maraviroc (1.89) ⁷¹	59
Scheme 24: Route to difluorocyclohexenones	60
Scheme 25: Synthetic route to Gefitinib (1.106) ⁷⁶	61
Scheme 26: Synthesis of fluorinated building block 1.105 ⁷⁷⁻⁷⁹	62
Scheme 27: Synthetic route to celebrex (1.114) ⁸¹	63

Scheme 28: A - structure of difluorocarbene, B - difluorocyclopropanation mechanism, C - outcome of difluorocyclopropanations on <i>cis</i> - and <i>trans</i> - alkenes .	63
Scheme 29: Thermal decomposition of NaCDFA (top) and the reaction of cyclohexene with NaCDFA (bottom).....	64
Scheme 30: Synthesis of <i>gem</i> -difluorocyclopropanes ⁹²	65
Scheme 31: Decomposition of MDFA to difluorocarbene	65
Scheme 32: Radical ring-opening reaction of difluorocyclopropanes followed by an RCM to furnish a <i>gem</i> -difluorocyclopentene motif ⁹³	66
Scheme 33: Synthesis of difluorocyclopropane intermediate 1.135	66
Scheme 34: Two methods of difluorocyclopropanation using Ruppert-Prakash reagent with the mechanism of decomposition for the sodium iodide conditions ..	67
Scheme 35: Route to Fmoc S ₅ using a chiral Ni(II)-ala-BPB auxiliary as reproduced by the author	69
Scheme 36: Alternative route to Fmoc S ₅ , utilising a tandem complex hydrolysis and Fmoc protection as reported by Li ³⁴	70
Scheme 37: Retrosynthetic analysis of 1.139	71
Scheme 38: Initial route to 1.140 from aldehyde 1.158	72
Scheme 39: Routes to key aldehyde starting material 41. Yields in blue are representative of the ozonolysis conditions and yields in red are representative of Swern oxidation conditions.....	72
Scheme 40: Tosylation of alcohol 1.160	73
Scheme 41: Exemplar Barton-M ^c Combie deoxygenation conditions ⁹⁹	74
Scheme 42: Mechanism of the Barton-McCombie deoxygenation reaction	74
Scheme 43: Attempted Barton-M ^c Combie deoxygenation of alcohol 1.160	75
Scheme 44: Potential mechanism of radical polymerisation of 1.179	76
Scheme 45: Second generation route to intermediate 1.140	77
Scheme 46: Cobalt catalysed esterification of TFA ¹⁰³	77
Scheme 47: Reported mechanism of the cobalt catalysed esterification	77
Scheme 48: Conditions employed in the THP protection of 1.191 ¹⁰⁴	78

Scheme 49: Proposed mechanism for self-condensation of compound 1.181 with LDA	79
Scheme 50: Modified second generation route to 1.140	80
Scheme 51: Finkelstein conditions employed in the synthesis of 1.182b	80
Scheme 52: Potential E2 elimination of 1.182	81
Scheme 53: An example deoxygenation and tandem ring opening reaction.....	82
Scheme 54: Proposed mechanism for the reaction shown in Scheme 21	83
Scheme 55: Reaction conditions for the tandem Matteson homologation and oxidation of a cyclopropyl pinacolboronate ester (top) and the mechanism of the key rearrangement (bottom) ¹⁰⁶¹⁰⁷	83
Scheme 56: Third generation route to intermediate 1.140.....	84
Scheme 57: Difluorocyclopropanation conditions from the literature reaction ¹¹⁰ ...	85
Scheme 58: Modified third generation route to intermediate 1.140	85
Scheme 59: Alternative acetate deprotection conditions used for large scale reactions	87
Scheme 60: Synthesis of alternative substrates for radical induced ring-opening ...	89
Scheme 61: Revised third generation route to compound 1.140	90
Scheme 62: Conditions utilised in the acidic TBDPS deprotection	91
Scheme 63: general conditions employed in the model substrate to optimise the TBDPS deprotection	92
Scheme 64: TBDPS deprotection and tosylation conditions from literature. Tosylate 1.227 was not isolated in this study and was used as crude in a further modification	93
Scheme 65: TBDPS deprotection conditions using TBAF	93
Scheme 66: Finkelstein reaction conditions employed in the synthesis of 1.140	94
Scheme 67: Final modified third-generation route to intermediate 1.140	95
Scheme 68: Standard conditions used to alkylate 1.144	95
Scheme 69: polyfluoroalkylation of malonate ¹¹⁹	96
Scheme 70: Potential elimination reaction with 1.140	98
Scheme 71: Conditions used to isolate amino acid 1.139	99

Scheme 72: Mechanism of the Lossen rearrangement of Fmoc-OSu to form Fmoc- β -alanine ¹²²	100
Scheme 73: Future work with the Ni-Ala-BPB Schiff base route	103
Scheme 74: Potential Schöllkopf conditions.....	104
Scheme 75: Construction of medium-sized rings containing a <i>gem</i> -difluoro group <i>via</i> RCM	105
Scheme 76: Future work with Fmoc protected amino acid 1.139.....	105
Scheme 77: Activation of cisplatin and its mechanism of action. Blueboxes represent DNA bases ¹⁴⁸	110
Scheme 78: Proline biosynthetic pathway from glutamic acid and ornithine ¹⁷²	116
Scheme 79: General alkylation conditions employed during the synthesis of pargyline analogues which used DIPEA as a base where Ar is an aryl group	129
Scheme 80: General alkylation conditions employed during the synthesis of pargyline analogues which used potassium carbonate as a base	129
Scheme 81: Appel conditions employed in the attempted synthesis of compound 2.33 resulting in a 2:5 mixture of 2.33:2.34	131
Scheme 82: Tosylation conditions employed in the attempted synthesis of 2.35..	131
Scheme 83: Bromination conditions employed in the synthesis of compound 2.33	132
Scheme 84: Tosylation conditions employed in the synthesis of 2.37	132
Scheme 85: Two-step synthesis of compound 2.39	133
Scheme 86: General reductive amination conditions employed during the synthesis of pargyline analogues	133
Scheme 87: Modified reductive amination conditions used in the synthesis of compound 2.51	135
Scheme 88: Modified reductive amination conditions used in the synthesis of compound 2.52	135
Scheme 89: Tentative reaction mechanism for the synthesis of 2.53.....	135
Scheme 90: SM conditions employed for analogue synthesis	136

Scheme 91: Potential side reactions and products of the SM conditions. A. Potential reactions of starting material 2.07. B. Potential reactions of starting material 2.55	136
Scheme 92: Amidation conditions used in the synthesis of compound 2.59.....	137
Scheme 93: Mesylation conditions used in the synthesis of compound 2.60.....	138
Scheme 94: Conditions used in the synthesis of compound 2.61	138
Scheme 95: Proposed fluorinated analogues (top); proposed route to compound 2.88 (bottom) ²²¹	160

Table of Tables

Table 1: Attempted alkylation conditions.....	78
Table 2: Attempted alkylation conditions for Weinreb amide	80
Table 3: Conditions screened for radical induced ring-opening.....	89
Table 4: Optimisation conditions utilised in the attempted alkylation of 1.144 with 1.140.....	96
Table 5: Properties of pargyline as calculated by ACD labs for the RSC ChemSpider database ¹⁹⁴	125
Table 6: Conditions used for alkylations	178
Table 7: Reaction Conditions of Difluorocyclopropanation	182
Table 8: Screening Conditions for Deoxygenation/Dehalogenation	190
Table 9: Reaction conditions deprotection optimisation using the model substrate	193
Table 10: Changes employed to attempt to optimise the alkylation conditions	198

1 Chapter 1: The Design and Synthesis of a Novel Fluorinated Amino Acid Hydrocarbon Staple

1.1 Introduction

1.1.1 Peptide Stapling

1.1.1.1 Proteins and α -Helix Formation

Proteins are polymers of amino acids which are arranged in such a way as to execute a specific biological process.¹ These processes are highly varied and can range from catalytic bond formation (kinases and phosphorylation) and hydrolysis (trypsin and digestion), and transport of materials to cells (haemoglobin and oxygen transport). Protein structure is complex and consists of four level of organisation: primary, secondary, tertiary and quaternary.¹ The primary structure is the amino acid sequence; the secondary structure is the repetitive arrangement of the primary sequence in space into α -helices and β -sheets; the tertiary structure is the overall three-dimensional shape of the protein and the quaternary is the arrangement of multiple protein subunits.¹

α -Helices are highly ordered structures with hydrogen bonding occurring between the carbonyl and NH of two amino acids at a distance of $i, (i+4)$ for a regular α -helix (**Figure 1**: structure of a typical α -helix).² The most common form is the 3.6_{13} helix, where 3.6 is the average number of residues in one turn and 13 is the number of atoms present in the ring formed by the hydrogen bond.² Most α -helices tend to be right handed, this is mainly due to natural amino acids having *L*-stereochemistry.³ However, if a sequence contains a high number of achiral glycine residues it is possible to have a left handed helix.³ The most common helix stabilising residues tend to be methionine, alanine, leucine, glutamic acid and lysine, while both proline and glycine tend to disrupt helices.⁴

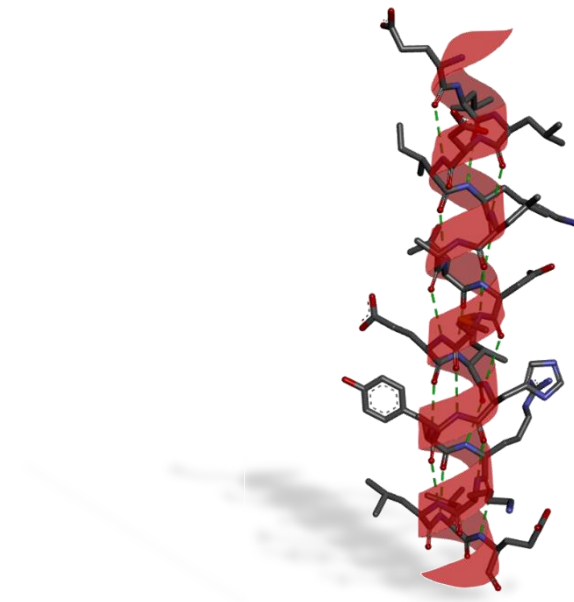


Figure 1: structure of a typical α -helix residues 361-381 from R335W mutant of human Lamin (PDB 3V4Q)⁵

The secondary structure of a peptide can be measured using circular dichroism (CD).⁶ This technique measures the interaction of a peptide with a mixture of right-handed and left-handed circularly polarised light (R-CPL and L-CPL, respectively) over the far UV range. If the peptide absorbs the L-CPL more than the R-CPL the CD will be positive and *vice versa*.⁷ The absorbance pattern of α -helices is particularly distinctive with two minima at 208 nm and 222 nm as outlined in **Figure 2**.⁶

CD Spectra of Typical Protein Secondary Structures

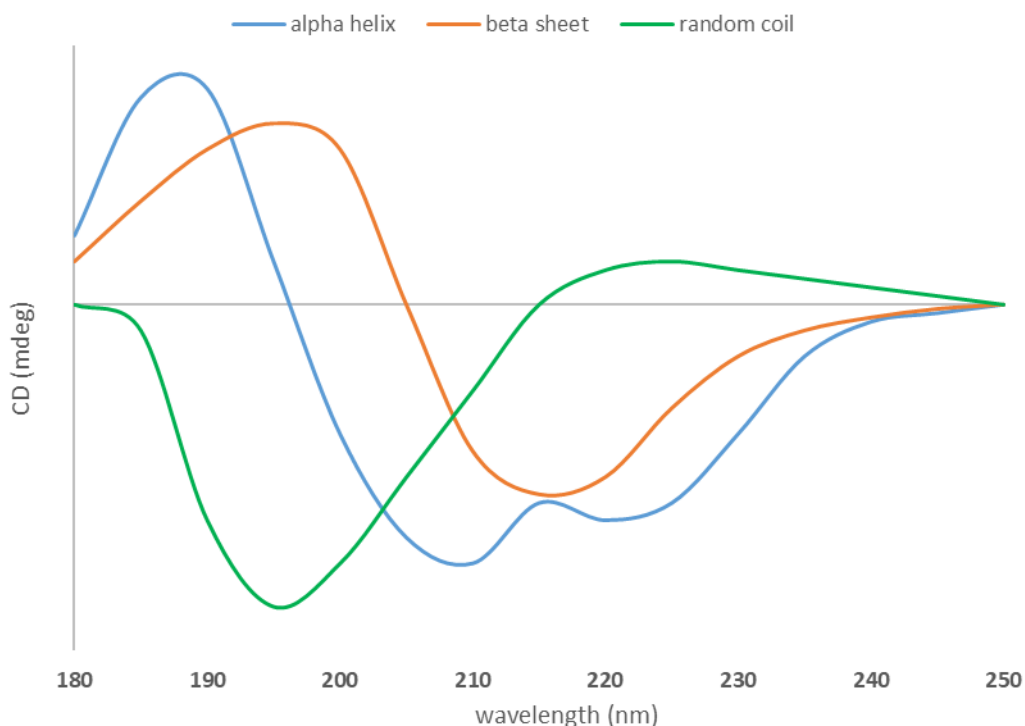


Figure 2: typical CD spectra of protein secondary structures

The helicity of a peptide can then be determined using the CD measurement at 222 nm using the equations below (**Equations 2-4**)^{8,9} after converting the units to ellipticity (θ) (**Equation 1**) although most modern instruments are able to automatically convert to the correct units.¹⁰

$$CD = \theta / 32.982$$

Equation 1: conversion factor between CD and ellipticity¹⁰

$$\% \text{ helicity} = ([\theta]_{222} / [\theta]_{max}) \times 100$$

Equation 2: calculation of the percentage helicity where; $[\theta]_{222}$ is equal to the mean residue ellipticity (calculated as in equation 3) and $[\theta]_{max}$ is equal to the maximum mean ellipticity (calculated as in equation 4)⁸

$$[\theta]_{222} = \theta_{222} / C \cdot n$$

Equation 3: calculation of mean residue ellipticity where; θ_{222} is the ellipticity obtained from the instrument at 222 nm; C is the molar concentration of the peptide and n is the number of residues in the peptide⁸

$$[\theta]_{max} = (-44000 + 250T)(1 - k/n)$$

Equation 4: calculation of the maximum mean ellipticity where; T is the temperature in °C; k is the number of non-hydrogen bonded carbonyls in the peptide and n is the number of residues^{8,9}

α -Helices are the most common type of protein secondary structure found within nature and as a result most protein-protein interactions (PPI) are based around α -helices.¹¹ An example of this is the interaction of E2-25K (blue) with ubiquitin⁺¹ (Ubb⁺¹ - red) (**Figure 3**). Here α -helix 9 (green) forms a PPI with the flat β -sheet of Ubb⁺¹ as it prepares the Ubb⁺¹ for ligation to a poly-ubiquitin chain.¹²

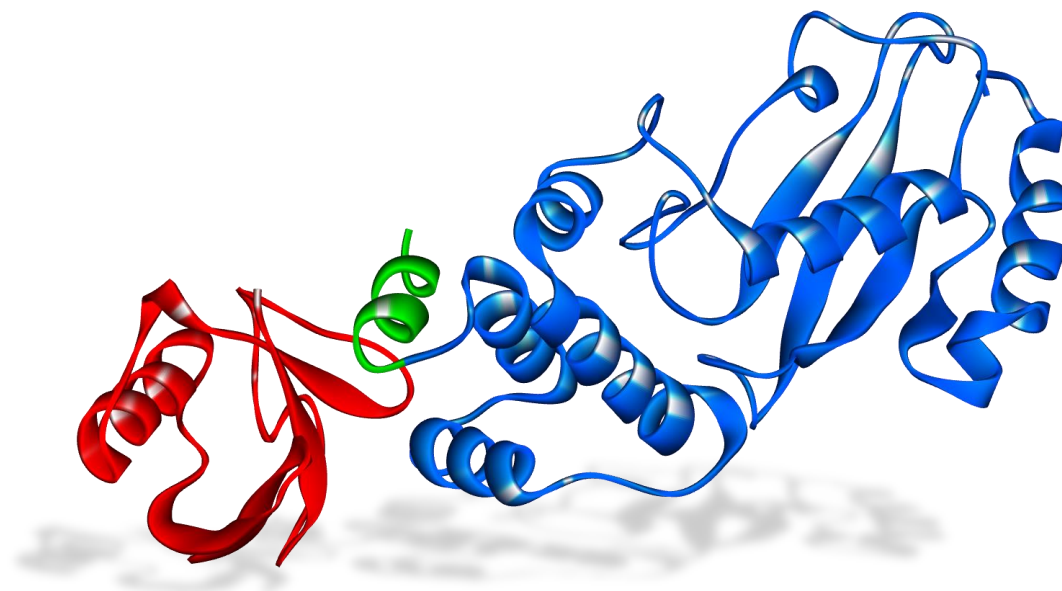


Figure 3: Interaction of Ubb⁺¹ (red) with α -helix 9 (green) of E2-25K (blue). Adapted from structure 3K9P from the RSCB PDB.¹²

As PPIs can provide access to less druggable targets, the pharmaceutical industry has increased research into short, synthetic peptides, which closely resemble the original target.¹³ For the inhibition of a given PPI to be successful, it is important that the peptide adopts the correct secondary structure. Unfortunately, this is not always the case and most short fragments, less than 20 residues long, are generally unstructured.¹⁴ Therefore, it is important to be able to constrain these peptides and force them to adopt the required structure whilst maintaining the strength of the PPI. This can sometimes be achieved by simply capping both the N- and C-termini to form an additional two amide bonds which are available for hydrogen bonding,¹⁴ however, most peptides require an extra interaction which typically mimics the hydrogen bonding interactions between the *i* and *i*+4 residues.

Several methods have been developed to stabilise the formation of an α -helix – some of which are outlined in section 1.1.1.2.

1.1.1.2 Methods of Helix Stabilisation

One of the most well-established means of stabilising α -helices is to exploit the functionality of naturally occurring amino acids such as lysine, glutamic acid, cysteine and methionine by incorporating them into the peptide sequence.

Among the first reported methods was to form a salt bridge between a lysine (Lys) residue and either a glutamic (Glu) or aspartic acid (Asp) residue or to lactamise the same three residues (**Figure 4**). While $i, (i+3)$ salt bridges are known to stabilise α -helix formation, they are less stable to extremes of pH and temperature than the most commonly used $i, i+4$.¹⁵

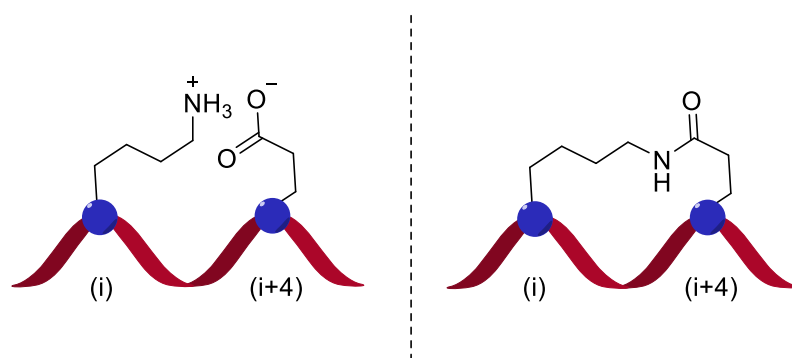


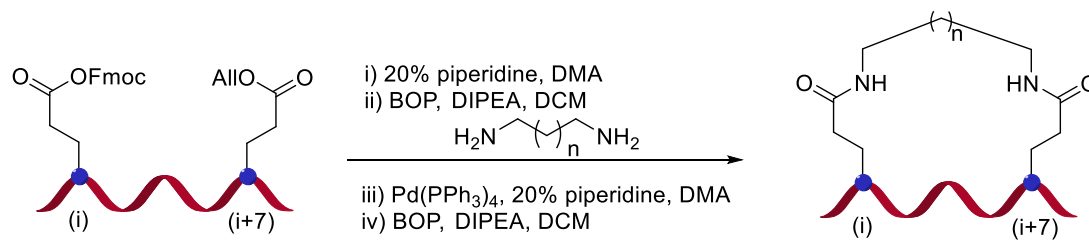
Figure 4: α -Helix stabilisation using glutamic acid and lysine at $i, i+4$. A salt bridge is illustrated on the left and a lactam bridge on the right.

A notable example of the use of a lactam bridge as a staple was in the synthesis of an analogue of parathyroid hormone related protein by Rosenblatt *et. al.* in 1991.¹⁶ Here Lys¹³ and Asp¹⁷ were lactamised, resulting in a much stronger PPI between the receptor and ligand (5-10 times depending on the type of assay used) than the corresponding non-stapled peptide.

Another method of peptide stapling is to covalently cross-link two compatible residues with an external linker. There are a number of strategies utilised for this technique which mainly depend on the amino acids present in the sequence.

In 1997, Phelan *et. al.* proposed that two glutamine residues in the $i, i+7$ positions would provide an acceptable handle for cross-linking with a hydrocarbon linker. However, synthesis of this motif proved difficult, and as an alternative two glutamic

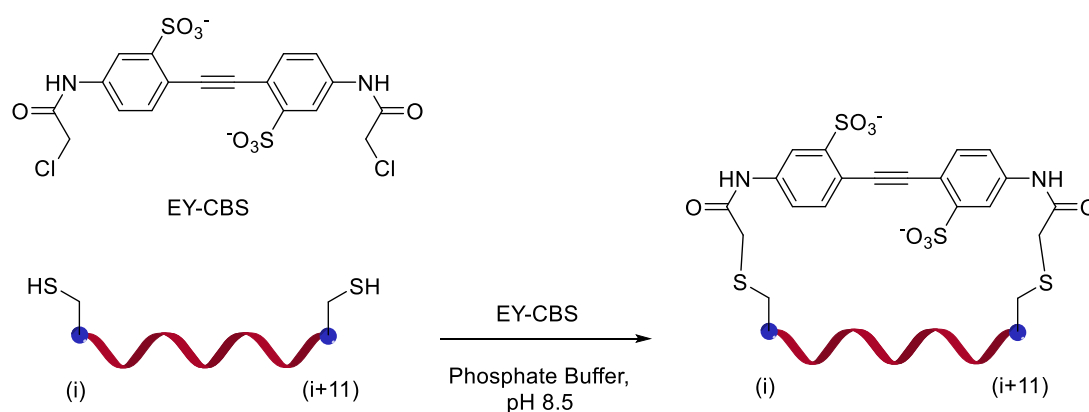
acid residues were instead amidated by a diamine with a 3-5 carbon linker using the strategy outlined below in **Scheme 1**.¹⁷



Scheme 1: Cross-linking strategy utilised by Phelan to link two Glu residues in the i, i+7 position. $n = 1, 2$ or 3

The technique was tested on the C-terminal helix of apamin (a component of bee venom) and a helical component of RNase A. 3-5 carbon cross-linkers were incorporated and the helicity measured by circular dichroism (CD). For apamin the 5-carbon linker was optimal, with 100% helicity being obtained, while for RNase A, the 4-carbon cross-linker was optimal with 82% helicity measured.

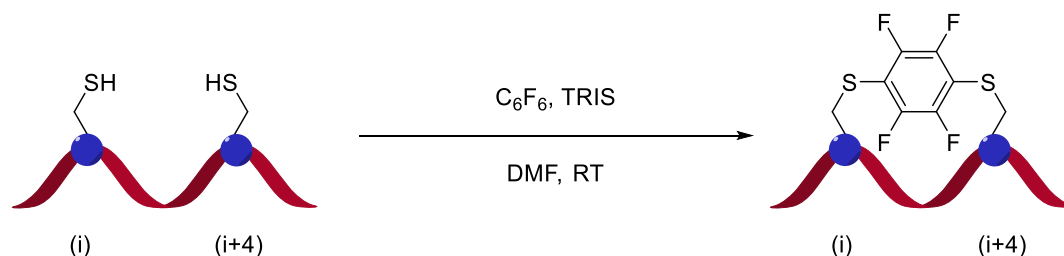
The sulfur atom of cysteine also lends itself to cross-linking strategies and is able to react with a wide variety of functional groups.¹⁸ This was exploited by Zhang *et. al.* in 2007 using the cross-linker EY-CBS (**Scheme 2**) to cover the i, i+11 positions, which equates to three turns of an α -helix. Here the two cysteine residues are alkylated by the linker.¹⁹



Scheme 2: Cross-linking of two cysteine residues in the i, i+11 positions

An 18 residue model peptide (FK11W) was treated using the conditions outlined above (**Scheme 2**) and the helicity measured as 100 % at 2 °C. The process was repeated for a longer 32 residue peptide (FK22W) and again showed remarkable helix stabilisation properties with 100 % helicity observed at 2 °C.

A similar concept by Spokoyny *et. al.* used perfluorobenzene as a staple between two cysteine residues in the i+, i+4 positions, as a means of introducing fluorine into peptides in order to use ^{19}F NMR spectroscopy for analysis.²⁰ Here, in the presence of tris(hydroxymethyl)-aminomethane (TRIS) at room temperature, two $\text{S}_{\text{N}}\text{Ar}$ reactions occur at both cysteine residues as outlined in **Scheme 3**.²⁰



Scheme 3: Cross linking of two cysteine residues in the i, i+4 position²⁰

The reaction was very efficient, with a greater than 90% conversion measured by LCMS, however, the CD spectrum obtained for the peptide was anomalous. Instead of the expected minima at 222 nm for a helical peptide, an absorbance maximum was observed. This was reasoned to be due to the staple and this was confirmed by measuring the CD spectra of compound **1.01** (**Figure 5**) by the observation of a maximum at 222 nm.²⁰

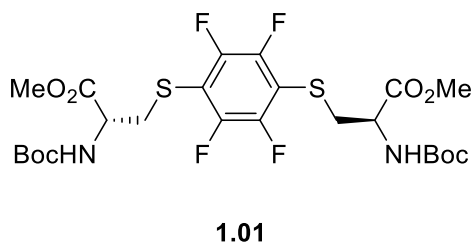
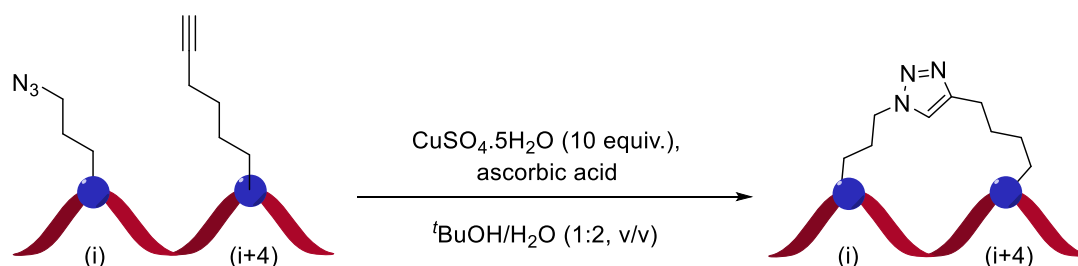


Figure 5: Structure of the model substrate used to determine the presence of an absorbance maximum at 222 nm in a CD spectrum²⁰

The helicity of the peptide was then estimated to be 53% with the presumption that the effect on the staple on the peptide was similar to that of **1.01**. While this technique does appear to stabilise α -helices, the interference of the staple in the CD spectrum is a major disadvantage as the helicity of the peptide cannot be accurately determined.²⁰

The use of unnatural amino acids for helix stabilisation is becoming more common with recent advancements in the chemistry toolbox. In this method the desired amino acids usually have to be independently synthesised (some synthetic routes to amino acids are outlined in **Section 1.12**). These can be derived from natural amino acids, such as *O*-allyl serine, or completely unnatural, such as the alkyne and azide containing residues used in copper catalysed alkyne-azide cycloadditions (CuAAC).

In 2010, Scrima *et. al.* utilised CuAAC to staple a model peptide based on para-thyroid hormone-related peptide which contained one azide containing amino acid residue and one alkyne containing residue in the (i), (i+4) position. A number of combinations were screened with the best conditions outlined below in **Scheme 4**.



Scheme 4: Scrima's conditions for helix stabilisation using CuAAC

This was further exemplified in 2011 when a similar technique was used to produce B-cell CLL/lymphoma 9 (BCL9) mimics for use as a potential cancer treatment.⁸ Here Kawamoto *et. al.* utilised both single and double CuAAC reactions to great effect with the greatest helicity obtained being 90% and 99% for single and double CuAAC, respectively. Both of the synthesised peptides were also found to be active in a BCL9 competitive fluorescence polarisation binding assay. Interestingly both peptides utilised a stereochemical mismatch utilising the (*S*)-residue on the azide component and the (*R*)-residue on the alkyne component as outlined below in **Figure 6**.

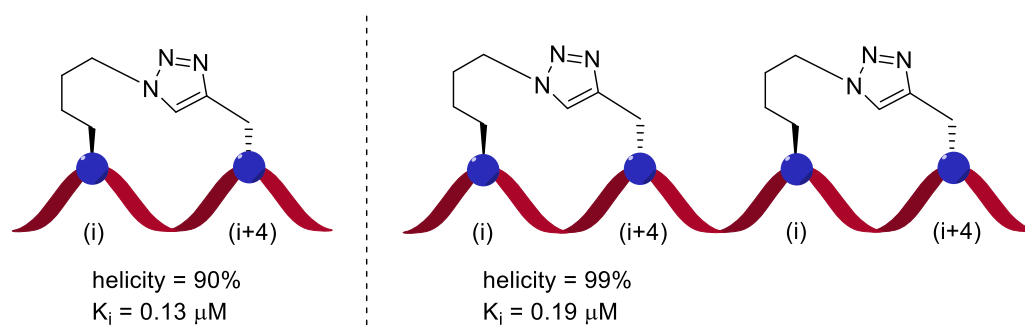
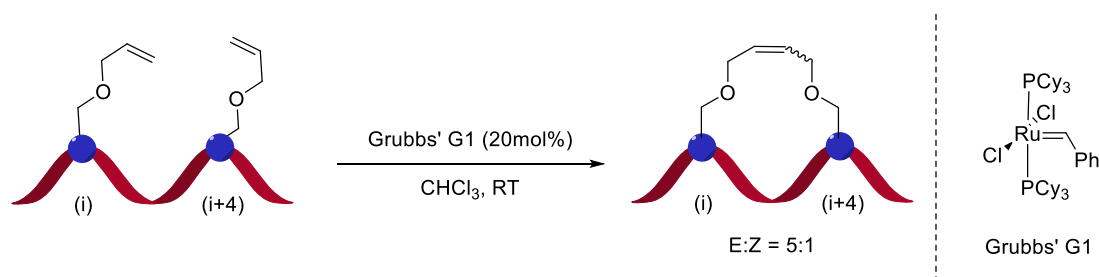


Figure 6: mismatched stereochemistry utilised by Kawamoto *et. al.* showing the helicity and binding constant for the single and double CuACC peptides on the left and right hand sides, respectively.⁸

This proved to be important for both binding and helicity with a stereochemical matched pair being lower for both peptides.⁸

In 1998, Grubbs utilised a ring-closing metathesis (RCM) to form the desired macrocycle between two *O*-allyl serine residues in the (i), (i+4) positions, using Grubbs' First-Generation Catalyst (Grubbs' G1 shown in **Scheme 5**).²¹



Scheme 5: RCM peptide stapling as developed by Grubbs

It was thought that the positioning of the two unnatural amino acids would allow both termini of the alkene moiety to be close enough to be brought together by the catalyst. Pleasingly, this was found to be the case and the reaction proceeded in 85% yield as a 5:1 mixture of *E* and *Z* isomers. The olefin was then reduced *via* hydrogenation and subjected to circular dichroism and found to be more helical than the unstapled peptide.²¹

Two years later Verdine developed a new type of amino acid staple as outlined in **Figure 7**. In the study it was established that α,α -disubstituted amino acids increased the helicity of peptides and that the length, position and stereochemistry of each staple was found to be key for the success of the RCM.²²

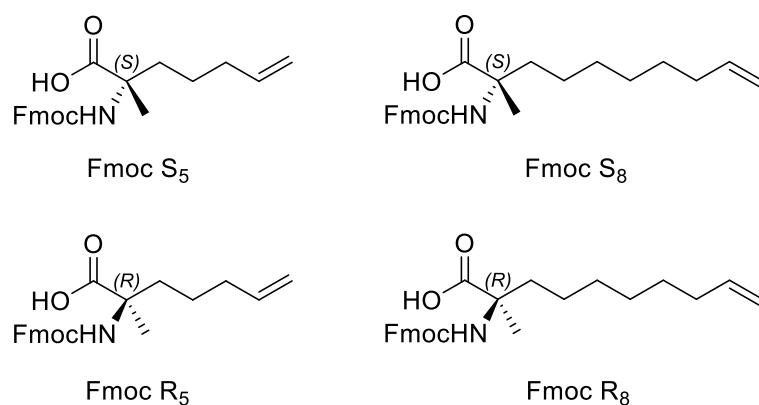
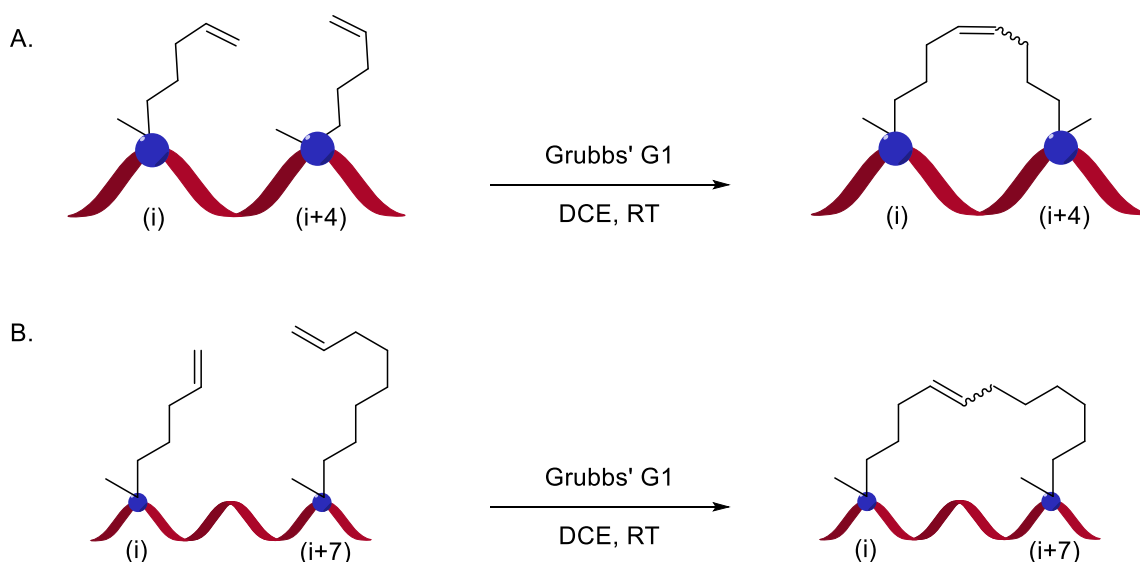


Figure 7: New amino acid staples developed by Verdine

It was found that amino acid staples which had a mismatch in stereochemistry had reduced success in the RCM reaction whilst RCM was optimal in the (i), (i+4) position using two matching, Fmoc S₅/R₅ staples (A. **Scheme 6**). For the (i), (i+7) positions it was found that matching Fmoc S₅/R₈ and Fmoc S₈/R₅ were optimal (B. in **Scheme 6**).



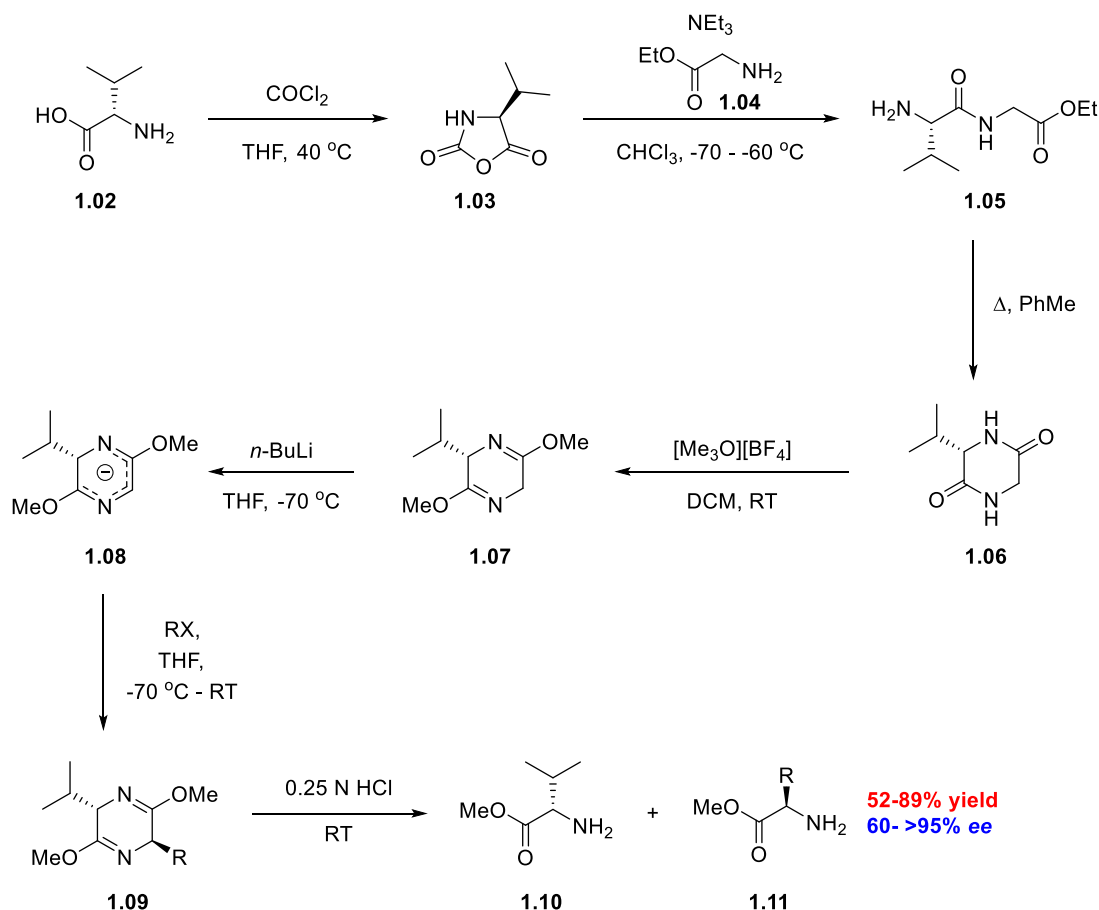
Scheme 6: A. All-hydrocarbon stapling in the i, i+4 positions as developed by Verdine. B. All-hydrocarbon stapling in the i, i+7 positions as developed by Verdine

This technique was further exemplified in the synthesis of artificial p53 analogues as a potential treatment for cancers which over express hDM2, an E3 ubiquitin ligase which targets p53 through a PPI with a 15 residue α -helix in the transactivation domain. Thus, analogues of this α -helix were synthesised using Fmoc-R₈ and Fmoc-S₅ in the i, i+7 positions. Substitutions to both serine and proline were found to be optimal for binding to the enzyme with a K_d of 0.92 nM, which was more potent than

the wild type peptide, and a helicity measured at 59%. However, while potent in *in vitro* enzyme assays, the peptide was not cell permeable and further modifications, such as exchanging all glutamic acid residues for glutamine, aspartic acid for asparagine and lysine for arginine, were made in order to test the peptide in cell-based assays. The potency of these peptides towards hDMD was reduced to 55 nM, which was still better than the wild type, and the helicity was improved with 85% observed. Most importantly, the peptide was cell permeable and was able to induce apoptosis in a cancer cell line which overexpressed hDM2.

1.1.2 Amino Acid Synthesis

Due to the reliance of unnatural amino acids on helix stabilisation, there is a need for efficient means of synthesising the required residues with a high degree of enantiopurity. One of the better-known ways of accomplishing this is the Schöllkopf method, which uses valine to form a chiral auxiliary.²³ This can then be alkylated after treatment with *n*-butyl lithium (*n*-BuLi), as outlined below in **Scheme 7**, to form the methyl ester of the desired amino acid in the opposite enantiomer to the starting valine. The stereocontrol is thought to be induced by the steric bulk of the valine blocking one face of intermediate **1.08**, forcing the alkyl group to approach from the least hindered side.²⁴



Scheme 7: Schöllkopf auxiliary method of amino acid synthesis

The reaction is moderate to high yielding with the excellent enantiomeric excess (*ee*) required for peptide synthesis on most, bulky substrates. However, for less sterically hindered substrates, the enantiomeric excess is less than ideal at around only 60%. The atom economy of the reaction is poor as a full equivalent of valine is discarded at the end of the reaction and it may also be difficult to separate the desired amino acid methyl ester from the unwanted valine.^{23,24} Furthermore, an ester deprotection step would then be required to expose the free amino acid, and the acidic or basic conditions usually employed to carry out this transformation may start to erode the enantiomeric excess through enolisation. The auxiliary also requires the use of phosgene in the first step of the synthesis which is a highly regulated and toxic gas, however, due to the popularity of this method auxiliary **1.07** and its precursor **1.06** are both commercially available in both the (*R*) and (*S*) enantiomers.^{25–28}

Another method utilises a nickel(II) Schiff base complex as a chiral auxiliary. Initially used to synthesise amino acids in 1985, the technique has undergone a degree of evolution to the present day in order to further optimise the enantioselectivity of the reaction.^{29–31} The first iteration of the nickel(II) Schiff base complexes utilised a benzyl proline aminobenzaldehyde (BPBA) based ligand as outlined in **Figure 8** below with future iterations utilising benzyl proline aminoacetophenone (BPAP) and benzyl proline aminobenzophenone (BPB) allowing for better control of enantioselectivity.^{29,30}

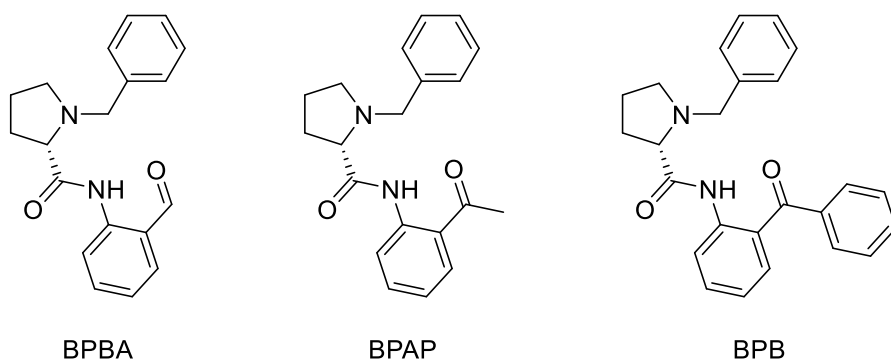


Figure 8: different chiral ligands used in the synthesis of Ni(II) Schiff bases

One positive aspect of this technique is the ability to isolate and recycle the chiral auxiliary, which may help address the relatively poor atom economy of the process, although the acidic decomplexation conditions could pose a significant risk of epimerisation at the α -proton of the proline system, which would erode the stereocontrol of subsequent reactions.³⁰ The stereoselectivity arises from the pendant benzyl group forming a π -stacking interaction with the aryl group directly bonded to the amide.³² This blocks one face of the complex leaving the less hindered side open to the electrophile as shown in **Figure 9**.³² As a result, the stereochemistry for the whole complex and subsequent amino acid is controlled by the stereochemistry around the proline centre, with (*S*)-amino acids being generated from *L*-proline and (*R*)-amino acids from *D*-proline, although with high equivalents of base it is possible to invert this process, presumably due to epimerisation of the stereocentre at proline.³³

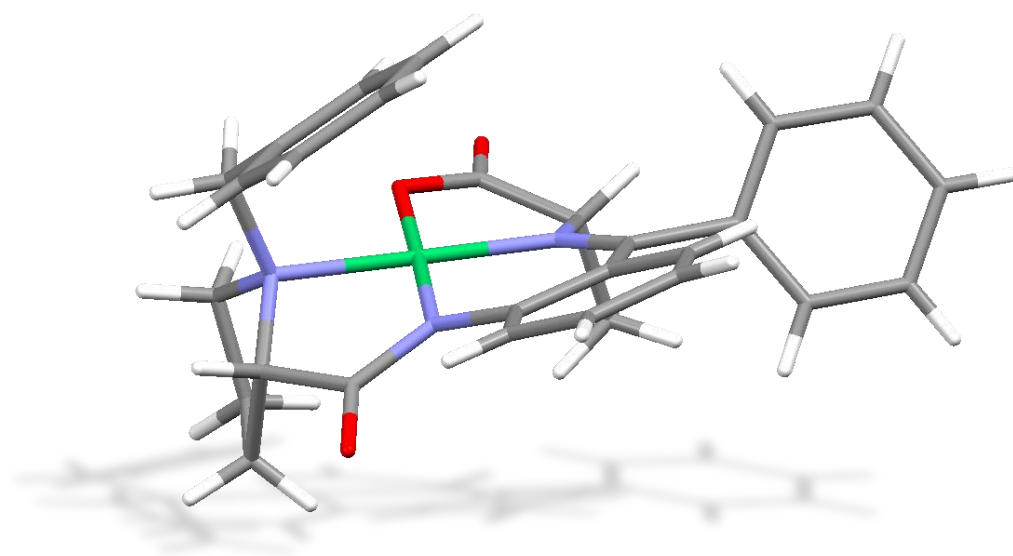
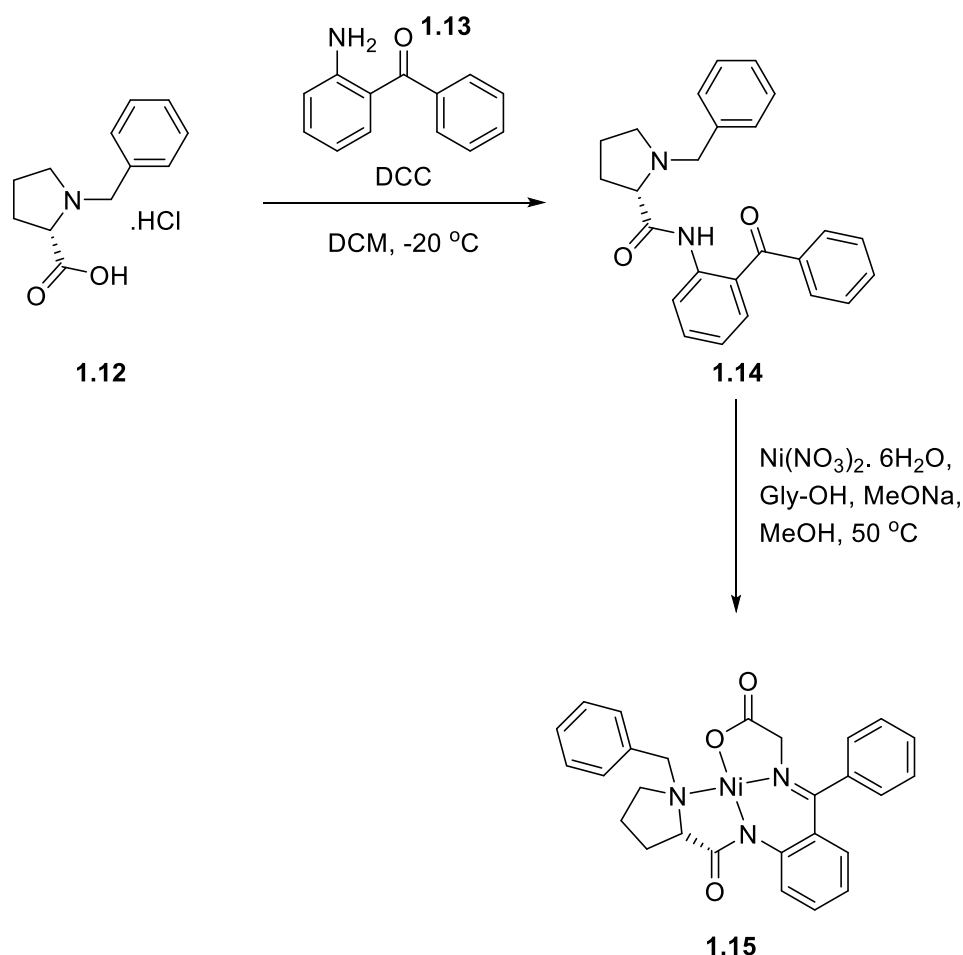


Figure 9: Crystal structure of Ni(II)-Ala-BPBP showing the π -stacking interaction between the benzyl group and the aromatic ring³²

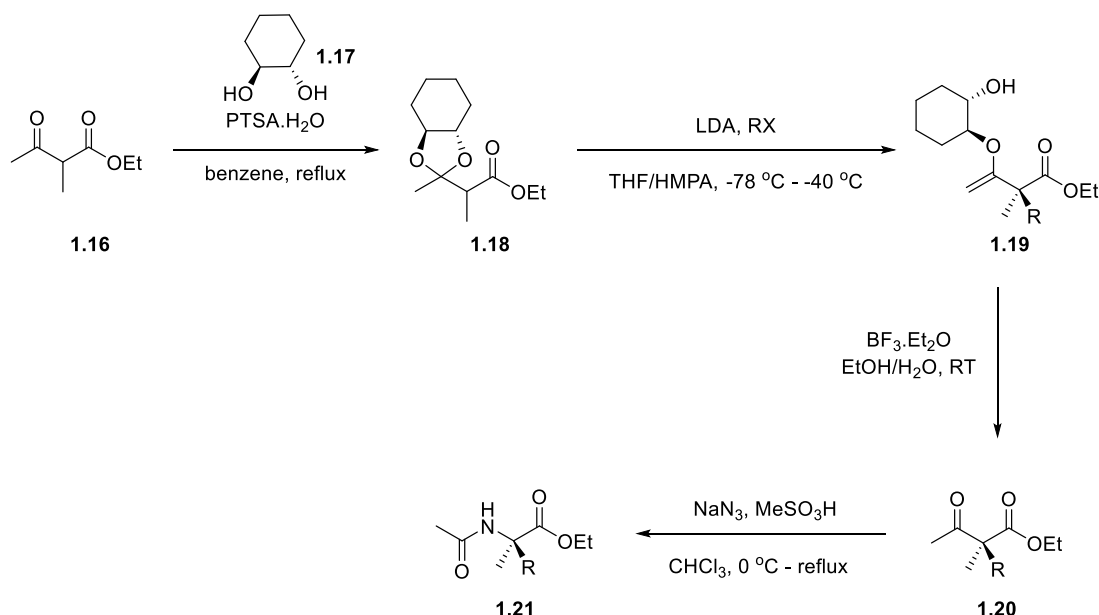
The most commonly used complex uses glycine and an example procedure is outlined below in **Scheme 8**.³²



Scheme 8: General route to Ni(II)-Gly-BPBP Schiff base complex³⁰

The intermediate nickel complex **1.15** is then able to undergo a variety of subsequent reactions to install the desired sidechain. To date this has been achieved utilising both alkylations with alkyl halides, aldol reactions with aldehydes and ketones and many others, with good levels of stereocontrol being reported for both reactions.^{29–31} The route is also not limited to glycine, and other amino acids, such as alanine, can be used to synthesise α,α -disubstituted amino acids.^{29–31,34,35} Unlike the Schöllkopf method, upon acidic hydrolysis the free amino acid is released meaning that further reactions are not required, potentially making the route more efficient.

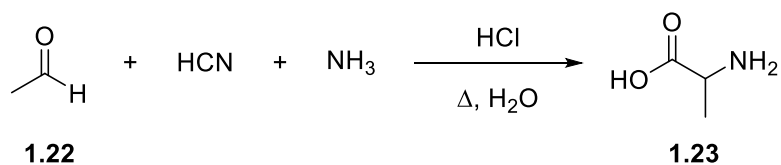
α,α -Disubstituted amino acids have also been prepared *via* alkylation of a β -keto-ester using a chiral diol (**1.16**) to establish the stereochemistry.^{36–38} The resulting α,α -disubstituted β -keto-ester (**1.19**) can then be converted to an *N*-acetyl- α -amino ester (**1.20**) using a Schmidt rearrangement as outlined in **Scheme 9**.



Scheme 9: Asymmetric alkylation of β -keto-esters with subsequent Schmidt rearrangement to form the protected amino acid

As with the Schöllkopf method, this reaction forms a protected amino acid and subsequent manipulations are required to form the free amino acid. Despite these shortcomings, the reaction is relatively high yielding with excellent stereocontrol with > 90% enantiomeric excess obtained for all substrates. The desired amino acid has the opposite stereochemistry to the diol with the inversion in stereochemistry arising from the change in priority with the introduction of the nitrogen.

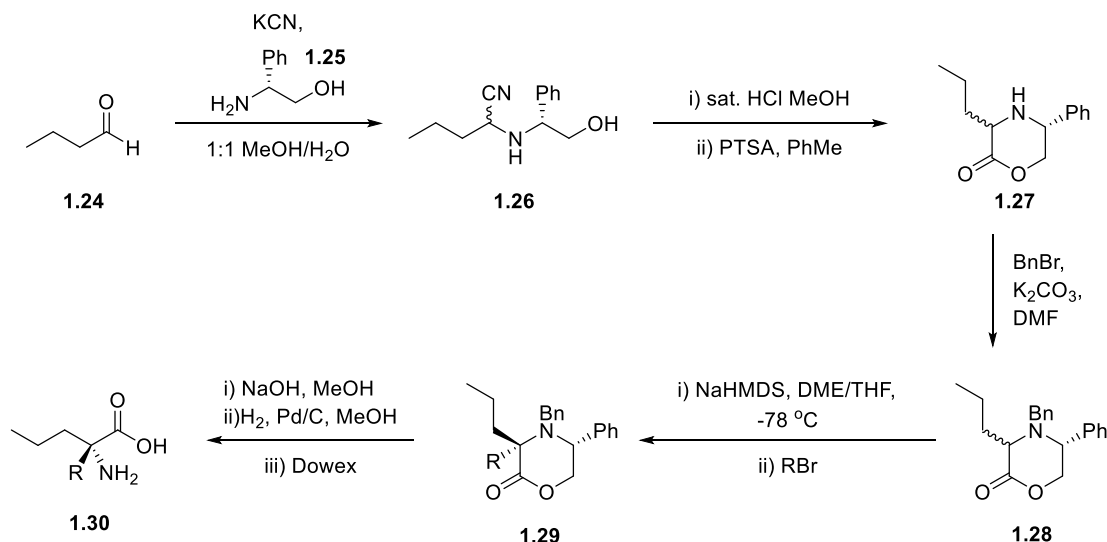
In 1850, Strecker reported the synthesis of alanine when acetaldehyde, hydrogen cyanide and ammonia were heated under acidic conditions.³⁹ This process has been used extensively to produce racemic amino acids and due to its multicomponent nature, the reaction is extremely atom efficient as shown in **Scheme 10**.



Scheme 10: Strecker multicomponent amino acid synthesis outlining the synthesis of alanine

Since the products of this reaction have no optical purity, many strategies have been developed in order to induce stereocontrol and avoid chiral separations.⁴⁰ One such

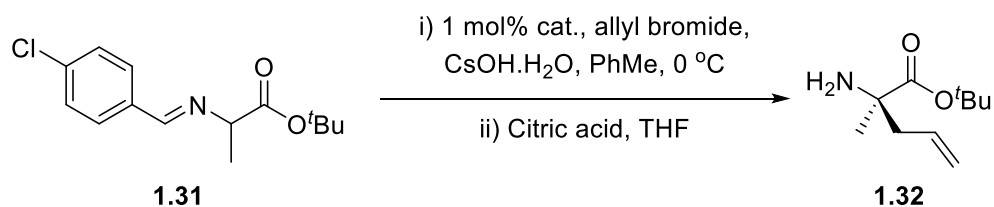
method has been the use of a chiral amino alcohol in order to form a chiral auxiliary *in situ* as outlined below in **Scheme 11**.⁴¹



Scheme 11: Asymmetric Strecker reaction using a chiral amino acid to set the stereochemistry

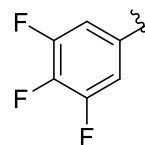
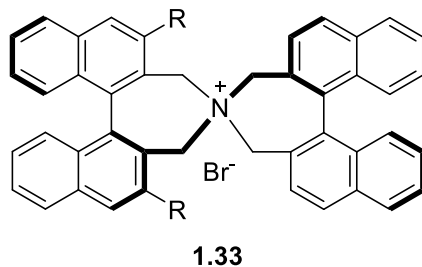
The reaction appears to give optically pure α,α-disubstituted amino acids after recrystallisation, however, no enantiomeric excesses are reported. The yields are also good, however, can depend heavily upon the substrates employed, as does the chirality of the final amino acid. The process is also not particularly atom efficient as the starting amino alcohol is not recoverable at the end of the reaction. The reaction also relies on potassium cyanide, which may discourage industry from adopting the process.

α,α-Disubstituted amino acids can also be synthesised from Schiff bases using a chiral phase transfer catalyst, as discovered by Marouka, shown below in **Scheme 12**.⁴²



cat. =

R =



Scheme 12: α,α -disubstituted amino acid synthesis by Maruoka chiral phase transfer catalysis

This reaction uses cheap, readily available starting materials and under mild conditions good yields of α,α -disubstituted aldehydes are obtained, which all have high enantiomeric excesses (> 90%). Unfortunately, the chiral phase transfer catalyst employed in this particular reaction (**1.33**) is not commercially available and must be synthesised. A structurally related catalyst (**Figure 10, 1.34**) is available commercially, however, it is very expensive (£3,633/mmol, Sigma Aldrich).⁴³ As the catalyst loading is very low, this counteracts the synthetic effort required for synthesis and the high cost of the commercial catalyst.⁴²

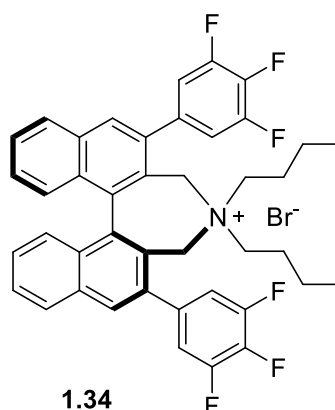


Figure 10: Structure of the commercially available Marouka chiral phase transfer catalyst

1.1.3 Fluorination

1.1.3.1 Fluorine in Medicinal Chemistry

Fluorine-containing molecules are becoming more prevalent within the pharmaceutical industry, with approximately 25% of drugs in the market today containing at least one fluorine atom (**Figure 11**).⁴⁴ This is mainly due to the beneficial effects that the incorporation of fluorine can have.

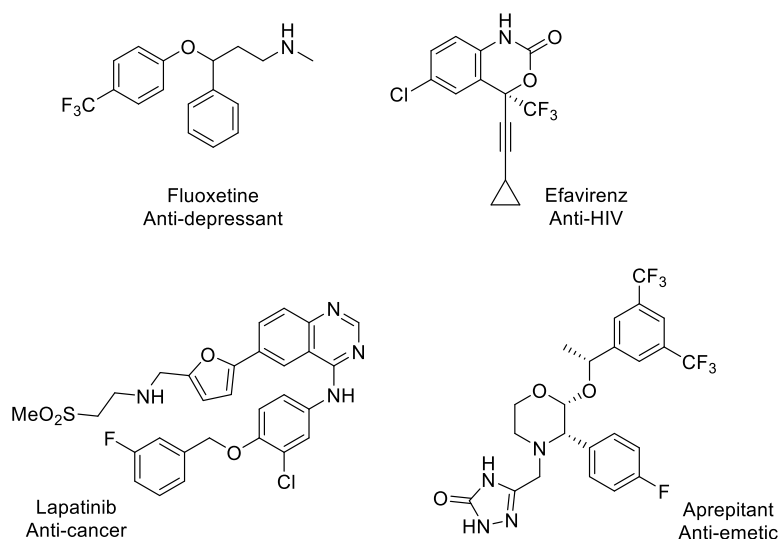


Figure 11: A selection of fluorine-containing drug molecules

Fluorine has been shown to enhance the potency of drugs by altering their $\log P$ and pK_a and increasing their metabolic stability.⁴⁵ This is a benefit as a lower dose of the drug can be used which could lead to a reduction in side effects.

$\log P$ is defined as the ratio of the concentration of a molecule which is partitioned between layers of octanol and water and is calculated using **Equation 5**. Therefore, the higher the $\log P$ the more lipophilic the molecule is.

$$\log P = \log \frac{[X_{\text{octanol}}]}{[X_{\text{water}}]}$$

Equation 5: Determination of $\log P$

This is important in pharmaceutical compounds, which according to Lipinski's rules⁴⁶ should ideally have a $\log P$ which is less than 5 to allow the drug to be able to pass through the cell membrane.⁴⁵ The addition of fluorine can both increase and decrease $\log P$ depending on where it is incorporated. Fluorine present on aromatic rings, and next to π -bonds increases lipophilicity as does polyfluorination and

perfluorination. However, counterintuitively, monofluorination and trifluoromethylation of saturated alkyl chains decreases lipophilicity. This is mainly due to the high electronegativity of fluorine, resulting in the generation of a dipole.⁴⁷

It is this extremely high electronegativity which also alters the acidity and basicity of drugs. Incorporation of fluorine to molecules will almost always increase their acidity.⁴⁷ This has been observed with a series of 5-HT_{2A} receptor antagonists where adding a single fluorine atom to the piperidine ring reduced its basicity as shown in **Figure 12**.⁴⁸

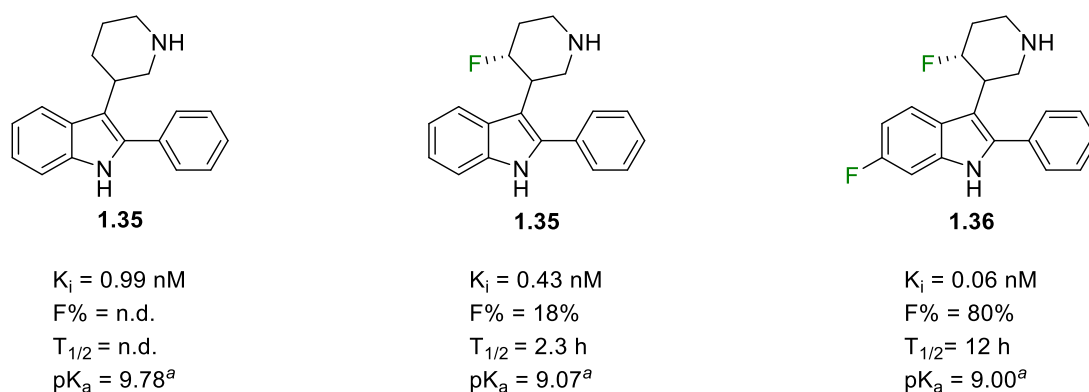


Figure 12: Effects of fluorine on bioavailability and half-life of selected 5-HT_{2A} receptor antagonists. ^a Calculated by ChemBioDraw

As shown in the example above, the strategic placement of fluorine can also increase the metabolic stability by preventing the formation of key metabolites in the pathway. The addition of a single fluorine atom in the 6-position of the indole ring in **1.36** prevented oxidation and eventual deactivation of the drug allowing the half-life ($T_{1/2}$) to increase to 12 hours from 2.3 hours, which also increased its bioavailability.⁴⁸ A further case study is in the development of flurithromycin (**Figure 13**) as a treatment for gastritis caused by *Helicobacter pylori* infections. The parent compound, erythromycin (**Figure 13**), which is used as an alternative antibiotic to penicillin for patients with an allergy, is not stable in the highly acidic conditions of the stomach and is therefore not a suitable treatment for this condition.⁴⁹ However, the incorporation of a single fluorine atom at the C8 position prevents an E1 elimination of water from the C6 (highlighted in red) in the acidic environment of the stomach which ensures that the molecule is stable enough to have an effect.⁵⁰

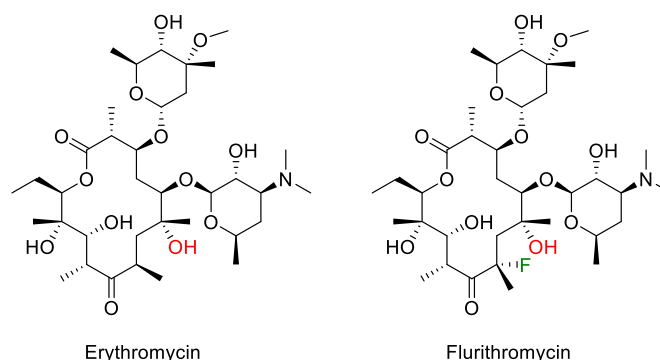


Figure 13: Structures of erythromycin and flurithromycin with hydroxy group which can be eliminated in acidic conditions highlighted in red

1.1.3.2 Fluorine as a Nuclear Magnetic Resonance (NMR) Probe

Fluorine exists as a single natural isotope, ^{19}F , which is NMR active. Due to its high natural abundance ^{19}F NMR is extremely sensitive and with the advancement of NMR technology and available experiments it is quickly becoming a valuable tool for monitoring reaction progress and elucidating reaction mechanisms.⁵¹

Another use for ^{19}F NMR is in the determination of binding constants of fluorinated ligands to a protein, or non-fluorinated ligands to a protein which is modified with fluorinated derivatives of natural amino acids such as those shown below in **Figure 14**.⁵²

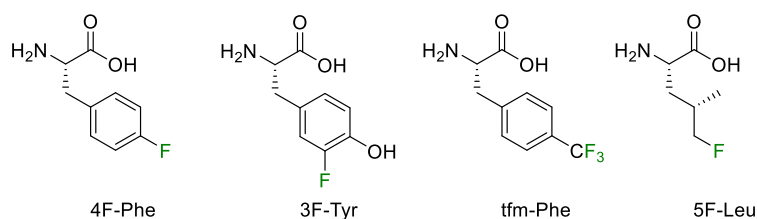


Figure 14: A selection of commonly used fluorinated amino acids

Due to the high sensitivity of ^{19}F NMR it would be possible to detect and quantify any changes in shift due to a change in environment of the fluorine atoms present e.g. in a “bound” and “unbound” state. One particularly useful method for high-throughput screening is known as fluorine chemical shift derived anisotropy and exchange for screening (FAXS). This method can be used to determine binding coefficients for both fluorinated and non-fluorinated substrates when used in the presence of a suitable fluorinated standard. This method exploits both the change in chemical shift as well

as the peak shape of a fluorine signal upon binding and release of a fluorinated molecule as outlined below in **Figure 15**.

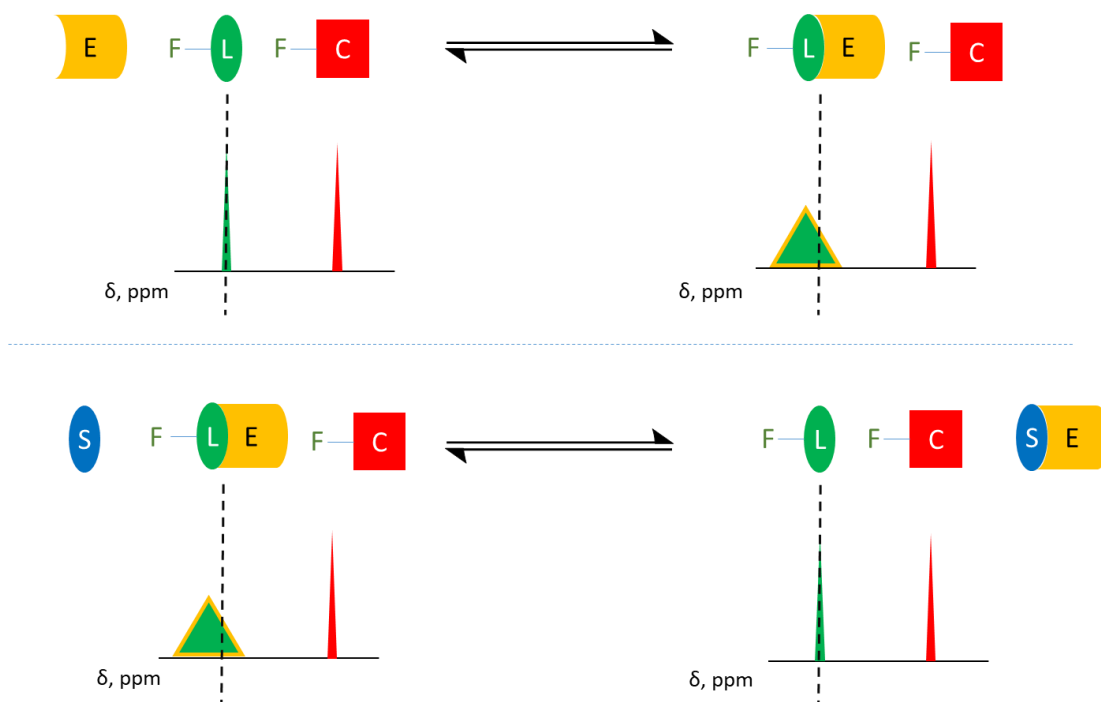


Figure 15: Outline of the changes in fluorine signal observed in a FAXS experiment. E is the enzyme, L is the fluorinated ligand, C is the fluorinated control and S is a non-fluorinated enzyme substrate. Top, changes in the ^{19}F signal of the ligand upon binding to the enzyme. Bottom, changes in the ^{19}F signal of the ligand upon displacement from the enzyme

This method is sensitive enough to be used with the typical NMR instrumentation found within most industrial and academic institutions and can also be run at low concentrations in biocompatible solvents, which allows for the study of poorly soluble substrates. It is also possible to run more than one fragment during the experiment, provided each chemical shift is distinct from the others and is well characterised. This especially useful for high-throughput screening as it is possible to identify multiple ligands in a single experiment as well as limits the amount of enzyme required for study.⁵³

1.1.3.3 Methods of Fluorination

Due to the increased level of incorporation of fluorine into pharmaceutically active molecules, and fluorinated molecules not being widely found in nature, robust synthetic methods of fluorination had to be developed.

Traditionally this was done using anhydrous hydrogen fluoride or fluorine gas which is an extremely atom efficient process. It is, however, difficult to control and incredibly dangerous due to the highly toxic and gaseous nature of these reagents. Therefore, specialist equipment and highly trained individuals are required, making the process expensive. To counteract these disadvantages easier to handle fluorinating agents were developed for laboratory use. These can be split into two main classes – electrophilic and nucleophilic.⁵⁴

Electrophilic fluorinating agents, such as Selectfluor®, xenon difluoride and *N*-fluorobenzenesulfonimide (NFSI) (**Figure 16**), are a source of a formal fluoronium cation (F^+). These mainly bench-stable crystalline solids are typically synthesised using fluorine gas which can make them expensive.⁵⁴

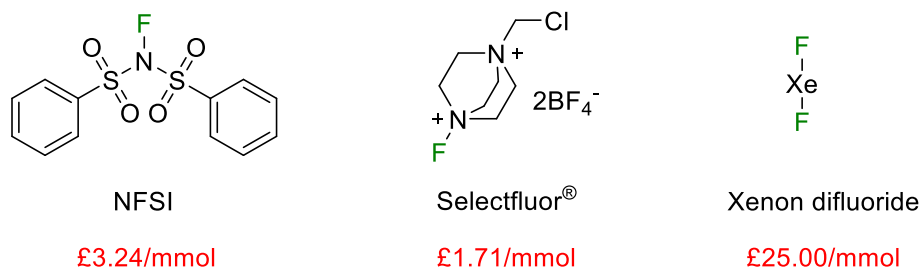
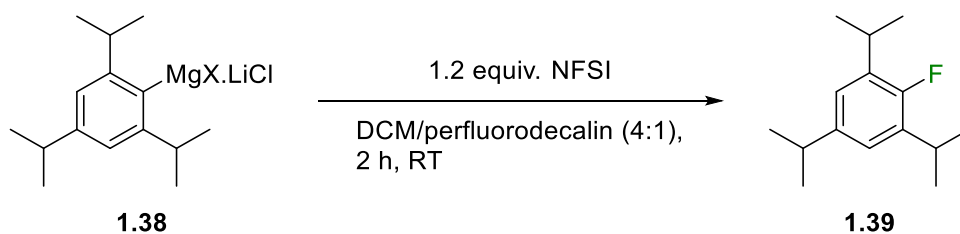


Figure 16: A selection of electrophilic fluorination agents including the cost per mmol as sold by Sigma Aldrich^{55–57}

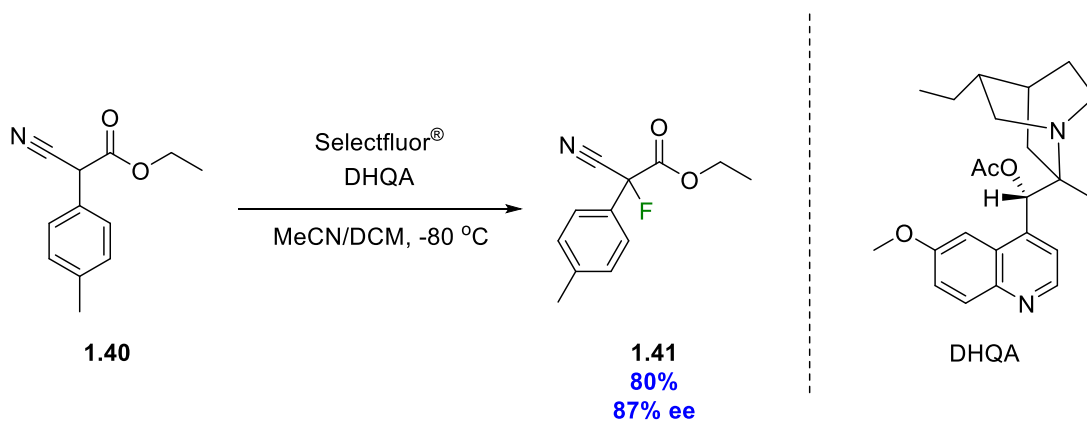
Electrophilic fluorinating agents are compatible with a wide range of substrates from aryl and heteroaryl Grignard reagents⁵⁸ to sp^3 hybridised alkyl chains.⁵⁹

Originally aryl Grignard reagents were selectively fluorinated with elemental fluorine.⁶⁰ In 2010 Knochel developed a method which could fluorinate a Grignard reagent complexed with lithium chloride (commonly known as a “turbo” Grignard). The Grignard is reacted with a slight excess of NFSI in a mixed solvent system to give the corresponding aryl fluoride as shown below in **Scheme 13**. The requirement for a fluorinated co-solvent was proposed to minimise proton abstraction from dichloromethane (DCM) by a suspected radical intermediate and pleasingly a range of functional groups and heterocycles were tolerated.⁵⁸



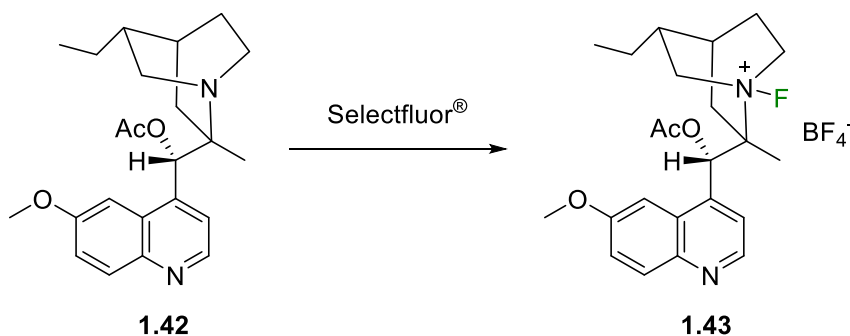
Scheme 13: Synthesis of aryl fluorides from turbo Grignard reagents as developed by Knochel

Electrophilic fluorinating agents are also able to fluorinate sp^3 carbon centres as shown below in **Scheme 14**.⁵⁹



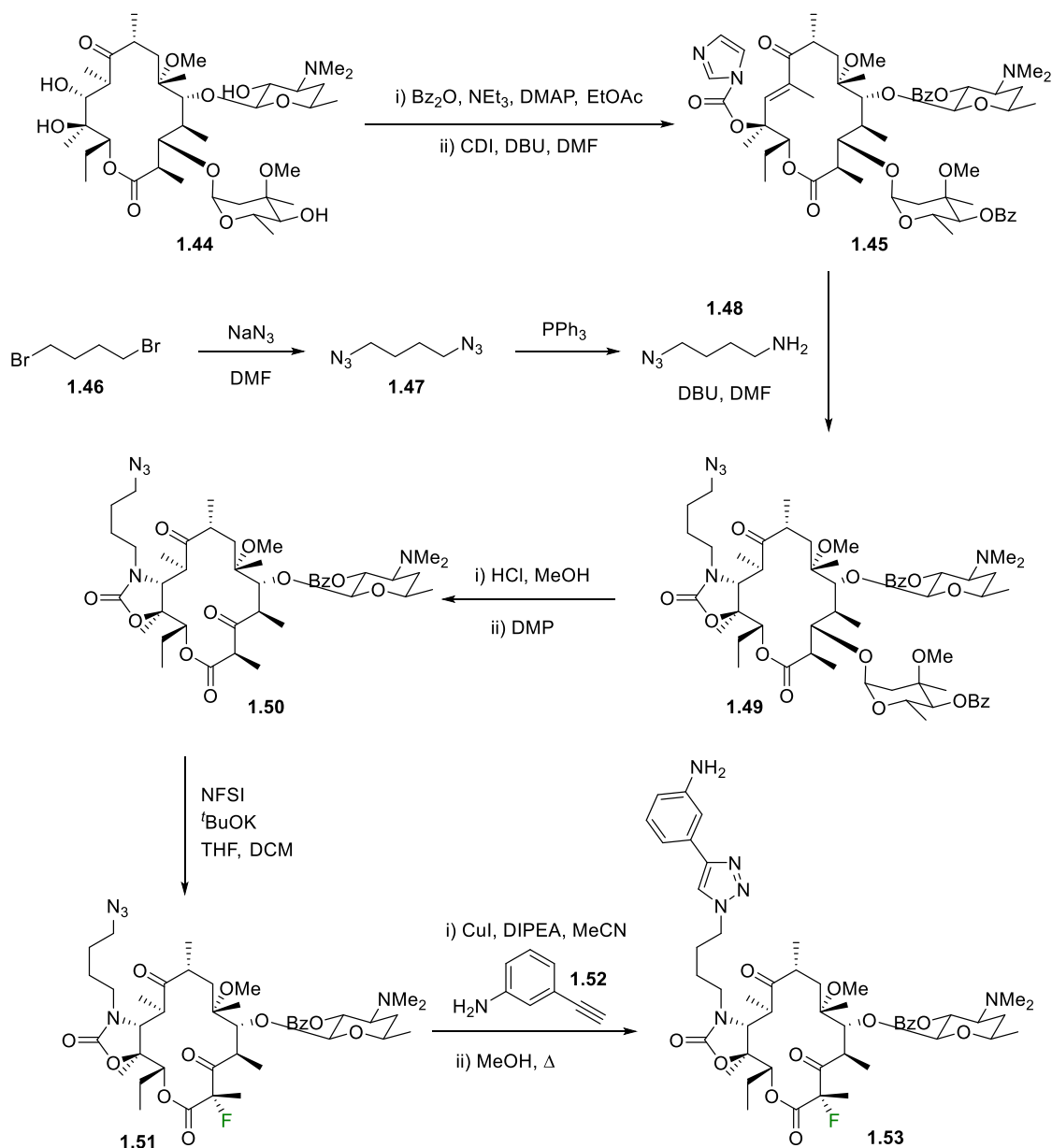
Scheme 14: Fluorination of sp^3 centres using Selectfluor[®]

The use of dihydroquinidine acetate (DHQA), a Cinchona alkaloid, has allowed the reaction to proceed enantioselectively with up to 91% *ee* being achieved. It is thought that initially the Selectfluor[®] fluorinates the alkaloid (**1.39**) *in situ* as shown below in **Scheme 15** and that it is this new, chiral fluorinating agent (**1.40**) which is responsible for the enantioselectivity observed in the products.



Scheme 15: Proposed mechanism of the reaction outlined in Scheme 4

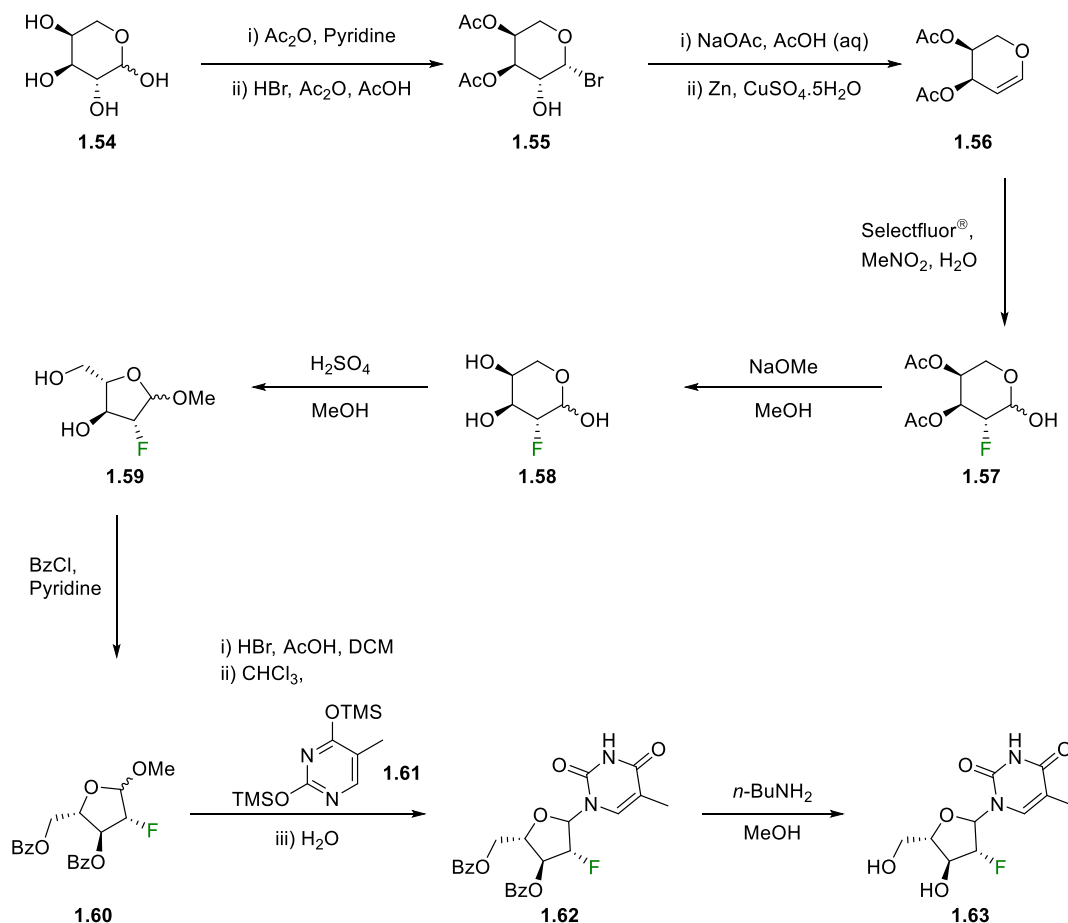
An example of a pharmaceutical which is synthesised using an electrophilic fluorinating agent is solithromycin (**1.53**), an antibiotic developed by Cembra Pharmaceuticals which is currently in phase III clinical trials for the treatment of community acquired bacterial pneumonia. The synthetic route is shown below in **Scheme 16**. The synthesis begins with the natural product clarithromycin and the single fluorine atom present in the molecule is added using NFSI.⁶¹



Scheme 16: Synthetic route to solithromycin (1.53**)**⁶¹

Clevudine (**1.63**) is an antiviral drug which has been approved for the treatment of chronic hepatitis B in South Korea and the Philippines. The synthetic route, shown in

Scheme 17, uses the natural product *L*-arabinose (**1.54**) as a starting material and the key fluorination step uses Selectfluor® as a fluorinating agent.^{61,62}



Scheme 17: Synthetic route to clevudine 1.63⁶²

Nucleophilic fluorinating agents are a formal source of a fluoride anion (F⁻). These can be as simple as a fluoride salt, such as potassium fluoride, to more complex structures such as (diethylamino)sulfur trifluoride (DAST) and XtalFluor-E® (**Figure 17**).

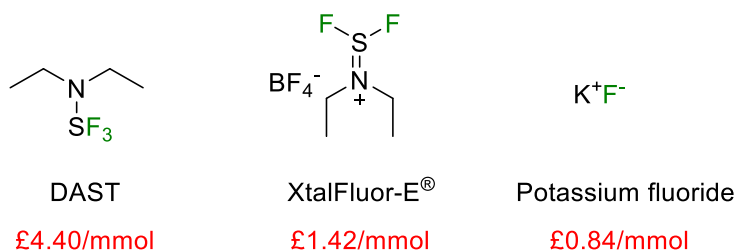
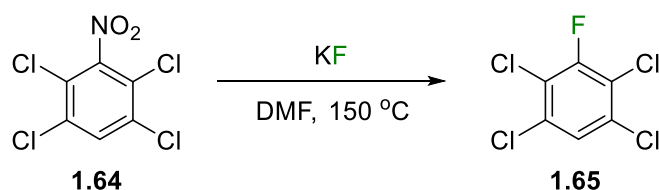


Figure 17: A selection of nucleophilic fluorinating agents including the cost per mmol as sold by Sigma Aldrich^{63–65}

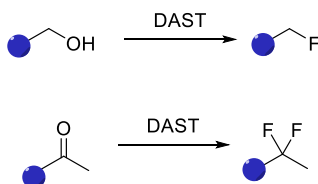
KF has the advantage of being relatively inexpensive, and has been shown to participate in nucleophilic aromatic substitutions (S_NAr) as early as the 1950's as shown in **Scheme 18**.⁶⁶



Scheme 18: S_NAr using KF

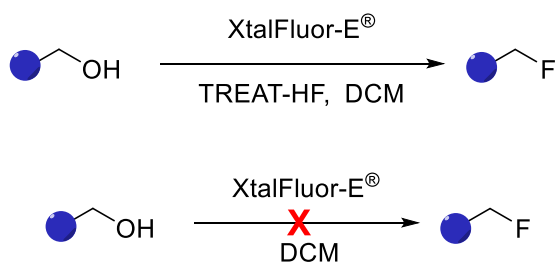
Here simply heating the reaction lead to the formation of fluorinated aromatic **1.65**, with the characteristic formation of brown NO_2 fumes indicating that it was the nitro-group which had been substituted.⁶⁶

Another use for nucleophilic fluorinating agents is in deoxyfluorination. In the presence of DAST, alcohols and ketones are found to be mono- and difluorinated, respectively as shown in **Scheme 19**.⁶⁷



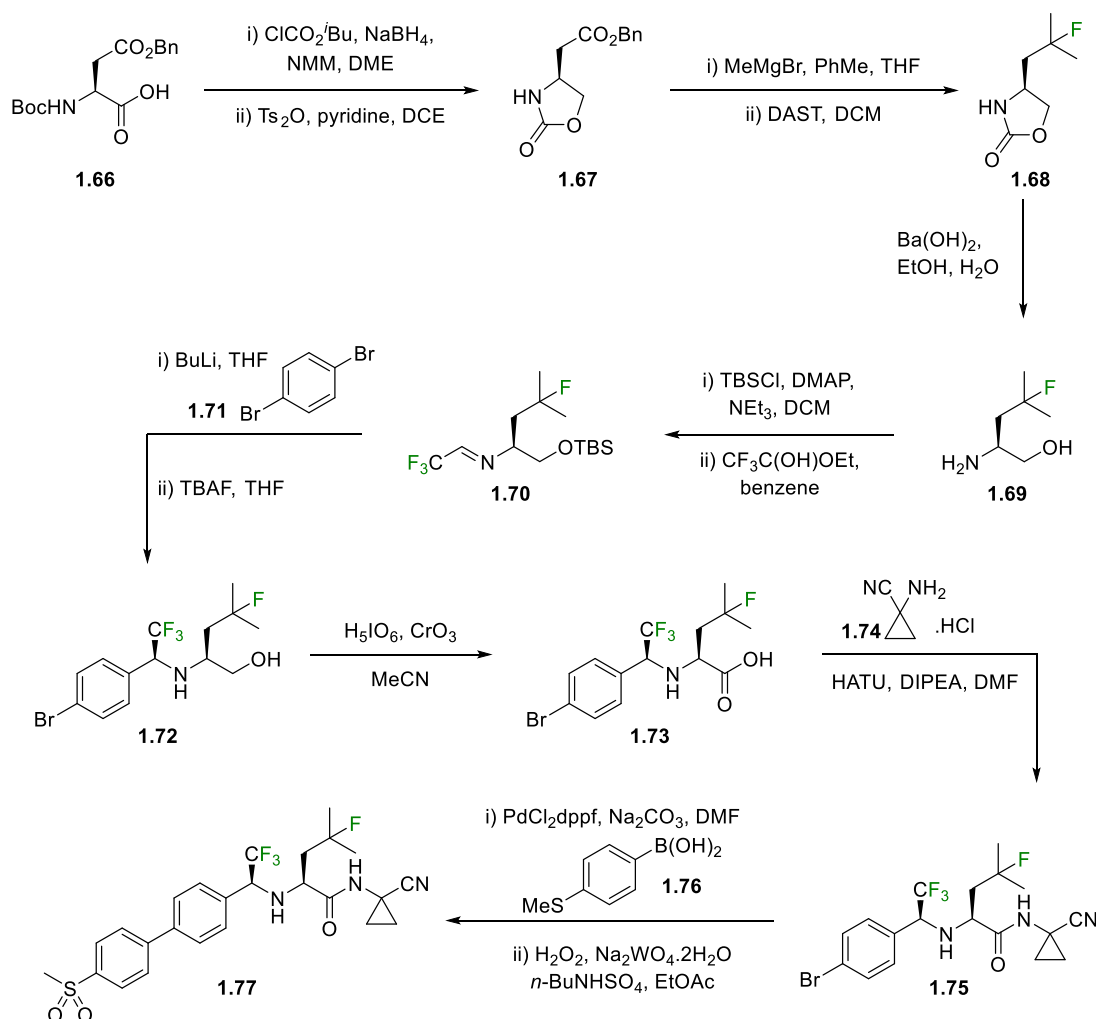
Scheme 19: Reactions of oxygen-containing molecules with DAST

However, DAST is a difficult to handle liquid, owing to its moisture sensitivity and propensity to explode when it undergoes a degradative process. A safer alternative is XtalFluor-E[®], which is a much more stable, crystalline solid. It is less reactive than DAST, and therefore a second fluoride source such as triethylamine trihydrofluoride (TREAT-HF) has to be used or the reaction does not proceed (**Scheme 20**).⁶⁸



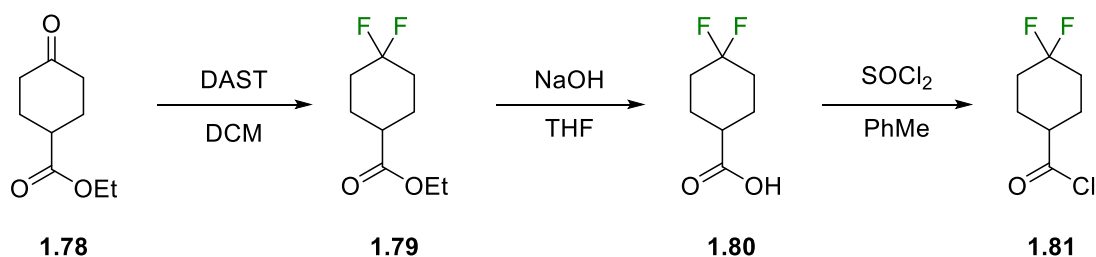
Scheme 20: Reactions of alcohols with XtalFluor-E

Deoxyfluorination with DAST is a key step in the synthesis of odanacatib (**1.77**, **Scheme 21**), an osteoporosis treatment discovered by Merck which is in Phase III clinical trials.⁶⁹

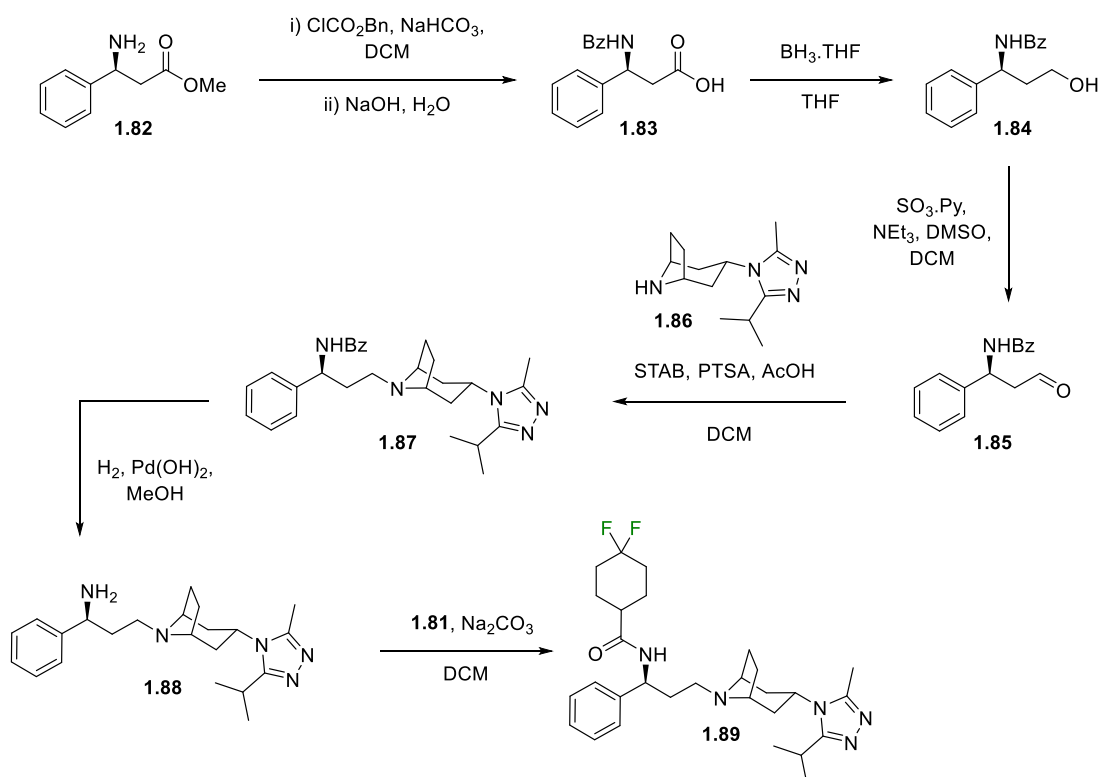


Scheme 21: Synthetic route to odanacatib (1.77**)**⁶⁹

Deoxyfluorination is also a key step to synthesise intermediate **1.81** (**Scheme 22**) which is utilised in the synthesis of the marketed HIV treatment Maraviroc (**1.89**), the synthesis of which is outlined in **Scheme 23**.^{70,71}



Scheme 22: Synthesis of key building block 1.81⁷⁰

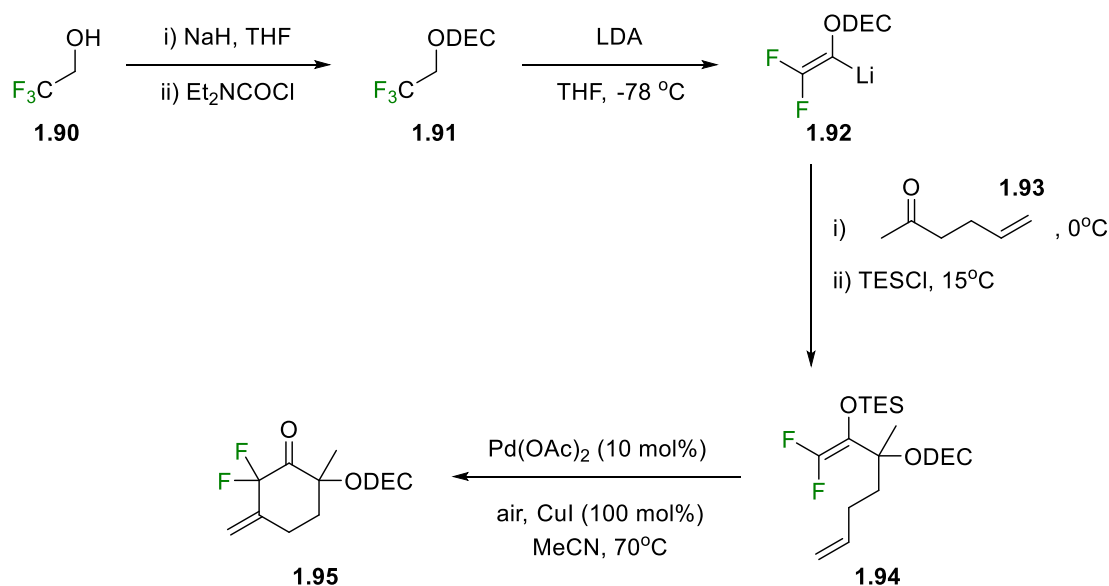


Scheme 23: Synthetic route to Maraviroc (1.89)⁷¹

Another way of incorporating fluorine into small molecules is the utilisation of a building block approach. This occurs when fluorine atoms are already attached to a carbon source and are incorporated *via* a carbon-carbon bond formation as opposed to a carbon-fluorine bond formation.⁷² These building blocks, such as trifluoroethanol, are usually unwanted by-products of large scale fluorinations, making them relatively inexpensive. For example, trifluoroethanol costs £0.07/mmol as sold by Sigma Aldrich.⁷³ However, due to the popularity of fluorine-containing molecules in both the pharmaceutical and agrochemical industries, more specialised building blocks are becoming more readily available. In a laboratory setting this is

usually a safer approach as the requirement of highly toxic fluorinating agents are not required.

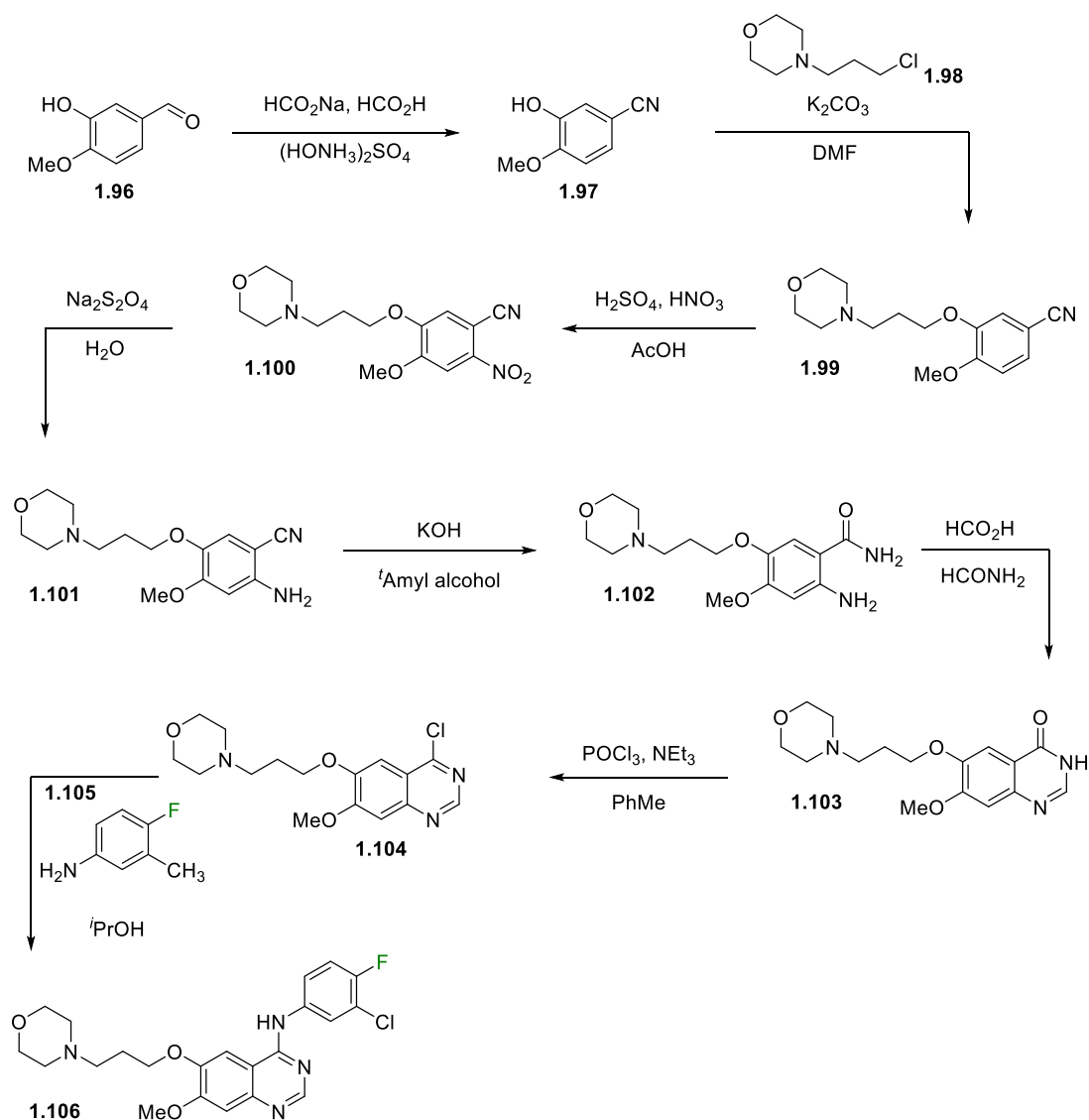
An example of the use of trifluoroethanol to build difluorinated cyclohexenones is shown in **Scheme 24**.



Scheme 24: Route to difluorocyclohexenones

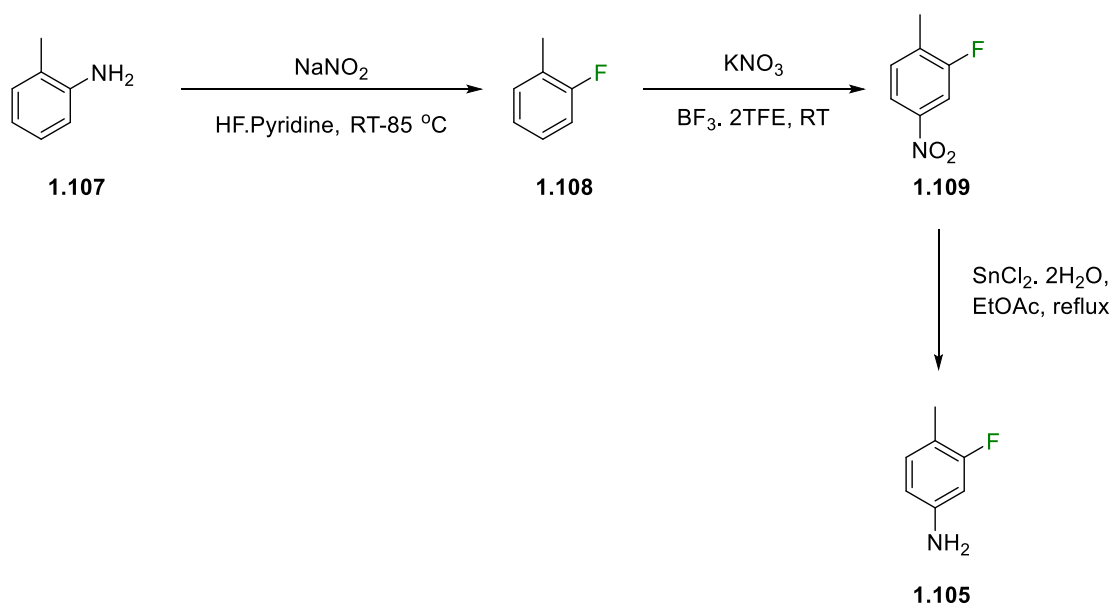
Here trifluoroethanol undergoes dehydrofluorination/lithiation to form species **1.92**, which is then trapped with an electrophile. The resulting diene is then cross coupled intramolecularly using a modified Saegusa–Ito cyclisation to give the resulting cyclohexenes in moderate yields.⁷⁴

Fluorinated building blocks are key for the synthesis of the majority of fluorinated pharmaceuticals. Gefitinib (**1.106**), an anti-cancer drug developed by Astra-Zeneca uses compound **1.105** (£0.13/mmol)⁷⁵ as the final step of an eight-step synthesis to install the required fluorine (**Scheme 25**).⁷⁶



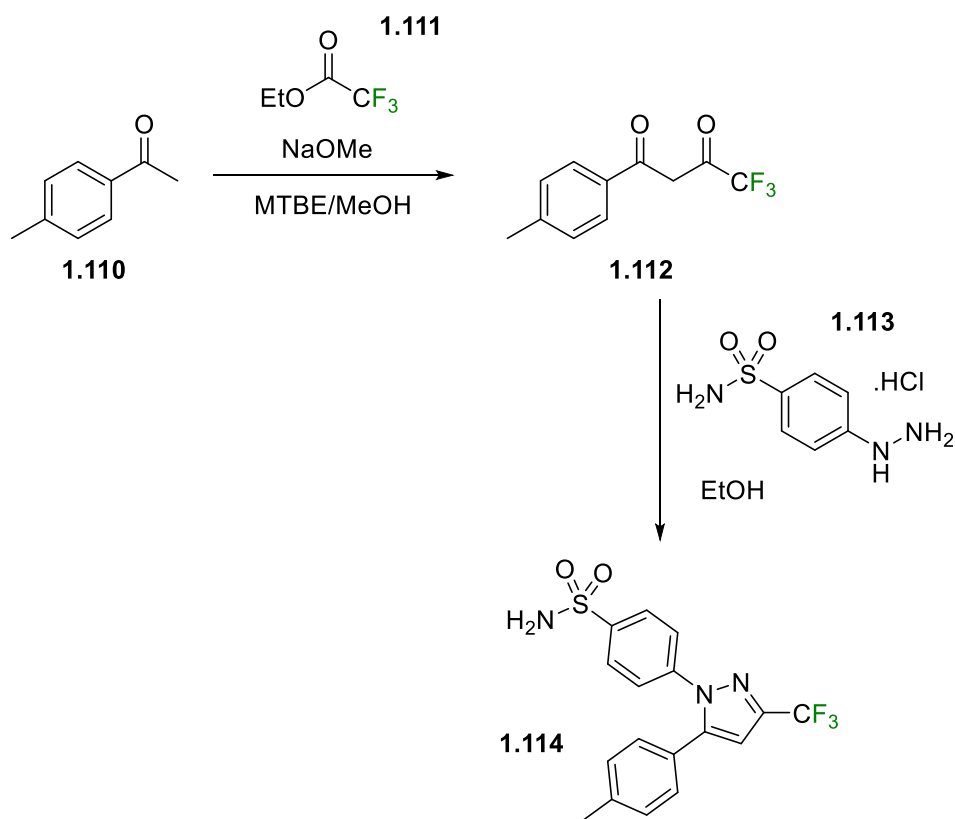
Scheme 25: Synthetic route to Gefitinib (1.106)⁷⁶

Fluorinated building block **1.105** can be synthesised using the following protocol (**Scheme 26**). Here 2-aminotoluene (**1.107**) is converted into 2-fluorotoluene (**1.108**) using a Sandmeyer-like reaction.⁷⁷ **1.108**, is then nitrated to give 2-fluoro-4-nitrotoluene (**1.109**)⁷⁸ which then undergoes a reduction to give fluorinated building block **1.105**.⁷⁹



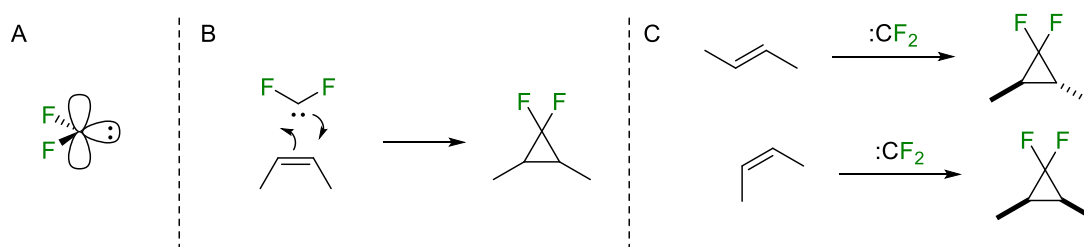
Scheme 26: Synthesis of fluorinated building block 1.105^{77–79}

Celebrex (**1.114**), Pfizer's non-steroidal anti-inflammatory drug, is also synthesised using a fluorinated building block. Here compound **1.111** (£0.09/mmol)⁸⁰ is used at the start of the two-step synthesis to install the required trifluoromethyl group as outlined below in **Scheme 27**.⁸¹



Scheme 27: Synthetic route to celebrex (1.114)⁸¹

Another important building block is difluorocarbene (:CF_2), which is principally used for difluorocyclopropanation. Difluorocarbene is a relatively stable carbene, which exists in the singlet state. This means that difluorocarbene has an empty p -orbital and a lone pair of electrons as shown below in **Scheme 28**.



Scheme 28: A - structure of difluorocarbene, B - difluorocyclopropanation mechanism, C - outcome of difluorocyclopropanations on *cis*- and *trans*- alkenes

This structure allows difluorocarbene to act as both a nucleophile and electrophile and it is known to react with alkenes in a concerted [2+1] cycloaddition as shown in **Scheme 28**.⁸² This is known to be the case as when a *trans*-alkene is used in the reaction the resulting cyclopropane has a *trans*-configuration and *vice versa*.

Due to its short lifespan, difluorocarbene must be generated *in situ* and many suitable reagents have been developed for this purpose (**Figure 18**).

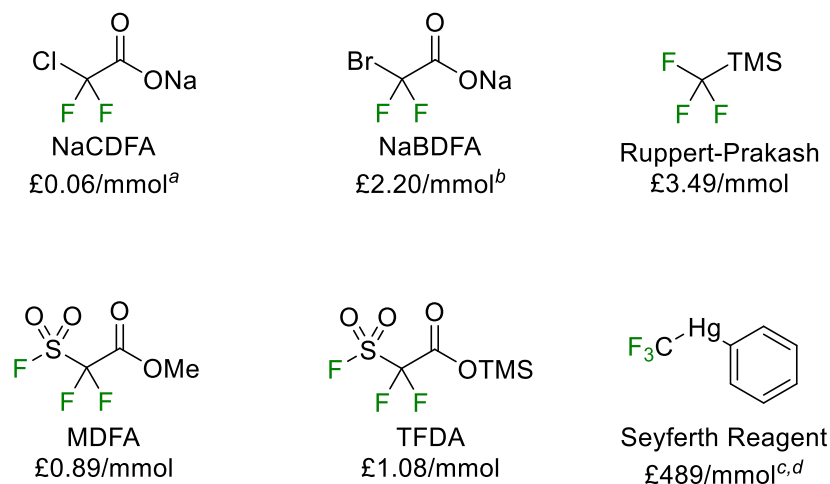
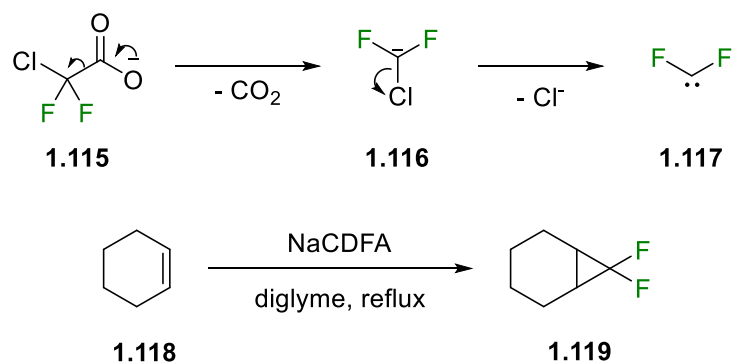


Figure 18: Difluorocarbene sources with their associated costs from Sigma Aldrich unless otherwise stated.^{83–85}
^a Sourced from Fluorochem,⁸⁶ ^b Sourced from Apollo Scientific,⁸⁷ ^c Sourced from Enamine,⁸⁸ ^d Exchange rate USD-GBP 08/05/2019⁸⁹

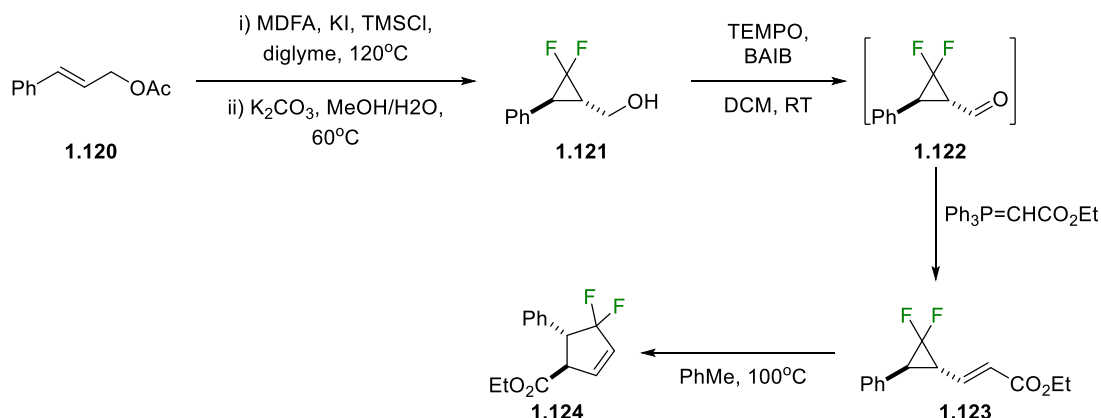
The first of this class of reagent to be discovered was sodium chlorodifluoroacetate (NaCDFA) in 1960 by Haszeldine. In this study, NaCDFA was shown to thermally decompose at high temperatures and react with cyclohexene as shown below in **Scheme 29** to generate the difluorocyclopropanated product in 22% yield.⁹⁰



Scheme 29: Thermal decomposition of NaCDFA (top) and the reaction of cyclohexene with NaCDFA (bottom)

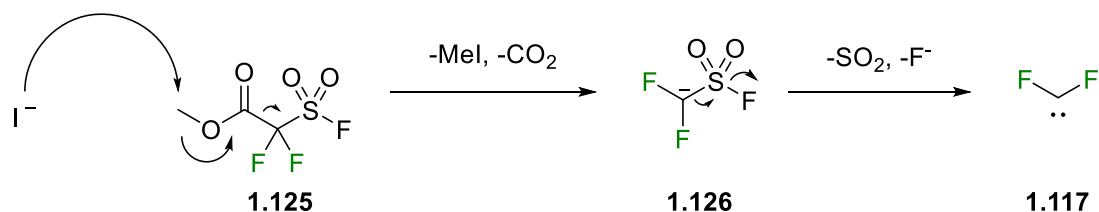
Sodium bromodifluoroacetate (NaBDFA) was discovered to be an effective difluorocarbene source by Amii *et.al.* in 2010. It decomposes under heating much like NaCDFA above, however, it is more reactive than NaCDFA and as a result this allows the reaction to proceed at lower temperatures.⁹¹

Difluorocyclopropanation, followed by a vinyl cyclopropane rearrangement (VCPR) has been used in the formation of *gem*-difluorocyclopentenes as shown in **Scheme 30**.⁹²



Scheme 30: Synthesis of *gem*-difluorocyclopanes⁹²

In this example, methyl 2,2-(difluorosulfonyl)acetate (MDFA) was used as the difluorocarbene source. MDFA is decomposed by iodide, with the loss of carbon dioxide and sulfur dioxide providing the driving force for the reaction. TMSCl is used to sequester the generated fluoride ion as shown in **Scheme 31**. This allowed the reactions to be run at a slightly lower temperature than those for NaCDFA.⁹²

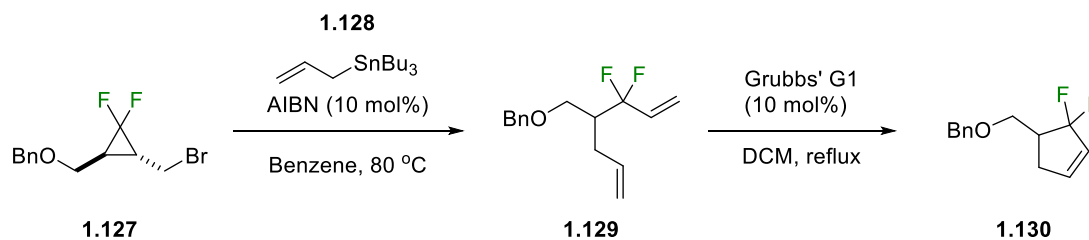


Scheme 31: Decomposition of MDFA to difluorocarbene

For the VCPR the presence of the *gem*-difluoro group facilitated the reaction, which was able to be conducted at lower temperatures than for non-fluorinated vinyl cyclopropanes.⁹²

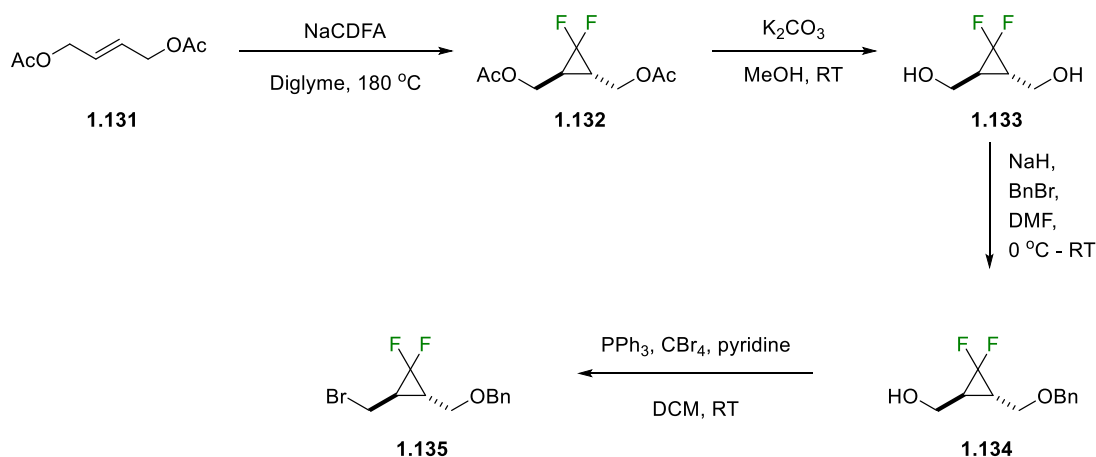
A similar motif can be reached through the radical based ring-opening reaction between difluorocyclopropane **1.127** and allyltributylstannane (**1.128**) initiated by azobisisobutyronitrile (AIBN) as shown below in **Scheme 32**.⁹³ This furnished *gem*-difluoro-bis-alkene (**1.121**) which then underwent an RCM reaction with 10 mol% of

Grubbs' G1 (structure shown in **Scheme 5**) to furnish the *gem*-difluorocyclopentene **1.130** in 97% yield.⁹³



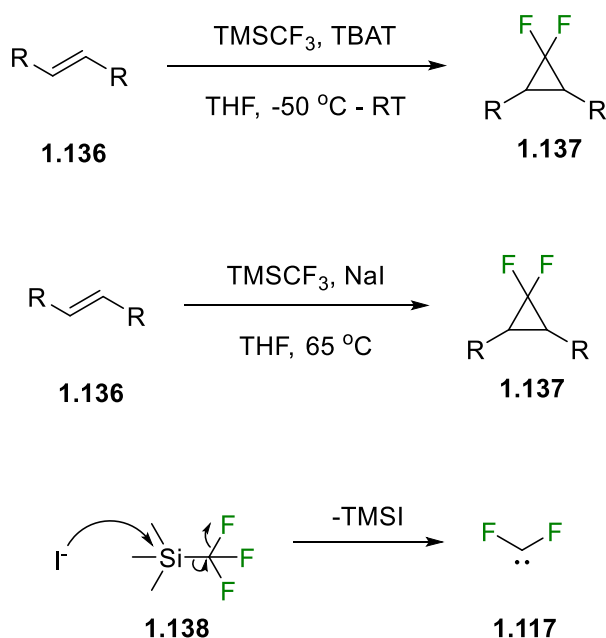
Scheme 32: Radical ring-opening reaction of difluorocyclopropanes followed by an RCM to furnish a *gem*-difluorocyclopentene motif⁹³

In this reaction, the difluorocyclopropane was prepared by the reaction of alkene **1.131** with NaCDFA followed by functional group manipulations as outlined in **Scheme 33** below.



Scheme 33: Synthesis of difluorocyclopropane intermediate **1.135**

Like MDFA, the Ruppert-Prakash reagent requires decomposition with an external anion to furnish difluorocarbene. There are several methods of accomplishing this, namely decomposition by tetrabutylammonium triphenyldifluorosilicate (TBAT) under cryogenic conditions or by using sodium iodide at elevated temperatures and reacts with a variety of alkenes to synthesise the corresponding difluorocyclopropanes in good to excellent yields as outlined below in **Scheme 34**.



Scheme 34: Two methods of difluorocyclopropanation using Ruppert-Prakash reagent with the mechanism of decomposition for the sodium iodide conditions

1.2 Aims

Due to the lack of functionalised amino acid staples and the favourable properties that fluorine could bring to the molecule, such as increased potency and metabolic stability, as well as a functional method of potentially measuring the binding constant with a cognate receptor using ^{19}F NMR, a fluorinated Fmoc S_5 analogue (**Figure 19**, **1.139**) was designed.

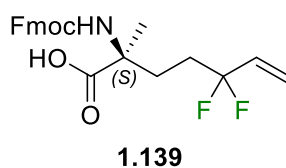


Figure 19: Fluorinated analogue of Fmoc S_5

The Jamieson group had also previously optimised a synthetic route to Fmoc S_5 which would be used as a starting point for the synthesis of analogue **1.139**. This route would be investigated to establish reproducibility before the synthesis of **1.139** commenced. The retrosynthetic analysis of **1.139** (outlined in section **1.3.2**) finds 3,3-difluoro-5-iodo-pent-1-ene (**Figure 20**, **1.140**) to be a pivotal intermediate. A building block strategy was adopted due to the expense, potential hazards and poor selectivity of traditional fluorinating agents, as discussed previously.

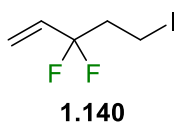


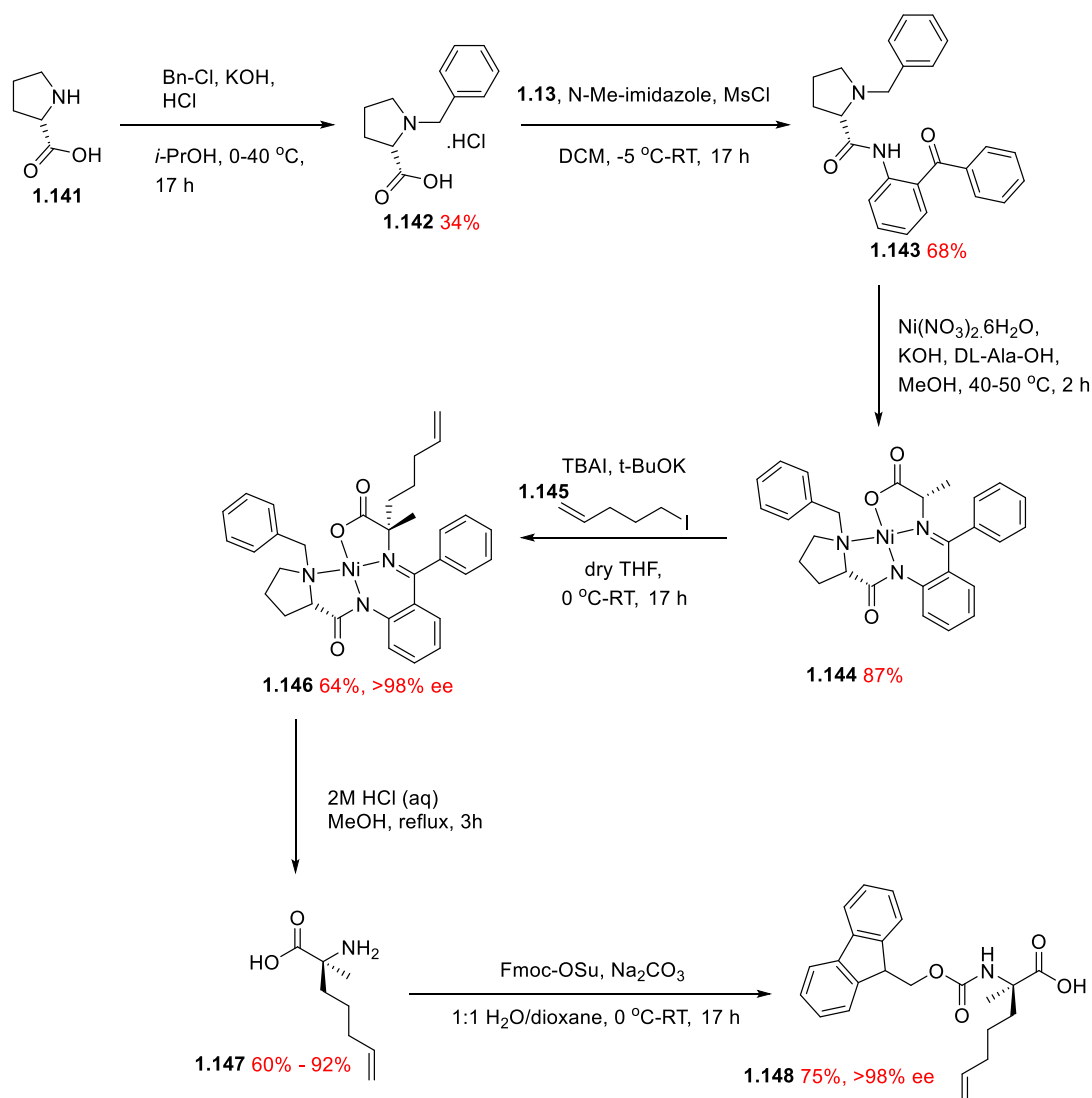
Figure 20: Key intermediate 1.140

The aim of this investigation was to develop a route to the key intermediate **1.140** using a building block approach and to construct the novel staple **1.139**. With novel staple **1.139** in hand, it would then be incorporated into a model peptide and the RCM optimised in order to compare the helicity and other key properties with a non-fluorinated analogue.

1.3 Results and Discussion

1.3.1 Synthesis of Fmoc S₅

As stated above, previous work within the Jamieson group has established a robust synthesis of Fmoc S₅ (**1.148**) using a chiral nickel(II)-alanine-benzylproline-benzophenone (Ni(II)-ala-BPB) auxiliary (**Scheme 35**). The requirement for this route was due to the high costs associated with the amino acid, and the varying degrees of enantiopurity of the commercial sources of **1.148**.³³ The route developed in our laboratories was found to have good yields, but most importantly for peptide synthesis, an excellent degree of enantiopurity (>98% ee by chiral HPLC).³³ This was subsequently reproduced by the author in the current study.

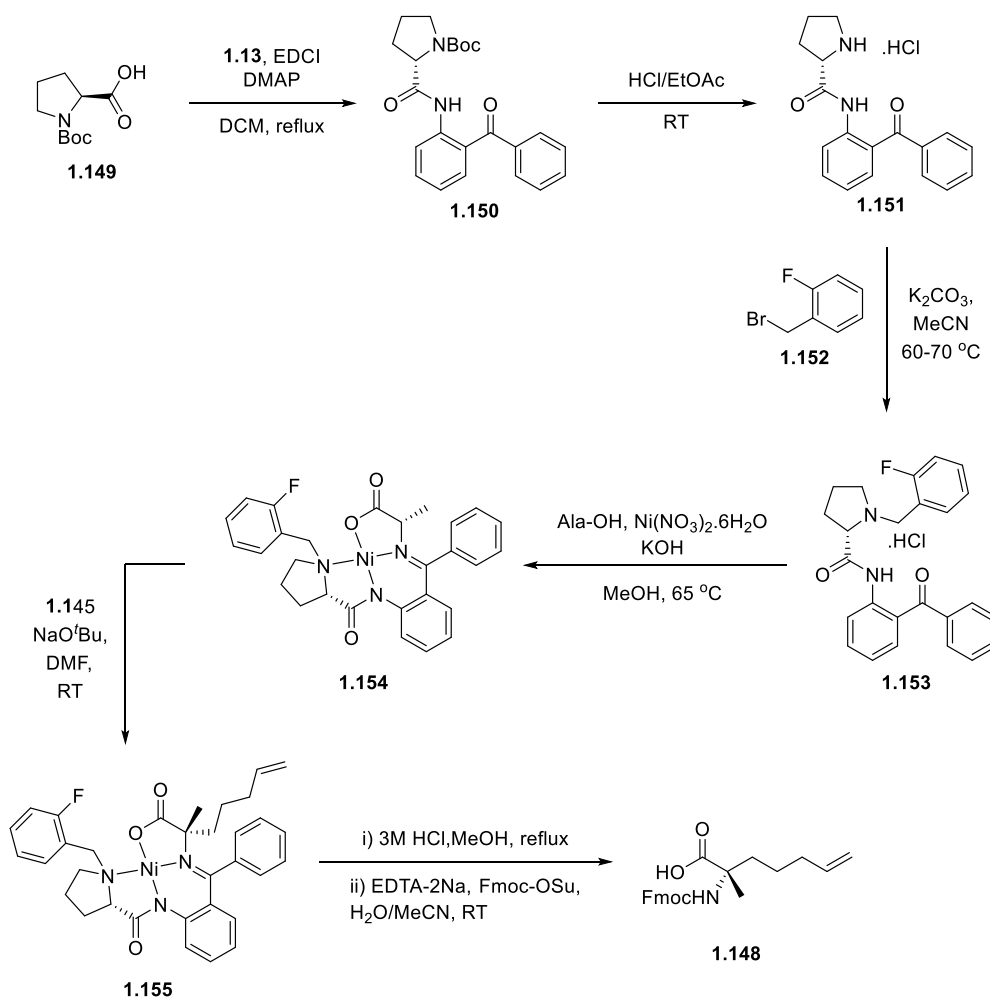


Scheme 35: Route to Fmoc S₅ using a chiral Ni(II)-ala-BPB auxiliary as reproduced by the author

To preserve the enantiopurity of the proline at the core of the synthesis, careful control of temperature and reaction time of the Ni-Ala-BPB complex (**1.144**) formation was found to be key.³³ This was established upon the generation of an X-ray crystal structure of compound **1.146** which indicated that both the desired (*S,S*) and (*R,R*) enantiomers were present in the final product.³³ This was subsequently confirmed by chiral HPLC and the reaction conditions were optimised to those outlined above in **Scheme 35**, where the potassium hydroxide was added as a solution in methanol in order to facilitate the short reaction times required to preserve the enantiopurity.³³

Pleasingly the route was found to be reproducible, in the current study, with excellent stereocontrol being achieved and it was therefore established as a basis for the synthesis of fluorinated analogue **1.139**.

Later, a similar route was published by Li *et. al.* in which the complex was hydrolysed and the Fmoc-protected amino acid isolated without having to first isolate the free amino acid as outlined below in **Scheme 36**.³⁴



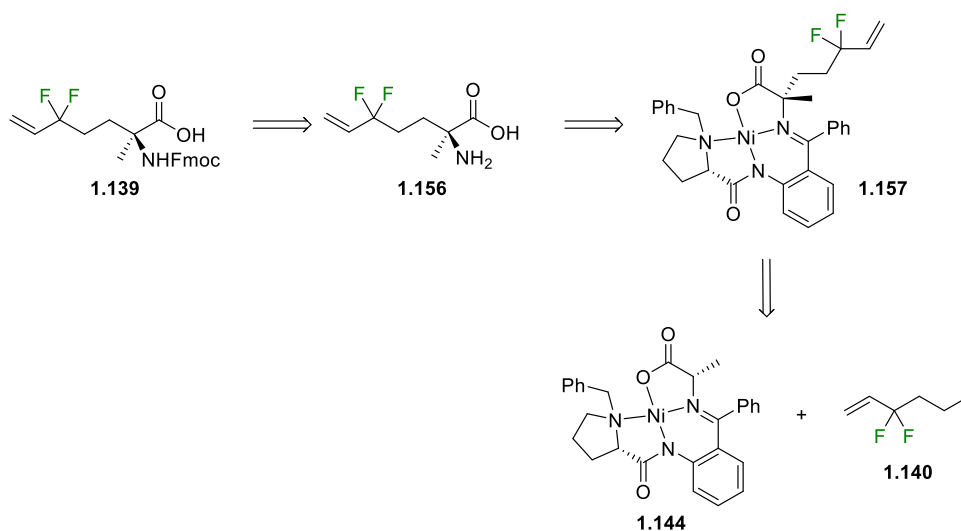
Scheme 36: Alternative route to Fmoc **S**₅, utilising a tandem complex hydrolysis and Fmoc protection as reported by Li³⁴

Moving forward, the route outlined above in **Scheme 35** could be improved by incorporating the final step of **Scheme 36** in place of the final two steps of the original synthesis. This would not only be one less step but would also avoid the protracted isolation of the free amino acid (**1.147**), which currently utilises the cationic exchange

resin DOWEX®. It was found that there was a wide variation on the quality of the DOWEX® supplied which resulted in inconsistencies in yields of **1.147**.

1.3.2 Retrosynthetic Analysis of Fluorinated Fmoc S₅

As shown in **Scheme 37**, the target fluorinated analogue of interest in the current study can be broken down into two principal fragments: **1.144** and **1.140**.



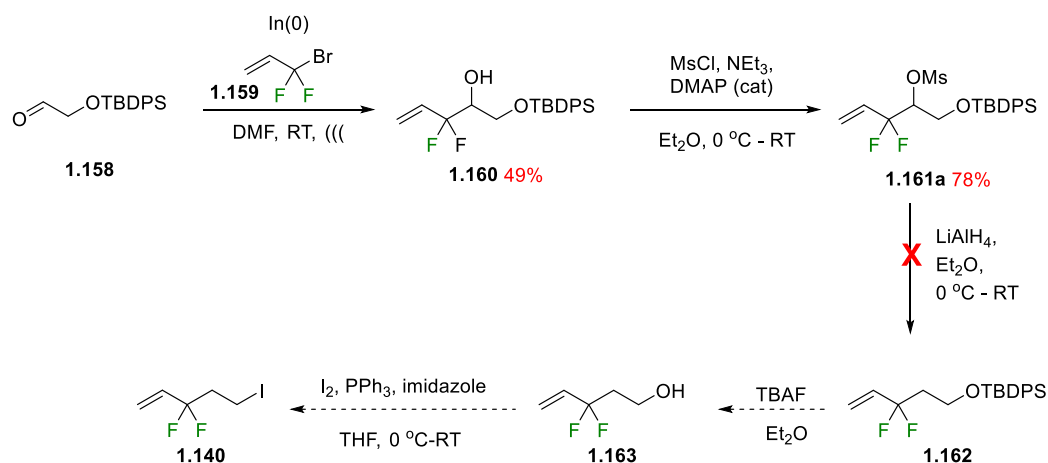
Scheme 37: Retrosynthetic analysis of 1.139

1.144 can be synthesised directly from the route described above in **Scheme 35**, however, **1.140** is a novel compound and a suitable route would have to be found. As stated above, due to the expense, hazards and selectivity issues of traditional fluorinating agents, it was decided that a building block approach would be assessed.

1.3.3 Synthesis of Key Fluorinated Building Block 1.140

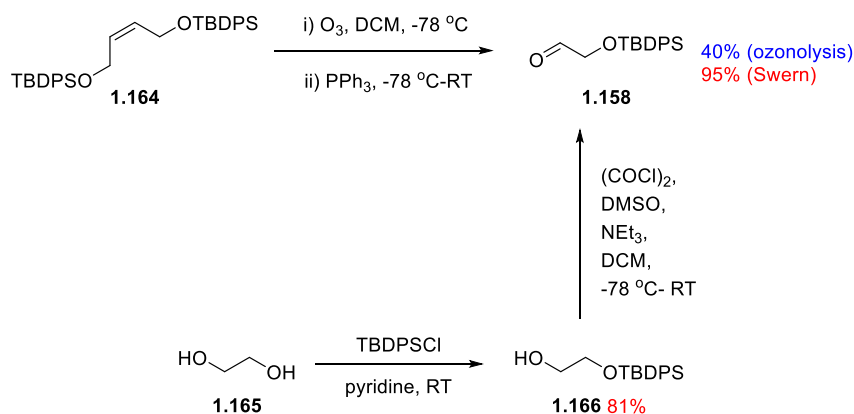
1.3.3.1 Generation 1

The initial route examined started from aldehyde **1.158**, which could then undergo an addition reaction with fluorinated building block **1.159** to furnish the secondary alcohol. Subsequent mesylation followed by hydride substitution and further functional group manipulations would then furnish the desired fluoroiodoalkene as outlined in **Scheme 38**.



Scheme 38: Initial route to 1.140 from aldehyde 1.158

tert-Butyldiphenylsilyl (TBDPS) ether was chosen as the protecting group due to its large molecular weight and the presence of a chromophore, making purification more straightforward, in addition to its stability over a variety of reaction conditions, including oxidations and reductions.⁹⁴ Aldehyde **1.158** was prepared either by ozonolysis of **1.164** or a monoprotection of ethylene glycol (**1.165**) followed by a Swern oxidation (**Scheme 39**).



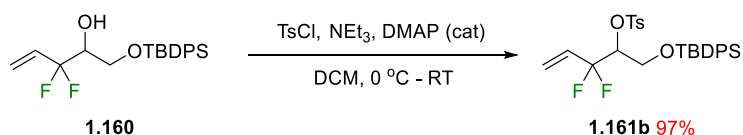
Scheme 39: Routes to key aldehyde starting material 41. Yields in blue are representative of the ozonolysis conditions and yields in red are representative of Swern oxidation conditions

Ozonolysis was chosen at first due to the excellent efficiency of the reaction, as two molecules of **1.158** are generated from one molecule of **1.164**. However, the poor yields (blue, **Scheme 39**), explosion hazards and issues associated with ozone generator led to the need for an alternative route to **1.158**.

A second route was then devised which started from ethylene glycol (**1.165**), a cheap and readily available feedstock (£3.19/mol, < £0.01/mmol Sigma Aldrich).⁹⁵ The ethylene glycol was then protected with TBDPS and oxidised using Swern conditions to give aldehyde **1.158** in a much greater yield (red, **Scheme 39**).

Once a source of starting material **1.158** was established, the next step was an indium mediated addition of fluorinated building block **1.159**.⁹⁶ The conditions employed were already known for the substrates used in this step of the route.⁹⁷ The requisite substrate **1.159** is commonly used as a component in refrigerants and as such is readily available.⁹⁸ Pleasingly the reaction proceeded in consistently good yields. The resulting alcohol (**1.160**) was then mesylated (**1.161a**, **Scheme 38**) to provide a competent leaving group, which could be reduced using lithium aluminium hydride. Whilst the mesylation occurred in excellent yields, there were some issues with the reduction. Analysis by thin layer chromatography (TLC) indicated that the starting material had been completely consumed, however the products isolated following flash chromatography contained no fluorine after analysis by ¹⁹F NMR. ¹H NMR spectroscopy indicated that the products were related to TBDPS, which suggested that TBDPS was not stable to these conditions, and the product had potentially degraded.

An attempt at varying the leaving group from mesyl to tosyl (**Scheme 40**) was made in the hypothesis that it would be more reactive towards hydride and that the reaction could be run in a shorter time, potentially allowing the TBDPS to be preserved. Unfortunately, this was not found to be the case, and the same issues as before were encountered, with namely decomposition being observed.



Scheme 40: Tosylation of alcohol 1.160

As the conditions using LiAlH₄ were unsuccessful, alternative reaction conditions were examined. The Barton-McCombie deoxygenation reaction uses tributyltinhydride (Bu₃SnH) to reduce the xanthate esters of both primary and

below.⁹⁹



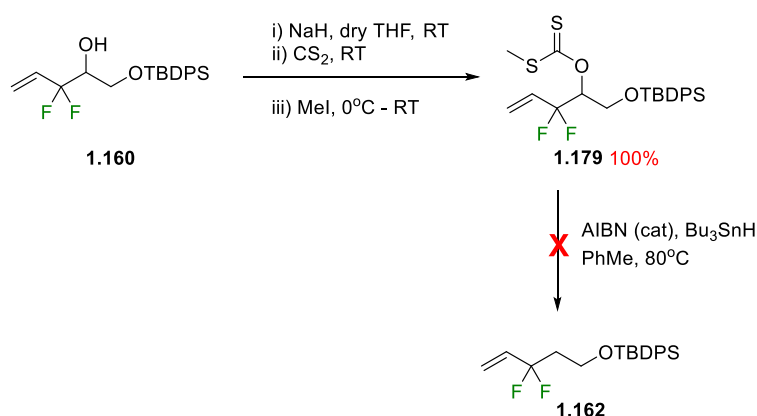
Scheme 41: Exemplar Barton-McCombie deoxygenation conditions⁹⁹

hydrogen from a further equivalent of tributyltin hydride as outlined in **Scheme 42**.¹⁰⁰



Scheme 42: Mechanism of the Barton-McCombie deoxygenation reaction

As shown in **Scheme 41** it was possible to carry out this reaction in the presence of alkenes, which is perhaps surprising as alkenes are usually reactive under radical conditions, and these types of reaction are usually used in the synthesis of polymers such as polystyrene.¹⁰¹ Based on this, it was decided to attempt the Barton-M^cCombie conditions to deoxygenate alcohol **1.160**. Alcohol **1.160** was then converted to the xanthate ester (**1.179**) using sodium hydride, carbon disulfide and iodomethane as shown in **Scheme 43**. Xanthate **1.179** was then subjected to azobisisobutyronitrile (AIBN) initiated, tributyltin hydride (Bu₃SnH) mediated, deoxygenation conditions without further purification.



Scheme 43: Attempted Barton-M^cCombie deoxygenation of alcohol 1.160

Unfortunately, ¹H NMR analysis of the crude reaction mixture showed that no alkene peaks were visible, and upon work up and isolation of the products and analysis by ¹⁹F NMR, a complex mixture of fluorinated products was obtained (**Figure 21**). This could be due to the polymerisation of starting material **1.179** under radical conditions (**Scheme 44**).

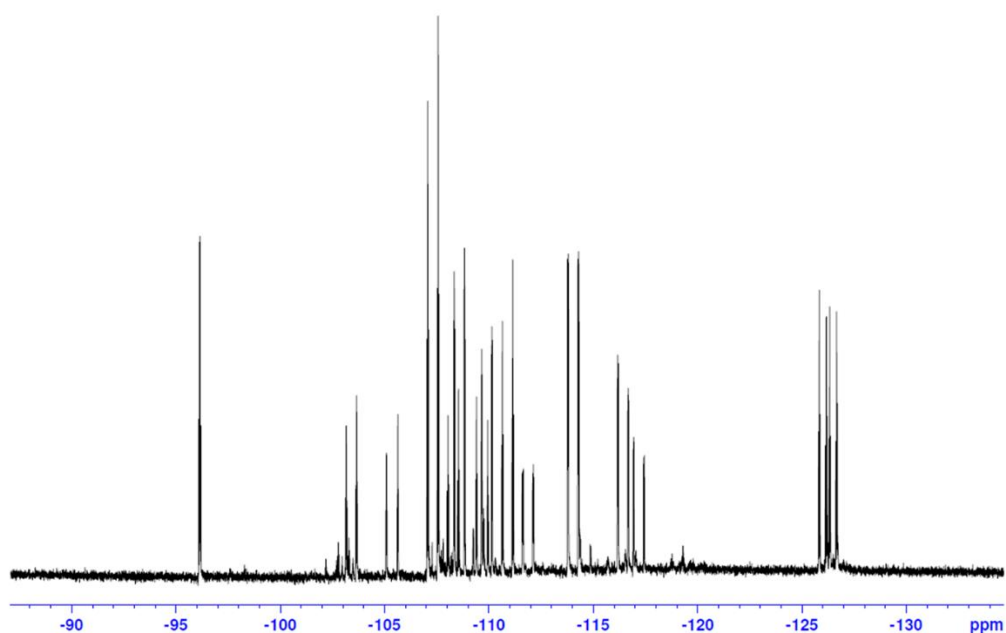


Figure 21: ^{19}F NMR of the Barton M $^{\text{c}}$ Combie reaction with **1.179** showing a complex mixture of fluorinated products

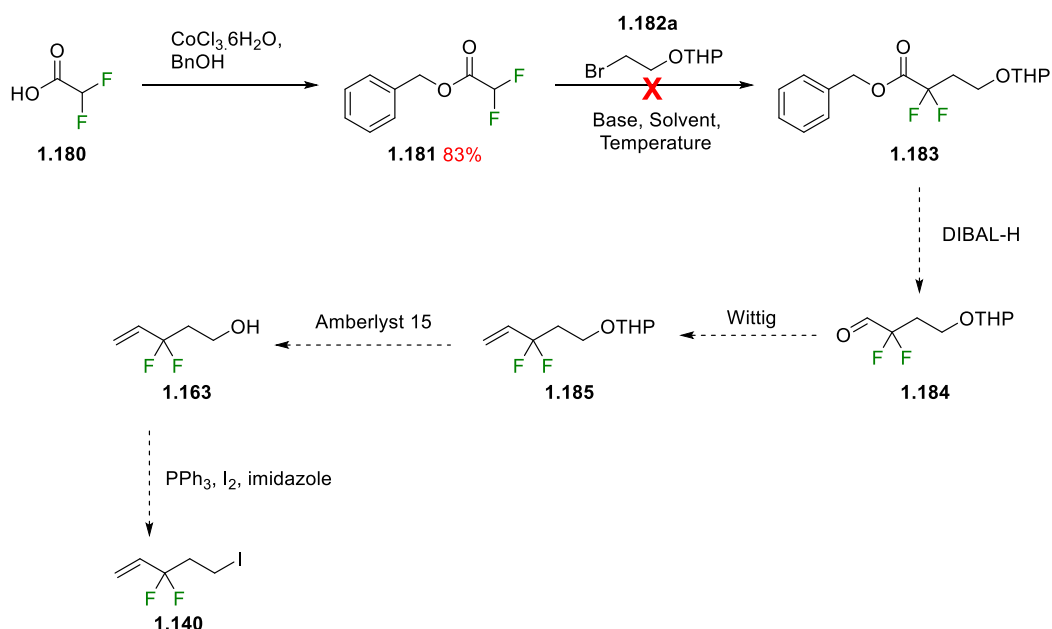


Scheme 44: Potential mechanism of radical polymerisation of **1.179**

Due to the difficulty in the deoxygenation of alcohol **1.160**, this route was determined to be unviable and was halted in favour of other approaches which are discussed in the subsequent sections.

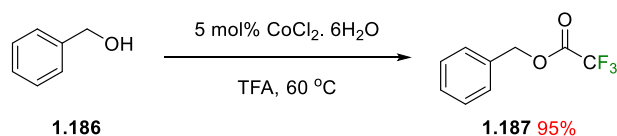
1.3.3.2 Generation 2

The next route evaluated was the alkylation of a benzyl ester, synthesised from difluoroacetic acid, by organohalide **1.182a**. This would be followed by a controlled reduction using diisobutylaluminium hydride (DIBAL-H) to generate the aldehyde required for a Wittig reaction to furnish alkene **1.185** which could undergo further functional group manipulation to give the desired alkene motif as outlined in **Scheme 45**.



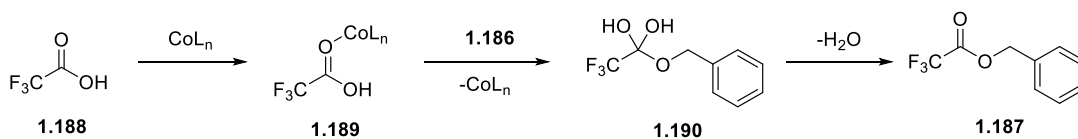
Scheme 45: Second generation route to intermediate 1.140

A benzyl ester functional group was chosen due to its high molecular weight and UV handle, allowing for easier purification. Initially a copper(I) catalysed coupling with benzyl alcohol using dicyclohexylcarbodiimide was attempted,¹⁰² however, the reaction failed. A new method was then sought and a literature search highlighted a cobalt catalysed esterification of trifluoroacetic acid as outlined in **Scheme 46**.¹⁰³



Scheme 46: Cobalt catalysed esterification of TFA¹⁰³

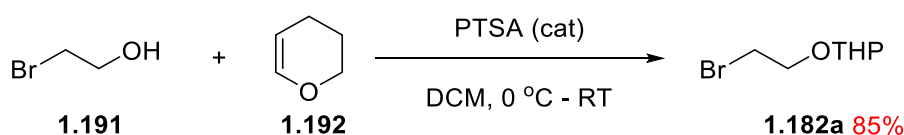
This reaction was attractive due to the high yields, fast reaction times and simple work-up, with both the excess acid and the cobalt catalyst being easily washed out of the crude reaction mixture. The reaction is believed to be promoted *via* Lewis acid catalysis as outlined below in **Scheme 47**.



Scheme 47: Reported mechanism of the cobalt catalysed esterification

As this process worked equally as well with acetic acid and TFA, it was reasoned that the same reaction conditions could be employed in the synthesis of ester **1.181**. Thus, the reaction conditions were repeated with difluoroacetic acid and the corresponding ester **1.181** was obtained in 83% yield.

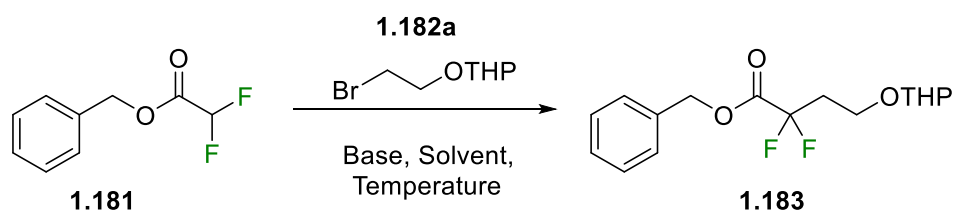
The electrophile of the reaction (**1.182a**) was also synthesised from 2-bromoethanol as outlined below in **Scheme 48**.¹⁰⁴ Here the tetrahydropyran (THP) protecting group was chosen due to its inertness to the basic conditions employed during the alkylation. Pleasingly, the reaction proceeded smoothly, with an 85% yield of **1.182a** isolated after purification.



Scheme 48: Conditions employed in the THP protection of **1.191**¹⁰⁴

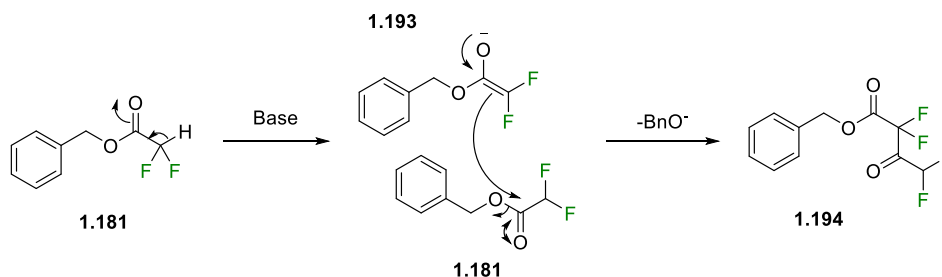
With a reasonable quantity of the ester and alkyl halide in hand, a range of alkylation conditions were screened as outlined in **Table 1**.

Table 1: Attempted alkylation conditions



Entry	Base	Solvent	Temperature (°C)	% Yield 1.183
1	LDA	THF	-78 - RT	0
2	K ₂ CO ₃	acetone	Reflux	0
3	NaOMe	MeOH	0 - RT	0
4	KO ^t Bu	THF	RT	0
5	NEt ₃	THF	RT	0
6	DBU	THF	RT	0
7	NaH	THF	0 - RT	0

Unfortunately, formation of **1.183** was not observed in any case. This could be due to the enolate self-condensing (**Scheme 49**) before the electrophile is added and a spot corresponding to benzyl alcohol was observed by TLC which strongly indicated that this was the case. When lithium diisopropyl amine (LDA) was used as a base (**Table 1**, entry **1**) the ^{19}F NMR of the crude reaction mixture showed that there was a complex mixture of fluorinated products (**Figure 22**).



Scheme 49: Proposed mechanism for self-condensation of compound **1.181** with LDA

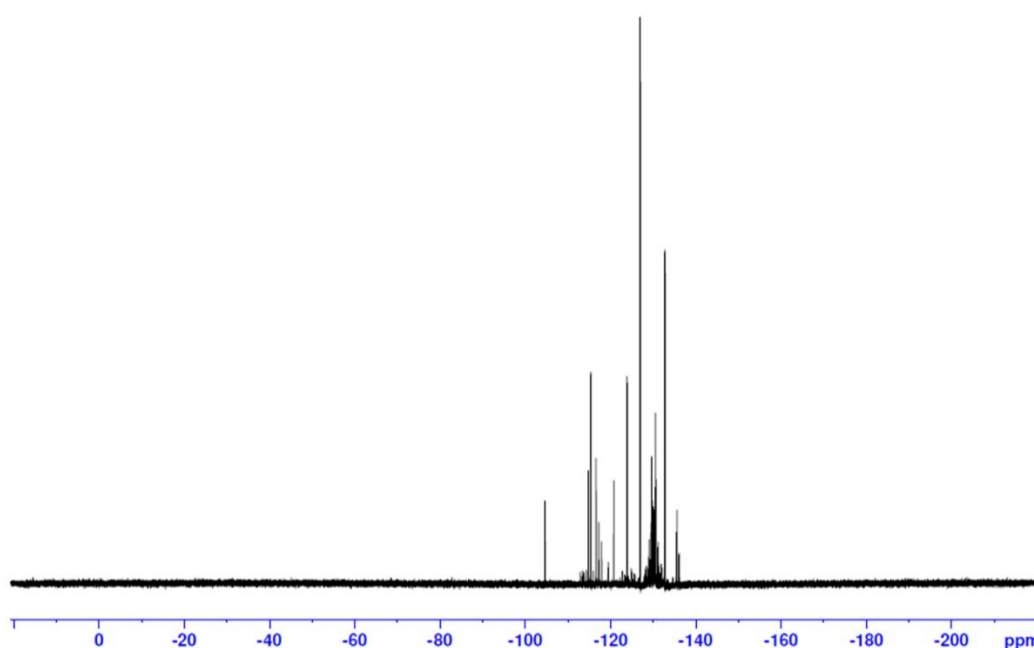


Figure 22: ^{19}F NMR of the crude reaction mixture used to prepare **1.155**

In an effort to lower the reactivity of the enolate, the Weinreb amide was considered. Here the cation of the enolate would be expected to coordinate to the oxygen atom of the Weinreb amide as outlined below in **Figure 23**. This would potentially stabilise the enolate and tune the reactivity towards the electrophile.

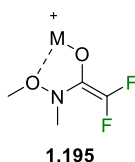
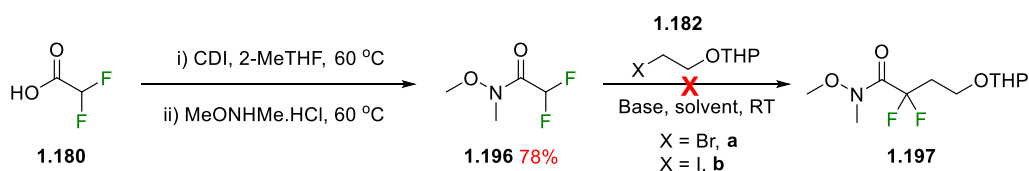


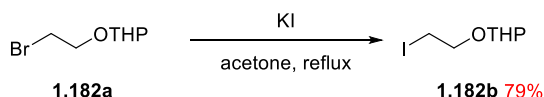
Figure 23: Stabilised enolate of Weinreb amide 1.196

Accordingly, Weinreb amide **1.195** was synthesised in good yield from difluoroacetic acid and *N,O*-hydroxylamine hydrochloride using carbonyldiimidazole (CDI) as a coupling agent (**Scheme 50**).



Scheme 50: Modified second generation route to 1.140

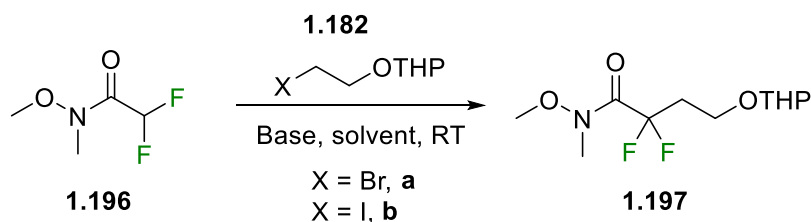
Iodo **1.182b** was also examined as a nucleophile as the iodide should be a better leaving group than the bromide and may help improve the reactivity towards the modified enolate. Thus, **1.182b** was synthesised from bromide **1.182a** using a Finkelstein reaction as outlined in **Scheme 51**. Pleasingly, this reaction also ran smoothly with an isolated yield of 79%.



Scheme 51: Finkelstein conditions employed in the synthesis of 1.182b

With all of the requisite starting materials in hand, a range of alkylation conditions were attempted using either THP protected bromoethanol or THP protected iodoethanol as outlined in **Table 2**.

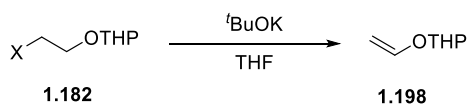
Table 2: Attempted alkylation conditions for Weinreb amide



Entry	X	Base	Solvent	% Yield 1.197
-------	---	------	---------	---------------

1	Br	NaOMe	MeOH	0
2	Br	DBU	THF	0
3	Br	NEt ₃	THF	0
4	Br	KO ^t Bu	THF	0
5	I	DBU	THF	0
6	I	NEt ₃	THF	0
7	I	KO ^t Bu	THF	0

The bases used in this study were those which gave the least evidence of self-condensation in the ester studies. As with the conditions screened in **Table 1**, no conversion to **1.197** was observed and instead polymerisation of **1.196** was believed to have taken place due to the observation of a spot in TLC which had the same R_f as benzyl alcohol. In the cases with potassium *tert*-butoxide (**Table 2**, entries **4** and **7**) an E2 elimination (**Scheme 52**) of the alkylhalide was observed as an alkene species was evident in a ¹H NMR of the crude reaction mixture (**Figure 24**).



Scheme 52: Potential E2 elimination of 1.182

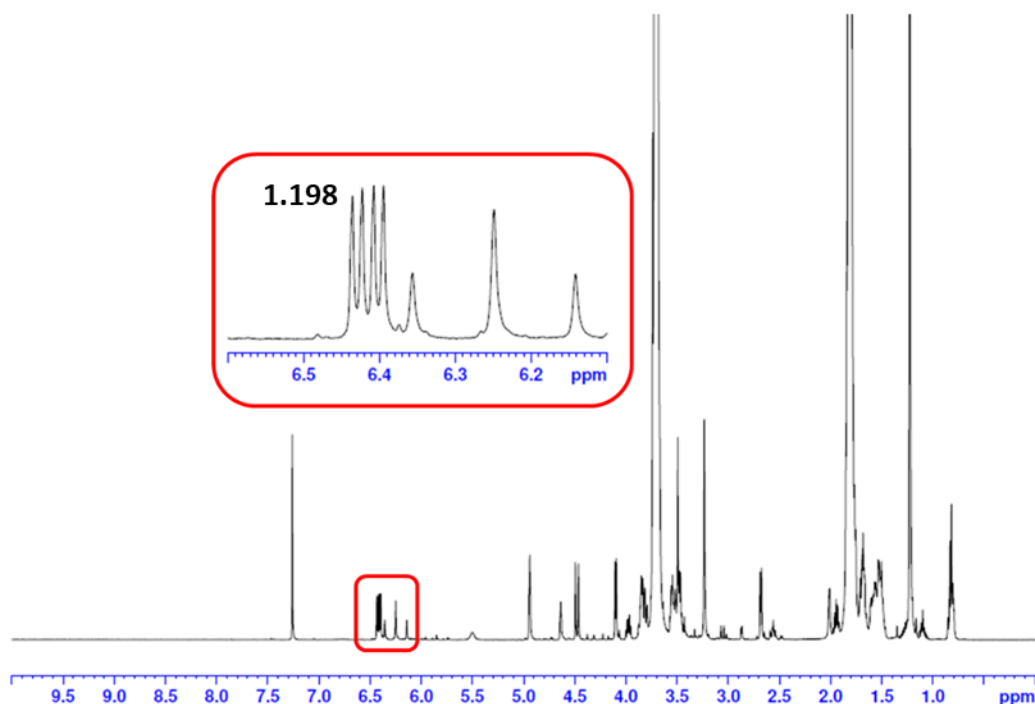
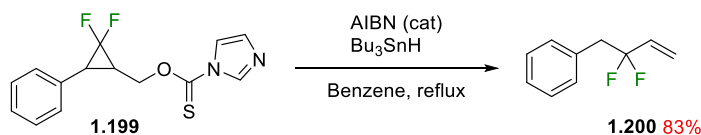


Figure 24: ^1H NMR of the crude reaction mixture, highlighting alkene species 1.198 (dd) and the presence of a CF_2H unit (t)

Since no alkylation was observed in either of the approaches examined, this method of synthesising **1.140** was quickly halted and alternative approaches evaluated.

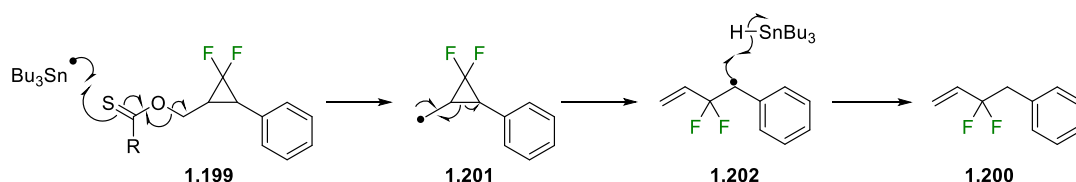
1.3.3.3 Generation 3

Through a literature search it was established that a radical induced deoxygenation of a *gem*-difluorocyclopropane was capable of opening the 3-membered ring and forming the corresponding alkene as outlined in **Scheme 53**.¹⁰⁵



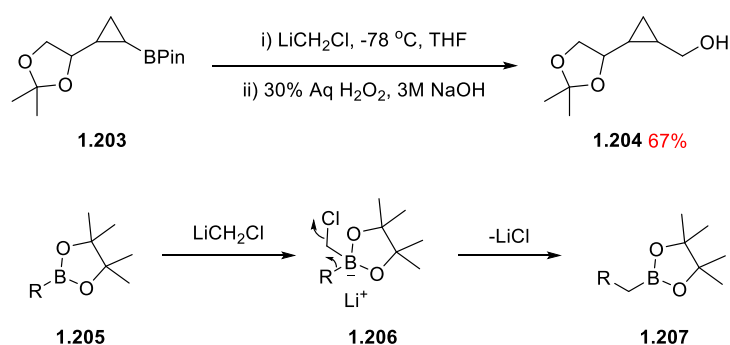
Scheme 53: An example deoxygenation and tandem ring opening reaction

The reaction is thought to form an unstable primary radical, which can then open the distal carbon-carbon bond to form a more stable secondary radical and induce homolytic cleavage of an equivalent of tributyltin hydride. This is shown below in **Scheme 54**.



Scheme 54: Proposed mechanism for the reaction shown in Scheme 21

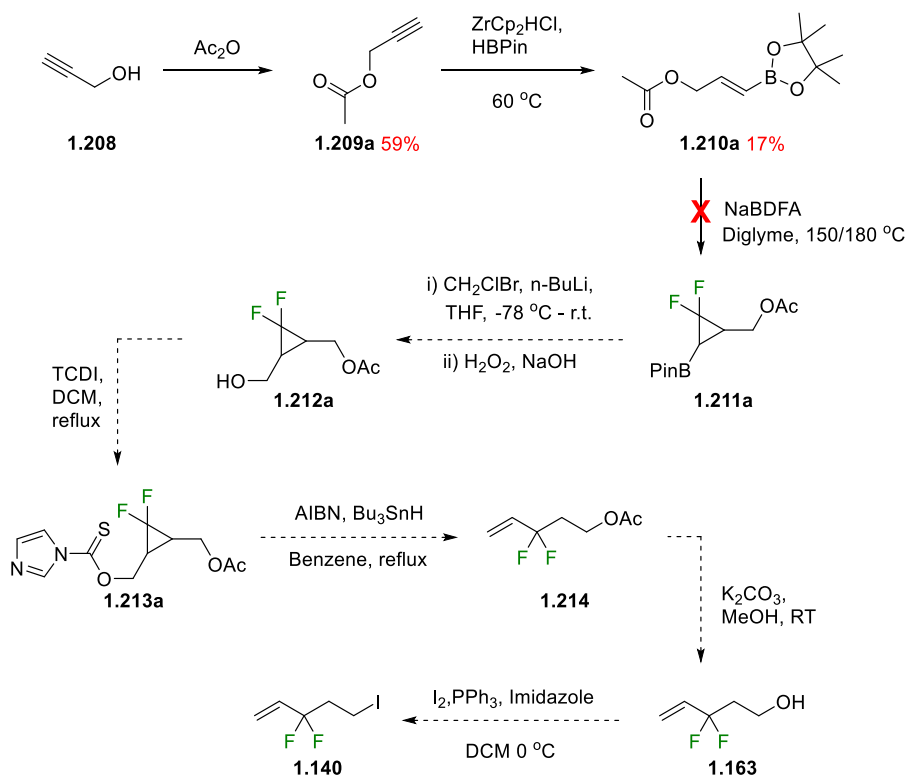
The first route evaluated for the synthesis of key building block **1.140** was based on this established procedure and is outlined below in **Scheme 56**. Due to previous experience in difluorocyclopropanation of vinyl pinacol boronate ester systems, these were chosen as the initial substrate, and we planned to employ a Matteson homologation and oxidation to install the necessary hydroxyl group as outlined in **Scheme 55**.¹⁰⁶ This reaction has previously been examined using cyclopropane **1.203** as outlined below in **Scheme 55**. The reaction proceeded in yields of 67% over two steps and the similarities in structure to difluorocyclopropane **1.211** suggested that the reaction conditions should be transferable to the difluorocyclopropane system. The mechanism of the key rearrangement step is also shown in **Scheme 55**. After forming the boronate with the lithiated species, there is a migration of the alkyl group onto the chloromethylene group with the expulsion of chloride to furnish homologated pinacol boronate ester **1.207**, which can then be oxidised using basic hydrogen peroxide.



Scheme 55: Reaction conditions for the tandem Matteson homologation and oxidation of a cyclopropyl pinacolboronate ester (top) and the mechanism of the key rearrangement (bottom)¹⁰⁶¹⁰⁷

Returning to the current study, propargyl alcohol was protected as the acetate derivative, where it was then hydroborated using catalytic Schwartz reagent and pinacol borane.¹⁰⁸ Unfortunately, vinyl BPin derivative **1.210a** was not stable on silica, making purification difficult and negatively impacting the isolated yield of

1.210a. Nevertheless, a sufficient quantity was isolated to attempt the difluorocyclopropanation. For this, sodium bromodifluoroacetate (NaBDFA) was chosen as the difluorocarbene source as it is slightly more reactive than NaCDFA.⁹¹ However, NaBDFA is more expensive than NaCDFA, and a batch was synthesised, following a literature procedure,¹⁰⁹ using 3-bromo-3,3-difluoroacetic acid and sodium hydroxide.



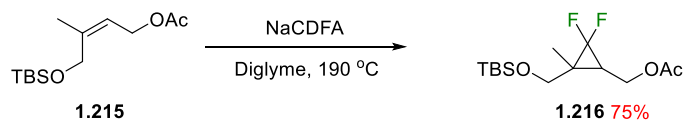
Scheme 56: Third generation route to intermediate 1.140

Unfortunately, vinyl BPin derivative **1.210a** failed to form **1.211a** and appeared to decompose under the reaction conditions as it was no longer visible in the ^1H NMR spectrum after 1 hour.

Exchanging the protecting group from acetate to a *tert*-butyldimethylsilyl (TBS) ether (**1.210b**), did not help improve the stability of the vinyl BPin to silica and unfortunately, the difluorocyclopropanation conditions using the cheaper, commercially available NaCDFA also failed.

Therefore, an alternative starting material was required. A further literature search revealed that a similar substrate to the alkene starting material of interest to the

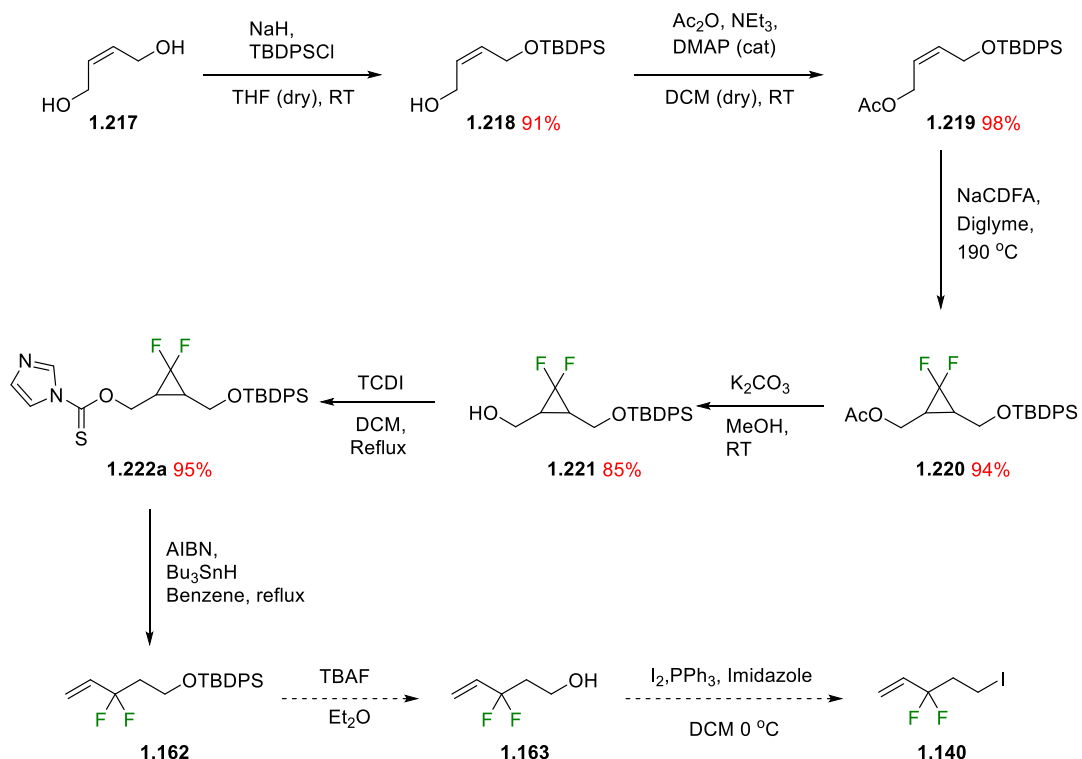
current study (**1.215**) had been synthesised previously as shown below in **Scheme 57**.¹¹⁰



Scheme 57: Difluorocyclopropanation conditions from the literature reaction¹¹⁰

In this report, a vast excess of NaCDFA (11 equivalents) was required for the reaction to proceed, as well as the requirement for a controlled dropwise addition over the course of one hour, with an additional 15 minutes heating after the addition was complete.

With a potential alternative difluorocyclopropanation procedure identified, the original third generation route (**Scheme 56**) was modified as shown below in **Scheme 58**.



Scheme 58: Modified third generation route to intermediate 1.140

The first two steps of the reaction involved the protection of *cis*-butene-1,4-diol (**1.217**) with TBDPS and acetate, respectively. Again, TBDPS was chosen for its high molecular weight, stability and UV chromophore which was anticipated to make

purification easier. Acetate was chosen as the second protecting group as it was facile to remove using mild conditions at a later point in the synthesis, and it is reported to be stable in the presence of difluorocarbene.⁹² With multi-gram quantities of the requisite alkene in hand, the next step was the difluorocyclopropanation. A repeat of the literature conditions described above led to a 2:1 ratio of difluorocyclopropane **1.220** to alkene **1.219** as determined by ¹H NMR (Figure 25).

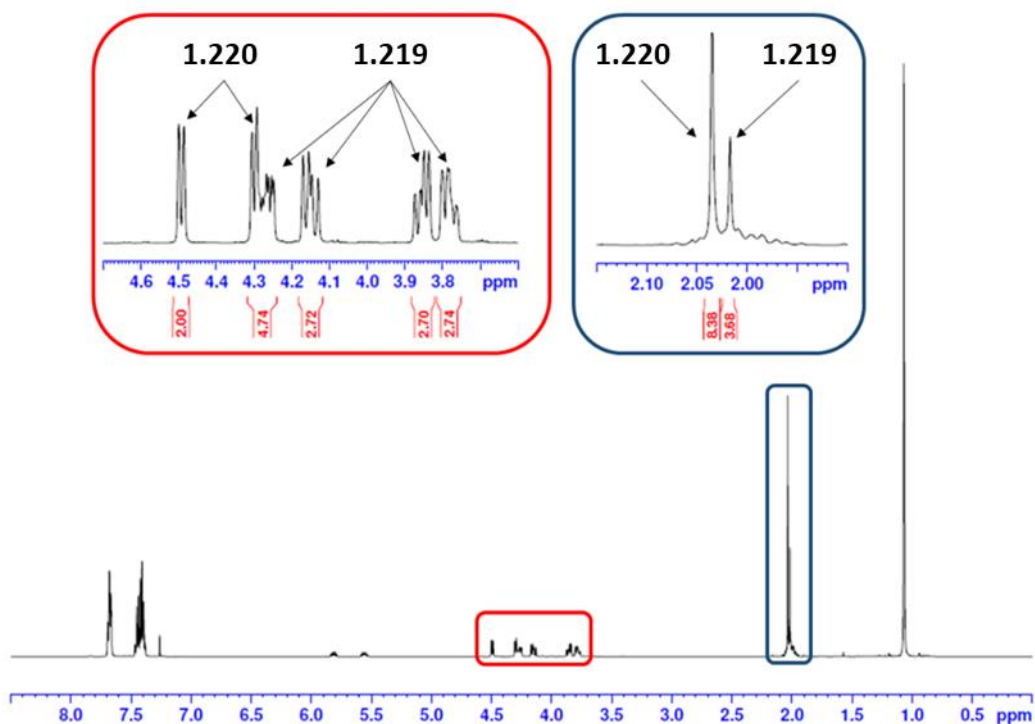


Figure 25: ¹H NMR of crude reaction mixture showing a 2:1 mixture of **1.220** to **1.219**

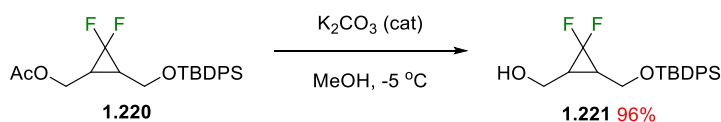
Unfortunately, **1.219** and **1.220** were inseparable by TLC and silica chromatography. Encouraged by this result, the reaction was optimised by increasing the addition time to 2 hours with an additional 1.5 hours of heating after the addition was complete. Pleasingly, these conditions proved to be successful with full conversion of **1.219** to **1.220** being achieved. This also led to a visual indication of complete conversion *via* TLC. Despite both compounds having the same *R_f*, alkene **1.219** stains blue in vanillin while difluorocyclopropane **1.220** does not stain in vanillin.

The poor solubility of NaCDFA in diglyme led to difficulties on the scale up of the reaction. Large volumes of the NaCDFA solution were required to be added dropwise using a syringe pump. This led to an initial limit of 3 mmol of reactant **1.219**. The use

of standard gauge needles coupled with poor solubility also led to frequent needle blockages due the precipitation of NaCDFA at the needle tip. While these were disadvantages, difluorocyclopropane **1.219** was stable in solution and it was possible to run numerous smaller batches for a collective work up procedure. Subsequently, employing a peristaltic pump and a wide bore needle, it was possible to scale up the reaction to in excess of 25 mmol, with fewer needle blockages and still maintaining the complete conversion of **1.219** to **1.220**, provided the NaCDFA reservoir was maintained under a positive nitrogen atmosphere.

Further difficulties also lay with the hygroscopic nature of NaCDFA, with older bottles of reagent having absorbed enough water to completely stop the reaction with alkene **1.219**. Thus, careful drying of NaCDFA at 50 °C under high vacuum was employed to remove water and residual 2-chloro-2,2-difluoroacetic acid before subjecting it to the difluorocyclopropanation conditions.

The acetate deprotection was carried out using potassium carbonate in a 3:1 methanol and water mix at room temperature. While this procedure worked well on smaller scales with 85% isolated yield, on larger scales the highly basic conditions resulted in the removal of the TBDPS protecting group. Initially, it was thought that this was happening upon removing the methanol after the reaction was neutralised with 2M HCl (aq) as TBDPS protected methanol was isolated during purification. However, upon inverting both steps of the work-up procedure, the isolated yield of the product was still low and the silanol by-product was isolated. In order to overcome this issue, the reaction conditions were changed to those outlined in **Scheme 59**.



Scheme 59: Alternative acetate deprotection conditions used for large scale reactions

In these conditions the stoichiometry of potassium carbonate was reduced from 1.5 equivalents to 0.5 equivalents and the reaction temperature was cooled to -5 °C. The reaction progress was monitored by TLC and found to be complete after 30 minutes.

The work-up procedure was also altered and the 2M HCl was exchanged for saturated ammonium chloride solution. Pleasingly, this resulted in trace amounts of unwanted by-products and **1.221** was isolated in 96% yield.

Following the procedure for the deoxygenation outlined above in **Scheme 58**, the thiocarbonylimidazolidine derivative **1.222a** was chosen as a direct comparison with the literature.¹⁰⁵ It was synthesised simply by refluxing **1.221** with an excess of thiocarbonyldiimidazole (TCDI) in DCM until the reaction was complete with analysis by TLC. The reaction proceeded smoothly with a 95% yield being obtained. However, **1.222a** was not bench stable and quickly changed from a pale-yellow gum to a dark brown gum when standing at room temperature and, to allow it to be used for multiple reactions, it was necessary to store it in a foil covered flask, in the freezer and under an atmosphere of argon. The initial Barton-M^cCombie conditions from the literature procedure¹⁰⁵ (**Table 3**, entry **1**) resulted in only a trace of desired product **1.162** which was visible in both ¹H NMR and ¹⁹F NMR (**Figure 26**). While this result was disappointing it did provide the proof of concept required and the reaction was then optimised by screening alternative conditions.

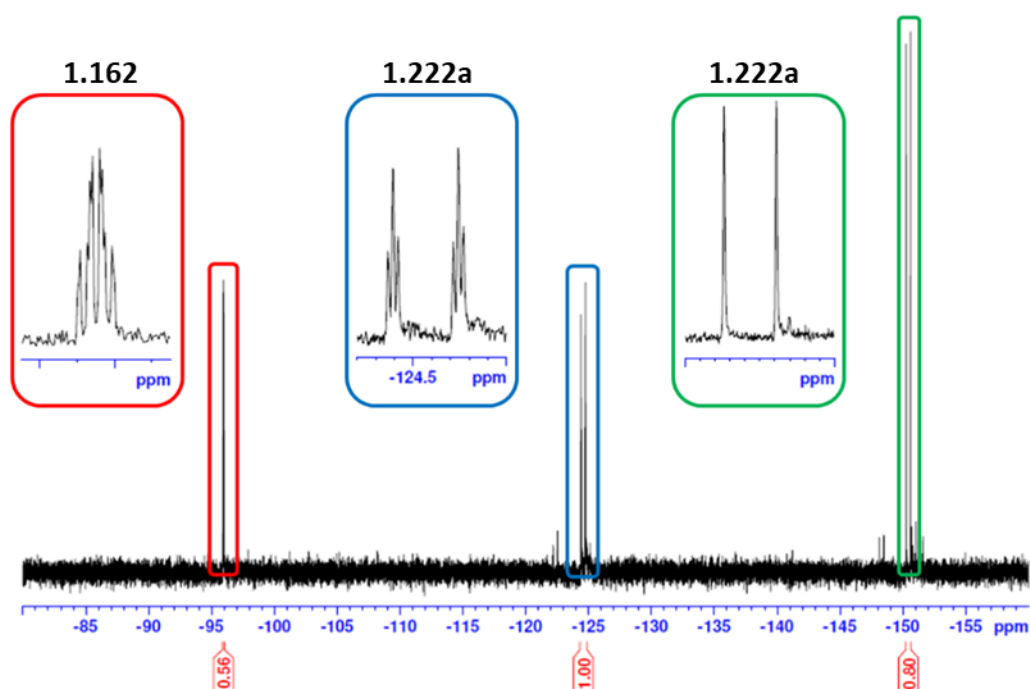
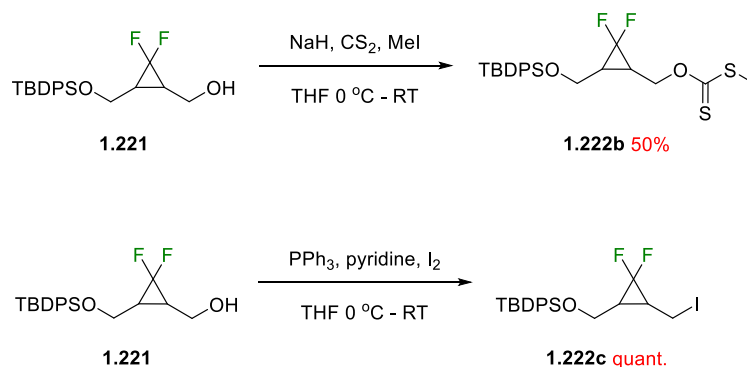


Figure 26: ¹⁹F NMR of crude reaction mixture for the deoxygenation and ring-opening of **1.222a**

As well as the original thiocarbonylimidazolidine (**1.222a**), xanthate **1.222b** and iodo **1.222c** were also synthesised as shown below in **Scheme 60**. The xanthate derivative **1.222b** was found to be bench stable, however, it did require extensive purification to obtain sufficiently pure material for the next step of the reaction. Iodo **1.222c** was also found to be bench stable, and the modified Appel reaction proceeded smoothly in excellent yield as shown in **Scheme 60**.

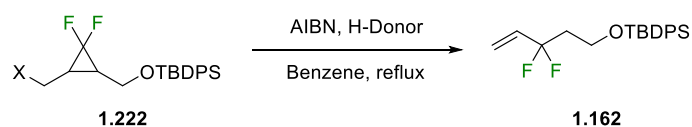


Scheme 60: Synthesis of alternative substrates for radical induced ring-opening

While changing the substrate was one approach to optimising the reaction, another method was to alter the hydrogen donor. Originally tributyltin hydride was used, however, there has also been some literature precedence with tris(trimethylsilyl)silane ((TMS)₃SiH).^{111–114} (TMS)₃SiH is a much safer alternative to the highly toxic tributyltin hydride traditionally used in the Barton-M^cCombie reaction.¹¹⁵ The bond dissociation energy of the Si-H bond of (TMS)₃SiH is approximately equal to that of the Sn-H bond of Bu₃SnH, making it an ideal modification.¹¹⁵ Furthermore, the bond dissociation energy of the Si-S bond (617 kJ/mol) is higher than that of the Sn-S bond (467 kJ/mol) which provides a stronger driving force for the reaction.¹¹⁶

Thus, a range of conditions were screened as in **Table 3** whilst keeping the solvent, concentration and temperature consistent.

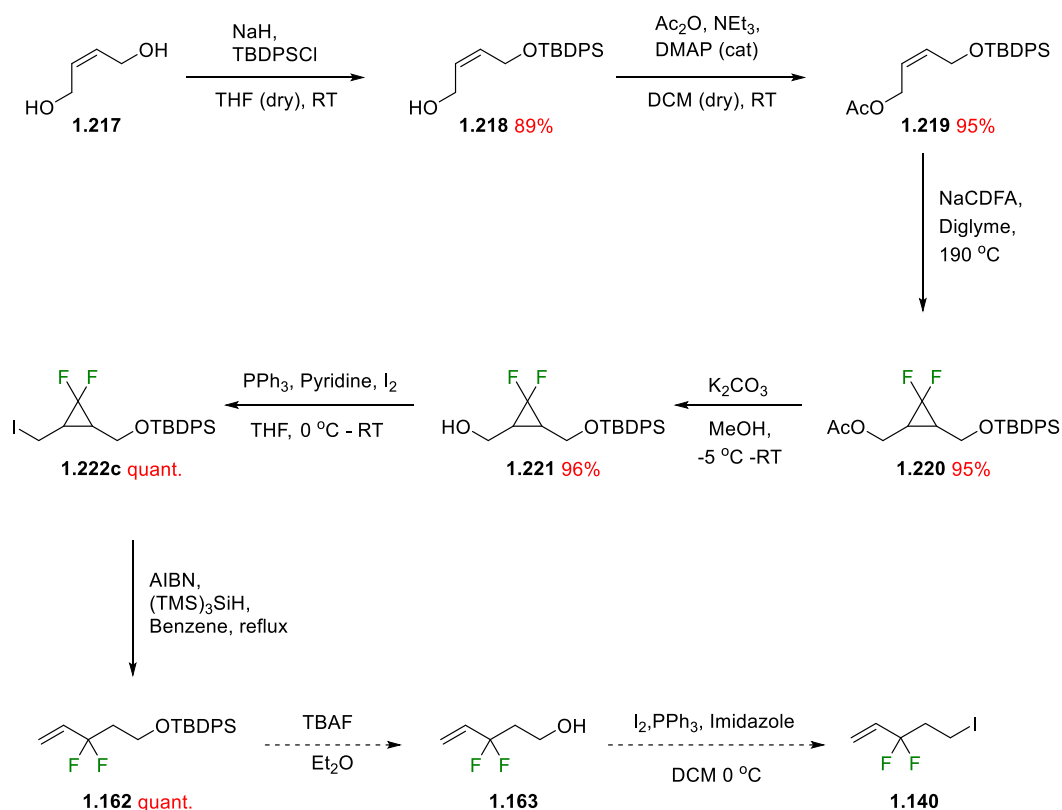
Table 3: Conditions screened for radical induced ring-opening



Entry	X	H-Donor	1.222:1.162 ^a
1	OC(S)Im	Bu ₃ SnH	5:1
2	OC(S)Im	(TMS) ₃ SiH	2:5
3	OC(S)SMe	Bu ₃ SnH	5:3
4	OC(S)SMe	(TMS) ₃ SiH	2:3
5	I	Bu ₃ SnH	2:3
6	I	(TMS) ₃ SiH	0:100

a – determined by ¹⁹F NMR

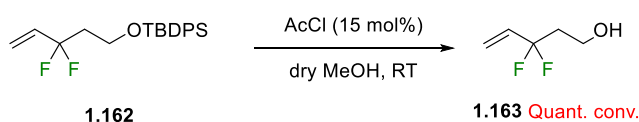
The conditions examined showed that (TMS)₃SiH was superior to tributyltin hydride in all cases and therefore, it was decided to switch to this reagent as the hydrogen donor. This also improved the safety of the reaction significantly as highly toxic organotin reagents do not have to be used. In terms of the substrate, the iodo-derivative **1.222c** performed the best, giving complete consumption of starting material. Based on all the modifications shown above, the route shown in **Scheme 61** was implemented.



Scheme 61: Revised third generation route to compound **1.140**

Due to the nature of the silyl by-products generated, it was difficult to obtain a pure sample of the TBDPS protected alcohol **1.162** on the scale the reaction was initially carried out on. Thus, the conditions from entry **6** in **Table 3** were scaled up in an effort to make isolation more facile. Unfortunately, this was not the case and **1.162** was still contaminated by a minor by-product which could be minimised using carefully controlled flash column chromatography utilising a petroleum ether and dichloromethane eluent system. Despite these difficulties, the yields of **1.162** remained very good with yields generally being greater than 95%.

The next step in the reaction involved the removal of the TBDPS group. Initially it was thought that solid supported tetrabutylammonium fluoride (TBAF) could be used in order to aid with isolation, as alcohol **1.163** was likely to be volatile as well as being potentially miscible with the aqueous solutions employed during work-up. Unfortunately, this approach was unsuccessful and TLC analysis after 16 hours showed no reaction had occurred. Alternative conditions were therefore examined utilising catalytic quantities of HCl in methanol (**Scheme 62**).¹¹⁷



Scheme 62: Conditions utilised in the acidic TBDPS deprotection

Pleasingly these conditions resulted in the full conversion of **1.162**. However, attempts to isolate the free alcohol were unsuccessful, mainly due to the volatility and thermal instability of **1.163**. Attempts to isolate the free alcohol using flash column chromatography with 40-60 °C petroleum ether and diethyl ether resulted in the loss of **1.163** during solvent removal and efforts to use Kugelrohr distillation at atmospheric pressure resulted in the degradation of **1.163** as shown in **Figure 27**. As this distillation was carried out in the presence of air it is likely that the alcohol was oxidising to the acid.

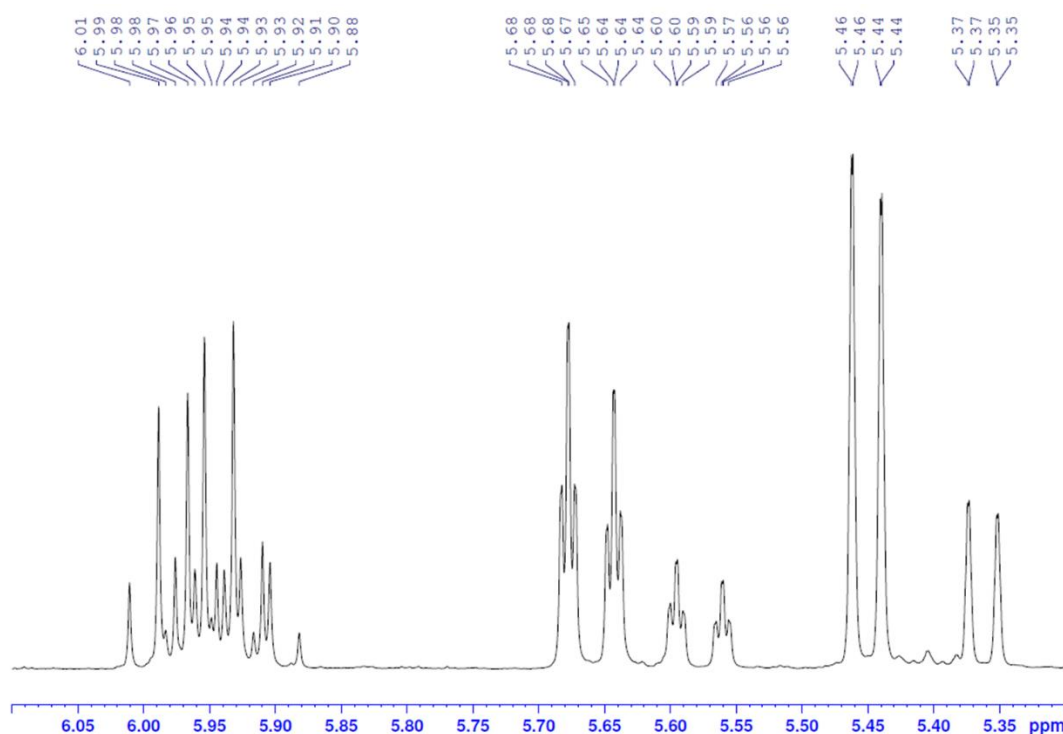
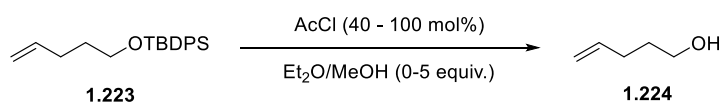


Figure 27: ^1H NMR spectrum of the alkene region of **1.163** after attempted Kugelrohr distillation. Two sets of alkene peaks are now visible, indicating the product was degrading under thermal conditions

At this stage the concept of converting the crude alcohol directly to the tosylate was assessed as the increased mass of the tosylate group would likely result in a less volatile product, thus being more facile to isolate than the free alcohol. However, to prevent the preferential formation of methyl tosylate, the amount of methanol employed in the first step of the reaction must be minimised, or more ideally, removed before commencing the tosylation step. Due to the lengthy synthesis of **1.162**, it was then decided to examine a model substrate based on pentenol as outlined below in **Scheme 63** to attempt to optimise the deprotection step.



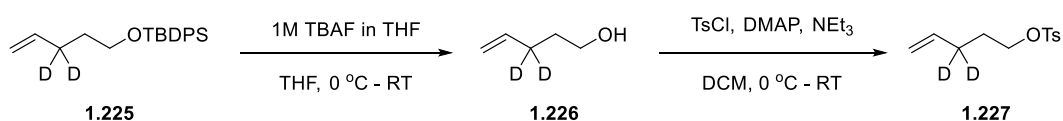
Scheme 63: general conditions employed in the model substrate to optimise the TBDPS deprotection

Changes to the concentration of methanol and quantities of acid were analysed and the conversion monitored by TLC.

Unfortunately, none of the conditions screened resulted in the full conversion of **1.223** to pentenol by TLC. Changing the concentration of acid did not seem to affect

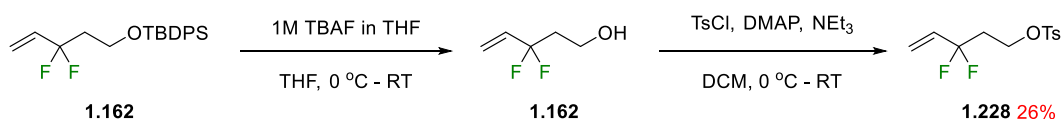
the reaction pathway with similarly low levels of conversion seen with 40 mol% and 100 mol%. There was, however, a correlation observed with the concentration of methanol, with more pentenol forming with higher concentrations of methanol. Since removing the quantity of methanol employed in the reaction did not appear to be feasible, an attempt to distil the methanol from the original reaction conditions was made. Unfortunately, it was difficult to remove all the methanol and the only product observed after employing tosylation conditions was methyl tosylate.

With the above route unsuccessful, conditions using TBAF to remove the TBDPS group were next employed. A procedure was identified from the examination of the literature which allowed for the direct conversion to di-deuteriotosylate **1.227** without isolating the intermediate alcohol as outlined in **Scheme 64** below.¹¹⁸



Scheme 64: TBDPS deprotection and tosylation conditions from literature. Tosylate **1.227** was not isolated in this study and was used as crude in a further modification

In this study, the tosyl derivative was not isolated and was used as crude in a further modification. Nevertheless, it proved that it was possible to isolate a structurally related substrate which was likely to have the same issues with volatility and aqueous solubility as the fluorinated compounds of interest in the current study. Thus, the reaction conditions were replicated using TBDPS protected alcohol **1.162** as outlined in **Scheme 65**.

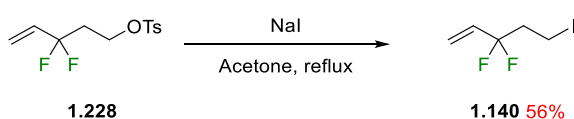


Scheme 65: TBDPS deprotection conditions using TBAF

Unfortunately, in our hands, these conditions resulted in the reaction not reaching completion, with the addition of further portions of tosyl chloride and triethylamine resulting in no further conversion of alcohol **1.162** to tosyl **1.228**. This resulted in an overall yield of 26% over both steps for the tosylate.

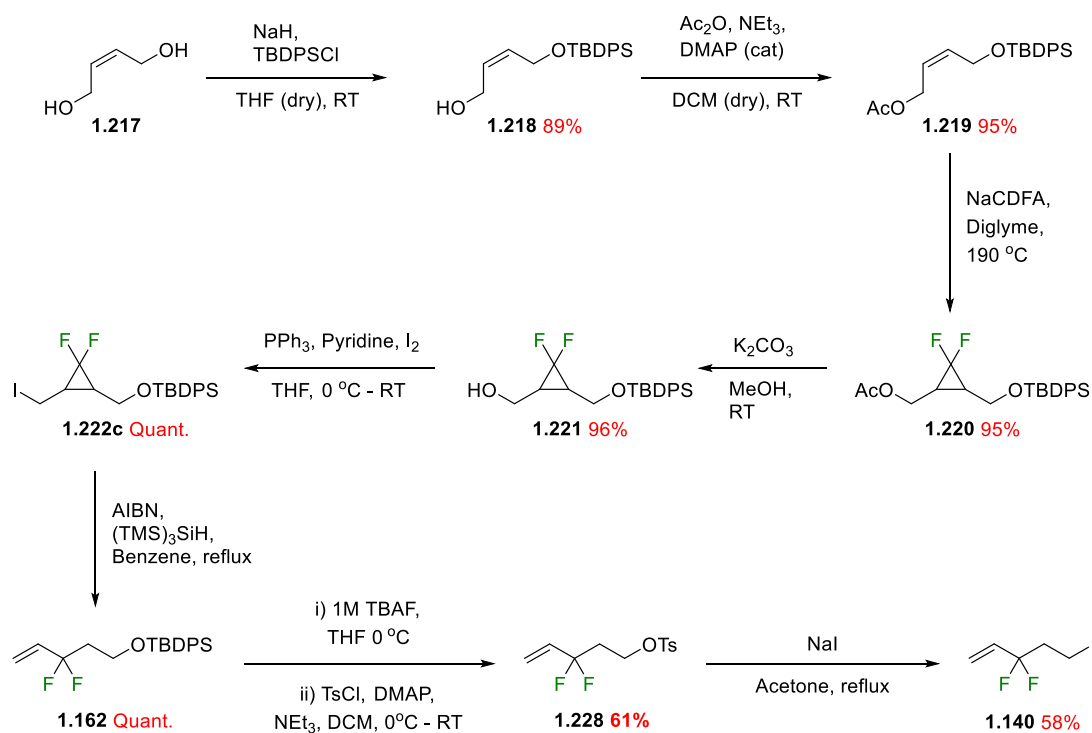
Based on this, it was then decided that isolation of intermediate alcohol **1.163** would facilitate the reaction as using clean pentenol as a model substrate resulted in quantitative yields of the corresponding tosylate. Flash column chromatography utilising pentane and diethyl ether (the most volatile solvent system available in our laboratory) yielded alcohol **1.163** which was concentrated to partial dryness to minimise loss to the rotary evaporator. This was then subjected to the tosylation conditions outlined above. Pleasingly, there was full conversion of alcohol **1.163** to tosylate **1.228** which was isolated in 42% yield over the two steps. The initial deprotection was thought to be the limiting step due to the inherent volatility of the alcohol. The reaction was initially conducted at room temperature overnight, and these conditions were thought to be a potential cause of loss of the alcohol. In an effort to improve the yield, the reaction was monitored by TLC and was found to be complete within an hour. Subsequent isolation of the alcohol gave a 61% yield of alcohol **1.163** (determined by ^1H NMR) as a 30% w/w solution in diethyl ether and pentane with this being converted in quantitative yields to the corresponding tosylate.

Having enabled a robust route to the target tosylate **1.228**, the final step was a Finkelstein reaction as shown below in **Scheme 66**.



Scheme 66: Finkelstein reaction conditions employed in the synthesis of **1.140**

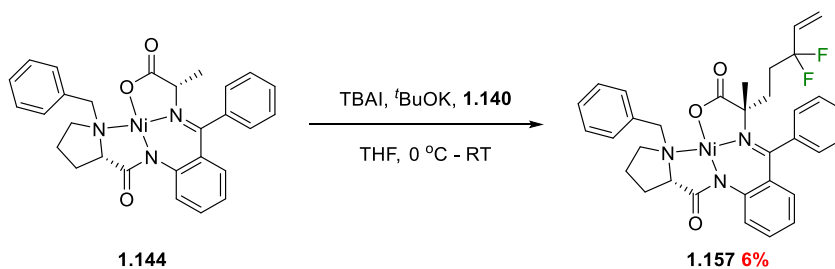
Pleasingly, this reaction proceeded smoothly with full conversion obtained. However, again due to the volatility of resulting iodo **1.140**, the yields obtained were comparatively low at 56%. Nevertheless, sufficient material was obtained to attempt to alkylate the Ni(II)-Ala-BPB complex on route to the target amino acid. The final overall route that was enabled to deliver the target fluorinated building block is shown below in **Scheme 67**.



Scheme 67: Final modified third-generation route to intermediate 1.140

1.3.4 Alkylation of nickel complex 1.144 with 1.140 and isolation of Fmoc amino acid 1.139

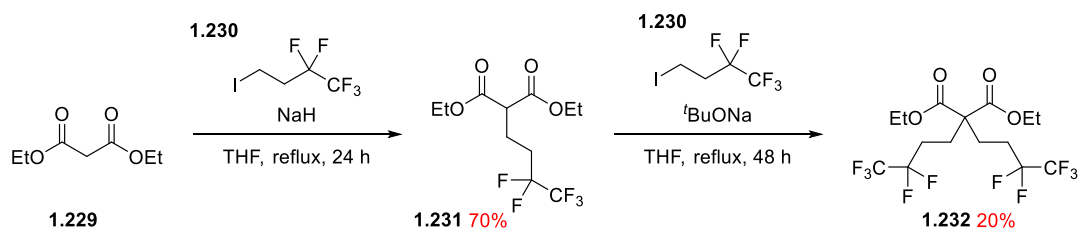
Using the conditions previously developed in our laboratory from the synthesis of Ni(II)-S₅-BPB as shown below in **Scheme 68**, only a 6 % yield of alkylated product **1.141** was isolated.



Scheme 68: Standard conditions used to alkylate 1.144

While disappointing that the yields did not compare favourably with those of the non-fluorinated substrate, it provided the proof of concept that the reaction could proceed, and that further optimisation would be necessary.

Unfortunately, as iodo **1.140** is a novel compound there are no direct literature comparisons for this reaction. However, alkylations with polyfluoroiodo alkanes with malonate are known and are outlined below in **Scheme 69**.¹¹⁹

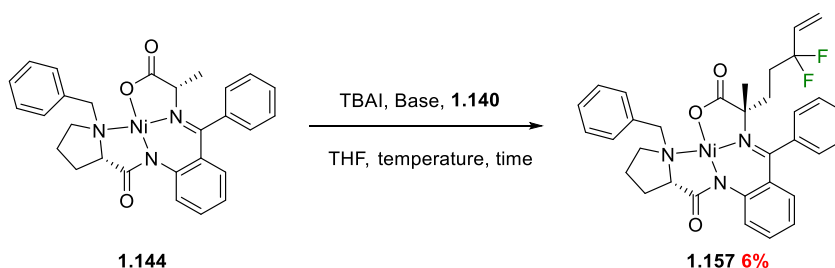


Scheme 69: polyfluoroalkylation of malonate¹¹⁹

In this set of reactions, the second alkylation most resembles the auxiliary alkylation conditions described above as this reaction also forms a quaternary carbon centre. The harsh conditions, protracted reaction times and poor yields suggest that this second alkylation is difficult. This, and the observation of poor yields for the synthesis of the alkylated auxiliary suggest that the alkylation of Ni-Ala-BPB **1.144** is also likely to be equally challenging.

Fortunately, sufficient quantities of iodo **1.140** were isolated to carry out a focused array of reaction conditions as outlined below in **Table 4**.

Table 4: Optimisation conditions utilised in the attempted alkylation of 1.144 with 1.140



Entry	Reaction Time (hr)	Concentration (M)	Temperature (°C)	Base (equiv.)	Average Conversion ^a (%)
1	72	0.1	0-RT	KO ^t Bu (2.5)	5.8 ± 0.4
2	24	0.1	0-40	KO ^t Bu (2.5)	16.9 ± 0.5

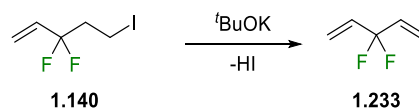
3	24	1	0-RT	KO ^t Bu (2.5)	3.3 ± 0.3
4	24	0.1	0-RT	KO ^t Bu (1.1)	21.5 ± 0.4
5	24	0.1	0-RT	NaHMDS (2.5)	0.9 ± 0.05
6	24	0.1	0-RT	DBU (2.5)	0
7	24	0.1	0-RT	BEMP (2.5)	0

^a Conversion measured in triplicate by HPLC using caffeine as an internal standard

The reactions were monitored in triplicate by HPLC using caffeine as an internal standard.

As the standard conditions showed poor conversion, and small amounts of **1.140** were isolated during flash column chromatography, it was reasoned that the reaction could be slower than that with the non-fluorinated derivative (**1.145**). Thus, the first attempt at exploring alternative reaction conditions increased the time of the reaction threefold. Unfortunately, there was no difference between the conversion, with an average of 5.8% conversion across three samples (**Table 4**, entry **1**). The second set of conditions examined increasing the reaction temperature (**Table 5**, entry **2**). In this case, the base was added at 0 °C and allowed to return to room temperature. Upon reaching this temperature, it was then heated to 40 °C overnight. Pleasingly, this resulted in an increase in the average conversion to 16.9%. However, this method is likely to epimerise the proline centre of **1.144** but unfortunately there was not sufficient material available to synthesise the opposite enantiomer in order to determine the enantiomeric excess by chiral HPLC. The next attempt at optimisation focused on increasing the reaction concentration (**Table 4**, entry **3**). The reaction concentration was increased 10-fold, from 0.1 M to 1 M and run overnight. Unfortunately, the average conversion was much lower than the standard conditions at only 3.3%, perhaps owing to the small reaction volume employed resulting in poor solubility and inefficient stirring. On a larger scale this may be easier to control and

may have improved results. **Table 4**, entry **4**, involved modifying the stoichiometry of potassium *tert*-butoxide employed in the reaction; reducing the equivalents of base from 2.5 to 1.1 in order to prevent any potential elimination reactions occurring with the electrophile as outlined in **Scheme 70** below.



Scheme 70: Potential elimination reaction with 1.140

As with the temperature study, this resulted in a greater average conversion to product **1.157**. However, this was at the expense of either starting material or product degradation as both TLC and HPLC analysis of the reaction mixture indicated significant amounts of a more polar by-product at a retention time of 5.5 minutes as shown in **Figure 28**. This was also observed to a much greater extent in the temperature study.

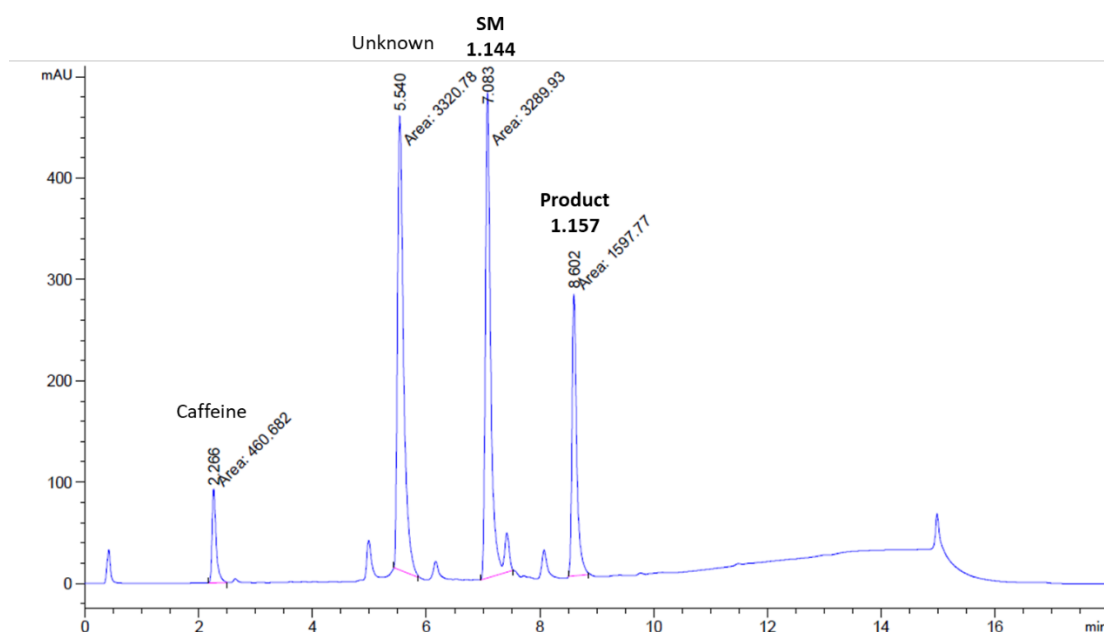


Figure 28: HPLC trace of the base equivalent study showing a large peak of an unknown analyte, potentially related to starting material 1.144, at 5.5 minutes

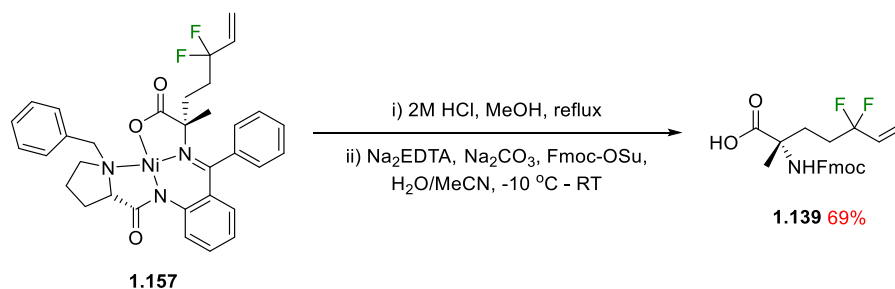
In order to determine whether or not the peak was related to the starting material or the product it would be necessary to isolate sufficient quantities of the by-product for analysis by ^{19}F NMR. Should no ^{19}F signal be observed it could then be determined that the non-fluorinated starting material (**1.144**) was being degraded in some

manner. A literature search did not yield any further insight into the identity of this unexpected by-product and thus, its formation would have to be investigated in future studies.

The final screening experiments examined involved substituting the potassium *tert*-butoxide for sodium hexamethyldisilazide (NaHMDS), 1,8-Diazabicyclo[5.4.0]undec-7-ene (DBU) or 2-*tert*-butylimino-2-diethylamino-1,3-dimethylperhydro-1,3,2-diazaphosphorine (BEMP), respectively (Table 4, entries 5-7). These bases were chosen as they had a range of pK_as (29.5, 12.5 and 19.0, respectively).¹²⁰ NaHMDS showed negligible conversion to **1.157** with an average solution yield of 0.9% (Table 4, entry 5). However, like the temperature and base equivalents study there was significant degradation of either the starting material or the product. Both DBU and BEMP showed no product formation.

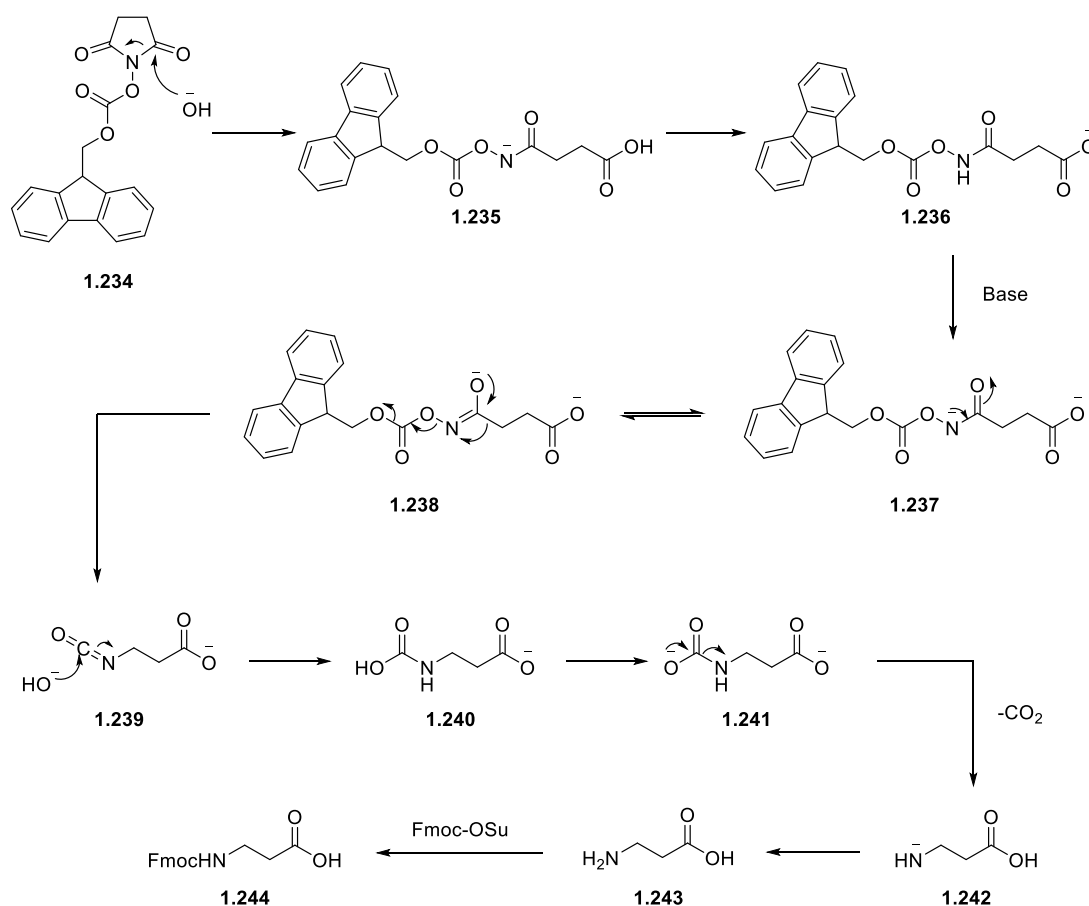
For DBU this could be explained by the base not being strong enough to deprotonate the starting material. The pK_a of related glycine complex **1.15** has been calculated to be 18.8 and it would be reasonable to assume that the pK_a of complex **1.144** would be similar.¹²¹ However, it would be expected that BEMP would be strong enough to deprotonate and it was surprising that no product **1.157** was observed. This served to establish the importance of the alkoxide base to the reaction.

Through combining entries **1**, **2**, and **4** in the optimisation study above, a sufficient quantity of the alkylated complex was obtained in order to attempt to synthesise the Fmoc amino acid as outlined below in Scheme 71. This would provide encouraging proof of concept that the target amino acid could be accessed, albeit in small quantities given the issues associated with the alkylation of the auxiliary.



Scheme 71: Conditions used to isolate amino acid 1.139

The initial hydrolysis step resulted in full conversion of **1.157** to the free amino acid as evidenced by TLC. The reaction mixture was then washed with DCM to remove ligand **1.14** and the aqueous layer evaporated. The residue was then taken up in an aqueous solution of sodium carbonate until the pH of the solution reached 9. Disodium ethylenediaminetetraacetate was then added to sequester the nickel salts following the earlier reported protocol.³⁴ The reaction was then cooled to -10 °C and Fmoc-OSu was then added dropwise as a solution in an equal volume of acetonitrile. The reaction appeared to run smoothly with full conversion to the fluorinated amino acid **1.139** observed by TLC. Unfortunately, there was an overlapping spot on the TLC which stained differently with ninhydrin, suggesting that what appeared to be a single product under UV visualisation was in fact two different compounds. Fmoc-OSu is known to undergo a base catalysed Lossen rearrangement to produce Fmoc- β -alanine as outlined below in **Scheme 72**.¹²²



Scheme 72: Mechanism of the Lossen rearrangement of Fmoc-OSu to form Fmoc- β -alanine¹²²

This unwanted side reaction could potentially account for the by-product observed in the ^1H NMR spectrum (**Figure 29**).

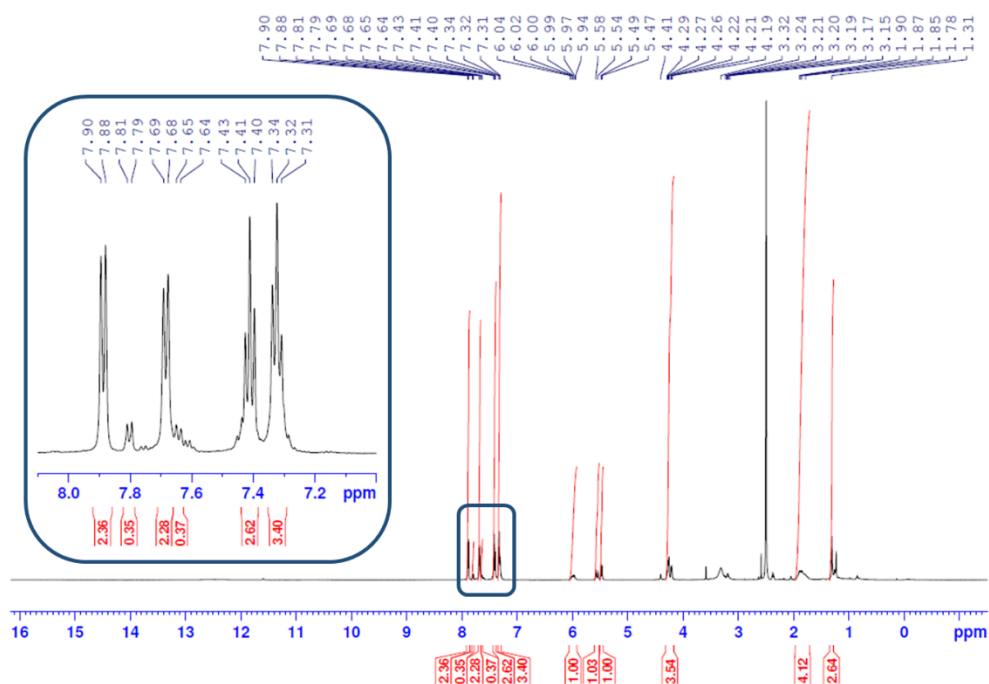


Figure 29: ^1H NMR spectrum of **1.139** after purification, showing minor contamination potentially by Fmoc- β -alanine

Nonetheless, upon purification with preparative TLC, a small quantity (9 mg) of the target Fmoc amino acid **1.139** was isolated in 69% yield with a purity of 73% as determined by LCMS analysis.

1.4 Conclusions

In conclusion, a fluorinated analogue of Fmoc-S₅-OH (**1.139**) has been synthesised, albeit currently on small scale. The retrosynthetic route towards the amino acid identified **1.140** to be a key intermediate and a thorough investigation into the synthesis was made with a total of three main routes examined.

The first-generation route towards **1.140** included an indium-mediated addition to an aldehyde. This route was deemed unsuitable due to the failure of the deoxygenation of the generated alcohol α to the *gem*-difluoro group. The second-generation alkylation strategy failed due to the inability to control the reactivity of

the difluorinated enolate, as it either self-condensed before reacting with the electrophile or did not react with the electrophile.

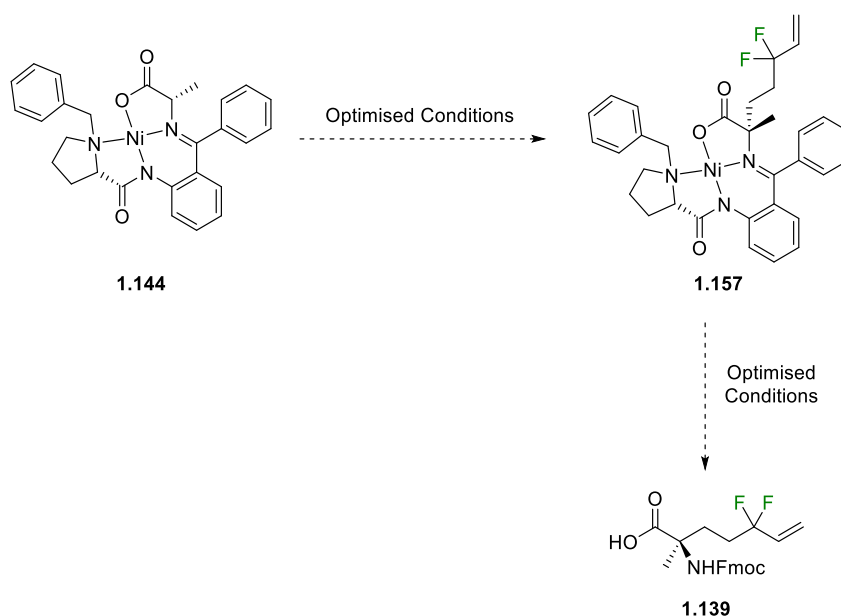
The third generation difluorocyclopropanation route, which exploited the highly strained, and reactive, nature of the cyclopropane ring system in a tandem dehalogenation and ring-opening reaction, was the most successful. The initial vinyl pinacol boronate ester systems were quickly eliminated due to their instability and poor reactivity and replaced with the much more stable bis-protected alkene **1.219**. Both the difluorocyclopropanation and the radical induced ring-opening reactions were initially low yielding and were optimised. The resulting TBDPS deprotection and iodination was quickly substituted for a two-step deprotection and tosylation strategy due to the highly volatile nature of the resulting alcohol. Tosylate **1.228** was then iodinated using a Finkelstein reaction to give the required fluorinated building block in 56% yield, an overall yield of 27% over 9 steps.

Sufficient quantities of iodoalkene **1.140** were isolated to attempt the alkylation of the BPB auxiliary **1.144** on route to the amino acid. Unfortunately, this occurred in only trace amounts and required further work to optimise the reaction conditions. Attempts to optimise the reaction with the limited amount of iodo **1.140** available showed an improvement in conversion by HPLC when the reaction temperature was increased to 40 °C, and when the equivalents of base was reduced from 2.5 equivalents to 1.1 equivalents. Unfortunately, there was also significant starting material or product degradation observed in both cases. Altering the concentration was worse than the standard conditions, potentially due to poor stirring, while altering the time resulted in no overall change in conversion. Changing the base from potassium *tert*-butoxide to either NaHMDS, DBU or BEMP resulted in little to no reaction, highlighting the importance of the alkoxide base to the success of the reaction.

1.5 Future Work

The future work of this project will primarily focus on optimising the alkylation of **1.144** with iodo **1.140** as outlined below in **Scheme 73**. The brief optimisation campaign employed in the current study did not examine alternative solvents; this is

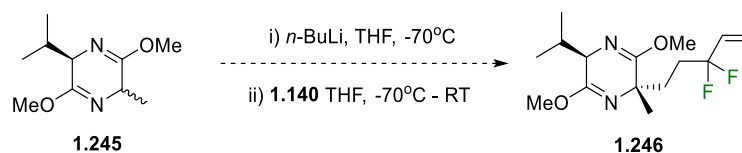
important to consider as solubility could be a factor in the poor yields. Further base screening would also be attempted. Literature reports have highlighted the use of sodium *tert*-butoxide as giving superior yields to potassium *tert*-butoxide due to the smaller size of the cation.³⁴ Thus, it may be of benefit to test both the lithium and the sodium salts to assess their reactivity in this reaction. Also, of importance is the enantiomeric excess of the reaction and the optimised conditions should produce **1.157** with an enantiomeric excess > 95%.



Scheme 73: Future work with the Ni-Ala-BPB Schiff base route

The number of variables present in the reaction could also allow for a Design of Experiments analysis.¹²³ This should help to find the optimal conditions faster by minimising the number of reactions that would have to be run. It also allows for the simultaneous analysis of multiple parameters and can identify which parameters are most important, allowing for a more efficient screen.

Should alkylating **1.144** prove unsuccessful, alternative starting materials may also be considered, for example, adopting the Schöllkopf auxiliary as outlined below in **Scheme 74**.¹²⁴



Scheme 74: Potential Schöllkopf conditions

Once the reaction has been optimised, for both yield and enantiomeric excess, work to optimise the tandem hydrolysis and Fmoc protection would commence. As product **1.139** did co-elute with an unknown amine which was Fmoc protected (proposed to be Fmoc β -alanine), the reaction would be optimised to minimise side-product formation. Here the equivalents of Fmoc-OSu, pH, reaction temperature and time could be examined in order to minimise the formation of the unwanted side-product. Alternative Fmoc protecting agents, such as Fmoc-Amox (**1.196**), could also be examined.¹²⁵ Here the succinimide has been replaced, which should stop the formation of Fmoc- β -alanine.

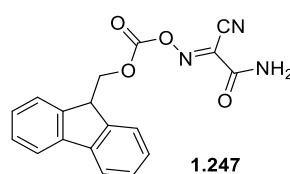
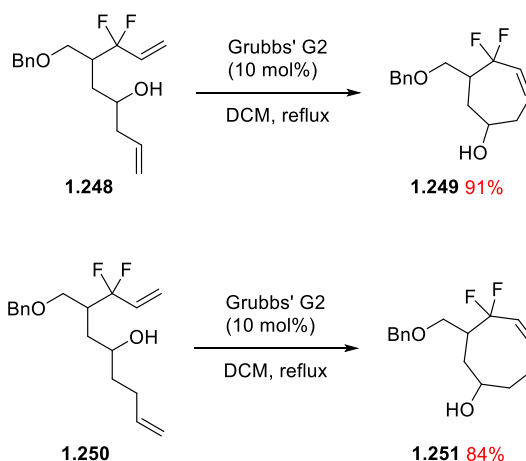


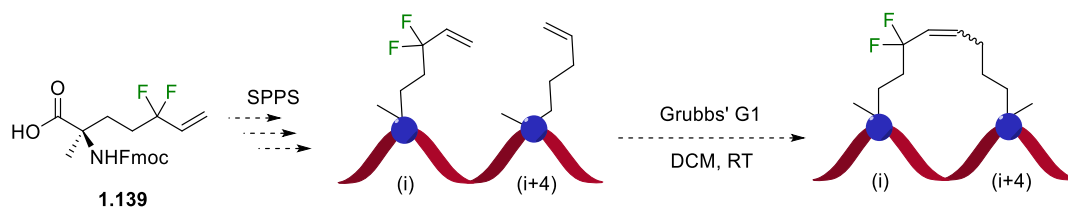
Figure 30: Structure of Fmoc-Amox¹²⁵

Finally, **1.139** would be incorporated into peptides using solid phase peptide synthesis (SPPS) and then stapled by an RCM, initially utilising Grubbs' G1 (**Scheme 76**). This process may also require optimisation to find the best catalyst system for the reaction, although there is literature precedence in small molecules for the successful RCM of the required allyl-difluoro alkene motif using Grubbs' G1 and Grubbs' G2.⁹³ This technique has been used to construct difluorocyclopentenes as described previously in **Section 1.1.3.3**. In the same report, the group also used RCM to construct difluorocycloheptenes and difluorocyclooctenes as shown in **Scheme 75**.



Scheme 75: Construction of medium-sized rings containing a *gem*-difluoro group via RCM

The peptides would then be analysed by circular dichroism to assess the helicity for comparison with the non-fluorinated analogues. The peptides could then be assessed by ^{19}F NMR to determine their suitability as tool compounds for determining binding to a cognate receptor in a protein-protein interaction.



Scheme 76: Future work with Fmoc protected amino acid 1.139

2 Chapter 2: The Design and Synthesis of Molecular Tools to Study the Role of PYCR1 in Oncology

2.1 Introduction

2.1.1 Cancer in Society

Cancer is the general name for a group of diseases which can be characterised by uncontrollable cell growth and proliferation.¹²⁶ It can affect any organ or tissue and people of all ages, races and genders without discrimination.¹²⁷ The condition is caused when DNA becomes damaged, such as with exposure to carcinogens or UV light, and the cell loses control of regulation.¹²⁸ Cells with DNA damage are usually prevented from dividing in order to attempt to repair the DNA.¹²⁹ If the DNA is unable to be repaired, the cell will be signalled to undergo apoptosis.¹²⁹ However, with cancerous cells mutations developed during the repair process suppress this mechanism and they continue to grow and divide in an abnormal fashion, eventually forming tumours as summarised in **Figure 31**.¹²⁸

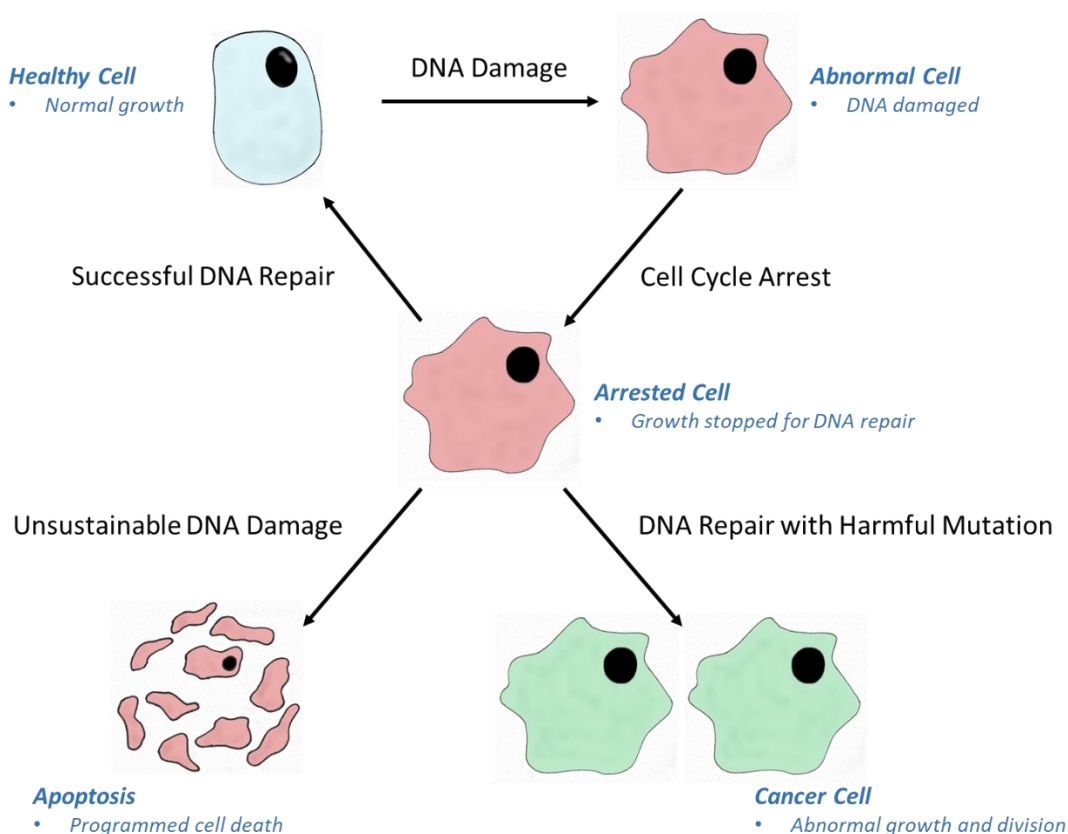


Figure 31: Cell cycle upon detection of DNA damage¹²⁹

For a cell to be classed as cancerous it must exhibit the six hallmarks of cancer.¹³⁰ These are: the ability to divide in the absence of cell growth factors, the ability to divide in the presence of tumour suppressants, the ability to avoid apoptosis, the ability to maintain the length of its telomeres through repeated cell division, the ability to undergo angiogenesis and the ability to invade surrounding tissue and metastasise.¹³⁰ As a result, there are a wide range of mutations possible within the cells and several potential targets are applicable. The mutations usually fall into two categories of genes: proto-oncogenes and tumour suppressor genes.^{131,132} Mutations in proto-oncogenes code for proteins which are usually involved in the acceleration of the growth and proliferation of cancer cells,¹³¹ whilst mutations in tumour suppressor genes usually render the resulting proteins ineffective at inhibiting cell growth.¹³² Notable genes involved in breast cancer are the oncogene coding for human epidermal growth factor receptor-2 (HER-2) and the tumour suppressor gene coding for breast cancer type 1 susceptibility protein (BCRA1).^{132,133}

HER-2 is a membrane bound growth factor receptor which contains a tyrosine protein kinase.¹³⁴ In some breast cancers HER-2 is overexpressed, and this signals the cell to undergo extensive proliferation. BCRA1 is a protein thought to be involved with DNA repair and can act as a checkpoint protein for DNA damage.¹³² In certain breast cancers, the gene is downregulated and as such the protein is not detectable. This allows cells with damaged DNA to continue to grow and proliferate. Spontaneous mutations in BCRA1 are rare and are usually inherited from one or both parents.

As a variety of gene mutations are usually present within a single cancer cell, there are many biological targets available for potential treatments, and this can make treatments complex.¹³⁵ Treatments can range from chemotherapy, which uses a small molecule to slow cell growth through the targeted inhibition of proteins associated with cell survival such as HER-2 as outlined above; radiotherapy, which directs ionising radiation to the tumour, damaging the DNA and forcing the cells to undergo apoptosis; immunotherapy, which programmes the patient's own immune system to target the cancerous cells and destroy them; and surgical excision of the tumour, where the cancerous tissue is completely removed from the patient.¹³⁵

Usually cancer treatments use a combination of one or more of the former.¹³⁵ The stage and location of the cancer also plays an important role in the treatment plan as some tumours may be inoperable or at too late a stage for it to be effective.¹³⁶

In 2015, there were 2.5 million people in the UK living with cancer and 2016 saw around 360,000 people diagnosed with cancer.¹³⁷ In 2008 this equated to a cost of £18.33 billion to the UK and the cost is expected to rise to £24.72 billion in 2020.¹³⁸ The number of people living with cancer has been increasing every year and by 2030 it is expected that the number of people in the UK living with cancer will rise to 4 million.¹³⁷ This equates to a 50% chance that a person in the UK will develop cancer.¹³⁹ As such, there is a pressing clinical need for new treatments to complement the current existing therapies, some of which are outlined below in **Figure 32**.

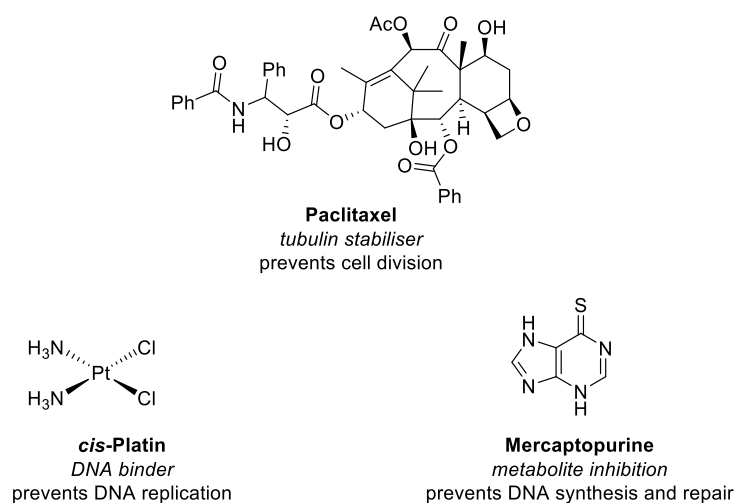


Figure 32: Commonly used chemotherapy drugs and their mechanisms of action.^{140–143}

Mercaptopurine (6MP) is used to treat acute lymphoblastic leukaemia.¹⁴⁴ It is itself a prodrug and it is metabolised into the active inhibitor thioinosine monophosphate (TIMP- Figure 33) by the action of hypoxanthine guanine phosphoribosyl transferase (HGPRT).¹⁴⁵

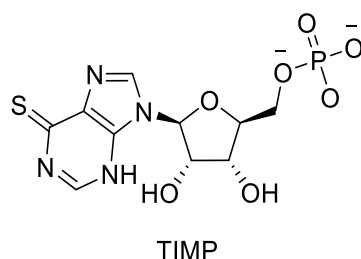


Figure 33: Structure of TIMP¹⁴⁶

From here the mechanism of action becomes complex as more than one pathway is involved in cytotoxicity as outlined in **Figure 34** below.¹⁴⁵ TIMP can then be methylated by thiopurine methyl transferase (TPMT) to form methyl-thioinosine monophosphate (MeTIMP), which can then inhibit phosphoribosyl pyrophosphate amidotransferase (PPAT).¹⁴⁵

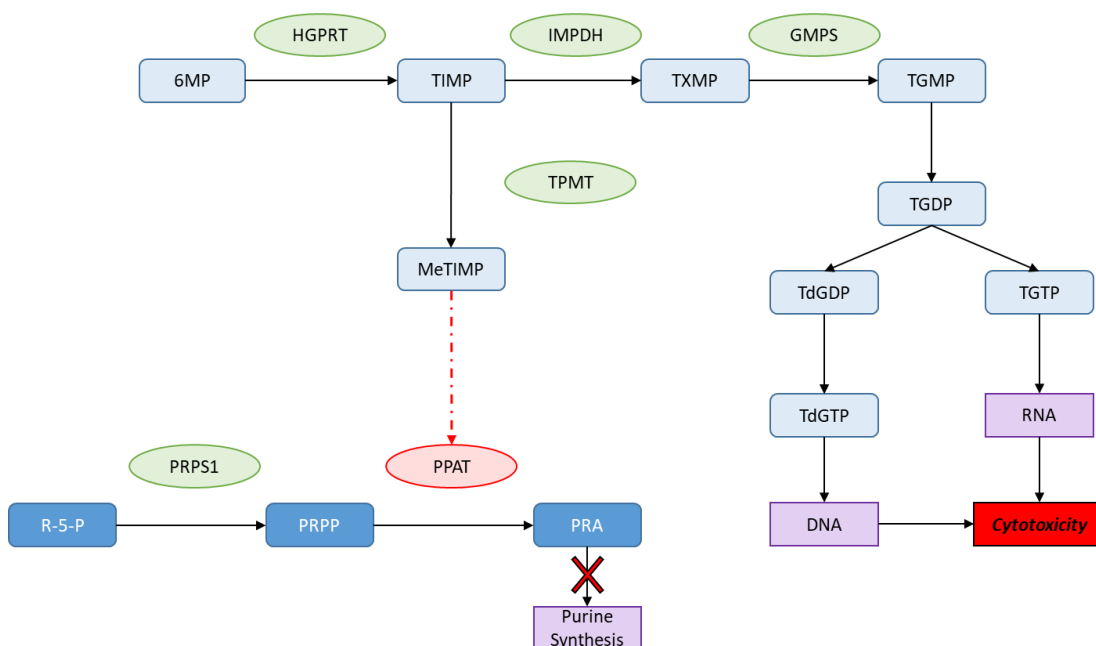
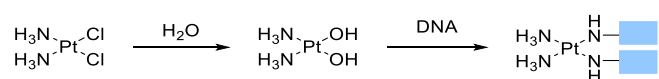


Figure 34: Metabolic fate and mechanism of action of 6MP. Pale blue boxes are metabolites of 6MP, blue boxes are materials required for *de novo* purine synthesis, green ovals are active enzymes, the pink enzyme is an inhibited enzyme, purple boxes are end products, red box and red cross are the effects of DNA and RNA incorporation and the effects of enzyme inhibition on purine synthesis¹⁴⁵

PPAT is involved in the synthesis of 5-phosphoribosylamine (PRA) from 5-phospho-D-ribose-1-pyrophosphate (PRPP), which is in turn synthesised from ribose-5-phosphate (R-5-P) by the action of phosphoribosyl pyrophosphate synthetase 1 (PRPS1).¹⁴⁵ PRA is an important feedstock for purine nucleotide synthesis and as PPAT is inhibited, the cell is unable to synthesise guanine and adenine through this

pathway.¹⁴⁵ TIMP can also be converted by inosine monophosphate dehydrogenase (IMPDH) to thioxanthine monophosphate (TXMP) which in turn is transformed by guanosine monophosphate synthetase (GMPS) to thioguanosine monophosphate (TGMP).¹⁴⁵ TGMP is then phosphorylated to thioguanosine diphosphate (TGDP) which then diverges into the DNA and RNA guanine nucleotide (TdGTP and TGTP, respectively). As the synthesis of normal purine bases is downregulated by the action of MeTIMP, TdGTP is incorporated into DNA which causes irreparable DNA damage. As both healthy cells and cancer cells use these mechanisms to survive, and the drug is given orally, it is difficult to target only the cancer cells. As a result, mercaptopurine has numerous side effects, which range from nausea to liver damage.¹⁴⁷

Cisplatin is a platinum(II) complex used in the treatment of various cancers; such as bladder, head and neck, and lung. Cisplatin is hydrolysed within the body to the *bis*-hydroxylated species as outlined below in **Scheme 77**.¹⁴⁸



Scheme 77: Activation of cisplatin and its mechanism of action. Blueboxes represent DNA bases¹⁴⁸

After hydrolysis, the activated cisplatin can then react with the purine DNA bases, causing crosslinking.¹⁴⁹ This damage is usually irreparable, which forces the cell to undergo apoptosis.¹⁵⁰ Like mercaptopurine, it is difficult to achieve selectivity between healthy and cancerous cells as almost all cells contain DNA and as a result there are usually severe side effects including organ damage (liver, kidney and heart) and hearing loss.¹⁵¹

Paclitaxel is a natural product, derived from the bark of the Pacific yew tree, which is used in the treatment of aggressive breast and ovarian cancers.¹⁵² It targets β -tubulin, a protein which forms microtubules which are essential for maintaining cell structure and forming spindle fibres which are present during mitosis.¹⁵³

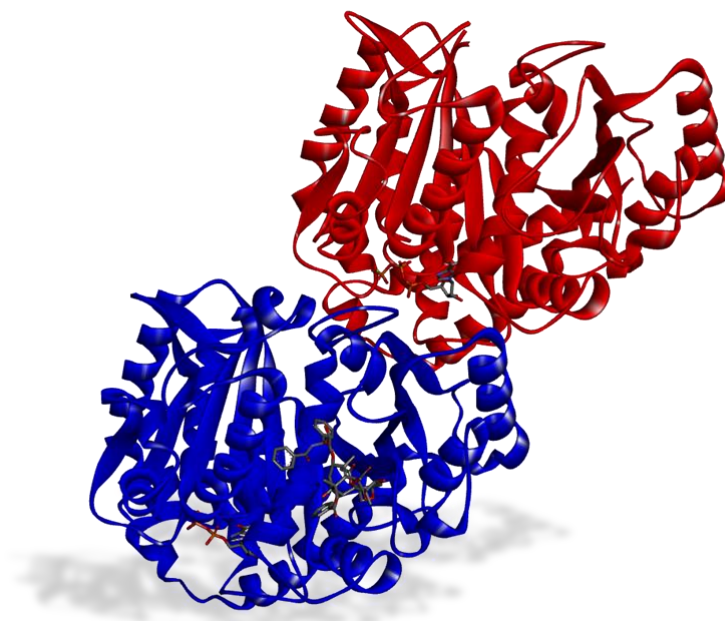


Figure 35: Structure of paclitaxel bound to tubulin as generated by electron microscopy PDB: 3J6G¹⁵³

When bound to β -tubulin, paclitaxel prevents microtubule disassembly and can stop the mitotic spindle fibres from attaching to the centrosomes of the chromatids.¹⁵² The cell then fails the mitotic checkpoint and enter mitotic arrest, which causes apoptosis.¹⁵² As most cells will continue to divide throughout their lifetime, paclitaxel is not selective to only cancer cells. However, as cancer cells have a higher rate of division it is most likely that these cells will be targeted preferentially. Paclitaxel also has several reported side effects such as fatigue, muscle and joint pain and neuropathy.¹⁵⁴

With the aforementioned chemotherapy treatments all targeting non-cancer specific pathways, the pharmaceutical industry has extensively studied the effects of targeting cancer specific pathways.¹⁵⁵ This has been facilitated by the advancement of genetic modification tools which can be used to analyse the functions of genes and their corresponding proteins, and identify if they are implicated in the disease, as well as generating new animal disease models.¹⁵⁵ It was initially thought that by targeting these cancer-specific proteins, it would reduce the side effects that commonly accompany the less specific treatments, however, all of the treatments described below have some side effects.

One of the first targeted treatments developed was imatinib (**Figure 36**) which is a tyrosine kinase inhibitor.¹⁵⁶

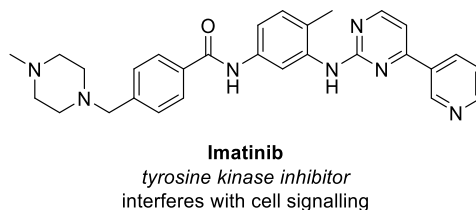


Figure 36: Structure of imatinib and its mechanism of action¹⁵⁷

In particular, it inhibits specifically the BCR-ABL kinase which arises from the expression of an oncogene created by the translocation of chromosomes 9 and 22. This particular mutation is found in most cases of chronic myelogenous leukaemia.¹⁵⁶ Imatinib binds to the ATP binding site and this prevents the phosphorylation of signalling proteins which lead to cell proliferation, which in turn reduces cell growth.¹⁵⁷

Similarly, gefitinib and erlotinib (**Figure 37**) are also marketed tyrosine kinase inhibitors, which are specific to the epidermal growth factor receptor (EGFR).^{158,159} In some cancers, such as non-small cell lung cancer, EGFR is overexpressed, which leads to increased cell proliferation.¹⁵⁸ Like imatinib, both drugs block the ATP binding site and stop signalling through this receptor which slows cell proliferation.^{159,160}

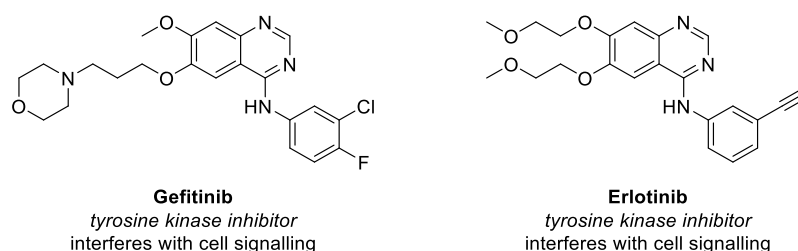


Figure 37: Structures of gefitinib and erlotinib and their mechanism of action^{159,160}

Another way to achieve selectivity for cancer cells over healthy cells is in the use of monoclonal antibodies.¹⁶¹ Here an antibody specific to a membrane bound receptor is administered. An example of this is trastuzumab, which targets HER-2.¹⁶² As discussed above, HER-2 is overexpressed in many breast cancers.¹³⁴ When the antibody identifies HER-2, it binds with it and blocks the receptor from dimerising upon the binding of a growth factor.¹⁶³ This in turn prevents downstream signalling

pathways and slows cell proliferation. Trastuzumab also has a secondary action by inducing immune cells to kill the cancer cells.¹⁶³

While these treatments are effective, eventually the cancer cells can develop resistance to the drugs.^{164,165} This can be in the form of over expressing efflux transporters, which pump the drug out of the cell before it can have an effect, or by mutating the targeted protein, which may reduce the ability of the drug to interact with the target.¹⁶⁶ As such, it is important to discover novel targets in order to adapt to the evolution of cancers, and to potentially find a targeted mechanism to which the cancer cells cannot develop resistance.

2.1.2 PYCR1 and its Role in Cancer

Amino acid deficiencies within the tumour are known to be caused in many cancers.^{167–169} Many cancers, such as acute lymphoblastic leukaemia, are highly sensitive to reductions in asparagine (Asn) and treatments, such as *L*-asparaginase (an enzyme which degrades Asn) have been developed to exploit this.¹⁷⁰ In order to discover new amino acids vulnerabilities implicated in cancers, the Agami group at the Netherlands Cancer Institute (NKI) developed a technique known as differential ribosome codon reading (diricore).¹⁶⁸ This technique counts the number of codons present on ribosome protected messenger RNA and associates them with their corresponding amino acid. As protein synthesis is halted when there is a deficiency in an amino acid, the greater the number of codons would indicate that there is a deficiency in that particular amino acid (**Figure 38**).¹⁷¹

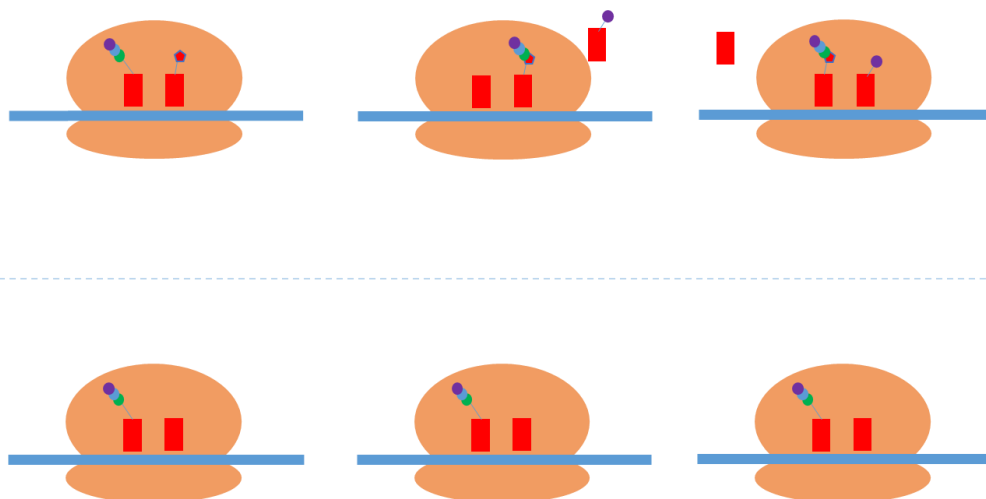


Figure 38: Simplified mechanism of ribosomal protein synthesis in the absence (top) and presence (bottom) of proline deficiency¹⁷¹

This technique was used to confirm that treatment of cancer cells with *L*-asparaginase caused a shortage of asparagine within the cancer cells. In response, it was found that the cells began to overexpress asparagine synthetase, the enzyme which synthesises asparagine, in order to overcome the deficiency.¹⁶⁸ With the technique having been validated, NKI then sought to discover new amino acids which were deficient in different cancers and could potentially be exploited in order to develop novel treatments. Cancerous tissue samples obtained from an excised kidney which were screened using the diricore technique found both methionine (Met) and proline (Pro) to be deficient within the tumour.¹⁶⁸ This was coupled with an increase in “uncharged” proline transfer RNA (**Figure 39**) which again suggested that proline was unavailable for protein synthesis.

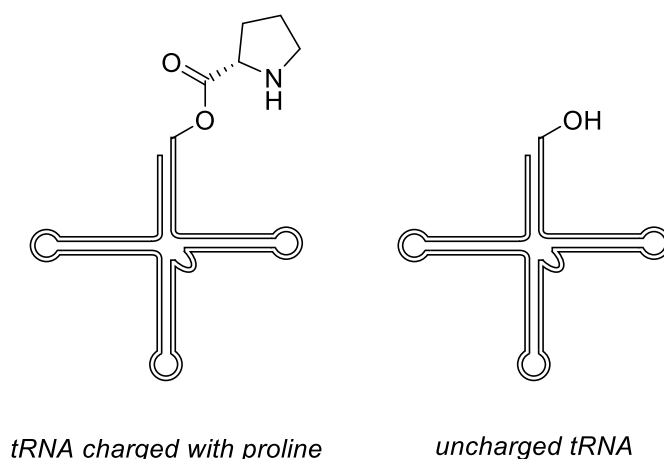


Figure 39: Transfer RNA in the charged and uncharged state¹⁷¹

Like with the asparagine shortage, the cancer cells had increased the expression of pyrroline-5-carboxylate reductase 1 (PYCR1), the enzyme required in the final step of proline biosynthesis, to surmount the deficiency to Pro, as shown below in **Figure 40**.¹⁶⁸

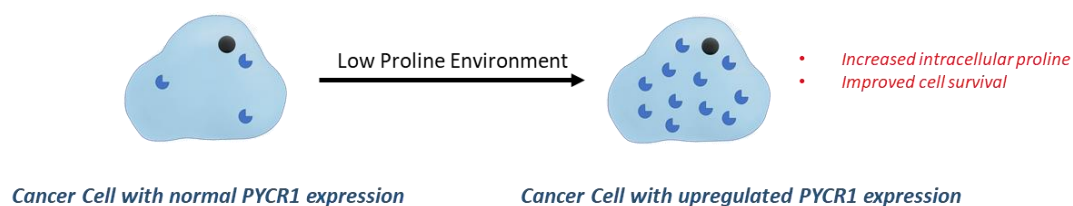


Figure 40: Cell adaptations to low proline environments showing the increased expression of PYCR1¹⁶⁸

Thus, it was proposed that inhibition of PYCR1 could potentially reduce *intracellular* levels of proline and arrest or retard the growth of cancer cells.

PYCR1 is the first member of the PYCR family which is expressed within the mitochondria and exists as a characteristic ring of five dimers as outlined in **Figure 41**.¹⁷²

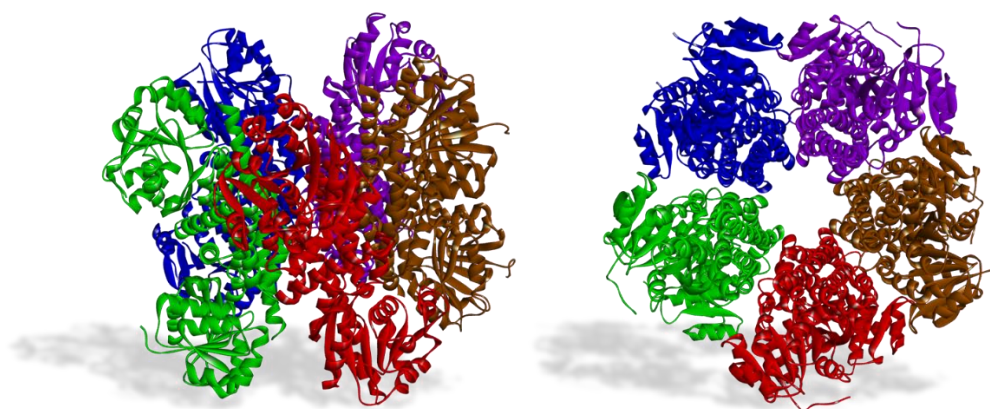
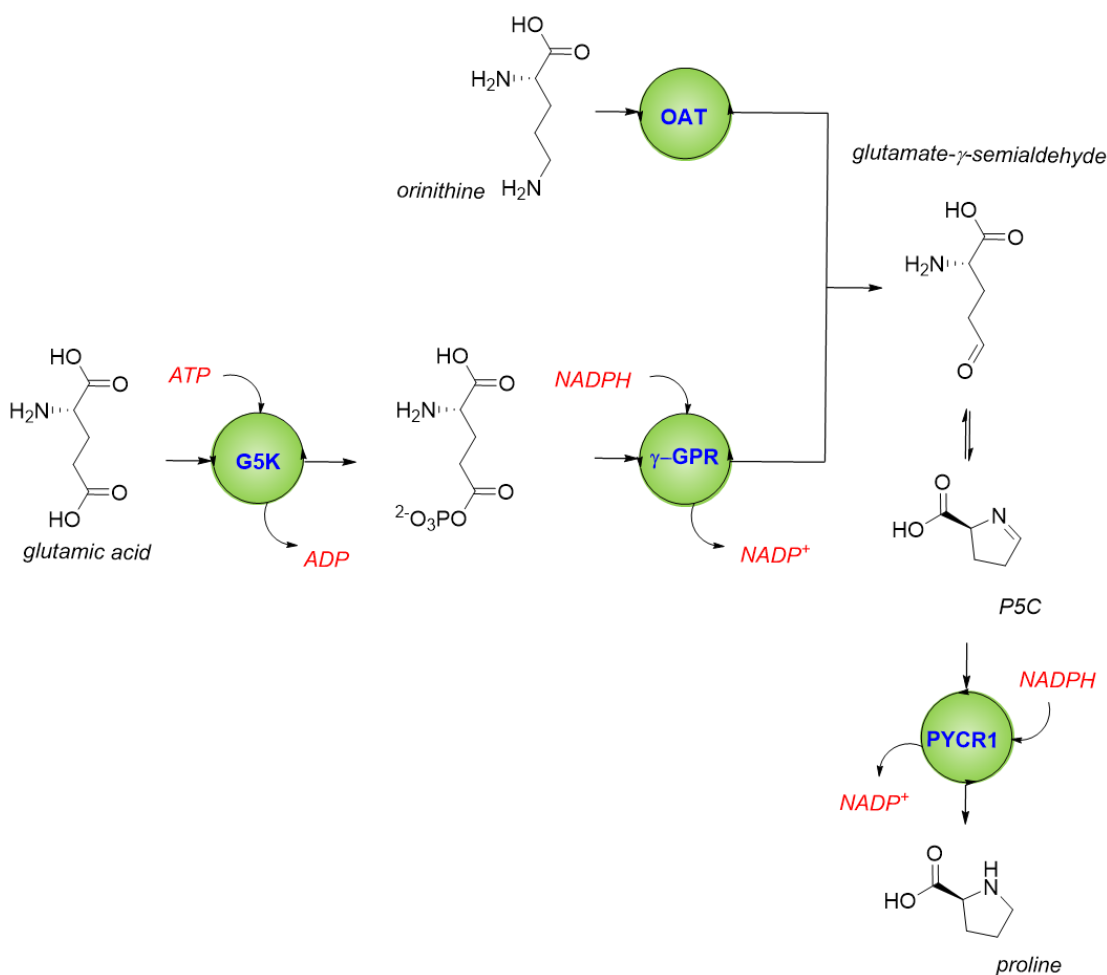


Figure 41: Biological assembly of PYCR1 showing the characteristic pentamer of dimers (PDB: 5UAV)¹⁷²

As mentioned above, PYCR1 is the final enzyme involved in proline biosynthesis.¹⁷² It reduces pyrroline-5-carboxylate (P5C) to proline with the aid of nicotinamide adenine dinucleotide phosphate (NADPH) as a co-factor as outlined below in **Scheme 78**.



Scheme 78: Proline biosynthetic pathway from glutamic acid and ornithine¹⁷²

The overall process follows two distinct pathways beginning with either glutamic acid (Glu) or ornithine (Orn). In the glutamic acid pathway, Glu is phosphorylated by glutamate-5-kinase (G5K) with the consumption of one unit of adenosine triphosphate (ATP). The phosphorylated Glu is then reduced by γ-glutamyl phosphate reductase (γ-GPR), again using NADPH as a co-factor, to furnish glutamate-γ-semialdehyde, which spontaneously cyclises to P5C. The Orn pathway directly converges on that of the Glu pathway by the formation of glutamate semi-aldehyde by the action of ornithine aminotransferase (OAT). This then forms P5C which is reduced to proline by PYCR1 as discussed above.¹⁷²

The active site of PYCR1 lies between both members of the dimer as outlined below in **Figure 42**.¹⁷²

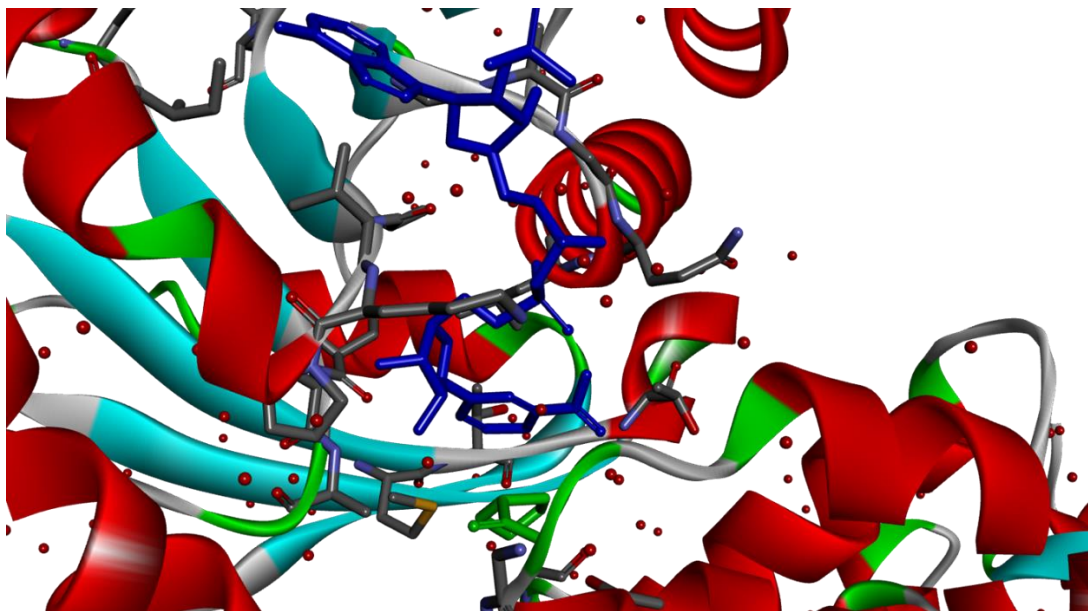


Figure 42: Active site of PYCR1 showing the interaction of NADPH (blue) and P5C mimic THFA (green). Image generated from PDB: 5UAV¹⁷²

NADPH lies within a Rossmann fold, which is a highly conserved structure in proteins which bind nucleotides, and forms hydrogen bonding interactions with the following amino acid residues (**Figure 43**, top right): Ala-8, Gln-10, Leu-11, Asp-36, Asn-56, Val-70 and Ala-97. All but Asn-56 form hydrogen bonds with the ribose or phosphate groups of NADPH, while Asn-56 bonds with a nitrogen atom of adenine. There is also an ionic interaction between the negatively charged oxygen atom of a phosphate group and Lys-71.¹⁷²

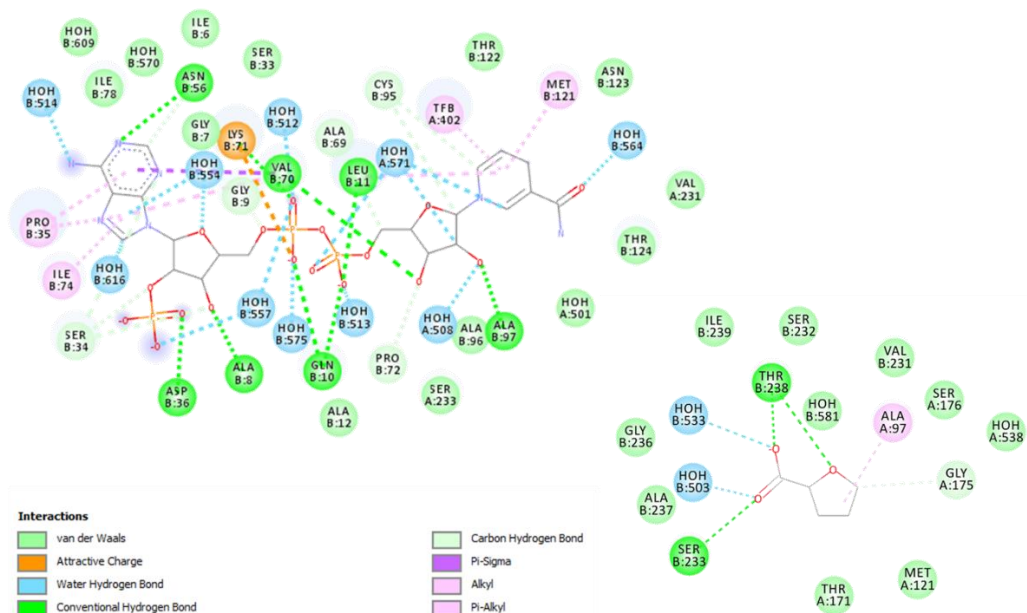


Figure 43: 2D interaction map for NADPH (top left) and THFA (bottom right) generated in Discovery Studio 2017 using PDB: 5UAV¹⁷²

As shown in **Figure 42**, the P5C mimic L-tetrahydro-2-furoic acid (THFA) lies directly below the nicotinamide portion of NADPH, a position where it is possible for hydride transfer between the NADPH and P5C. The THFA forms hydrogen bonding interactions between the carboxylate and Ser-233 and Thr-283. Thr-283 also forms another hydrogen bond between the ethereal oxygen in THFA (**Figure 43**, bottom right).¹⁷²

Proline has several important roles within cells. It is essential for protein synthesis and in turn influences the secondary structure of proteins, where it disrupts helicity and produces kinks and turns. This is due to the rigidity of the 5-membered ring system.¹⁷³ Proline and its derivatives, such as hydroxyproline, are also the main amino acids found in collagen, which is the most abundant structural protein found within the body. It also helps to maintain the redox balance of the cell in a process known as the proline cycle which is outlined below in **Figure 44**.^{174,175}

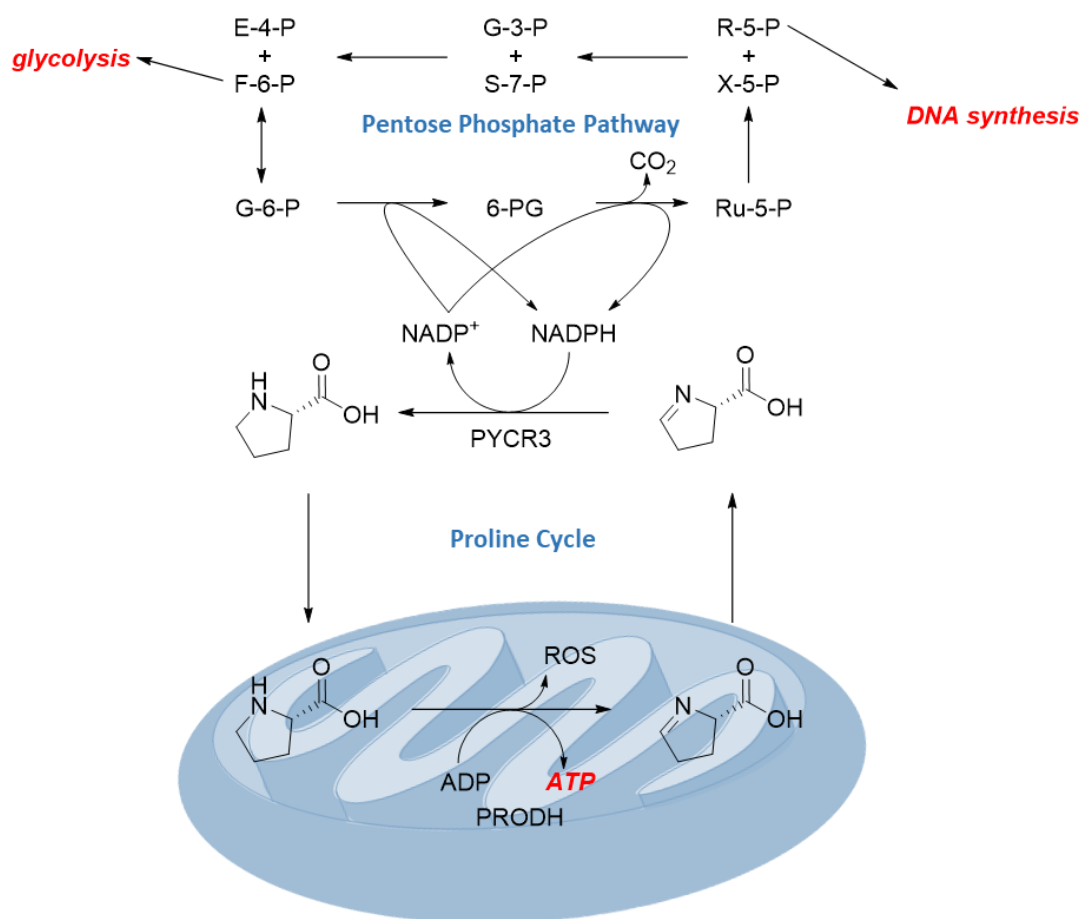


Figure 44: The proline cycle and the pentose phosphate pathway. The structures of the sugars are outlined in Appendix 1

During this cycle, proline dehydrogenase (PRODH) oxidises proline back to P5C in the mitochondria, releasing a molecule of ATP in the process, which can go on to provide energy for other cell processes. P5C then enters the cytosol, where it is then reduced back to proline by PYCR3, a cytosolic variant of PYCR1. The proline is then taken up by the mitochondria and the cycle begins again. The NADP⁺ produced by the reduction of proline can then be used as a co-factor in the pentose phosphate pathway where glucose-6-phosphate (G-6-P) is converted to fructose-6-phosphate (F-6-P), which is the starting material required for glycolysis. Ribose-5-phosphate (R-5-P) is an intermediate along this pathway and is essential for nucleotide synthesis.¹⁷⁶ Furthermore, this regenerates NADPH which can then be used in other cell processes. All of the above processes contribute to cell survival.¹⁷⁷

In healthy cells, these processes are highly regulated and essential for maintaining normal function. However, as stated above, in many cancers the expression of PYCR1 has been found to be upregulated, which increases the amount of Pro available to the cell and exacerbates these effects.^{168,178–181} Independent PYCR1 knock out studies in both *in vitro* human prostate and lung cancer as well as *in vivo* xenograft human breast cancer models indicated that removing PYCR1 results in phenotypic changes within the cell.^{168,178,181}

In the prostate cancer cell studies, genetic knockout of PYCR1 was achieved in two prostate cancer cell lines (PC-3 and DU145) which over expressed PYCR1. The cell lines were then incubated and the proliferation of the cells in comparison to an unmodified control group was measured by absorbance using an MTT assay.¹⁷⁸ In this assay the tetrazolium salt is reduced by viable cells to the formazan which absorbs light at 595 nm as outlined below in **Figure 45**.¹⁸²

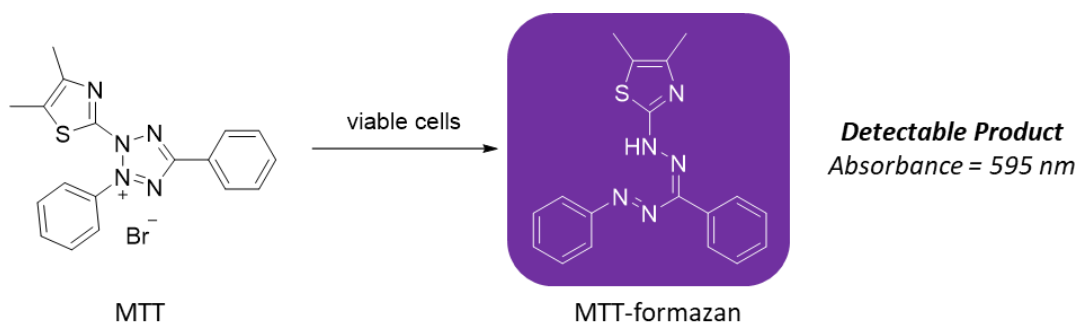


Figure 45: Format of the MTT assay showing the detectable product¹⁸²

As shown in **Figure 46**, the cells which were PYCR1 negative had lower absorbance values which indicated that less cells were present in the well, suggesting that the lack of PYCR1 was affecting cell proliferation *in vitro*.¹⁷⁸

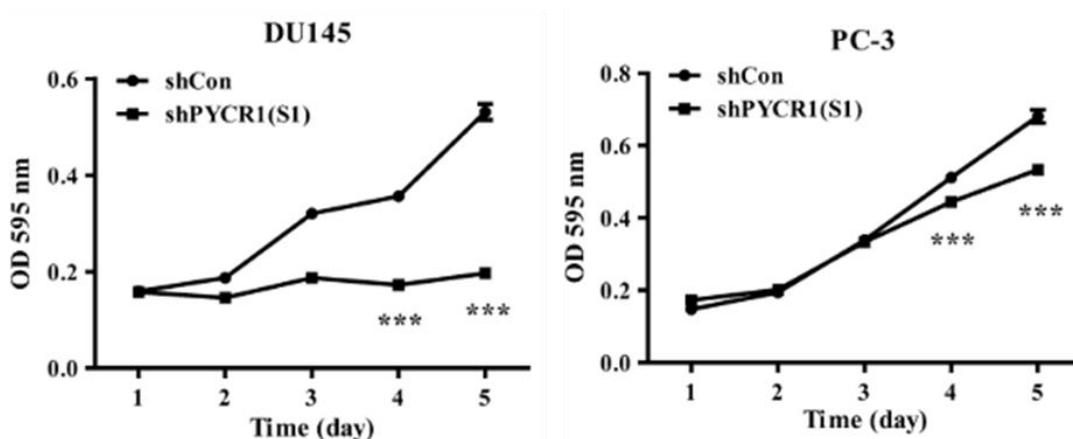


Figure 46: Cell proliferation data for both DU145 and PC-3 prostate cancer cell lines showing reduced cell proliferation was present in the cell lines where PYCR1 was knocked out¹⁷⁸

This result was corroborated in a similar experiment from an independent group using two lung cancer cell lines (SPC-A1 and H1703) which were also found to over express PYCR1.¹⁸¹ Again, PYCR1 was knocked out and the cell proliferation measured by absorbance at 450 nm using a similar WST-8 assay protocol as outlined below in **Figure 47**.¹⁸³

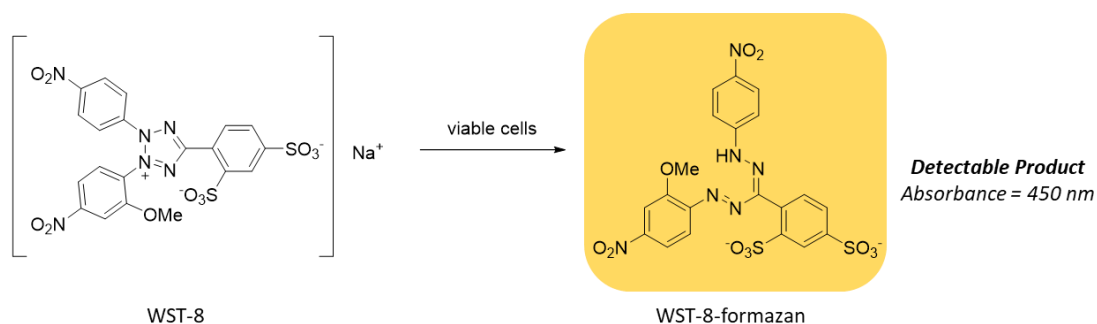


Figure 47: Format of the WST-8 assay showing the detectable product¹⁸³

Like the prostate cancer proliferation studies, the lung cancer cells where PYCR1 was knocked out showed lower absorbance than the control cells (**Figure 48**), again indicating that there were less cells present in the well and that PYCR1 was responsible for the reduced cell proliferation.

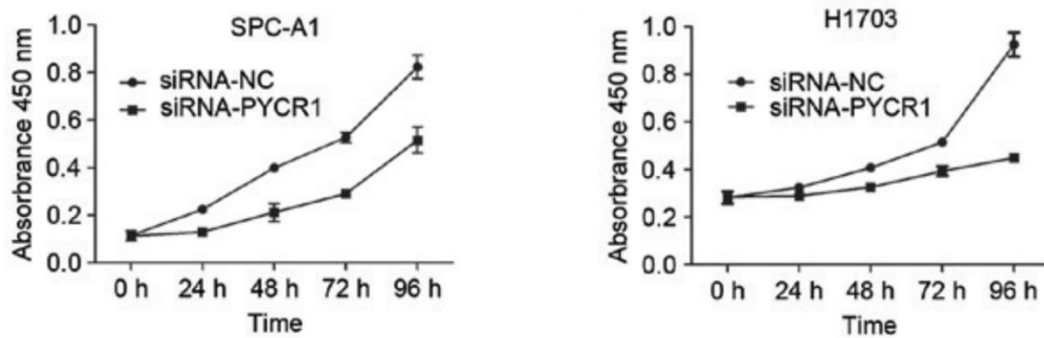


Figure 48: Cell proliferation data for both SPC-A1 and H1703 lung cancer cell lines showing reduced cell proliferation was present in the cell lines where PYCR1 was knocked out¹⁸¹

This observation was also replicated in *in vivo* xenograft breast cancer mouse models in the SUM-159-PT breast cancer cell line which was found to over express PYCR1.¹⁶⁸ In this experiment, PYCR1 was knocked out using CRISPR Cas 9 and the cells implanted into immunocompromised mice.¹⁶⁸ The tumour volume was then measured every 3-5 days. As shown in **Figure 49** below, the tumours comprising of the PYCR1 knock out cells did not appear to increase in size in comparison to the control group.¹⁶⁸ Again, this suggested that the absence of PYCR1 was, in this case, preventing the cells from proliferating *in vivo*.

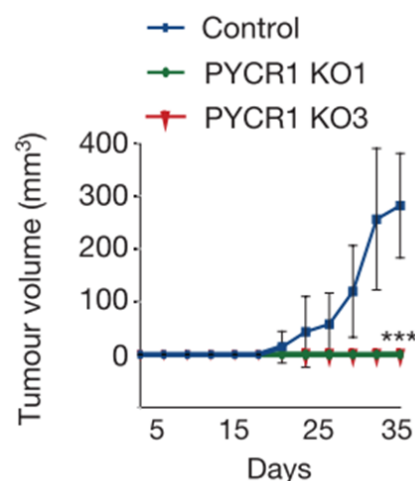


Figure 49: Data from the *in vivo* PYCR1 knock out tumour growth studies showing a reduction in tumour growth in the cells where PYCR1 was knocked out¹⁶⁸

With three independent studies indicating that knocking out PYCR1 reduced the growth and proliferation of five different types of cancer cells this strongly suggests that inhibition of PYCR1 could be a new oncology target.

While genetic knockouts are a useful tool for probing the function of a particular gene or protein, their use in therapeutics is very limited, and no knockout treatments have yet been approved as a treatment in any disease. This is mainly due to poor understanding of the human genome and the current technological limitations of the technique. It also raises a host of ethical debates.^{184,185} Furthermore, mutations in PYCR1 have been linked to the connective tissue disorder *cutis laxa*, a disease that is characterised by loose skin, hypermobile joints and in severe cases it can affect the structural support of the internal organs of the patient.¹⁸⁶ Thus, the potential, yet unknown, side effects of completely ablating PYCR1 as a cancer treatment could be life-changing for the person involved as they would be permanent.

In order to further validate PYCR1 as a potentially druggable target, the observations in the genetic knock out data would have to be replicated using a molecular probe or tool.¹⁸⁷ A molecular probe is usually a well characterised small molecule which can be used to determine the function of a particular protein within a cell.¹⁸⁷ As many are used to test the potential druggability they quite often share several properties with drug molecules.¹⁸⁷ Lipinski's rule of 5 states that a drug molecule will have a logP which is less than 5 and have less than 5 hydrogen bond donors and less than 10 hydrogen bond acceptors and rotatable bonds.⁴⁶ This is also true of many molecular probes.¹⁸⁷ Both drugs and molecular tools must be selective for the targeted protein, however the pharmacokinetics of the tool compound can be less than those of drug compounds as they are not intended for therapeutic use. Probes usually have similar potencies to drug molecules, and will most often have a known mechanism of action.¹⁸⁸ As many probes are used in cell based assays, it is important that the permeability of these compounds is high in order for the probe to pass through the cell membrane. As they share many properties with drugs they are also able to be developed into a lead candidate through structure activity relationship studies, perhaps in order to improve the physicochemical or pharmacokinetic properties.¹⁸⁸ Some notable tool compounds are outlined below in **Figure 50**.

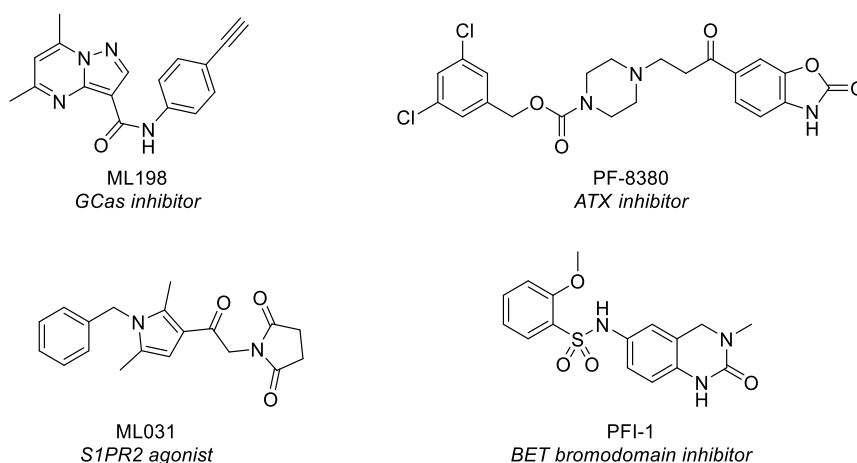


Figure 50: Structures and targets of some known tool compounds^{188–190}

With the knockout studies successfully showing that altering PYCR1 had a significant reduction in tumour growth, PYCR1 became the enzyme of interest for the development of a small molecule inhibitor. As this was a novel target, with no known small molecule inhibitors, a biological assay which would be used for screening was developed by the Agami group at NKI. The assay mimicked the natural conditions of the enzyme and monitored the consumption of NADH, a structurally related analogue of NADPH, by measuring the absorbance of the wells at 340 nm, the wavelength of absorption of NADH, over time as outlined below in **Figure 51**.

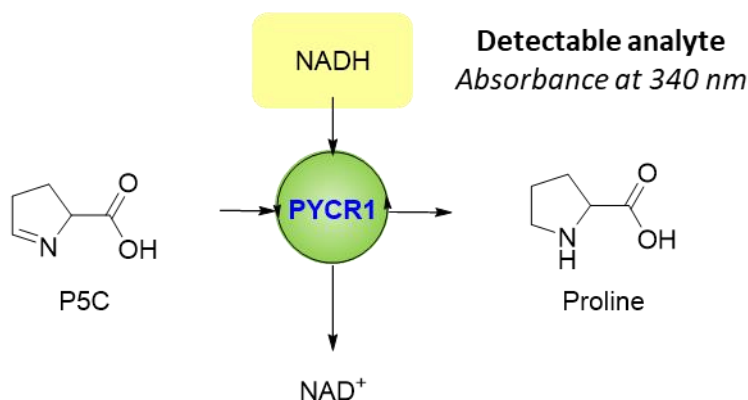


Figure 51: Assay conditions developed by NKI to study the effect of small molecule inhibitors of PYCR1

Once suitable assay conditions were in hand, NKI screened the target against a commercially available library of pharmaceutically active compounds (LOPAC[®]¹²⁸⁰, Sigma Aldrich).¹⁹¹ It was this screen that identified pargyline (**2.01**, **Figure 52**) as a fragment-like hit.

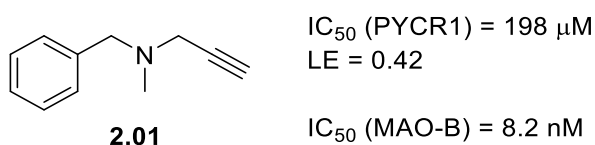


Figure 52: Structure of pargyline and its activity and ligand efficiency (LE) for both PYCR1 and MAO-B)

Fragments are typically weakly binding small molecules which are usually incorporated into libraries in order to explore a wide range of chemical space.¹⁹² Like drug molecules, fragments also have their own selection rules, known as the rule of three.¹⁹³ These rules state that a fragment should have a molecular weight lower than 300 Da, have a ClogP which is less than 3, have less than 3 hydrogen bond donors (HBD), acceptors (HBA) and freely rotatable bonds (FRB) and a polar surface area (PSA) less than 60 Å².¹⁹³ **Table 5** below outlines the properties of pargyline and compares them with the rule of three.

Table 5: Properties of pargyline as calculated by ACD labs for the RSC ChemSpider database¹⁹⁴

Property	Rule of 3 value	Pargyline value	Obeys rule of 3
Molecular weight (Da)	< 300	159.23	Yes
HBD	≤ 3	0	Yes
HBA	≤ 3	1	Yes
ClogP	≤ 3	2.48	Yes
FRB	≤ 3	4	No
PSA (Å²)	≤ 60	3	Yes

As shown above pargyline obeys most of the rule of 3 guidelines as it has a low molecular weight and ClogP, as well as fewer than 3 hydrogen bond donors and acceptors and a polar surface area which is less than 60 Å². The only failing is on the number of freely rotatable bonds, which at 4 is one greater than the recommended 3. As all the above criteria had good agreement with the rule of three, this makes pargyline an attractive fragment-like hit.

Typically, fragments have binding constants in the range of 100 μM to 1 mM.¹⁹⁵ However, despite their relatively weak interactions, their small size enables them to bind very efficiently with the target protein.¹⁹² This can be evaluated by a parameter

known as ligand efficiency (LE). Ligand efficiency is calculated by dividing the change in Gibbs' free energy of the fragment upon binding to the target protein by the number of heavy atoms (HA) or non-hydrogen atoms present in the fragment as shown in **Equation 6**.¹⁹²

$$LE = \frac{\Delta G_{bind}}{No. HA}$$

Equation 6: Calculation of LE. ΔG_{bind} = change in Gibbs' free energy upon binding, No. HA = number of heavy atoms (non-hydrogen atoms)

ΔG can be represented as shown in **Equation 7** where R is the universal gas constant, T is the temperature and K_d is the dissociation constant.¹⁹² This means **Equation 6** can be combined with **Equation 7** to obtain **Equation 8**.

$$\Delta G_{bind} = -RT \ln K_d$$

Equation 7: Calculation of ΔG

$$LE = -\frac{RT \ln K_d}{No. HA}$$

Equation 8: Combination of Equation 6 and Equation 7

Equation 8 can be further manipulated to give **Equation 9**, which can be simplified if standard conditions ($R = 1.985 \times 10^{-3}$ Kcal K^{-1} mol, $T = 298$ K, $c = 1$ M) are assumed to **Equation 10**.¹⁹⁶

$$LE = -\frac{2.303RT}{No. HA} \log (K_d/c)$$

Equation 9: Manipulation of Equation 8

$$LE = \frac{1.37pK_d}{No. HA}$$

Equation 10: Simplification of Equation 9 upon assuming standard conditions, where $pK_d = -\log K_d$

The dissociation constant (K_d) can also be substituted with IC_{50} to give **Equation 11**.

$$LE = \frac{1.37pIC_{50}}{No. HA}$$

Equation 11: Substitution of K_d for IC_{50}

The threshold for the ligand efficiency of a fragment is 0.3, which is based on the ligand efficiency of a 500 Da drug with a dissociation constant of 10 nM. In this analysis, it is assumed that the 500 Da drug would have 38 heavy atoms.¹⁹⁶ Therefore, with a ligand efficiency of 0.42, pargyline also fits the ligand efficiency profile of a good fragment.

Pargyline is a known monoamine oxidase B (MAO-B) inhibitor which has an IC_{50} of 8.2 nM.^{197,198} It is an irreversible inhibitor and covalently bonds to the flavin cofactor found within the enzyme in a similar manner to that of rasagiline, a structurally related MAO-B inhibitor, as shown in **Figure 53**.¹⁹⁹

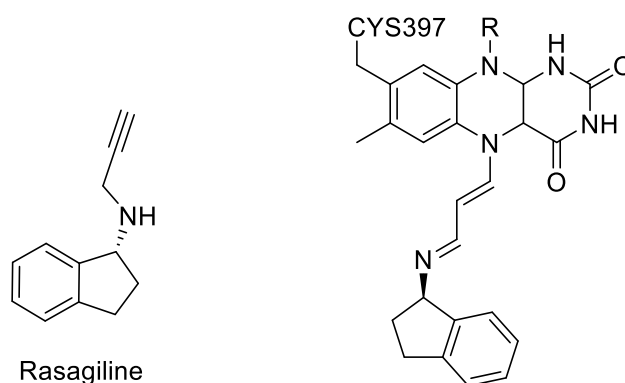


Figure 53: Structure of rasagiline and its binding to the flavin cofactor found within MAO-B

Originally designed as an antihypertensive, pargyline was eventually withdrawn from use due to the large number of harmful drug and food interactions.¹⁹⁹

This high affinity for MAO-B makes pargyline potentially an unsuitable tool compound for studying PYCR1, however as discussed above, its molecular properties and modular structure make it an ideal candidate for use in a fragment-like study.¹⁹⁶ However, no structural data of PYCR1 with pargyline exists which would make subsequent structure activity relationship studies more difficult.

2.2 Aims

The main aim in this chapter was to design and synthesise a series of pargyline analogues in order to probe the structure activity relationship (SAR) with PYCR1 to produce potential tool compounds which were more potent, and potentially more selective towards PYCR1 than the progenitor compound. Ideally, these compounds

would be active in both *in vitro* enzyme and cell studies and *in vivo* cancer models, thus enabling the validation of PYCR1 as an emerging oncology target suitable for further development. The final aim of this chapter was to also generate a co-crystal structure of an inhibitor with PYCR1 which would allow for the discovery of the binding site as well as elucidating a possible mechanism of action. The crystal structure could then be used to delineate areas for further development around the template, facilitating efficient lead optimisation.

2.3 Results and Discussion

2.3.1 Synthesis of Pargyline Analogues

Firstly, a sample of pargyline hydrochloride was obtained and analysed to confirm identity and purity before being retested to confirm its activity at PYCR1. With the activity confirmed, the synthesis of pargyline analogues commenced. As mentioned above in **section 2.1**, pargyline has a modular structure with three main areas that are readily amenable to modification: the benzyl group, *N*-methyl group and propargyl group as outlined in **Figure 54**. These were highly chemically tractable modifications which could be accessed through either alkylation chemistry or reductive amination, usually in one step.

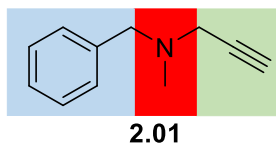
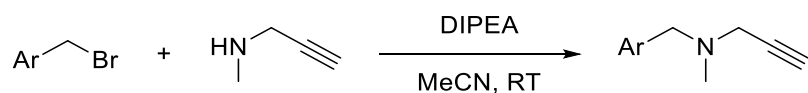


Figure 54: Structure of pargyline showing the three main areas of interest: benzyl group (blue), *N*-methyl (red) and propargyl (green)

Over 60 structurally related analogues were successfully synthesised in total using either alkylation chemistry or reductive amination between the corresponding amine and aryl or alkyl halide or pseudo-halide or amine and aldehyde or ketone, respectively.

Two sets of alkylation conditions were utilised throughout the synthesis of the pargyline analogues, firstly using diisopropylethylamine (DIPEA) as a base as outlined below in **Scheme 79**.



Scheme 79: General alkylation conditions employed during the synthesis of pargyline analogues which used DIPEA as a base where Ar is an aryl group

These conditions were initially chosen as they were mild and as they had excellent yields and functional group tolerance as stated in the literature.²⁰⁰ Four compounds were synthesised using this method as outlined below in **Figure 55**.

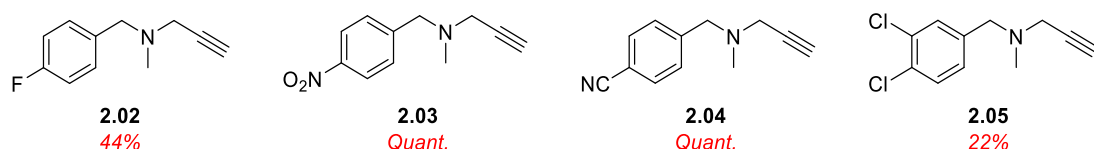
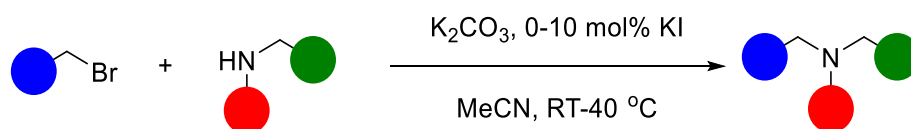


Figure 55: Compounds synthesised by alkylation using DIPEA as a base

While the reaction worked well for two of the substrates (**2.03** and **2.04**) with quantitative yields obtained, for the other two compounds the yields were significantly lower. For compound **2.02** the poor yield was likely due to the volatility of the compound. The first time this reaction was conducted the product was lost upon concentration with compressed air, and subsequent re-synthesis of the compound yielded 44%. For compound **2.05**, the reaction failed to reach completion, despite having a longer reaction time than the literature conditions, which resulted in the reduced yields. With DIPEA also being a tertiary amine and in slight excess, the separation with the product was more challenging and may have created issues with further analogues, which led to the adoption of the potassium carbonate conditions outlined below in **Scheme 80**.



Scheme 80: General alkylation conditions employed during the synthesis of pargyline analogues which used potassium carbonate as a base

Again, these conditions were mild and the use of an inorganic base meant that the excess could be filtered off at the end of the reaction, making the final purification more facile. Most of the bromides used were fairly activated, such as benzyl or allyl derivatives and did not require further additives to aid the reaction progression.

Some of less activated alkyl bromides, such as the propyl and cyclopropyl systems, required the use of catalytic potassium iodide to form the alkyl iodide *in situ* via a Finkelstein reaction. The compounds synthesised using this method are shown below in **Figure 56**.

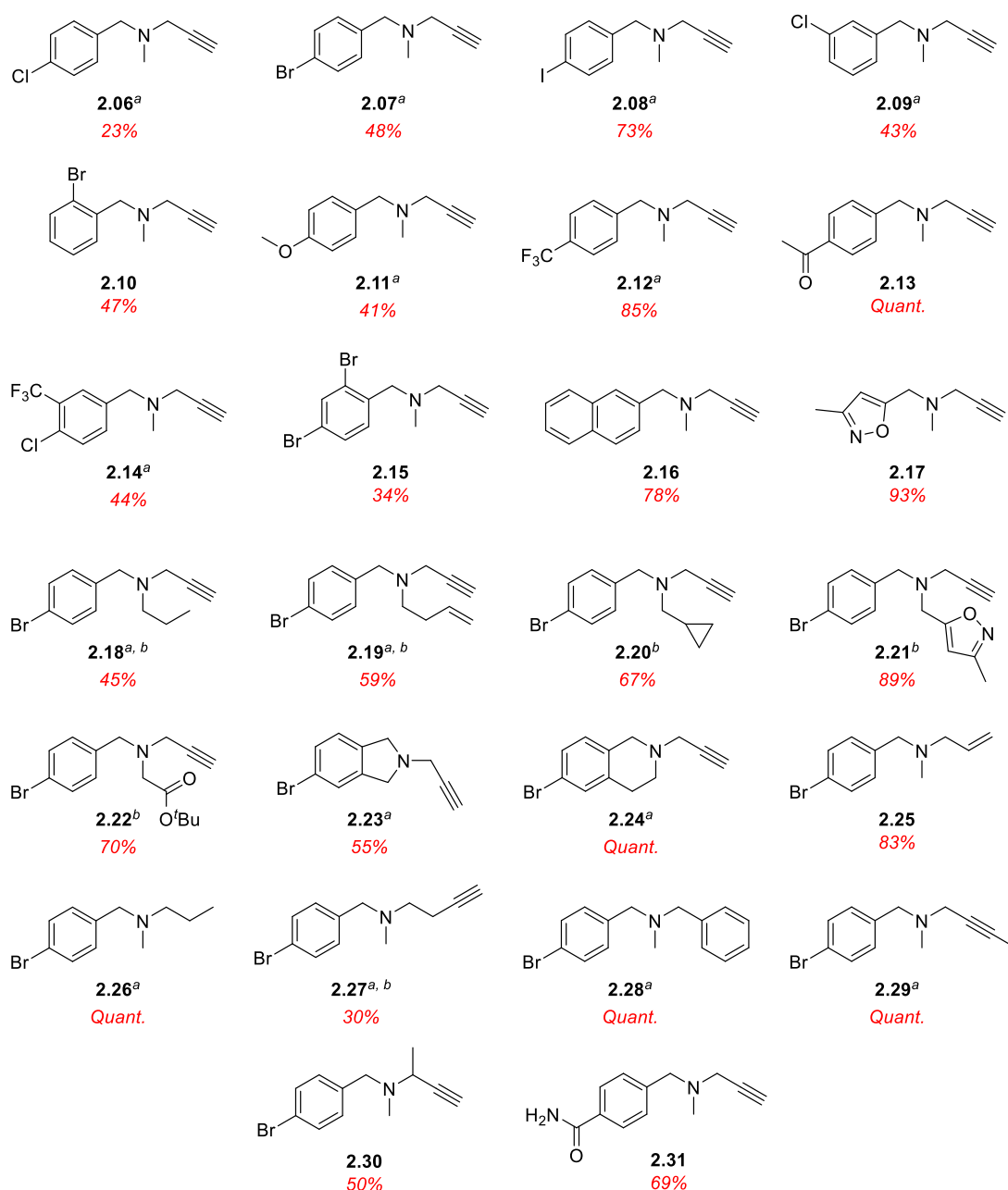
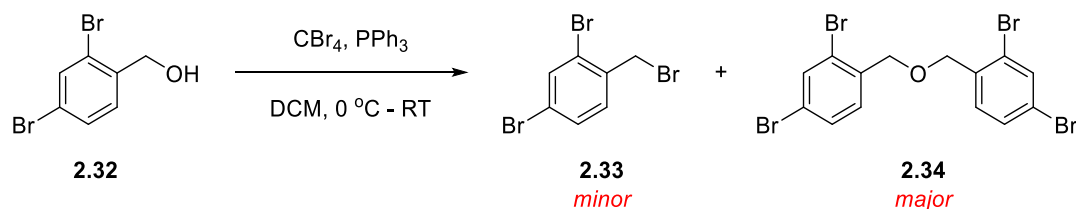


Figure 56: Compounds synthesised by alkylation using potassium carbonate as a base. ^aIsolated as the HCl salt, ^bsynthesised using 10 mol% potassium iodide

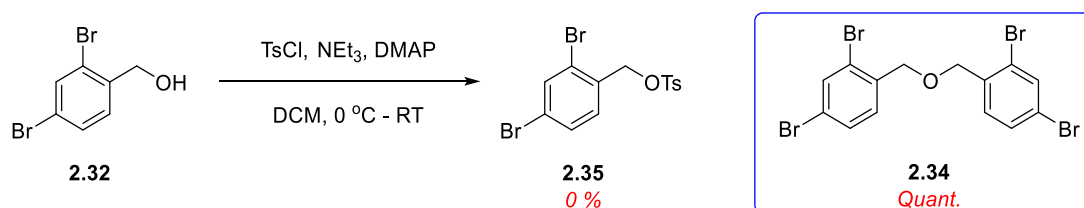
Compound **2.15** required synthesis of a suitable starting material due to a lack of commercial availability of 2,4-dibromobenzyl bromide. However, 2,4-dibromobenzyl alcohol (**2.35**) was available and Appel conditions as outlined below in **Scheme 81**

were the first conditions screened.²⁰¹ While the reaction appeared to be complete by TLC, after purification it was revealed that there were two compounds present, which at the time were unknown, but were later discovered to be ether **2.34** and product **2.33** (Green, **Figure 57**). Unfortunately, the ratio of **2.33** and **2.34** (2:5, respectively, as measured by ¹H NMR) was greater in favour towards the ether and as both products were inseparable, alternative reaction conditions were sought.



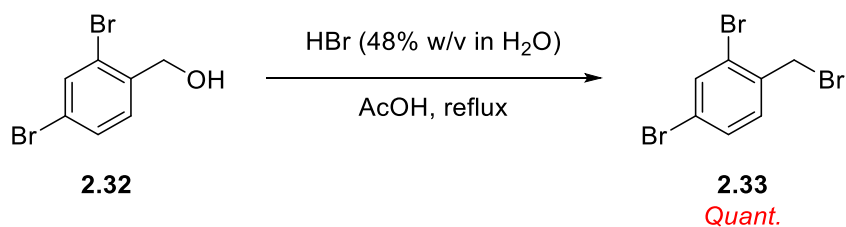
Scheme 81: Appel conditions employed in the attempted synthesis of compound **2.33** resulting in a 2:5 mixture of **2.33**:**2.34**

The next set of conditions utilised the alcohol functionality of **2.06** by forming the tosylate as shown in **Scheme 82**. Again, the reaction appeared to be successful by TLC, with full conversion to a less polar spot observed. However, upon purification and analysis, this spot was revealed, not to be the desired tosylate **2.35**, but ether **2.34** (Red, **Figure 57**). This was presumably due to the unreacted alcohol reacting with the newly formed tosylate during the reaction.



Scheme 82: Tosylation conditions employed in the attempted synthesis of **2.35**

The final conditions used hydrobromic acid to brominate in the benzylic position (**Scheme 83**). Here, the highly acidic reaction conditions facilitated the removal of water from **2.32**. As with the previous conditions, TLC indicated complete conversion of the starting material to a single product. Pleasingly, this was identified as product by ¹H NMR (blue, **Figure 57**) and used directly in the next step in the reaction without further purification.



Scheme 83: Bromination conditions employed in the synthesis of compound 2.33

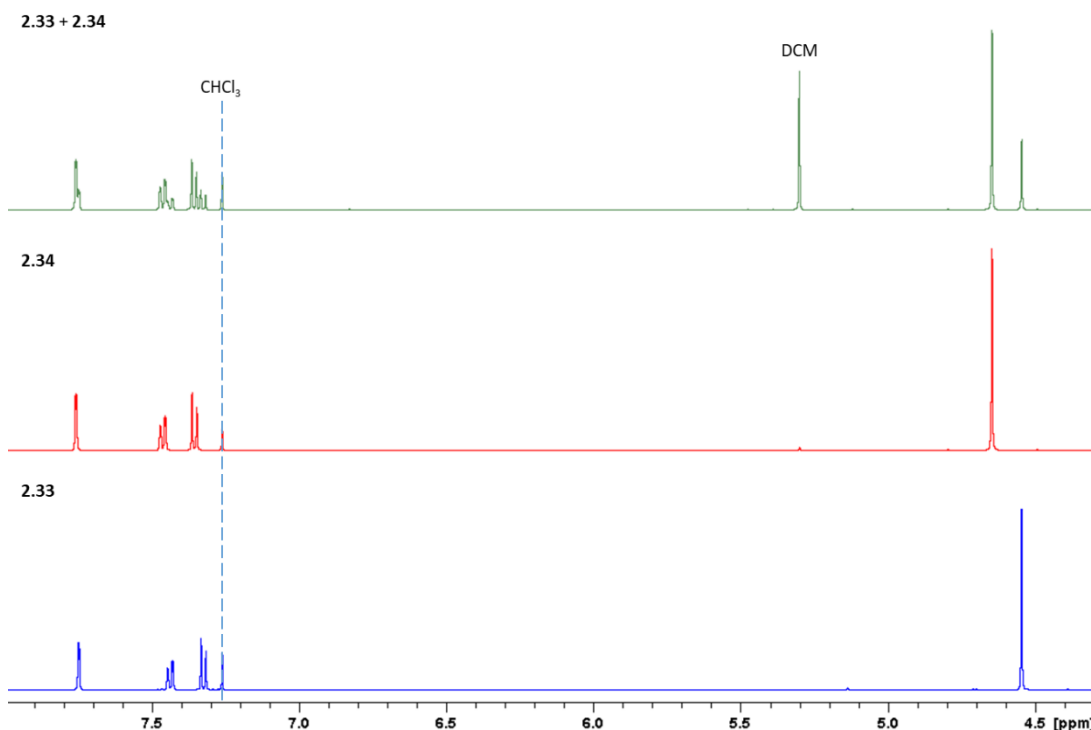
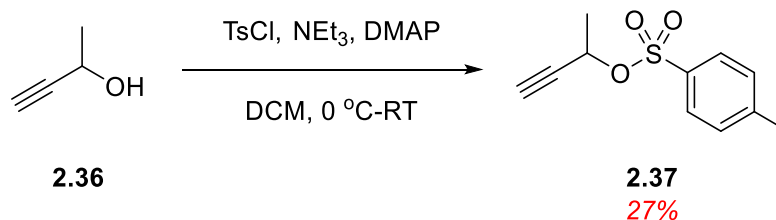


Figure 57: ^1H NMR of the resulting compounds of each set of reaction conditions (green, Appel; Red, tosylation; blue, bromination) between $\delta = 8\text{-}4.5$ ppm

The final compound **2.30** also required the synthesis of the tosylate system **2.37** from the commercially available **2.36** as outlined in **Scheme 84**.

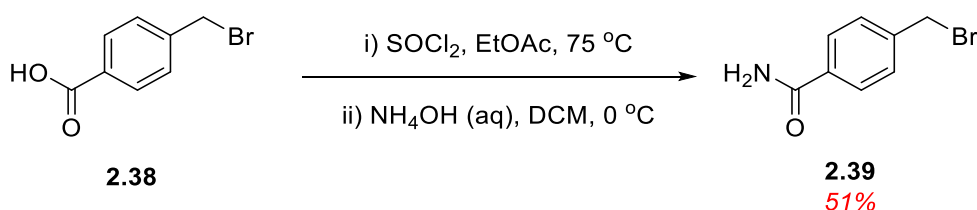


Scheme 84: Tosylation conditions employed in the synthesis of 2.37

While the reaction was successful, it was unfortunately low yielding. TLC indicated that both starting material **2.36** and tosyl chloride had been consumed, and as a result the yield should be high. The loss in yield could be due to the workup

procedure. Prior to washes with saturated copper(II) sulfate and saturated sodium bicarbonate, the reaction was filtered through a pad of celite to remove the majority of the salts formed in the reaction and some of the product could have become trapped in the filter aid. Nevertheless, sufficient material was obtained for the alkylation step.

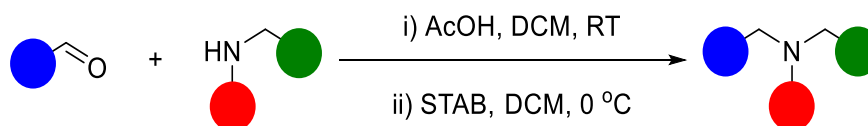
The last of the alkylation products, **2.31**, also required the synthesis of aryl bromide **2.39**. Compound **2.39** was commercially available; however, it was very expensive (£207.32 for 1 g).²⁰² Aryl bromide **2.38** was also commercially available at a fraction of the price (£31.30 for 5 g)²⁰³ and there was literature precedence to reach **2.39** in a two-step reaction as outlined in **Scheme 85**.²⁰⁴



Scheme 85: Two-step synthesis of compound 2.39

The first step formed the acid chloride which was then quenched by the addition of an excess of aqueous ammonia. **2.39** then precipitated out of the reaction media and was purified by recrystallisation. While the yield was lower than the reported 81%, sufficient material was isolated for use in the alkylation.

As mentioned above, the pargyline analogues could also be accessed by reductive amination. For the most part, these were performed on a secondary amine, using an excess of aldehyde as outlined in **Scheme 86** below.



Scheme 86: General reductive amination conditions employed during the synthesis of pargyline analogues

Initially, the reductive aminations failed to produce the desired product. This was due to the use of a decomposed stock of sodium triacetoxyborohydride (STAB) and

subsequent reactions with fresh reagent proceeded smoothly as shown below in **Figure 58**.

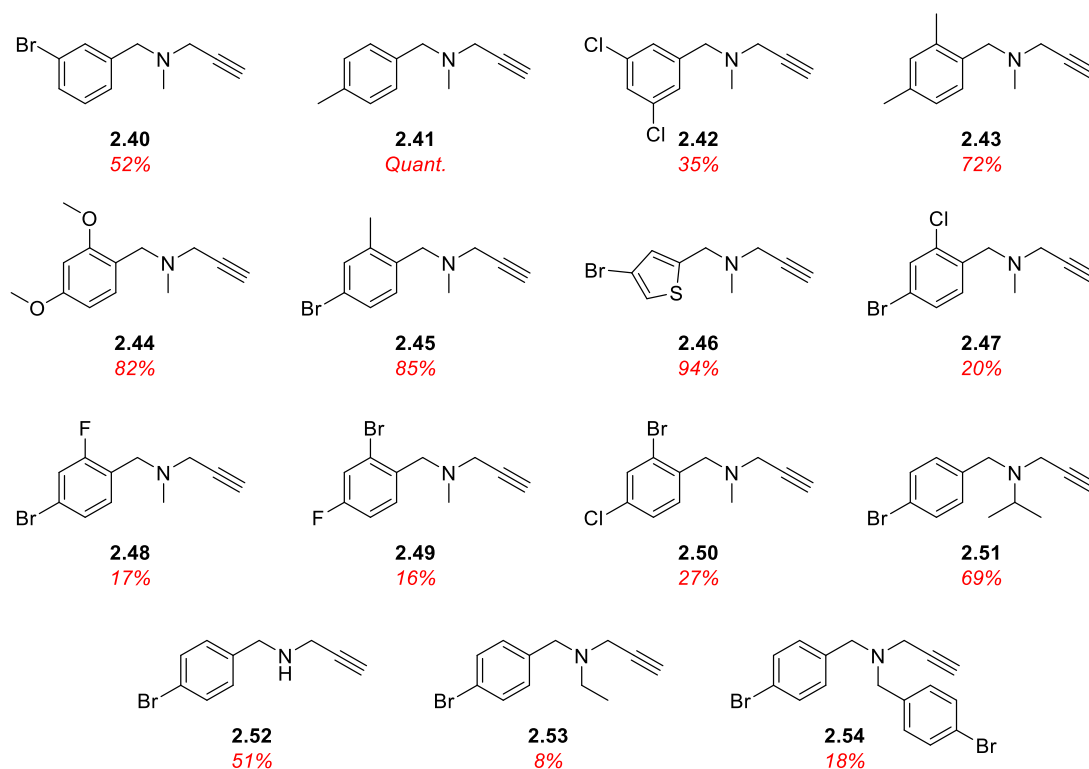
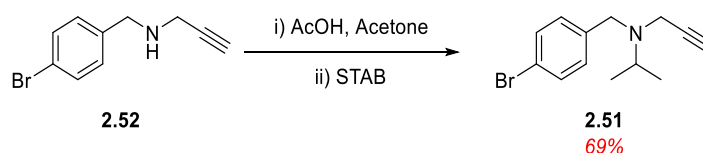


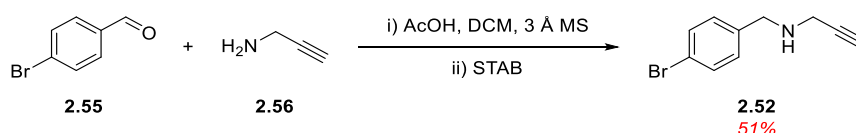
Figure 58: Pargyline analogues synthesised by reductive amination

The standard conditions were modified in the synthesis of compound **2.51** (**Scheme 87**). In this case, DCM was replaced by acetone, which served as both the solvent and the reactive partner. The formation of the iminium intermediate was very slow, as was the reduction meaning that the reaction took four days in total. As the formation of the iminium intermediate is a reversible process, the presence of water in the reaction could be one of the reasons the reaction was slow. One way to accelerate the process would be to sequester the water formed during the reaction. This would disturb the equilibrium and help to move it in the direction of product formation. Unfortunately, acetone undergoes aldol reactions in the presence of molecular sieves and as such it was not possible to add these to the reaction as a drying aid.²⁰⁵



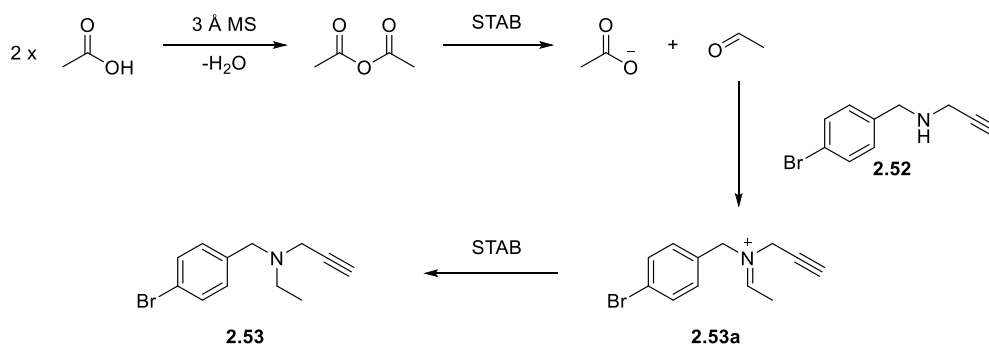
Scheme 87: Modified reductive amination conditions used in the synthesis of compound 2.51

Compound **2.52** also required a modification to the general reaction conditions. To minimise the doubly aminated product **2.54**, propargylamine was in slight excess and 3 Å molecular sieves (MS) were used to sequester the water formed during the reaction as outlined in **Scheme 88** below.



Scheme 88: Modified reductive amination conditions used in the synthesis of compound 2.52

This reaction was relatively successful with 51% of the desired product isolated. As expected, due to **2.52** being more nucleophilic than **2.56**, compound **2.54** was a by-product in this reaction and was isolated in an 18% yield. Unexpectedly, compound **2.53** was also isolated from this reaction mixture. Presumably, the ethyl group is being supplied by the acetic acid in this reaction as it is the only two carbon unit present within the reaction mixture. A tentative reaction mechanism is proposed below in **Scheme 89**.

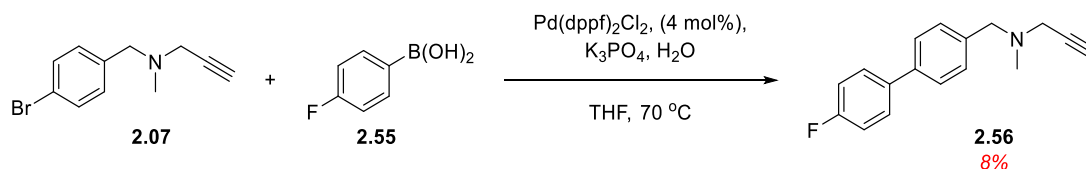


Scheme 89: Tentative reaction mechanism for the synthesis of 2.53

Here, two equivalents of acetic acid are dehydrated by the molecular sieves to form acetic anhydride which is then potentially reduced to acetate and acetaldehyde. The acetaldehyde can then undergo iminium formation with an equivalent of compound

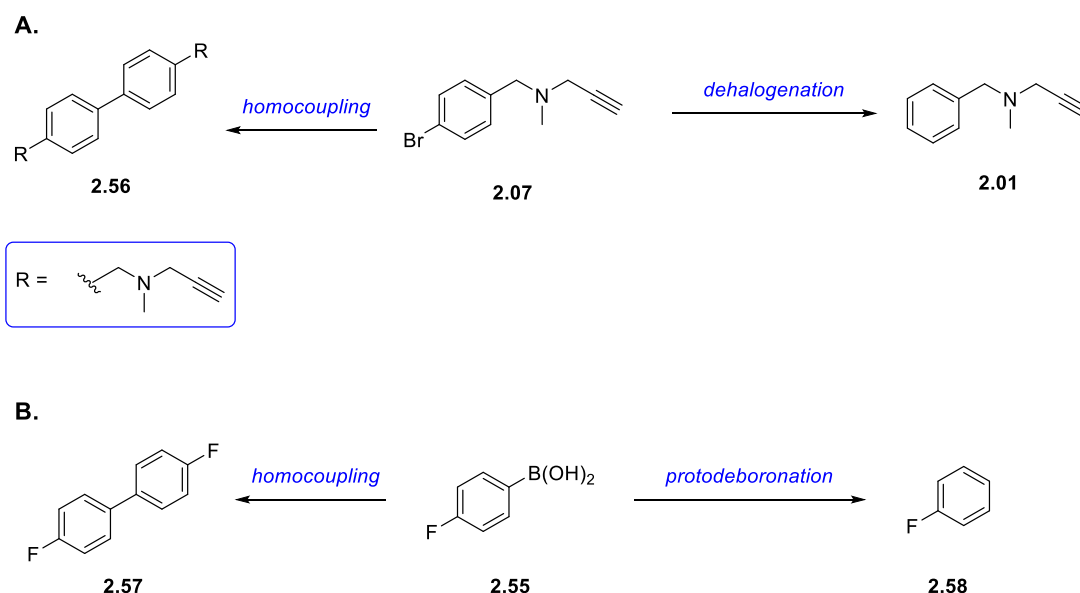
2.52 which is then reduced to compound **2.53**. However, further mechanistic work, such as isotope labelling, would be required to prove this hypothesis.

Suzuki-Miyaura (SM) cross coupling was used to prepare compound **2.56** from a stock of compound **2.07** as shown below in **Scheme 90**.²⁰⁶



Scheme 90: SM conditions employed for analogue synthesis

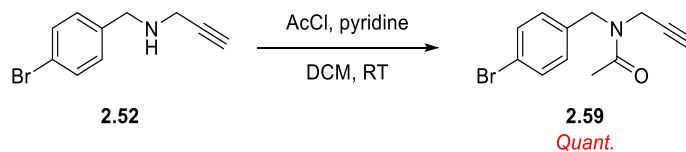
The yield of this reaction was very poor, with only 8% isolated from the reaction mixture. TLC did indicate full consumption of both **2.07** and **2.55**, however this is not indicative of complete conversion to the product as both starting materials have the potential to undergo side reactions such as homocoupling and protodeboronation as outlined below in **Scheme 91**.²⁰⁷



Scheme 91: Potential side reactions and products of the SM conditions. A. Potential reactions of starting material 2.07. B. Potential reactions of starting material 2.55

The reaction profile indicated the presence of several UV active compounds by TLC which could support the presence of either of the compounds outlined in **Scheme 91**. However, these compounds were not isolated or analysed and remain unknown.

Amidation of compound **2.52** with acetyl chloride (**Scheme 92**) furnished compound **2.59** in quantitative yields.

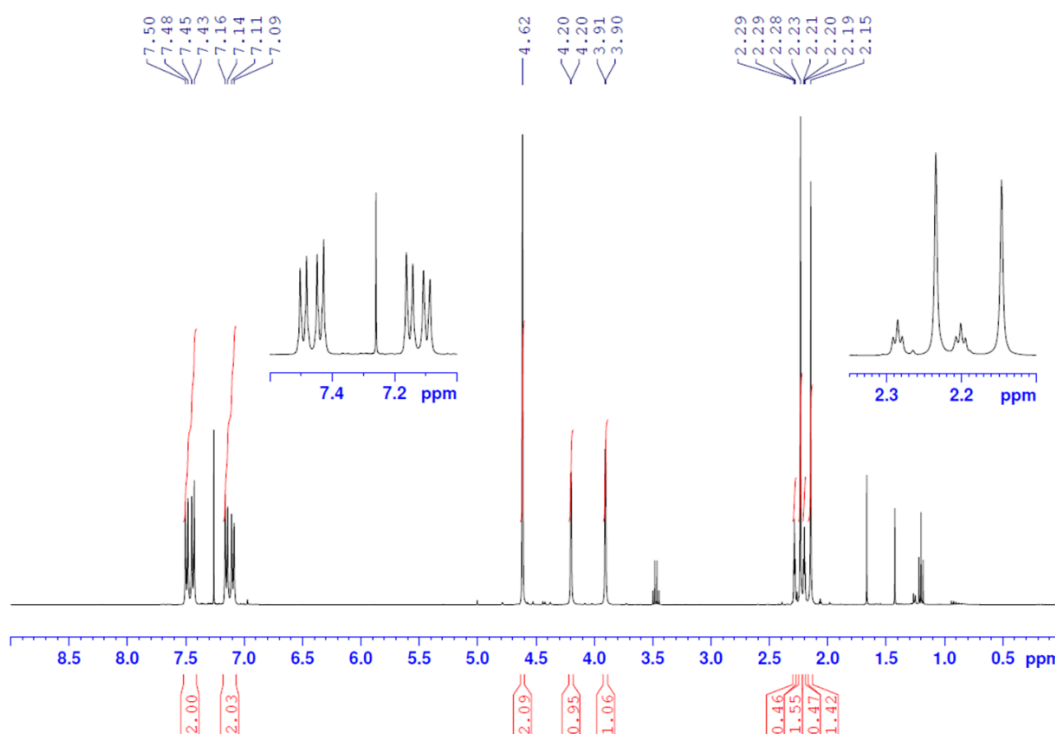


Scheme 92: Amidation conditions used in the synthesis of compound **2.59**

TLC of the isolated material indicated a single compound. However, the ^1H NMR and ^{13}C NMR showed a 1:1 mixture of what could have been two amides (**Figure 59**).

Figure 59: ^1H NMR of compound **2.59**

Su



Subsequent LCMS analysis also returned a single peak which had the correct m/z ratio for $[\text{M}+\text{H}]^+$ (**Figure 60**).

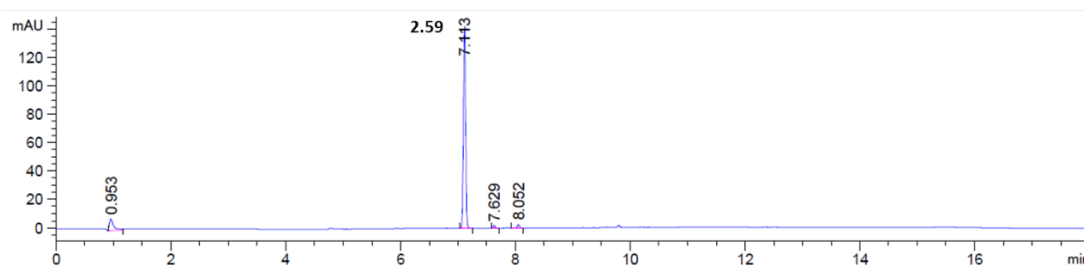
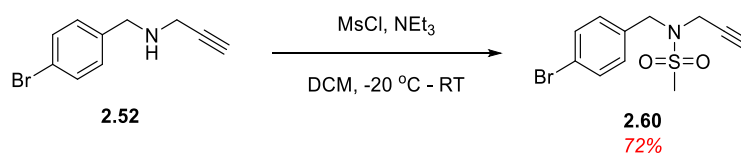


Figure 60:UV trace from the LCMS analysis showing compound **2.59** at $R_t = 7.1$ mins

As both TLC and LCMS indicated **2.59** was a single product, it was determined from the ^1H and ^{13}C NMR that compound **2.59** was rotameric. Attempts to resolve the rotamers by cooling to 214 K and heating to 325 K were unsuccessful. However, the higher temperature experiment did resolve the aromatic peaks. Due to the use of CDCl_3 as the NMR solvent, the temperature range that could be employed was limited and using a higher boiling point solvent, such as dimethylsulfoxide, may better the resolution as higher temperatures could be applied to attempt to break the energy barrier and allow free rotation around the amide bond.

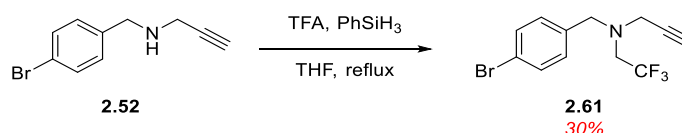
Compound **2.52** was also converted to sulfonamide **2.60** as outlined in **Scheme 93**.



Scheme 93: Mesylation conditions used in the synthesis of compound **2.60**

Synthesis of **2.60** was straightforward and a yield of 72% was obtained after minimal purification.

Finally, attempts were made to add a trifluoroethyl group onto compound **2.52** using chemistry developed by Denton as outlined below (**Scheme 94**).²⁰⁸



Scheme 94: Conditions used in the synthesis of compound **2.61**

While the reaction proceeded as expected, it was difficult to separate the final product with silyl by-products and sufficient purity for biological screening (> 90%)

was not achieved and therefore the compound was not tested in the SAR studies outlined later in the chapter.

2.3.2 Benzyl Group Substitutions

The benzyl group was the first moiety to be assessed by substituting halogens in various positions around the aromatic ring (**Figure 61**).

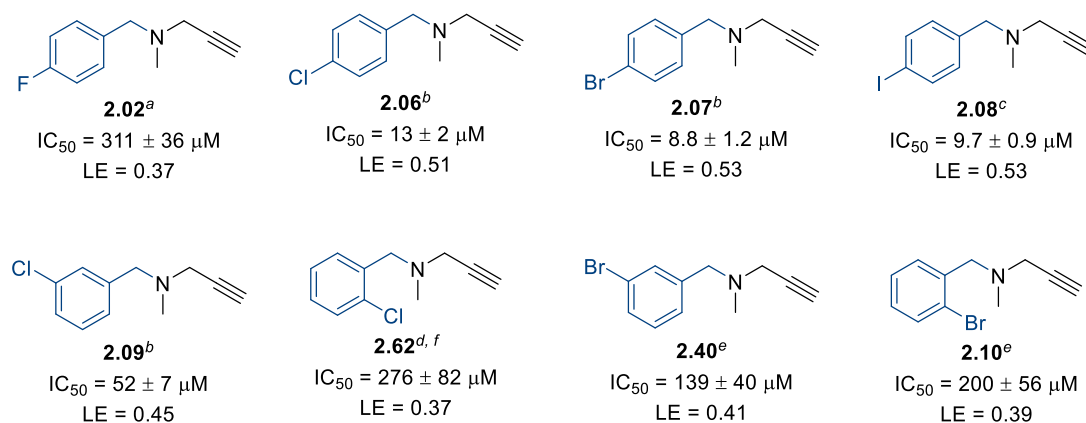


Figure 61: Activities and LE of single halogen substitution of the benzyl group. ^a Pargyline was used as the standard, $IC_{50} = 372 \pm 46 \mu M$; ^b pargyline was used as the standard, $IC_{50} = 198 \pm 29 \mu M$; ^c 2.07 was used as the standard, $IC_{50} = 9.2 \pm 1.0 \mu M$; ^d 2.07 was used as the standard, $IC_{50} = 23 \pm 6 \mu M$; ^e 2.07 was used as the standard, $IC_{50} = 8.6 \pm 2.4 \mu M$; ^f synthesised by another member of the laboratory²⁰⁹

Halogens were the first functional groups introduced due to their synthetic availability and extensive use within the pharmaceutical industry.²¹⁰ Fluorine and chlorine, in particular, have a number of uses within drug discovery and are mainly used to alter the physicochemical properties of compounds.²¹⁰ They have been used to improve the bioavailability of drugs by blocking metabolism at metabolic hotspots, as well as increasing lipophilicity which can help compounds to pass through the blood brain barrier.^{211,212} They are also able to form halogen bonding interactions with electron rich species found within the protein of interest which can include serine, lysine, tyrosine and the amide carbonyl of the protein backbone.²¹³ These halogen bonds have the result that the compounds have a stronger interaction with the protein, which can lead to an increase in potency. Halogen bonding arises when the electron density of a halogen is drawn towards the aromatic ring, which creates an area which has a partially positive charge known as a σ -hole. The σ -hole can then interact with an electron rich system face on.²¹⁴

Pleasingly, all the analogues synthesised were more active than pargyline with the exception of the 2-chlorobenzyl (**2.62**) and the 2-bromobenzyl (**2.10**) derivatives, which had lower activity. This study also identified a trend in the positioning of the halogen atoms around the ring, with the most active compounds having a halogen in the 4-position (**2.06** and **2.07**), and compounds with a halogen in the 2-position being the least active (**2.62** and **2.10**). Compounds substituted in the 3-position (**2.09**, **2.40**) had intermediate levels of activity. This effect could be due to a steric clash in the, as yet unknown, binding pocket of the enzyme. The potencies of the analogues also increased with the increasing size of the halogen atom. This could be a further indication of halogen bonding between the compound and PYCR1 since the strength of a halogen bond increases moving down the group due to the atoms becoming more diffuse.²¹³ It could also be due to steric effects, with the larger group better occupying the space in the binding site. However, further structural data in the form of an X-ray co-crystal structure would be required to corroborate this theory.

The ligand efficiencies (LE) of compounds **2.06**, **2.07**, **2.08**, and **2.09** were also improved. This is mainly due to the increased potency offsetting the effect of adding the additional molecular weight to the compounds.

As it would be much easier to observe the effects of changes in more potent compounds, compound **2.07**, the substrate with the highest potency thus far, was used as a standard in the biological screening from this point on.

In order to further examine the benzyl group, a number of different functional groups were substituted as outlined in **Figure 62**. The functional groups included both electron withdrawing (EWG) and electron donating groups (EDG) primarily in the 4-position, owing to the trend of higher potencies associated with this position in the halogen analogues, although some compounds had substitutions in the 2- and 3-positions (**2.15** and **2.16**) as match pairs to both the chloro- and bromo-analogues.²¹⁵

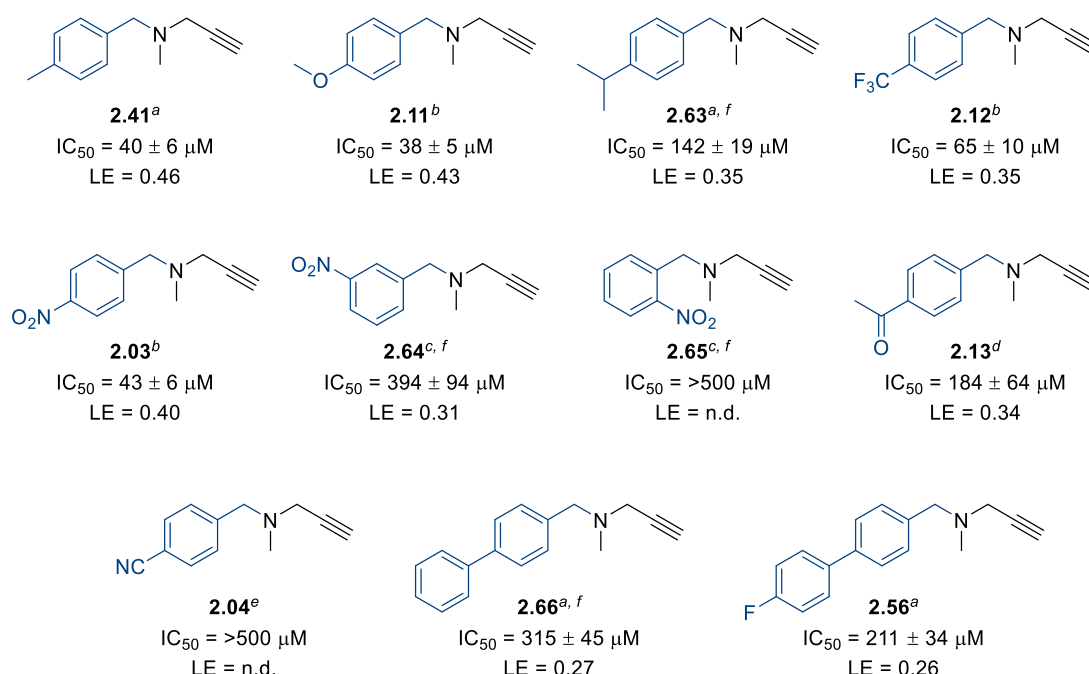


Figure 62: Activities and LE of single substitution of the benzyl group. ^a 2.07 was used as the standard, IC₅₀ = 8.3 ± 1.2 μM; ^b pargyline used as the standard, IC₅₀ = 198 ± 30 μM; ^c 2.07 was used as the standard, IC₅₀ = 10 ± 2 μM; ^d 2.07 was used as the standard, IC₅₀ = 9.7 ± 1.0 μM; ^e pargyline was used as the standard, IC₅₀ = 372 ± 46 μM, ^f synthesised by another member of the laboratory²⁰⁹

Again, most compounds appeared to be more active than pargyline, however, they were not as active as compound **2.07**. Pleasingly, the same pattern of substitution on activity was identified in the nitro-series (**2.03**, **2.64** and **2.65**) with the 4-nitrobenzyl group being the most active of the three, and the 2-nitrobenzyl group being the least active, suggesting that the 4-position was indeed the favoured position for substitution. There also appeared to be no clear preference for EWG or EDG systems, with compounds **2.11** (EDG) and compound **2.03** (EWG) having similar potencies.

With more potent analogues being observed by increasing the size of the halogen in the 4-position, it was decided that larger groups in the 4-position of the benzyl group may have a similar result. Due to the similarities in size between iodine and a benzene ring, it was reasoned that they should fill the same space within the enzyme.^{216,217} Thus, compound **2.07** was subjected to Suzuki-Miyaura (SM) cross coupling with phenylboronic acid and 4-fluorophenylboronic acid using the conditions outlined above in **Scheme 90**.²⁰⁶

Unfortunately, both **2.66** and **2.56** were less active than both pargyline and compound **2.07**. However, this also strengthens the hypothesis that the increase in

potency is not purely due to the size of the group present in the 4-position but also relies on another effect, which potentially could be halogen bonding where the strength of a H-X bond increases with increasing size of halogen atom.¹²⁹

With the previous examples only exemplifying single substitutions on the aromatic ring of the benzyl group, it was decided to incorporate several disubstituted analogues as outlined in **Figure 63**. Again, this was initially examined using various substitution patterns on dichlorobenzyl moieties, in part due to their observed activities as a single substitution as well as their synthetic availability.

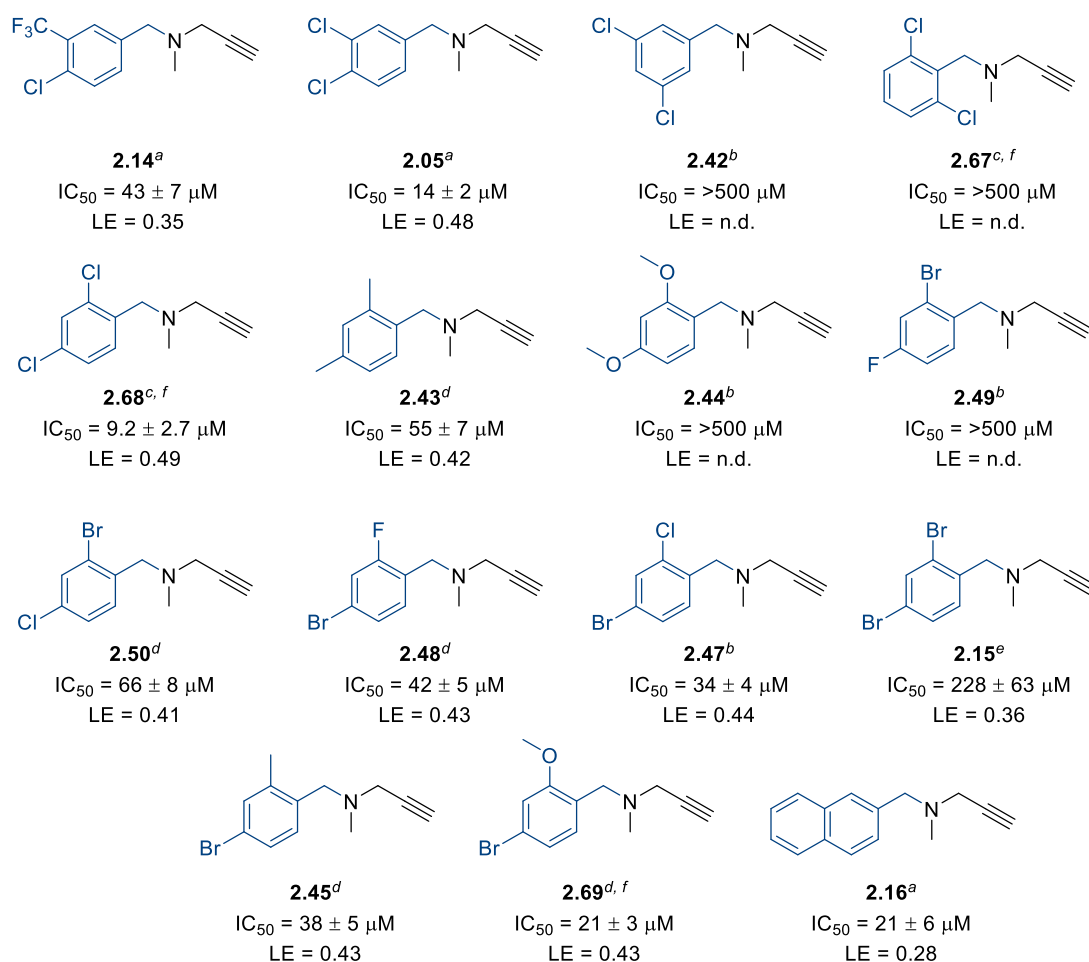


Figure 63: Activities and LE of disubstitution of the benzyl group. ^a 2.07 was used as the standard, IC₅₀ = 9.2 ± 1.0 μM; ^b 2.07 was used as the standard, IC₅₀ = 30 ± 6 μM; ^c 2.07 was used as the standard, IC₅₀ = 23 ± 6 μM; ^d 2.07 was used as the standard, IC₅₀ = 26 ± 3 μM; ^e 2.07 was used as the standard, IC₅₀ = 8.6 ± 2.4 μM; ^f synthesised by another member of the laboratory²⁰⁹

Both the 3,5-dichlorobenzyl (**2.42**) and the 2,6-dichlorobenzyl (**2.67**) analogues were inactive in the assay, while the 3,4-dichlorobenzyl (**2.05**) maintained potency in comparison to the 4-chlorobenzyl derivative (**2.06**). A clear preference for

substitution in the 2,4-positions was observed, with compound **2.68** being slightly more potent than **2.07**. This was unexpected, as on its own, the 2-position had the lowest activity in comparison to the 3- and 4-positions. Thus, it can be reasoned that there may be a second interaction in the binding site which could result in the slight increase in potency observed. With the 2,4-substitution pattern appearing to be favoured, it was then decided to probe this area further by examining the effect of other halogens and alternative functional groups. Unfortunately, none of these analogues matched the activity of **2.68** with respect to **2.07**, although they were all more potent than pargyline. With **2.07** showing a preference for a 4-bromobenzyl group, it was then decided to maintain this as a common factor and alter the functional groups in the 2-position. Pleasingly, a further two compounds showed equal activity with respect to **2.07**, the 4-bromo-2-chlorobenzyl (**2.47**) and the 4-bromo-2-methoxybenzyl (**2.69**) groups. While showing equal activity with **2.07**, compounds **2.68**, **2.47** and **2.69** had a greater number of non-hydrogen atoms and, as such, a lower ligand efficiency. It was also decided to examine a naphthyl derivative as a further modification in the 3,4-position (**2.16**). Much like compound **2.05**, this compound was less active than **2.07** and, again, due to the greater number of non-hydrogen atoms, had a less favourable LE of 0.28.

The first three modification strategies also appeared to follow a Topliss-like pattern with compounds **2.06**, **2.07**, **2.68**.²¹⁸ The Topliss decision tree (Appendix 2) is a method of deciding which aromatic substitutions were most likely to increase the potency of an analogue by comparing the lipophilic (π -value) and electronic (σ -value) effects of a substitution in comparison to the phenyl analogue (in this case, pargyline).²¹⁸ The 4-chloro substitution was the first analogue suggested (**2.06**) which has increased π - and σ -values.²¹⁸ **2.06** was found to be more active than **2.1** and the decision tree then suggested that the next analogue should be the 3,4-dichloro analogue (**2.05**) which should have a further increase to the π - and σ -values.²¹⁸ As **2.05** was equipotent to **2.06**, it suggests either that there could be a steric interaction at the 3-position, or that the lipophilicity is adversely affecting binding. The decision tree then suggests the 4-trifluoromethyl analogue (**2.12**) which has fewer steric interactions, a lower π -value and similar σ -value to **2.06**.²¹⁸ **2.12** was less potent than

2.06, potentially due to halogen bonding in the binding site as discussed above. Topliss also suggests the 4-bromo (**2.07**) and 4-iodo (**2.08**) as alternatives to the 4-trifluoromethyl.²¹⁸ These have a higher π -value but a much lower σ -value and both **2.07** and **2.08** were more potent than both **2.05** and **2.12**, suggesting that the lipophilicity of the substituent is more important for binding than the electronic effects of the substituent. Thus, the next suggested analogue, the 2,4-dichloro **2.68** was examined. This has a similar lipophilicity to **2.08** but does have a larger σ -value. This analogue should limit any steric effects observed with the 3,4-dichloro analogue, however, as discussed above the 2-chloro analogue (**2.62**) was found to have the lowest potency of the 2-, 3- and 4-substituted analogues. It was therefore surprising that compound **2.62** was found to be more potent than compound **2.07**, which could be attributed to an extra interaction in the binding site. Finally, the Topliss tree tests the effect of a high σ -value and low π -value by suggesting the synthesis of the 4-nitro analogue (**2.03**).²¹⁸ This analogue was less active than **2.07** and **2.68**, which suggests that the π -value is more important than the σ -value for the pargyline series.

The final modifications considered the requirement of the benzyl group for binding. Here, the benzyl group was homologated by a single carbon unit, exchanged for 5-membered heterocycles or branched with methyl groups as outlined below in **Figure 64**.

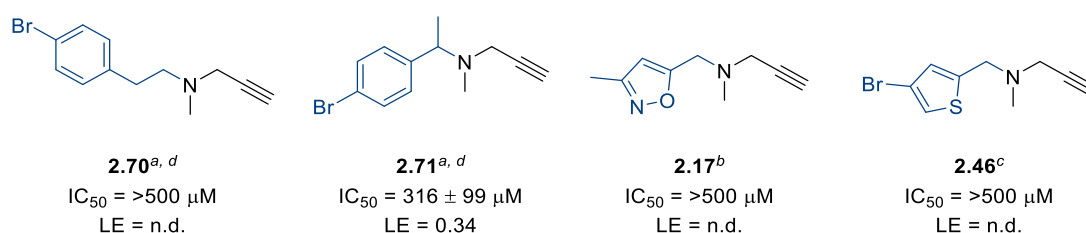


Figure 64: Activities and LE of modifications to the benzyl group. ^a**2.07** was used as the standard, IC₅₀ = 23 \pm 6 μ M; ^b**2.07** was used as the standard, IC₅₀ = 9.2 \pm 1.0 μ M; ^c**2.07** was used as the standard, IC₅₀ = 30 \pm 6 μ M; ^dsynthesised by another member of the laboratory²⁰⁹

It was observed that the benzyl group was essential for activity as both the isoxazole (**2.17**) and thiophene (**2.46**) were inactive. This was particularly surprising as thiophene is an isostere of benzene and therefore the potency of **2.46** would be expected to be similar to **2.07**.²¹⁹ However, overlaying compounds **2.07** and **2.46** (**Figure 65**) revealed that the bromine atom of **2.46** (red, **Figure 65**) could be in the

wrong orientation for binding, resulting in the lower potency of **2.46** in comparison to **2.07**.

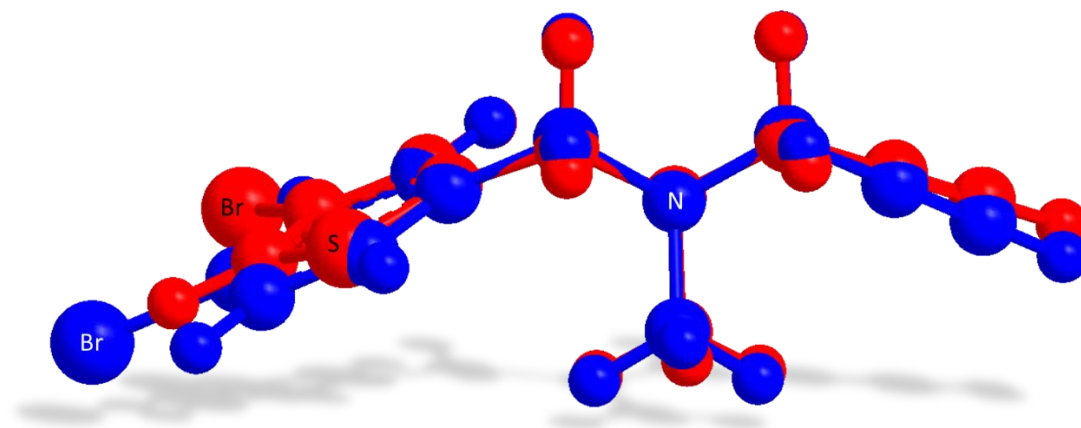


Figure 65: Overlay of compounds **2.07** (blue) and **2.46** (red) generated in ChemBioDraw3D 17.1. Both structures were energy minimised using the MM2 energy minimisation calculation

Homologated compound **2.70** was also inactive. Adding branching to the benzyl group (**2.71**) also significantly reduced activity in comparison to both pargyline and compound **2.07**. This could again be attributed to a steric clash in the binding site.

With compound **2.07** showing the greatest ligand efficiency and excellent potency in comparison to the other analogues, it was decided to maintain the presence of the 4-bromobenzyl moiety in the rest of the study.

2.3.3 *N*-Methyl substitutions

The next stage in the SAR study was modifications to the *N*-methyl group. This location was one of the areas which should tune the selectivity of the compounds towards PYCR1 as literature states that any group larger than a methyl group was inactive at MAO-B.¹⁹⁷ The modifications attempted by Swett *et. al.* are outlined below in **Figure 66**. The assay conditions utilised in this study were markedly different from those utilised by NKI which are outlined above. Here the concentration of a dark brown pigment, which was formed by the action of MAO (a mixture of both A and B were used in the study), was measured and the lighter the colour, the more the enzyme is being inhibited by the compound.

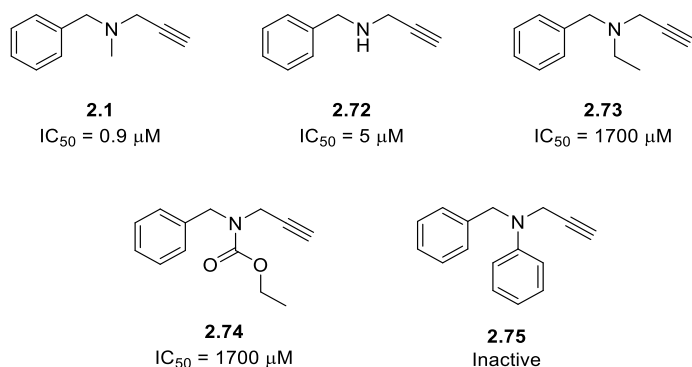


Figure 66: Strategies attempted by Swett *et. al.* to attempt to increase the potency of pargyline towards MAO by altering the *N*-methyl group, all modifications resulted in reduced activity

Thus modifications to the length and branching of the alkyl chain were made as well as the nature of the *N*-alkyl group as outlined below in **Figure 67**.

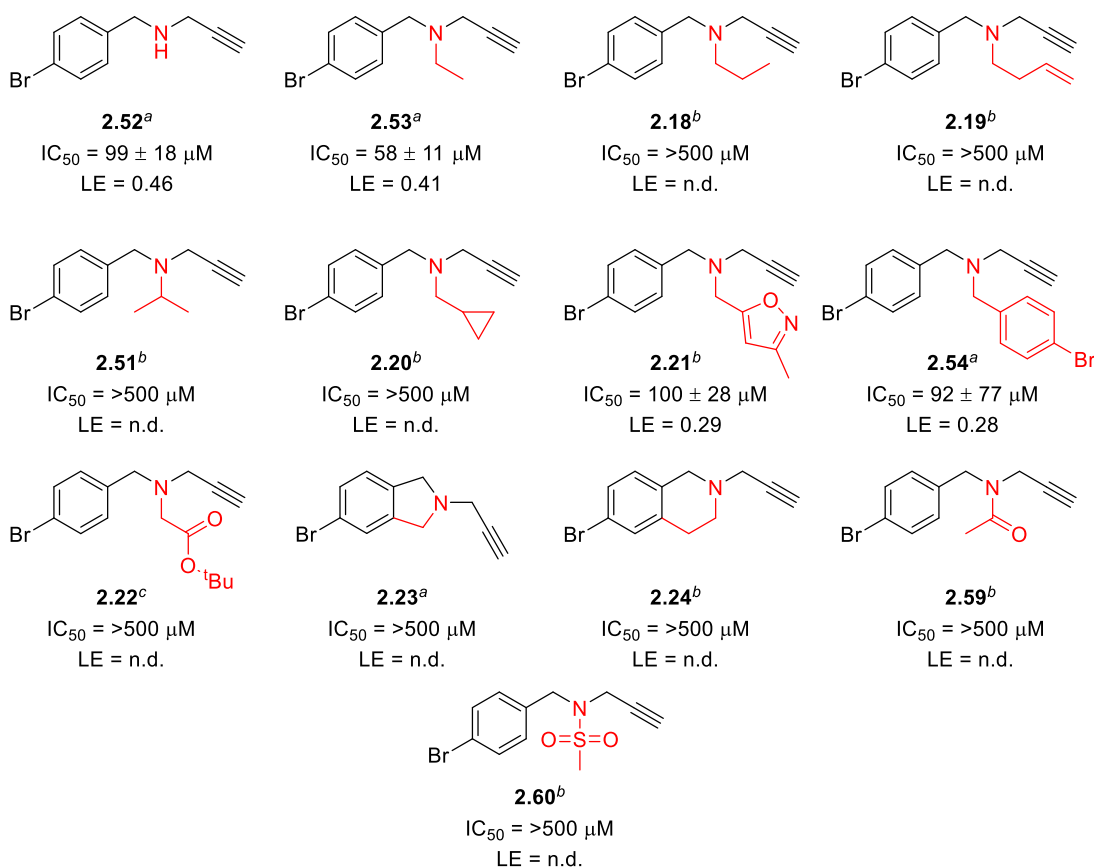


Figure 67: Activities and LE of modifications to the *N*-methyl group. ^a2.07 was used as the standard, $IC_{50} = 15 \pm 3 \mu M$; ^b2.07 was used as the standard, $IC_{50} = 23 \pm 6 \mu M$; ^c2.07 was used as the standard, $IC_{50} = 26 \pm 3 \mu M$

Unlike the benzyl group, there was less tolerance in this area with only four analogues showing any activity against the enzyme. Much like the SAR around pargyline any moieties larger than a methyl group were mostly inactive. The exceptions were the

secondary amine (**2.52**), ethyl group (**2.53**) and surprisingly the aryl compounds **2.21** and **2.54** which had some activity at the enzyme, however, all three were significantly less active than **2.07**. Again, the lack of activity could possibly be attributed to the steric requirements of the alkyl chains, however, this hypothesis is not consistent with the activity observed for the aryl groups. In this case, there could be additional interactions, such as π -stacking or hydrogen bonding within the binding pocket, which could give rise to the observed activity and structural data would be able to confirm this hypothesis. The next modification examined was the tethering of the alkyl chain to form the isoindoline and tetrahydroisoquinoline (**2.23** and **2.24**, respectively). Both of these analogues were inactive, perhaps due to the rigidity of the fused ring systems of the isoindoline and tetrahydroisoquinoline, respectively, restricting the ability of the compound to rotate into the correct conformation for binding. Finally, the basicity of the nitrogen core was removed by forming the amide and sulfonamide (**2.59** and **2.60**). Again, the analogues were inactive, suggesting that a basic nitrogen centre is required for activity, indicating a potential π -cation interaction with the enzyme if the amine is protonated at physiological pH. The amide could also be restricting free rotation as the compound was isolated as a mixture of rotamers, which could prevent the compound from reaching the ideal conformation for binding.

The original *N*-methyl group displayed the greatest activity in the enzyme assay and it was decided that it was optimal for potency at PYCR1. This motif was then incorporated within the final batch of analogues. Unfortunately, this moiety could make it difficult to lower the affinity of the potential tool compounds towards MAO-B.

2.3.4 Propargyl Group Substitutions

The final area of modification to be studied was the propargyl group. This area was also of interest as alterations to this group can also help reduce activity at MAO-B. As outlined below in **Figure 68**.¹⁹⁷

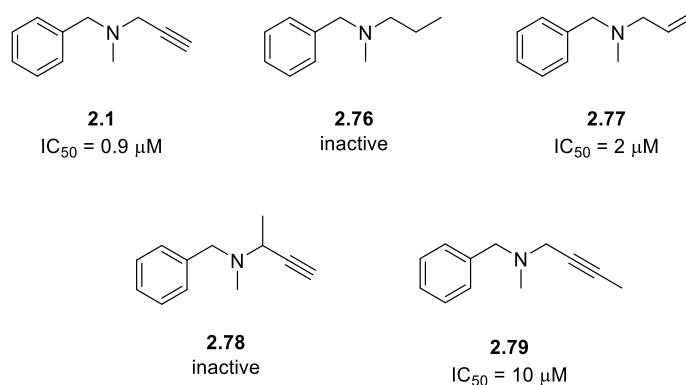


Figure 68: Strategies attempted by Swett *et. al.* to attempt to increase the potency of pargyline towards MAO by altering the propargylic group, all groups showed reduced activity.

Swett *et. al.* identified that almost all modifications to the propargyl group reduced the potency of pargyline towards MAO and it was reasoned that adopting the alterations above would help to improve the selectivity of the tool compounds towards PYCR1. Thus, a series of analogues were synthesised as outlined below in **Figure 69**.

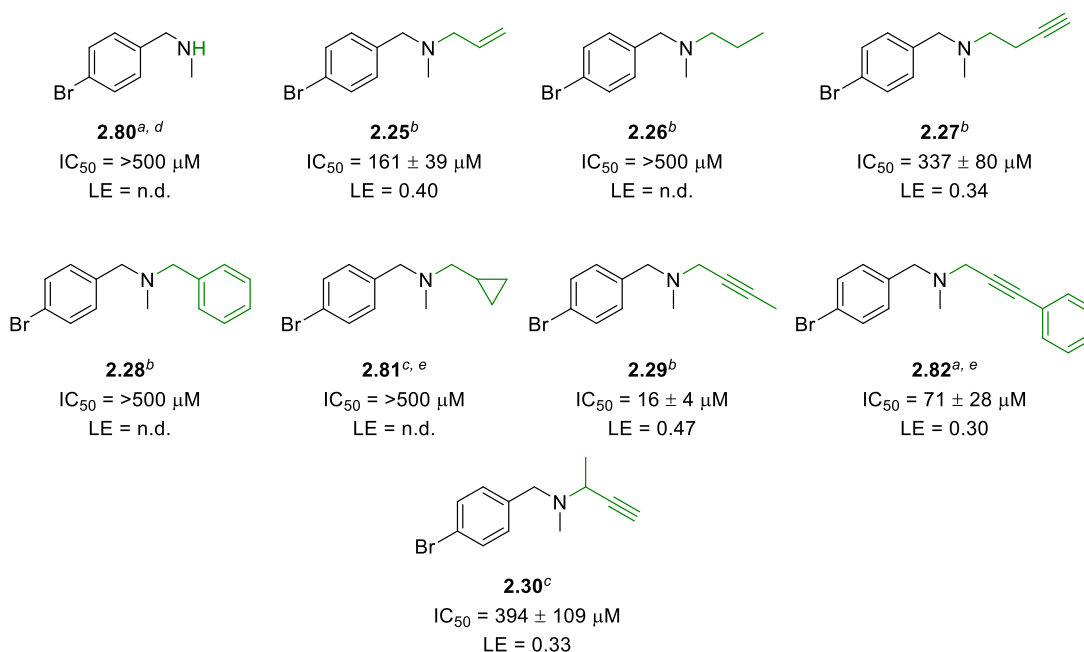


Figure 69: Activities and LE of modifications to the propargyl group. ^a2.07 was used as the standard, $IC_{50} = 15 \pm 3 \mu M$; ^b2.07 was used as the standard, $IC_{50} = 10 \pm 2 \mu M$; ^c2.07 was used as the standard, $IC_{50} = 8.6 \pm 2 \mu M$; ^dcommercially available; ^esynthesised by another member of the laboratory²⁰⁹

As with the *N*-methyl group, there was limited scope for modification. Completely removing the propargyl group (**2.80**) resulted in an inactive compound, suggesting that the propargyl group is required for activity. The next compounds screened the

effects of modifying the propargyl group to the allyl and propyl groups (**2.25** and **2.26**, respectively). The propyl group was inactive; however, the allyl group showed some residual activity. The activity was equivalent to pargyline but markedly less active than **2.07**. Single carbon homologation in the linker region (**2.27**) was even less active, suggesting that the propargylic nature of the group was preferred for activity. This was further exemplified when the propargyl group was exchanged for a benzyl and cyclopropyl group (**2.28** and **2.81**) with both being inactive. Branching in the linker region (**2.30**) also reduced activity, which could be caused by steric effects in the binding pocket. Finally, the nature of the alkyne was assessed, by comparing terminal alkynes with internal alkynes as again this could be another means to limit the activity for MAO-B. Pleasingly, compounds **2.29** and **2.82** were found to be active with **2.29** having a similar potency to compound **2.07**. This proved that there was no requirement for a terminal alkyne. However, compound **2.82** was significantly less potent than **2.07**, perhaps due to the steric bulk of the phenyl ring in the binding site of the enzyme.

This part of the study therefore concluded that the original propargyl group of compound **2.07** was optimal for potency.

Throughout the study, it has been found that the SAR of the pargyline analogues at PYCR1 closely follows that of MAO-B in that both the *N*-methyl group and the propargyl group are required for activity and most alterations resulted in compounds with much reduced activity at PYCR1 as outlined below in **Figure 70**. This could make it difficult to acquire selectivity for PYCR1 over MAO-B. There was, however a much greater scope around the benzylic moiety, with a large range of functional groups tolerated, and a clear preference for halogen substituents was identified. As stated above, this could potentially be due to halogen bonding with the enzyme. It was found that substitutions in both the 4-position and 2,4-positions were optimal for potency and compounds **2.07** and **2.68** were found to be the most potent compounds tested which correlated with a Topliss decision tree. However, compound **2.07** had the best ligand efficiency and it was taken forward into further testing as the lead compound in assays which could be used to validate PYCR1 as an oncology target.

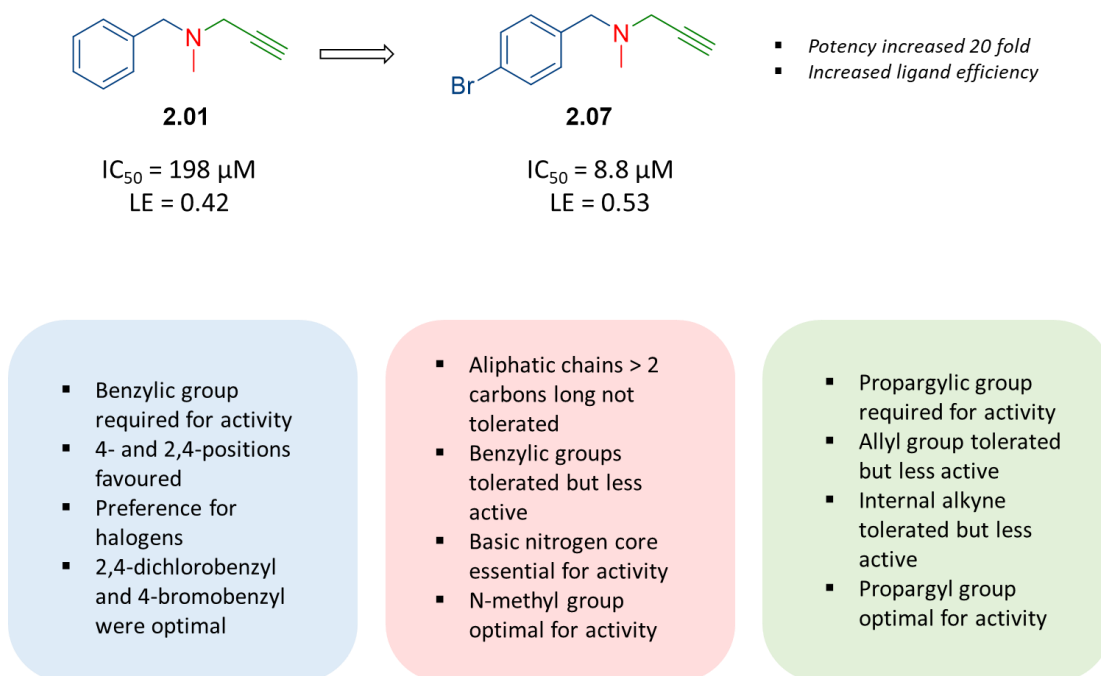


Figure 70: Summary of the SAR studies on the pargyline analogues showing the differences between the parent compound 2.1 and the lead compound 2.07

2.3.5 Further Biological Studies with Compound 2.07

Firstly, our collaborators in the Agami group at NKI attempted to grow a co-crystal with compound **2.07** and PYCR1, in order to establish the binding site and mode for the series, which could be used for *in silico* screening and structure-based compound design. Unfortunately, while there were crystals of PYCR1 present, when submitted to the X-ray conditions, compound **2.07** was not detected. Nevertheless, it was decided to go ahead with further biological evaluation of lead compound **2.07**.

Our collaborators then performed a commercial MAO assay kit to determine the activity of **2.07** at MAO-B. The assay was based around the breakdown of tyramine by MAO-B. This reaction released an equivalent of hydrogen peroxide which activated horseradish peroxidase (HRP) and oxidised the fluorometric probe OxyRed™ to resorufin as outlined in **Figure 71**. The fluorescence at 535 nm and 587 nm is then recorded and compared to a calibration curve to determine the concentration of hydrogen peroxide which can then be used to calculate the IC_{50} .

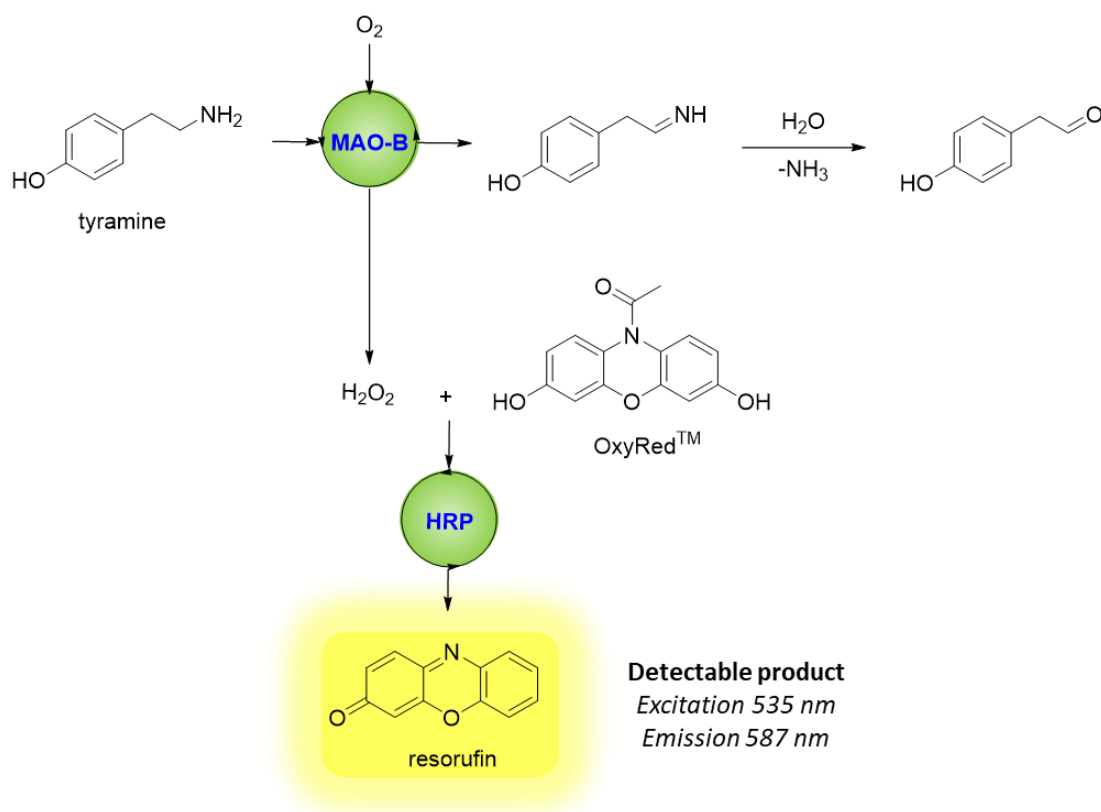


Figure 71: Assay format used in the determination of the inhibition of MAO-B

Fortunately, the compound was less active at MAO-B than pargyline, with an IC_{50} of 300 nM as opposed to an IC_{50} of 8.2 nM. However, this activity was still higher than the activity of **2.07** at PYCR1. While disappointing, this provided proof of concept that the activity towards PYCR1 could be improved by modifying the benzyl group and with the aid of an X-ray co-crystal structure, it may be possible to further tune this activity towards complete selectivity for PYCR1.

Despite the observed MAO-B activity, it was decided to carry out some *in vitro* cell-based assays to investigate if it was possible to observe any pathway-relevant phenotypic effects. Since PYCR1 catalyses the formation of proline within the cell, it was reasonable to assume that inhibition of PYCR1 should result in lowered levels of proline. This hypothesis was corroborated by the incubation of a human breast cancer cell line (SUM-159-PT) which relies on PYCR1 for cell proliferation and tumour expansion with and without compound **2.07**, using pargyline as a positive control as outlined below in **Figure 72**. The cells were then lysed and the amount of proline within the cells quantified using liquid chromatography-mass spectroscopy (LCMS).

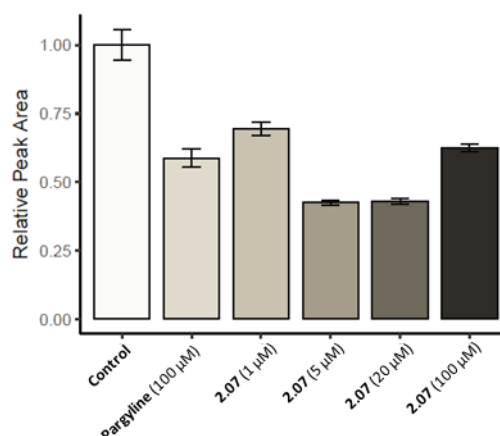


Figure 72: Effect of pargyline and compound **2.07** on the proline levels of the SUM-159-PT breast cancer cell line carried out by the Agami group at NKI

Pargyline was found to reduce the Pro levels by approximately 50% at a concentration of 100 µM. Pleasingly, compound **2.07** had a similar effect to pargyline but at a lower concentration of 1 µM with a dose dependent response observed with increasing concentrations of **2.07** until 100 µM where the effect is apparently diminished. This was attributed to the poor solubility of the compound in the cell media. With both pargyline and **2.07**, levels of the essential amino acids phenylalanine (Phe), methionine (Met), leucine (Leu), tryptophan (Trp), valine (Val) and isoleucine (Ile) were not affected (**Figure 73**) which shows that, for amino acids, **2.07** is selective only towards the inhibition of proline, indicating a pathway relevant effect. This suggests that the reduction of proline observed is mediated through PYCR1 inhibition.

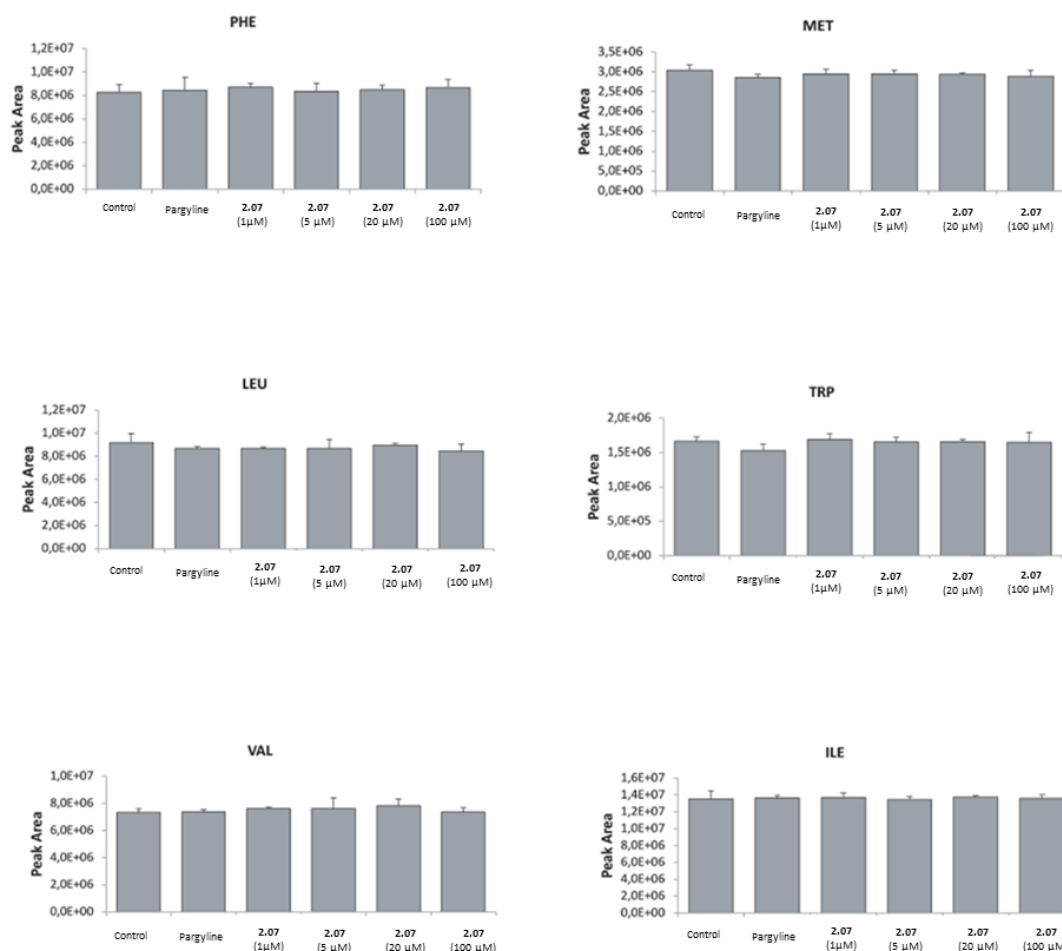


Figure 73: Effect of pargyline and compound 2.07 on the levels of essential amino acids in SUM-159-PT cells carried out by the Agami group at NKI

The reduction in proline was further exemplified by utilising a ^{13}C glutamine (Gln) flux experiment. Glutamine is a precursor to glutamic acid which serves as the starting point for proline biosynthesis. Here the cells were incubated with a mixture of fully ^{13}C labelled glutamine ($[\text{U-}^{13}\text{C}]\text{-Gln}$) and unlabelled glutamine, which is broken down into glutamic acid, and the level of ^{13}C incorporation in proline measured by mass spectroscopy. As Gln has five carbon atoms, the mass of the fully labelled proline would be expected to be $[\text{M}+5]$. However, Gln is also able to participate in other cellular processes and as such a small amount of $[\text{M}+3]$ was also detected. As shown below in **Figure 74**, cells incubated for 24 hours with compound **2.07** had less ^{13}C incorporation than those which had not. This data again strongly indicated that the reason for the reduced proline levels within the cells incubated with compound **2.07** was due to the inhibition of PYCR1.

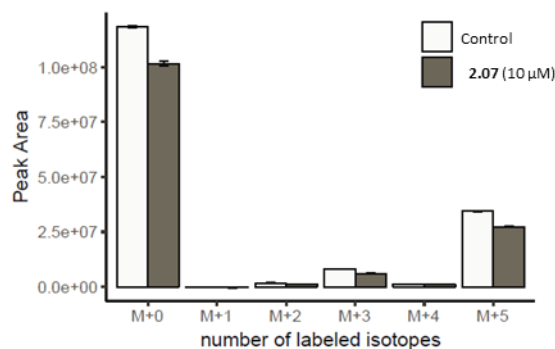


Figure 74: Results of the glutamine flux assay which show reduced incorporation of ^{13}C in cells treated with compound **2.07** (10 μM) carried out by the Berkers group at Utrecht University

The final *in vitro* experiments performed studied the effect of compound **2.07** on the proliferation of cells. Here, two breast cancer cell lines which were known to overexpress PYCR1 (MDA-MB-231 and SUM-159-PT) were incubated with compound **2.07** and the cell proliferation measured as the percentage confluence across a given area. The control experiments were run without compound **2.07** and both with and without exogenous proline. There was no significant difference between both experiments with both cell lines (**Figure 75**) which showed that the presence of Pro had no negative effect on the proliferation of the cells.

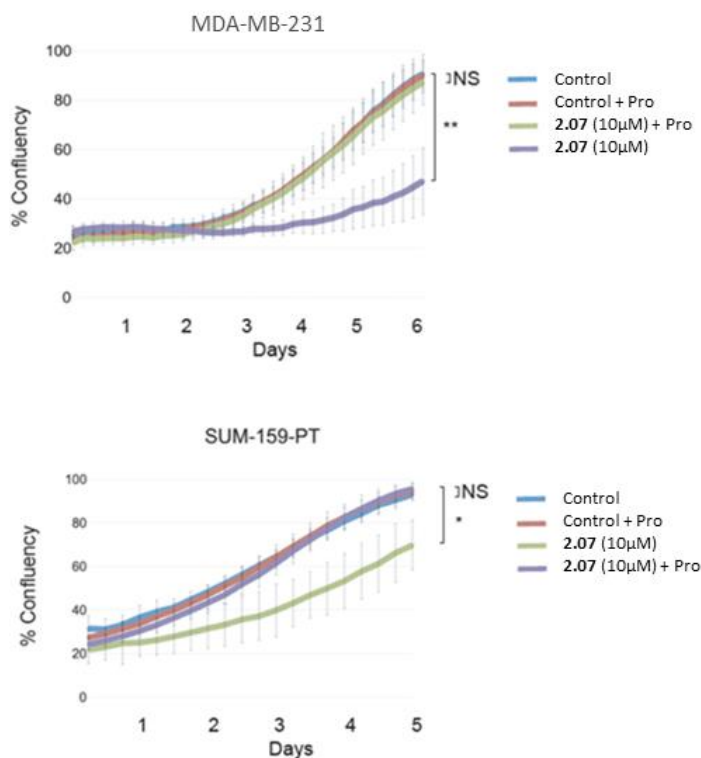


Figure 75: Results of the *in vitro* cell proliferation study in both MDA-MB-231 and SUM-159-PT breast cancer cell lines as carried out by the Agami group at NKI

However, when the cells were incubated with compound **2.07** at a concentration of 10 µM, the percentage confluency decreased by around 40% for the MDA-MB-231 cell line (top, **Figure 75**) and 30% for the SUM-159-PT cell line, suggesting that compound **2.07** was inhibiting cell proliferation. In an effort to prove that this phenomenon was due to the effect of reduced proline caused by the inhibition of PYCR1, the experiment was repeated in the presence of exogenous proline. In both cell lines, growth was rescued by the proline with no significant difference found with the control experiments. This proved unequivocally that the reduction of cell proliferation observed was due to compound **2.07** inhibiting PYCR1 and causing a reduction in Pro, which disrupted the cell cycle.

The success of the *in vitro* experiments then led to testing efficacy *in vivo*. Due to the presence of metabolic hotspots, it was suspected that compound **2.07** may be cleared rapidly when dosed orally or intravenously. The metabolism of pargyline had already been studied and a range of metabolites reported (**Figure 76**).²²⁰ These

include *N*-dealkylations of the benzyl, propargyl and methyl groups as well as *N*-oxidation.²²⁰

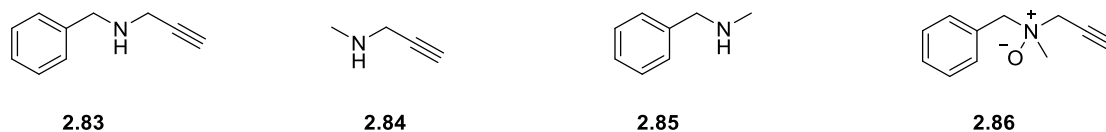


Figure 76: Metabolic fate of pargyline²²⁰

As compound **2.07** was structurally related to pargyline, it could be reasoned that it would have a similar metabolic fate and could generate the following metabolites (Figure 77).

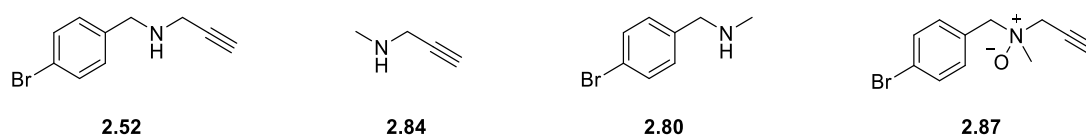


Figure 77: Potential metabolic fate of compound **2.07**

As shown above in sections **2.3.3** and **2.3.4**, compound **2.52** had reduced activity at PYCR1 and compound **2.80** was inactive and would greatly reduce any observed activity of **2.07** *in vivo*.

Accordingly, clearance studies were carried out in mice. 5 mice were dosed with compound **2.07** to achieve an initial blood concentration of 100 nM. The concentration of compound present in the blood was then measured after 5 hours. As suspected, due to these metabolic hotspots, compound **2.07** was rapidly cleared from the blood in only 5 hours as shown below in Figure 78.

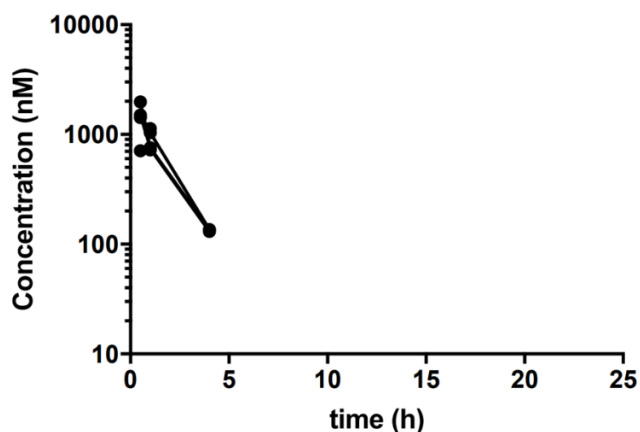


Figure 78: Results of the *in vivo* clearance studies as carried out by the Agami group at NKI

In view of the suboptimal pharmacokinetic data, it was thought that direct injection of compound **2.07** into the tumour compartment would help to overcome the high clearance observed and therefore, the study commenced using the same two breast cancer cell lines as the *in vitro* cell proliferation studies: MDA-MB-231 and SUM-159-PT. The cancer cells were injected into a single mammary fat pad of 20 immunocompromised mice per cell line and divided into the control and treatment groups. The control groups did not receive compound **2.07**, while the treatment group were dosed with compound **2.07** (50 μ L of a 200 μ M stock solution of compound **2.07**, daily for 14 days) by injection into the tumour compartment. The tumour volume of each group was measured three times per week for 11 weeks for the MDA-MB-231 cell line and three times per week for 9 weeks for the SUM-159-PT cell line as shown below in **Figure 79**.

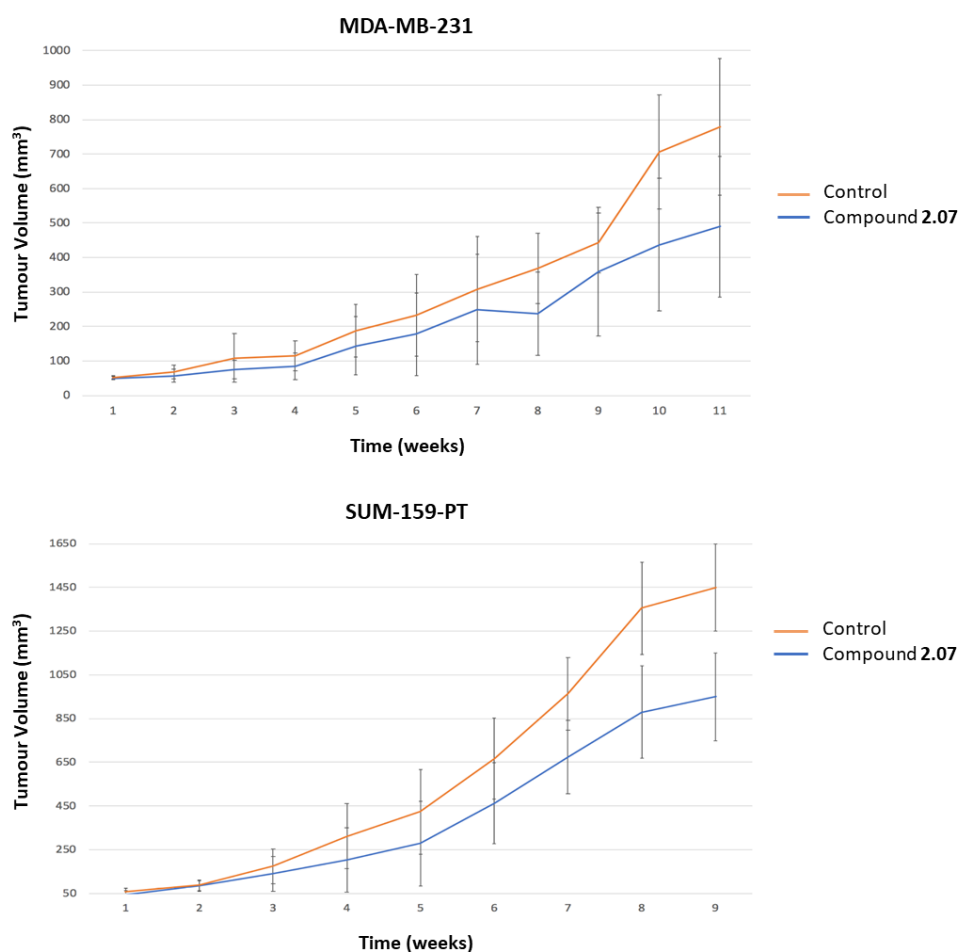


Figure 79: Results of the *in vivo* tumour growth studies in xenograft mouse models of MDA-MB-231 and SUM-159-PT cell lines as carried out by the Agami group at NKI

Pleasingly, both cell lines showed a reduction in the tumour volume, however only the SUM-159-PT cell line showed a statistically significant effect. This showed that compound **2.07** is capable of slowing the growth of tumours *in vivo* despite the poor pharmacokinetics.

To the best of our knowledge, this is the first known example of a small molecule inhibitor of PYCR1 which has been shown to directly affect the production of proline and the proliferation of breast cancer cell lines *in vitro* and shown some effect on slowing the growth of tumours *in vivo*. The outcomes of these studies were consistent with those of the knockout studies performed by NKI (discussed above in **section 2.1**) and further exemplified PYCR1 as a valid oncology target.

2.4 Conclusion

In conclusion, 60 pargyline analogues were synthesised and tested in an enzyme activity assay. The key findings of this SAR study found that there was very little tolerance in the propargyl and *N*-methyl groups, with these moieties showing the greatest activity. There was more scope for variation around the benzyl group, with the 4-substitution and the 2,4-disubstitution being the most tolerated. The 4-bromobenzyl group (**2.07**) was found to be the most active, with an improved ligand efficiency of 0.53 and IC₅₀ of 8.8 µM, representing a 20-fold increase in activity compared to pargyline. Based on this, compound **2.07** was taken through as a lead compound into further pathway-relevant *in vitro* and *in vivo* studies. These studies showed that compound **2.07** was effective, reducing proline levels, and this could be attributed to inhibition of PYCR1. This effect resulted in a reduction of cell proliferation both *in vitro* and displayed modest effects on tumour growth *in vivo*, the first time this phenomenon has been observed for a small molecule PYCR1 inhibitor. Unfortunately, compound **2.07** was more selective towards MAO-B than PYCR1 and attempts to limit this activity were unsuccessful as literature-based strategies also resulted in a loss of activity at PYCR1. Attempts at generating an X-ray co-crystal structure of PYCR1 and **2.07** were also unsuccessful and, to date, the binding site and mode of action of **2.07** are still unknown.

2.5 Future work

As there is currently a plateau in the activity for PYCR1, future work for this project depends greatly on the successful generation of an X-ray co-crystal structure. This would allow for *in silico* screening, which would potentially aid the design and synthesis of more potent and selective compounds. There is also a lack of heterocyclic and saturated compounds, such as pyridyl or cyclohexyl, prepared in the benzyl position. The pyridyl analogues would add an extra hydrogen bond acceptor which may increase the potency and selectivity at PYCR1 as Swett *et. al.* had tested a 2-pyridyl analogue of pargyline, which was found to be less potent towards MAO-B.¹⁹⁷ The cyclohexyl motif was also found to be inactive in the MAO-B assay employed by Swett and if active in PYCR1 it could provide the selectivity required for a tool compound.¹⁹⁷ It may also be beneficial to test other pargyline-related drugs, such as rasagiline, as this may also provide useful scaffolds for future development (**Figure 80**).

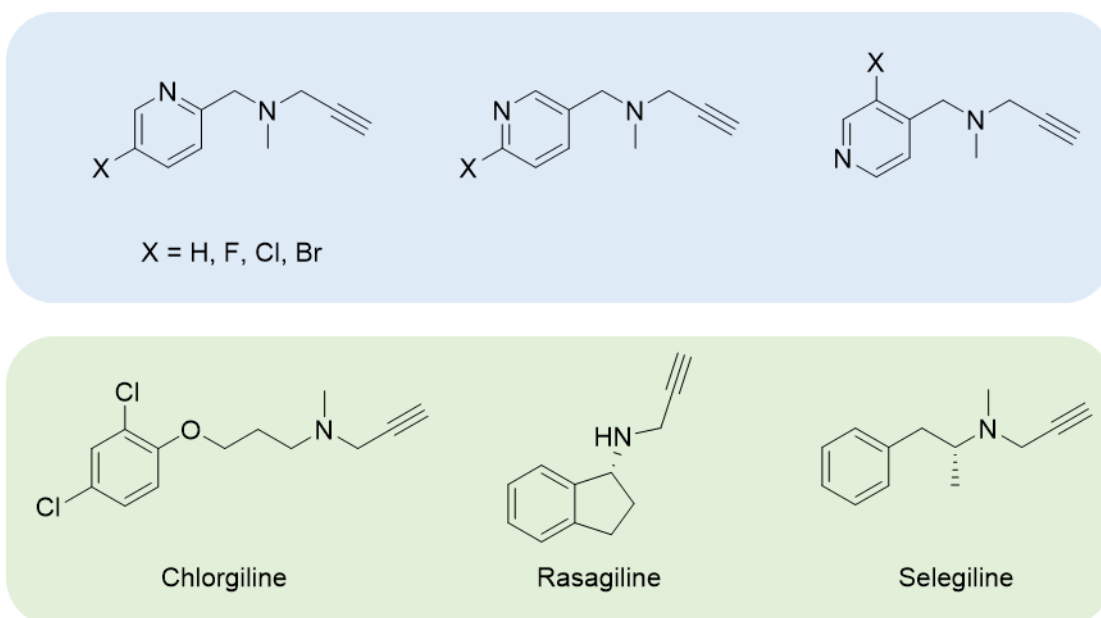
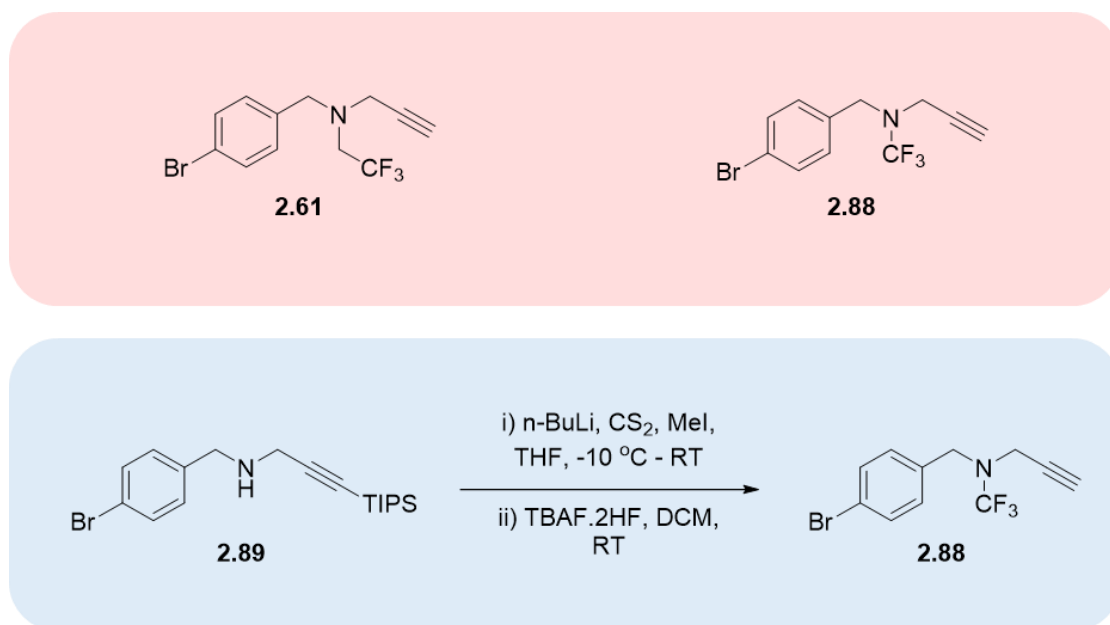


Figure 80: Some new analogues for testing in the PYCR1 assay. Top: heterocyclic incorporation into the benzyl region. Bottom: Other pargyline-related drugs.

It would also be of use to determine if compound **2.07** was a reversible or irreversible inhibitor and further insight into the mechanism of action may be gained from an X-ray crystal structure, or further biochemical assays.

It would also be a benefit to further examine methods of improving the pharmacokinetics of the analogues. However, attempts to block the benzylic and propargylic positions with methyl groups resulted in inactive compounds. Thus, it may be of benefit to revisit the fluorination chemistry in order to block metabolism of the *N*-methyl group, while minimising the steric effects. Thus, the analogues proposed in **Scheme 95** could be synthesised. The synthesis of compound **2.61** has already been discussed in **section 2.3.1**, however, it was difficult to purify. Further purification attempts would be applied to this compound in order to reach the desired purity. Compound **2.88** could be synthesised using the reaction conditions outlined below in **Scheme 95**.²²¹ The alkyne would have to be protected using triisopropyl silane (TIPS) to prevent unwanted side reactions with *n*-butyl lithium and the 4-bromo had been utilised in the literature using these conditions and found to deliver the desired product of the first step in 87% yield.



Scheme 95: Proposed fluorinated analogues (top); proposed route to compound 2.88 (bottom)²²¹

Overall, there is further scope within the series to address the issues identified leading to improved compounds which could be re-evaluated in the *in vitro* and *in vivo* assays described above.

3 Experimental

3.1 General

NMR spectra were recorded on Bruker AV3HD-500 and AV3-400 spectrometers using the deuterated solvent as the lock and the residual solvent as the internal reference. Chloroform is referenced at 7.26 ppm in ^1H NMR and 77.16 ppm in ^{13}C NMR. DMSO is referenced at 2.50 ppm in ^1H NMR and 39.52 ppm in ^{13}C NMR. Methanol is referenced at 3.31 ppm in ^1H NMR and 49.00 ppm in ^{13}C NMR. ^{13}C NMR was proton decoupled and all signals are singlets unless reported otherwise. $^{13}\text{C}\{^{19}\text{F}\}$ NMR is fluorine decoupled to the relevant fluorine shift and signals are all ^1H coupled. Multiplicities are presented as follows: s – singlet, d – doublet, t – triplet, q – quartet, quin – quintet, sept – septet, m – multiplet, dd – doublet of doublets, dt – doublet of triplets, dq – doublet of quartets, ddd – doublet of double doublets, br – broad, qd – quartet of doublets, td – triplet of doublets.

High resolution mass spectrometry was carried out at the EPSRC National Mass Spectrometry Facility at Swansea University using either a Thermo Scientific LTQ Orbitrap XL or Waters Xevo G2-S.

Fourier Transformed Infra-Red (FTIR) spectra were obtained using either an A2 Technologies ATR 32 IR spectrophotometer or a Shimadzu IRAffinity-1 FTIR spectrophotometer.

Chiral normal phase HPLC was carried out using an Agilent 1260 Infinity system using a Chiralpak IA (Amylose tris(3,5-dimethylphenylcarbamate)) column with hexane and 2-propanol as the eluent system.

Reverse phase HPLC was carried out using an Agilent 1260 Infinity system using a Machery-Nagel Nucleodur C18 column with 0.1% TFA spiked water and 0.1% TFA spiked acetonitrile as the eluent system.

Analytical TLC was performed on pre-coated silica gel plates with aluminium backing (E. Mercke, A.G. Darmstadt, Germany. Silica gel 60 F254, 0.2 mm). Spots were visualised under UV light (254 nm) or with vanillin, ninhydrin or potassium permanganate stains. Preparative TLC was performed on 20 x 20cm glass plates pre-

coated with silica gel (Whatman. PK6F silica gel 60 Å, 1000 µm thickness). Bands were visualised under UV light (254 nm) scraped with a clean scalpel and the product eluted with a suitable solvent system through a fritted cartridge. Column chromatography was carried out using silica gel (Zeochem, Zeoprep 60HYD, 40-63 nm) using a glass column and analytical grade solvents. Kugelrohr distillation was carried out using a Büchi Kugelrohr oven at atmospheric pressure or with a high vacuum pump. Phase separations were accomplished using Isolute SPE Accessories phase separators.

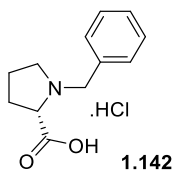
Glassware used for anhydrous reactions was dried in an oven overnight at 150 °C and cooled under an argon or nitrogen atmosphere. Diglyme was distilled over CaH₂ and stored at room temperature over 3 Å molecular sieves under argon or nitrogen. Benzene was dried over 3 Å molecular sieves and stored at room temperature under a nitrogen atmosphere. Methanol was dried over 3 Å molecular sieves then distilled and stored over molecular sieves. Acetone was dried by standing over oven-dried magnesium sulfate in an oven-dried conical flask under an atmosphere of argon for 24 hours. All other dry solvents were obtained from a PurSolv system from Innovative Technology Inc. and stored over 3 Å molecular sieves. Potassium *tert*-butoxide was sublimed before use. LDA was prepared as a solution in dry THF from freshly distilled diisopropyl amine and 2M *n*-butyl lithium in hexanes. Sodium chlorodifluoroacetate was dried in an oven-dried Schlenck tube under high vacuum at 50 °C for 5 hours and stored under nitrogen. Sodium methoxide was prepared freshly by dissolving sodium metal in dry methanol. All other solvents and reagents were used as received.

All compounds sent to NKI for biological testing were > 90% pure (peak area of compounds > 90% of total peak area) as determined by reverse phase HPLC. The eluent system and column used was described above

3.2 Chapter 1 – Experimental

3.2.1 Fmoc S₅ Synthesis

3.2.1.1 Synthesis of *N*-Benzylproline Hydrochloride (**1.142**)

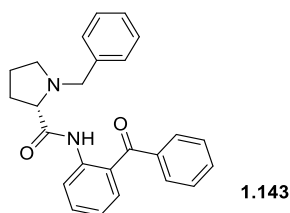


L-Proline (20 g, 175 mmol) was suspended in 2-propanol (115 mL, 0.6 mL/mmol of proline) and warmed to 40 °C. The mixture was stirred at this temperature for 40 minutes, where most of the suspension had dissolved, then cooled to 0 °C using an ice bath. Ground potassium hydroxide was then added, and the reaction stirred for 30 minutes at 0 °C, followed by the dropwise addition of benzyl chloride (30.2 mL, 262.5 mmol) over 15 minutes. When addition was complete, the reaction was warmed to 40 °C and stirred at this temperature for 21 hours. In this time a precipitate had formed and colour change, from colourless to yellow, had occurred. The reaction was cooled to room temperature and the pH adjusted to pH 4 using concentrated hydrochloric acid before being diluted with dichloromethane (200 mL). The mixture was refrigerated overnight, and the resulting potassium chloride precipitate was removed by filtration. The filtrate was concentrated under reduced pressure and the residue diluted with acetone. A white precipitate formed which was collected by filtration to give the title compound **1.142** (14.43 g, 59.7 mmol, 34% yield).

¹H NMR (400 MHz, d₆-DMSO) δ = 7.40-7.27 (m, 5H, 5 x Ar-*H*), 4.05 (d, *J* = 13.0 Hz, 1H, Bn-*CH*), 3.74 (d, *J* = 13.0 Hz, 1H, Bn-*CH*), 3.36 (dd, *J* = 8.8 Hz, 5.6 Hz, 1H, Pro-*CH*), 3.08-3.03 (m, 1H, Pro-*CH*), 2.61-2.55 (m, 1H, Pro-*CH*), 2.15-2.05 (m, 1H, Pro-*CH*), 1.91-1.66 (m, 3H, 3 x Pro-*CH*)

The data recorded are consistent with literature.³³

3.2.1.2 Synthesis of *N*-Benzylproline Benzoacetophenone Schiff Base (BPB) (**1.143**)

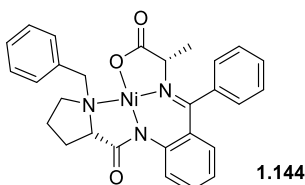


N-benzylproline hydrochloride **1.142** (14.33 g, 59 mmol) was taken up in dry DCM (200 mL, 3.4 mL/mmol **1.142**) in an oven dried 3-necked flask under an atmosphere of nitrogen. 1-methylimidazole (13.2 mL, 165 mmol) was added via syringe and the mixture was cooled to -10 °C. Mesyl chloride (5 mL, 65 mmol) was then added dropwise, keeping the temperature below 0 °C. The reaction was stirred at this temperature for 30 minutes then 2-aminobenzoacetophenone was added in a single portion. The cooling bath was removed, and the mixture warmed to room temperature and stirred for 63 hours. The reaction was quenched with saturated ammonium chloride followed by extraction with 3 portions of DCM. The combined organics were dried with magnesium sulfate, filtered and concentrated *in vacuo*, to give 30.8 g of crude brown oil. The residue was then purified using silica chromatography with a gradient of 0-75% ethyl acetate in petroleum ether to give the title compound **1.143** as a yellow crystalline solid (15.47 g, 40.1 mmol, 68% yield).

¹H NMR (400 MHz, CDCl₃) δ = 11.52 (s, 1H, NH), 8.57 (dd, *J* = 8.4 Hz, 0.9 Hz, 1H, ArH), 7.79-7.77 (m, 2H, 2 x ArH), 7.63-7.48 (m, 5H, 5 x ArH), 7.38-7.36 (m, 2H, 2 x ArH), 7.15-7.07 (m, 4H, 4 x ArH), 3.92 (d, *J* = 13.0 Hz, 1H, Bn-CH), 3.59 (d, *J* = 13.0 Hz, 1H, Bn-CH), 3.31 (dd, *J* = 10.5 Hz, 4.7 Hz, 1H, Pro-CH), 3.24-3.19 (m, 1H, Pro-CH), 2.44-2.37 (m, 1H, Pro-CH), 2.31-2.20 (m, 1H, Pro-CH), 1.85-1.75 (m, 2H, Pro-CH)

The data recorded are consistent with the literature.³³

3.2.1.3 Synthesis of (S) Ni-Ala-BPB Auxiliary (**1.144**)

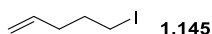


BPB **1.143** (2 g, 5.2 mmol), nickel (II) nitrate hexahydrate (3 g, 10.4 mmol), and DL-alanine (926 mg, 10.4 mmol) were taken up in methanol (18 mL, 3.5 mL/mmol **1.143**) in an oven-dried three-necked flask fitted with a condenser under an atmosphere of nitrogen. The reaction was warmed to 40 °C and potassium hydroxide (3 g, 36.4 mmol) was added as a solution in methanol (7 mL, 0.2 mL/mmol KOH) dropwise over 10 minutes. The temperature was increased to 50 °C and the reaction stirred at this temperature for 2 hours the cooled to room temperature. The reaction was neutralised using acetic acid then quenched with water. Dichloromethane was added, and the mixture stirred overnight. The layers were separated, and the aqueous layer extracted with two portions of DCM. The combined organics were dried using a phase separator and concentrated *in vacuo* to give crude red oil. The residue was purified using silica chromatography using gradients of 50-100% ethyl acetate in petroleum ether and 0-20% methanol in ethyl acetate to give the title compound as a red crystalline solid (2.33 g, 4.5 mmol, 87% yield).

¹H NMR (500 MHz, CDCl₃) δ = 8.10-8.06 (m, 3H, 3 x ArH), 7.53-7.44 (m, 3H, 3 x ArH), 7.36 (t, *J* = 7.6 Hz, 2H, 2 x ArH), 7.26-7.25 (m, 2H, 2 x ArH + residual CHCl₃), 7.20 (t, *J* = 7.2 Hz, 1H, ArH), 7.15-7.12 (m, 1H, ArH), 6.95 (d, *J* = 7.6 Hz, 1H, ArH), 6.67-6.61 (m, 1H, ArH), 4.42 (d, *J* = 13 Hz, 1H, Bn-CH), 3.91 (q, *J* = 6.8 Hz, 1H, Ala-α-CH), 3.77-3.67 (m, 1H, Pro-CH), 3.58-3.53 (m, 2H, Bn-CH + Pro-CH), 3.48 (dd, *J* = 11.6 Hz, 5.8 Hz, 1H, Pro-CH), 2.77-2.72 (m, 1H, Pro-CH), 2.57-2.49 (m, 1H, Pro-CH), 2.24-2.18 (m, 1H, Pro-CH), 2.10-2.04 (m, 1H, Pro-CH), 1.59 (d, *J* = 6.8 Hz, 3H, Ala-CH₃)

The data recorded are consistent with the literature.³³

3.2.1.4 Synthesis of 5-Iodopent-1-ene (1.145)



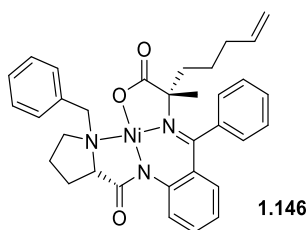
Potassium iodide (10.96 g, 66 mmol) was taken up in acetone (19.8 mL, 0.6 mL/mmol of 5-bromopent-1-ene) in a round bottomed flask equipped with a reflux condenser. 5-bromopent-1-ene (3.97 mL, 33 mmol) was added and the reaction heated to reflux for 5 hours. The reaction was cooled to room temperature and diluted with water and diethyl ether. The layers were separated, and the organic layer washed with 2

portions of water. The combined aqueous layers were then washed with a portion of diethyl ether and the combined organics were then dried with magnesium sulfate, filtered and concentrated *in vacuo* to give a brown oil. The excess diethyl ether was then removed by Kugelrohr distillation at 60 °C, atmospheric pressure, to give the title compound **35** as brown oil (4.03 g, 20.5 mmol, 62% yield).

^1H NMR (500 MHz, CDCl_3) δ = 5.80 - 5.70 (m, 1H, $\text{CH}=\text{CH}_2$), 5.11 - 5.00 (m, 2H, $\text{CH}=\text{CH}_2$), 3.19 (t, J = 6.9 Hz, 2H, Alkyl CH_2), 2.19 - 2.13 (m, 2H, Alkyl CH_2), 1.91 (quin, J = 7.1 Hz, 2H, Alkyl CH_2)

The data recorded are consistent with the literature.³³

3.2.1.5 Synthesis of (S) Ni-S₅-BPB Auxiliary (1.146)



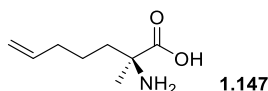
Ni-Ala-BPB **1.144** (1.72 g, 3.36 mmol), was taken up in dry THF (33.6 mL, 10 mL/mmol **1.144**) in an oven dried round bottomed flask under an atmosphere on nitrogen. The solution was then cooled to 0 °C using an ice bath and *tert*-butylammonium iodide (124 mg, 0.336 mmol), followed by freshly sublimed potassium *tert*-butoxide (941 mg, 8.39 mmol) were added. The mixture was stirred at 0 °C for 5 minutes before **1.145** (1.64 g, 8.4 mmol) was added dropwise over 5 minutes. The reaction was then allowed to warm to room temperature and stirred for 24 hours. The reaction was quenched with 0.1 M hydrochloric acid and stirred for 1 hour. The reaction was diluted with DCM, stirred for 1 hour, then the phases separated. The aqueous layer was then extracted with two portions of DCM and the combined organics dried using a phase separator and concentrated *in vacuo* to give red oil. The residue was then purified using silica chromatography with a gradient of 0-5% methanol in ethyl acetate to give the title compound **1.146** as a red solid (980 mg, 1.7 mmol, 50%).

ee = 97% by chiral chromatography.

^1H NMR (500 MHz, CDCl_3) δ = 8.09 - 8.04 (m, 2H, 2 x ArH), 8.02 - 7.98 (m, 1H, 2x ArH), 7.51 - 7.44 (m, 2H, 2 x ArH), 7.43 - 7.35 (m, 3H, 3 x ArH), 7.34 - 7.26 (m, 2H, 2 x ArH), 7.15 - 7.10 (m, 1H, ArH), 7.00 - 6.95 (m, 1H, ArH), 6.67 - 6.59 (m, 2H, 2 x ArH), 5.86 (d, J = 6.7 Hz, 1H, $\text{CH}=\text{CH}_2$), 5.12 - 4.99 (m, 2H, $\text{CH}=\text{CH}_2$), 4.50 (d, J = 13.0 Hz, 1H, Bn-CH), 3.70 (d, J = 13.0 Hz, 1H, Bn-CH), 3.67 - 3.62 (m, 1H, Pro-CH), 3.43 (dd, J = 10.7 Hz, 6.0 Hz, 1H, Pro-CH), 3.32 - 3.20 (m, 1H, Pro-CH), 2.73 - 2.65 (m, 1H, Pro-CH), 2.53 - 2.34 (m, 2H, 2 x Pro-CH), 2.17 - 2.00 (m, 5H, Pro-CH + 4 x alkyl CH), 1.76 - 1.64 (m, 2H, 2 x alkyl CH), 1.24 - 1.21 (m, 3H, $\alpha\text{-CH}_3$)

The data recorded are consistent with the literature.³³

3.2.1.6 Synthesis of S_5 Free Amino Acid (**1.147**)

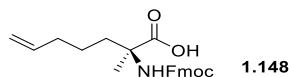


Ni- S_5 -BPB **1.146** (980 mg, 1.7 mmol) was taken up in methanol (22.1 mL, 13 mL/mmol **1.146**) in a round bottomed flask equipped with a reflux condenser. Aqueous 2M hydrochloric acid solution was added (30.6 mL, 18 mL/mmol **1.146**) then the mixture heated to reflux for 16 hours. In that time the reaction had turned from a red solution to a yellow solution. The reaction was then cooled to room temperature and the pH adjusted to pH 9 using concentrated aqueous ammonia (colour change: yellow to blue). Water and DCM were added, and the layers separated. The aqueous layer was then extracted with two portions of DCM and the concentrated *in vacuo* to give a pale-blue solid. The residue was then taken up in a 1:1 mixture of methanol and water and loaded onto a column packed with DOWEX 50WX8 H-form resin. Impurities were eluted by washing with methanol and water and the product eluted with 25% aqueous ammonia which was concentrated *in vacuo*, then re-dissolved in water and freeze dried to give the title compound **1.147** as a fluffy, white solid (180 mg, 1.1 mmol, 67% yield).

^1H NMR (500 MHz, $\text{d}_6\text{-DMSO}$) δ = 7.49 (br s, 3H, $\text{COOH} + \text{NH}_2$), 5.82 - 5.72 (m, 1H, $\text{CH}=\text{CH}_2$), 5.04 - 4.93 (m, 2H, $\text{CH}=\text{CH}_2$), 1.97 (q, J = 7.1 Hz, 2H, alkyl CH_2), 1.66 - 1.60 (m, 1H, alkyl CH), 1.53 - 1.41 (m, 2H, alkyl CH_2), 1.32 - 1.18 (m, 4H, alkyl $\text{CH}_2 + \alpha\text{-CH}_3$)

The data recorded are consistent with the literature.³³

3.2.1.7 Synthesis of Fmoc S₅ (1.148)



The free S₅ amino acid **1.147** (160 mg, 1.02 mmol), was taken up in a 1:1 mixture of water and 1,4-dioxane (6.8 mL, 6.6 mL/mmol of **1.147**) then cooled to 0°C using an ice bath. Sodium carbonate (216 mg, 2.04 mmol) was added followed by the slow addition of Fmoc-O-Su over 2 hours. After the addition was complete, the reaction was allowed to return to room temperature and stirred for 22 hours. The solvent was then removed *in vacuo* and the residue taken up in diethyl ether and water. The layers were separated, and the aqueous layer was then extracted with 2 portions of diethyl ether. The combined organics were discarded and then the pH was adjusted to pH 4 using aqueous 1M hydrochloric acid. The aqueous layer was then extracted with two portions of ethyl acetate and the combined organics washed with 1M hydrochloric acid, dried with magnesium sulfate, filtered and dried concentrated *in vacuo* to give a crude yellow oil. The residue was purified with silica chromatography using a gradient of 0-5% methanol in DCM to give the title compound **1.148** as a sticky, pale-yellow gum.

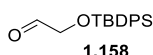
ee = > 98% by chiral chromatography

¹H NMR (500 MHz, *d*₆-DMSO) δ = 7.89 (d, *J* = 7.6 Hz, 2H, ArH), 7.71 (br d, *J* = 7.5 Hz, 2H, ArH), 7.41 (t, *J* = 7.5 Hz, 2H, ArH), 7.33 (d, *J* = 7.3 Hz, 3H, ArH + CONH), 5.82 - 5.71 (m, 1H, CH=CH₂), 5.04 - 4.91 (m, 2H, CH=CH₂), 4.29 - 4.18 (m, 3H, Fmoc CH + Fmoc CH₂), 1.98 (br d, *J* = 6.4 Hz, 2H, alkyl CH₂), 1.83 - 1.63 (m, 2H, alkyl CH₂), 1.36 - 1.26 (m, 5H, alkyl CH₂ + α -CH₃)

The data recorded are consistent with the literature.³³

3.2.2 Generation 1

3.2.2.1 Synthesis of Aldehyde 1.158



Route A – Ozonolysis

Bis-TBDPS protected *cis*-butene-1,4-diol **1.164** (3 g, 5 mmol, synthesised by another member of the laboratory) was taken up in DCM (7 mL, 1.4 mL/mmol **1.164**) in a three-necked flask then cooled to -78 °C using a dry ice/acetone bath. Ozone was then bubbled through the solution until a faint blue colour was observed. The excess ozone was then blown out of the flask with oxygen and the reaction immediately quenched with triphenylphosphine (1.44 g, 5.5 mmol). The cooling bath was removed, and the reaction protected from light and allowed to return to room temperature and stirred for 18 hours. The reaction was concentrated *in vacuo* then re-dissolved in DCM, excess triphenylphosphine was removed by filtration then the filtrate concentrated *in vacuo*. The residue was purified using silica chromatography using a gradient of 0-30% diethyl ether in petroleum ether to give the title compound **1.158** as a pale-yellow oil (2.04 g, 6.8 mmol, 68% yield).

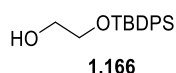
¹H NMR (500 MHz, CDCl₃) δ = 9.73 (s, 1H), 7.68 - 7.65 (m, 4H), 7.47 - 7.43 (m, 2H), 7.43 - 7.39 (m, 4H), 4.23 - 4.21 (m, 2H), 1.11 (s, 9H)

¹³C NMR (101 MHz, CDCl₃) δ = 201.8, 135.6, 134.9, 132.6, 130.2, 129.8, 128.1, 70.2, 26.8

The recorded data are consistent with the literature.²²²

Route B – Oxidation

Step 1 – Monoprotection of Ethylene Glycol



Ethylene glycol (15 mL) and pyridine (15 mL) were placed into a round bottomed flask. TBDPS chloride was added dropwise at room temperature and stirred for 3 hours. The reaction was diluted with ethyl acetate, then diluted with water. The layers were separated, and the organic layer washed: twice with saturated aqueous sodium bicarbonate, twice with water, twice with 1M aqueous hydrochloric acid, and twice with brine. The organic layer was the washed once again with saturated sodium

bicarbonate, water and brine then dried with magnesium sulfate, filtered and concentrated *in vacuo*. The residue was then purified using silica chromatography with a gradient of 0-50% Et₂O in petroleum ether to give the monoprotected ethylene glycol **1.166** (7.35 g, 24 mmol, 81%)

¹H NMR (400 MHz, CDCl₃) δ = 7.71 - 7.65 (m, 4H, 4 x ArH), 7.47 - 7.37 (m, 6H, 6 x ArH), 3.77 (d, *J* = 5.0 Hz, 2H, OCH₂), 3.69 (d, *J* = 5.3 Hz, 2H, OCH₂), 1.08 (s, 9H, 3 x CH₃)

¹³C NMR (101 MHz, CDCl₃) δ = 135.7, 133.4, 129.9, 127.9, 65.1, 63.9, 27.0, 19.4

Step 2 – Swern Oxidation

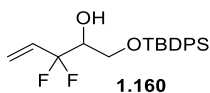
Oxalyl chloride (0.7 mL, 8.04 mmol) was added to a dry three necked flask containing DCM (28 mL, 4.2 mL/mmol **1.166**) under an atmosphere of argon at -78 °C. DMSO (2.4 mL, 33.5 mmol) was then added dropwise and the reaction stirred at -78 °C for 15 minutes. **1.166** (2 g, 6.7 mmol) was then added dropwise and the reaction stirred for a further hour before adding triethylamine. The cooling bath was removed, and the reaction allowed to return to room temperature and stirred for 2 hours. The reaction was diluted with water and the layers separated. The aqueous layer was extracted with two portions of DCM and the combined organics washed with three portions of brine and dried using a phase separator. The solvent was removed *in vacuo* and the residue purified with silica chromatography to give the title compound **1.158** as a pale-yellow oil (1.90 g, 6.4 mmol, 95%).

¹H NMR (500 MHz, CDCl₃) δ = 9.73 (s, 1H), 7.68 - 7.65 (m, 4H), 7.47 - 7.43 (m, 2H), 7.43 - 7.39 (m, 4H), 4.23 - 4.21 (m, 2H), 1.11 (s, 9H)

¹³C NMR (101 MHz, CDCl₃) δ = 201.8, 135.6, 134.9, 132.6, 130.2, 129.8, 128.1, 70.2, 26.8

The recorded data are consistent with the literature.²²²

3.2.2.2 Synthesis of Alcohol 1.160



Aldehyde **1.158** (1.15 g, 3.86 mmol), 3-bromo-3,3-difluoropropene (0.4 mL, 3.86 mmol), and indium powder (443 mg, 3.86 mmol) were combined in a round bottomed flask containing DMF (7.72 mL, 2 mL/mmol of **1.158**). The reaction was then sonicated for 8 hours, then stirred for a further 19 hours. The reaction was then quenched with 1M aqueous hydrochloric acid and extracted with three portions of diethyl ether. The combined organics were washed with brine, dried with magnesium sulfate, filtered and concentrated *in vacuo*. The residue was purified with silica chromatography using a gradient of 0-25% diethyl ether in petroleum ether to give the title compound **1.160** as a colourless oil (714.1 mg, 1.9 mmol, 40% yield).

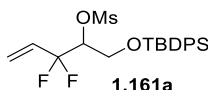
^1H NMR (500 MHz, CDCl_3) δ = 7.69 - 7.63 (m, 4H, 4 x ArH), 7.48 - 7.38 (m, 6H, 6 x ArH), 5.99 (dq, J = 17.5 Hz, 11.7 Hz, 1H, C=CH), 5.72 - 5.66 (m, 1H, C=CH), 5.49 (d, J = 11.1 Hz, 1H, C=CH), 3.95 - 3.79 (m, 3H, OCH + OCH₂), 2.82 - 2.77 (m, 1H, OH), 1.08 (s, 9H)

^{13}C NMR (101 MHz, CDCl_3) δ = 135.7 (d, J = 2.7 Hz), 132.7 (d, J = 3.7 Hz), 130.4 (t, $^2J_{\text{CF}}$ = 25.8 Hz, overlapping with 130.1), 130.1, 128.0, 120.9 (t, $^3J_{\text{CF}}$ = 9.8 Hz), 119.4 (t, $^1J_{\text{CF}}$ = 243.9 Hz), 73.3 (t, $^2J_{\text{CF}}$ = 29.5 Hz), 62.4 (t, $^3J_{\text{CF}}$ = 3.8 Hz), 26.9, 19.4

^{19}F NMR (471 MHz, CDCl_3) δ = -107.6 (dt, J = 253.6 Hz, 10.2 Hz, 1F), -110.9 (dt, J = 253.6 Hz, 11.1 Hz, 1F)

The data recorded are consistent with the literature.⁹⁶

3.2.2.3 Synthesis of Mesylate **1.161a**



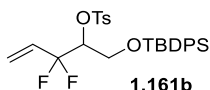
Alcohol **1.160** (714 mg, 2 mmol), was taken up in diethyl ether (5 mL, 2.5 mL/mmol **1.160**) in a round bottomed flask and cooled to 0 °C using an ice bath. Triethylamine (0.33 mL, 2.3 mmol), and DMAP (22 mg, 0.2 mmol) were added followed by the dropwise addition of mesyl chloride (0.18 mL, 2.4 mmol) over five minutes. The reaction warmed to room temperature and stirred for 5 hours. The reaction was then quenched with 1M sodium hydroxide and the layers separated. The organic layer was washed with water and brine then dried with magnesium sulfate, filtered and

concentrated *in vacuo* to give the title compound **1.161a** as a colourless oil (695.3 mg, 1.5 mmol, 78% yield) which was used without further purification.

^1H NMR (500 MHz, CDCl_3) δ = 7.69 - 7.62 (m, 4H, 4 x ArH), 7.48 - 7.37 (m, 6H, 6 x ArH), 5.88 (dq, J = 11.2, 17.5 Hz, 1H, C=CH), 5.73 - 5.66 (m, 1H, C=CH), 5.54 (d, J = 11.0 Hz, 1H, C=CH), 4.93 - 4.86 (m, 1H, OCH), 3.95 - 3.87 (m, 2H, OCH_2), 3.11 (s, 3H, SO_2CH_3), 1.08 - 1.05 (m, 9H, 3 x CH_3)

^{19}F NMR (471 MHz, CDCl_3) δ = -105.7 (dt, J = 256.7 Hz, 10.3 Hz, 1F), -107.5 (dt, J = 256.1 Hz, 10.5 Hz, 1F)

3.2.2.4 Synthesis of Tosylate 1.161b



Alcohol **160** (1.57 g, 4.2 mmol), tosyl chloride (1.6 g, 8.36 mmol), and DMAP (50 mg, 0.4 mmol) were taken up in dry DCM (50 mL, 12 mL/mmol **160**) in a round bottomed flask, then cooled to 0 °C using an ice bath. Triethylamine (1.75 mL, 12.5 mmol) was then added dropwise and the reaction warmed to room temperature and stirred for 21 hours. The reaction was quenched with aqueous saturated sodium bicarbonate and the layers separated. The organic layer was washed twice with water and brine then dried with magnesium sulfate, filtered and concentrated *in vacuo*. The residue was then purified using silica chromatography with a gradient of 0-20% diethyl ether in petroleum ether. A mixture of starting material and product was obtained which was submitted to fresh tosylation conditions as outlined above to give the title compound as a pale-yellow solid (2.22 g, 4.2 mmol, 100% yield)

^1H NMR (500 MHz, CDCl_3) δ = 7.77 (d, J = 8.4 Hz, 2H, 2 x ArH), 7.61 (ddd, J = 8.0 Hz, 3.5 Hz, 1.4 Hz, 4H, 4 x ArH), 7.46 - 7.36 (m, 6H, 6 x ArH), 7.24 (d, J = 7.9 Hz, 2H, 2 x ArH), 5.84 (dq, J = 17.5 Hz, 11.5 Hz, 1H, C=CH), 5.58 (dt, J = 17.3 Hz, 2.3 Hz, 1H, C=CH), 5.43 (d, J = 11.0 Hz, 1H, C=CH), 4.89 - 4.82 (m, 1H, OCH), 3.91 - 3.79 (m, 2H, OCH_2), 2.40 (s, 3H, Ts, CH_3), 1.05 - 1.02 (m, 9H, 3 x CH_3)

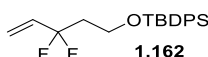
^{13}C NMR (101 MHz, CDCl_3) δ = 144.9, 135.7 (d, J = 7.78 Hz), 134.2, 130.0 (d, J = 7.78 Hz), 129.8, 129.3 (t, $^2J_{\text{CF}}$ = 24.9 Hz), 128.0, 128.0, 127.9, 121.9 (t, $^3J_{\text{CF}}$ = 10.9 Hz), 117.5 (t, $^1J_{\text{CF}}$ = 245.7 Hz), 81.2 (t, $^2J_{\text{CF}}$ = 31.1 Hz), 61.7 (t, $^3J_{\text{CF}}$ = 3.2 Hz), 26.8, 21.8, 19.3

^{19}F NMR (471 MHz, CDCl_3) δ = -104.6 (dt, J = 255.6, 10.9 Hz, 1F), -107.1 (dt, J = 256.0, 8.8 Hz, 1F)

HRMS ($\text{C}_{28}\text{H}_{36}\text{F}_2\text{O}_4\text{NSSi}$): $[\text{M}+\text{NH}_4]^+$ required 548.2103, found $[\text{M}+\text{NH}_4]^+$ 548.2106

IR (neat): 3067, 2961, 1597, 1366, 1180, 1042, 980, 934 cm^{-1}

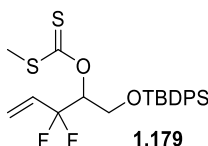
3.2.2.5 Attempted Synthesis of TBDPS protected alcohol **1.162**



Lithium aluminium hydride (114 mg, 5 mmol) was suspended in dry diethyl ether (12.5 mL, 8.3 mL/mmol **1.161a**) in an oven dried round bottomed flask under an atmosphere of argon. **1.161a** (695.3 mg, 1.5 mmol) was added dropwise over 10 minutes and the reaction warmed to room temperature and stirred for 18 hours. The reaction was quenched with 1M sodium hydroxide (5 mL) and filtered through a pad of celite. The two layers were separated, and the organic layer dried with magnesium sulfate, filtered and concentrated *in vacuo*. The residue was purified by silica chromatography using a gradient of 0-100% diethyl ether in petroleum ether. Title compound was not isolated. Reaction failed.

The same procedure was used for tosylate **1.161b**.

3.2.2.6 Synthesis of Xanthate **1.179**



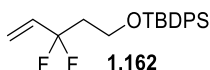
Sodium hydride (60% dispersion in mineral oil, 78 mg, 1.95 mmol) was suspended in dry THF (6 mL, 4.6 mL/mmol **1.160**) in an oven dried round bottomed flask under an atmosphere of argon. Alcohol **1.160** (500 mg, 1.3 mmol) was then added dropwise as a solution on dry THF (6 mL, 4.6 mL/mmol **1.160**) and the reaction stirred at room temperature for 1 hour. Carbon disulfide (80 μL , 1.3 mmol) was added as a solution

in dry THF (1 mL, 0.8 mL/mmol CS₂) and the reaction stirred for a further 30 minutes at room temperature. The reaction was cooled to 0 °C and iodomethane (90 µL, 1.43 mmol) was added and the reaction stirred at 0 °C for 30 minutes before being warmed to room temperature for 1 hour. The reaction was diluted with diethyl ether and poured into saturated aqueous ammonium chloride. The layers were separated, and the aqueous layer extracted with two portions of diethyl ether. The combined organics were then washed twice with water and brine, dried with magnesium sulfate, filtered through a plug of silica and concentrated *in vacuo* to give the title compound **1.179** as a yellow oil which was used in the next step without further purification (662.9 mg, 1.4 mmol, quant. yield).

¹H NMR (500 MHz, CDCl₃) δ = 7.66-7.64 (m, 4H, 4 x ArH), 7.45-7.37 (m, 6H, 6 x ArH), 6.30 – 6.24 (m, 1H, CHOCS), 5.95 (dq, *J* = 17.3 Hz, 11.1 Hz, 1H, C=CH), 5.50 (dt, *J* = 17.0 Hz, 3.0 Hz, 1H, C=CH), 5.50 (d, *J* = 11.2 Hz, 1H, C=CH), 4.05-3.96 (m, 2H, OCH₂), 2.59 (s, 3H, SCH₃), 1.02 (s, 9H, 3 x CH₃)

¹⁹F NMR (471 MHz, CDCl₃) δ = -104.7 (dt, *J* = 254.3 Hz, 10.9 Hz, 1F), -108.7 (dt, *J* = 256.5 Hz, 10.9 Hz, 1F)

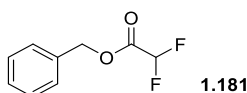
3.2.2.7 Attempted Synthesis of TBDPS Protected Alcohol **1.162**



Xanthate **1.179** (606 mg, 1.3mmol), AIBN (11 mg, 0.06 mmol), and Bu₃SnH (1 mL, 3.9 mmol) were combined in an oven dried round bottomed flask, equipped with a reflux condenser, under an atmosphere of argon. Dry toluene (6.5 mL, 1.5 mL/mmol of **1.179**) was added and the reaction heated for 80 °C for 18 hours. The reaction was cooled to room temperature and analysed by ¹H NMR and ¹⁹F NMR. No alkene peaks were visible in the ¹H NMR and multiple fluorinated products were observed in the ¹⁹F NMR. The title compound **1.162** was not formed and the reaction failed.

3.2.3 Generation 2

3.2.3.1 Synthesis of Benzyl 2,2-difluoroacetate (**1.181**)



2,2-difluoroacetic acid (15 mL, 0.5 mL/mmol benzyl alcohol), cobalt dichloride hexahydrate (357 mg, 1.5 mmol, 5 mol%) and benzyl alcohol were combined and heated to 60 °C. The reaction was stirred for 2.5 hours then cooled to room temperature. The mixture was partitioned with diethyl ether and water and the organic layer washed three times with saturated sodium bicarbonate, twice with water and twice with brine. The organics were dried with magnesium sulfate, filtered and concentrated *in vacuo*. The residue was purified by silica chromatography, eluting with 100% DCM to give the title compound **1.181** as a pale-yellow oil (4.62 g, 24 mmol, 83% yield).

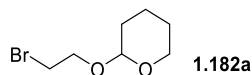
^1H NMR (500 MHz, CDCl_3) δ = 7.43 - 7.37 (m, 5H, 5 x ArH), 5.93 (t, J = 54.8 Hz, 1H, CF_2H), 5.31 (s, 2H, BnCH_2)

^{13}C NMR (126 MHz, CDCl_3) δ (ppm) = 162.5 (t, $^2J_{\text{CF}}$ = 28.7 Hz), 134.1, 129.1, 128.9, 128.7, 106.8 (t, $^1J_{\text{CF}}$ = 245.6 Hz), 68.5

^{19}F NMR (471 MHz, CDCl_3) δ = -126.6 (d, J = 53.8 Hz)

^1H NMR is consistent with the literature.²²³

3.2.3.2 Synthesis of THP Protected Bromoethanol (1.182a)



Para-toluenesulfonic acid (10 mg, 0.06 mmol), was taken up in dry DCM (78 mL, 1.8 mL/mmol bromoethanol) in an oven dried three-necked flask, equipped with a thermometer, under an atmosphere of argon. 2-bromoethanol (2.8 mL, 40 mmol) was added and the mixture cooled to 0 °C using an ice bath. Dihydropyran (4.4 mL, 48 mmol) was then added dropwise, maintaining the internal temperature at 0 °C. Once addition was complete, the reaction was warmed to room temperature and stirred for 17 hours. It was then cooled to 0 °C and quenched with saturated aqueous sodium bicarbonate. The resulting biphasic mixture was partitioned, and the organic layer washed with water and brine, dried with magnesium sulfate, filtered and concentrated *in vacuo*. The residue was purified by Kugelrohr distillation (115 °C, high

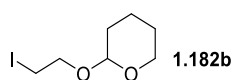
vacuum) to give the title compound **1.182a** as a colourless oil (7.19 g, 34.4 mmol, 86% yield).

^1H NMR (500 MHz, CDCl_3) δ = 4.66 (t, J = 3.4 Hz, 1H, OCHO), 4.00 (dt, J = 11.4 Hz, 6.2 Hz, 1H, OCH), 3.91 - 3.84 (m, 1H, OCH), 3.76 (dt, J = 11.3 Hz, 6.3 Hz, 1H, OCH), 3.54 - 3.45 (m, 3H, OCH and BrCH_2), 1.88 - 1.78 (m, 1H, THP-CH), 1.76 - 1.68 (m, 1H, THP-CH), 1.64 - 1.49 (m, 4H, 4 x THP-CH)

^{13}C NMR (126 MHz, CDCl_3) δ = 99.0, 67.6, 62.4, 30.9, 30.5, 25.5, 19.4

The data recorded are consistent with the literature.¹⁰⁴

3.2.3.3 Synthesis of THP Protected Iodoethanol (1.182b)



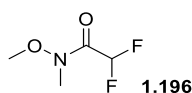
THP protected bromoethanol **1.182a** (1 g, 4.8 mmol) was taken up in acetone (3 mL, 0.6 mL/mmol of THP-bromoethanol) in a round bottomed flask equipped with a reflux condenser. Potassium iodide (1.59 g, 9.56 mmol) was added and the mixture heated to reflux for 17 hours. the mixture was then partitioned between water and diethyl ether and the aqueous layer extracted with two portions of diethyl ether. The combined organic layers were then dried with magnesium sulfate, filtered and concentrated *in vacuo*. The residue was the purified by silica chromatography using a gradient of 0-10% diethyl ether in petroleum ether to give the title compound **1.182b** as a colourless oil (966 mg, 3.8 mmol, 79% yield).

^1H NMR (500 MHz, CDCl_3) δ = 4.67 (br s, 1H, OCHO), 4.04 - 3.83 (m, 2H, 2 x OCH), 3.79 - 3.67 (m, 1H, OCH), 3.52 (br d, J = 6.9 Hz, 1H, OCH), 3.29 (br s, 2H, 2 x OCH), 1.90 - 1.78 (m, 1H, THP-CH), 1.77 - 1.68 (m, 1H, THP-CH), 1.66 - 1.47 (m, 4H, THP-CH)

^{13}C NMR (126 MHz, CDCl_3) δ = 98.8, 68.4, 62.4, 30.6, 25.5, 19.4, 3.6

The data collected are consistent with the literature.²²⁴

3.2.3.4 Synthesis of 2,2-difluoro-*N*-methoxy-*N*-methylacetamide (1.196)



2,2-difluoroacetic acid (1.3 mL, 20.8 mmol) was taken up in 2-MeTHF (58 mL, 2.8 mL/mmol difluoroacetic acid) in a round bottomed flask fitted with a reflux condenser and heated to 60 °C. Carbonyldiimidazole (4 g, 25 mmol) was then added and the reaction stirred for 2 hours. *N,O*-dimethylhydroxylamine hydrochloride (8.1 g, 83.3 mmol) and stirred for 17 hours. The reaction was cooled to room temperature, filtered and concentrated *in vacuo*. The residue was purified by silica chromatography using a gradient of 0-100% diethyl ether to give the title compound **1.196** as a colourless oil (2.25 g, 16 mmol, 78%)

^1H NMR (500 MHz, CDCl_3) δ = 6.25 (t, J = 53.8 Hz, 1H, CF_2H), 3.74 (s, 3H, OCH_3), 3.23 (br s, 3H, NCH_3)

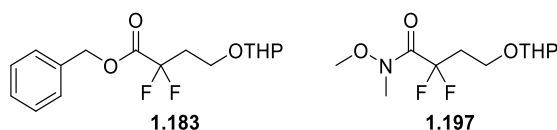
^{13}C NMR (126 MHz, CDCl_3) δ = 162.4 (t, $^2J_{\text{CF}}$ = 25.7 Hz), 106.4 (t, $^1J_{\text{CF}}$ = 244.1 Hz), 62.2, 32.3

^{19}F NMR (471 MHz, CDCl_3) δ = -126.9 (br d, J = 53.8 Hz, 1F)

HRMS: ($\text{C}_4\text{H}_8\text{F}_2\text{NO}_2$) $[\text{M}+\text{H}]^+$ requires 180.0831, found $[\text{M}+\text{H}]^+$ 180.0827

The data recorded are consistent with the literature.²²⁵

3.2.3.5 Attempted Synthesis of Ester **1.183** and Amide **1.197**



General Procedure for Attempted Alkylation Reaction

The same procedure was used for ester **1.183** and amide **1.197** with THP-bromoethanol **1.182a** and THP-iodoethanol **1.182b** using the conditions outlined in **Table 4**.

Base (1.2 equiv.) was taken up in solvent (2 mL/mmol of nucleophile **1.181** or **1.196**) at temperature **T**. Nucleophile **1.181** or **1.196** (1 equiv.) was added dropwise followed by the addition of electrophile **1.182a** or **1.182b** (1.2 equiv). The reaction was allowed to stir at the specified temperature for the time specified in **Table 6** and analysed by ^1H NMR and ^{19}F NMR.

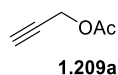
No alkylation product was observed in any case

Table 6: Conditions used for alkylations

Entry	Nucleophile 1.181 or 1.196	Electrophile 1.182a or 1.182b	Base	Solvent	Temperature (°C)	Time (h)
1	1.181	54a	LDA	THF	-78 - RT	1
2	1.181	54a	K ₂ CO ₃	Acetone	Reflux	3.5
3	1.181	1.182a	NaOMe	MeOH	0 - RT	1
4	1.181	1.182a	KO ^t Bu	THF	Reflux - RT	19
5	1.181	1.182a	KO ^t Bu	THF	RT	19
6	1.181	1.182a	NEt ₃	THF	RT - 60	19
7	1.181	1.182a	DBU	THF	RT	17
8	1.181	1.182a	NaH	THF	0 – RT	2
9	1.196	1.182a	NaOMe	MeOH	RT	1
10	1.196	1.182a	DBU	THF	RT	17
11	1.196	1.182a	NEt ₃	THF	RT	17
12	1.196	1.182a	KO ^t Bu	THF	RT	17
13	1.196	1.182b	DBU	THF	RT	17
14	1.196	1.182b	NEt ₃	THF	RT	17
15	1.196	1.182b	KO ^t Bu	THF	RT	17

3.2.4 Generation 3

3.2.4.1 Synthesis of Prop-2-yn-1-yl Acetate (1.209a)



Propargyl alcohol (5.2 mL, 89 mmol) and sodium acetate pentahydrate (730 mg, 8.9 mmol) were combined in a round bottomed flask. Acetic anhydride (9.2 mL, 98 mmol) was added dropwise using a pressure equalised dropping funnel and the reaction stirred for 3.5 hours at room temperature. The reaction was diluted with diethyl ether and quenched with saturated sodium bicarbonate. The layers were separated, and

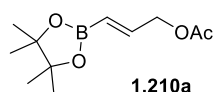
the organic layer washed once with aqueous saturated sodium bicarbonate, twice with water and twice with brine, dried with magnesium sulfate, filtered and concentrated *in vacuo*. The residue was purified by Kugelrohr distillation (125 °C under house vacuum) to give the title compound **1.209a** as a colourless oil (5.12 g, 52.2 mmol, 59% yield).

^1H NMR (400 MHz, CDCl_3) δ = 4.64 (d, J = 2.5 Hz, 2H, CH_2), 2.45 (t, J = 2.5 Hz, 1H, alkyne CH), 2.07 (s, 3H, COCH_3)

^{13}C NMR (101 MHz, CDCl_3) δ = 170.2, 77.7, 74.9, 52.0, 20.7

The recorded data are consistent with the literature.^{226,227}

3.2.4.2 Synthesis of Vinyl BPin **1.210a**



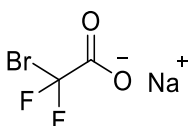
Schwartz reagent (230 mg, 0.89 mmol) was placed in an oven dried two-necked flask, fitted with a reflux condenser, under an atmosphere of argon. Prop-2-yn-1-yl acetate **1.209a** (1 g, 17.8 mmol) was added and the mixture heated to 60 °C for 30 minutes. Pinacol borane (2.8 mL, 19.6 mmol) was then added dropwise over ten minutes and the reaction stirred for 18 hours. The reaction was cooled to room temperature and purified with silica chromatography using a gradient of 0-20% diethyl ether in petroleum ether to give the title compound **1.210a** as a colourless oil (720 mg, 3.2 mmol, 17% yield).

^1H NMR (500 MHz, CDCl_3) δ = 6.59 (dt, J = 4.7, 18.2 Hz, 1H, C=CH), 5.70 - 5.62 (m, 1H, C=CH), 4.64 (dd, J = 1.7, 4.6 Hz, 2H, OCH_2), 2.07 (s, 3H, COCH_3), 1.27 - 1.24 (m, 12H, 4 x CH_3)

^{13}C NMR (126 MHz, CDCl_3) δ = 170.6, 146.0, 120.3 (b, C=CHBPin), 83.5, 65.5, 24.8, 20.9

The recorded data are consistent with the literature.²²⁸

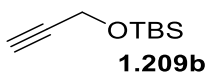
3.2.4.3 Synthesis of Sodium 2-Bromo-2,2-Difluoro Acetate



Sodium hydroxide (5 g, 28.6 mmol) was placed into an oven dried flask under an atmosphere of argon and cooled to 0 °C. 2-Bromo-2,2-difluoroacetic acid (1.14 g, 28.6 mmol) was added dropwise as a solution in methanol (8.6 mL, 0.3 mL/mmol of acid). When addition was complete, the reaction was stirred at 0°C for 15 minutes before warming to room temperature and stirred for five hours. The solvent was then removed *in vacuo* to give the title compound as a white solid (5.59 g, 28.6 mmol, quantitative yield).

^{19}F NMR (471 MHz, d_6 -DMSO) δ = -53.2 (s)

3.2.4.4 Synthesis of TBS Protected Propargyl Alcohol **1.209b**

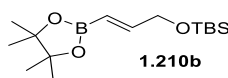


Propargyl alcohol (1.04 mL, 17.8 mmol) was taken up in dry DCM (7.1 mL, 0.4 mL/mmol propargyl alcohol) in a round bottomed flask fitted with a reflux condenser. TBS chloride (2.68 g, 17.8 mmol) was added followed by imidazole (2.42 g, 35.6 mmol) at room temperature and the reaction warmed to reflux for 2 hours. The reaction was cooled to room temperature, quenched with water and filtered through celite. The layers were separated, and the aqueous layer extracted with three portions of DCM. The combined organics were dried with magnesium sulfate, filtered and concentrated *in vacuo*. The residue was then purified by Kugelrohr distillation (50°C, high vacuum) to give the title compound **1.209b** as a colourless oil (3 g, 17.8 mmol, 100% yield).

^1H NMR (500 MHz, CDCl_3) δ = 4.31 (d, J = 2.3 Hz, 2H, CH_2), 2.38 (t, J = 2.4 Hz, 1H, alkyne CH), 0.91 (s, 9H, 3 x CH_3), 0.12 (s, 6H, 2 x SiCH_3)

The recorded data are consistent with the literature.²²⁹

3.2.4.5 Synthesis of Vinyl BPin 1.210b

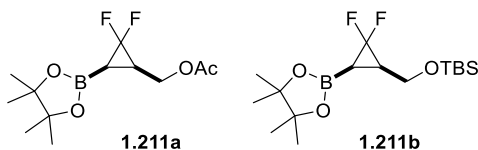


Schwartz reagent (74 mg, 0.29 mmol) was placed in an oven dried two-necked flask, fitted with a reflux condenser, under an atmosphere of nitrogen. TBS protected propargyl alcohol **1.209b** (500 mg, 2.9 mmol) was added followed by triethylamine (40 μ L, 0.29 mmol) and the reaction stirred at room temperature for 10 minutes. Pinacol borane (0.44 mL, 3.0 mmol) was added dropwise over 5 minutes and the reaction heated to 60 $^{\circ}$ C for 20 hours. The reaction was cooled to RT, diluted with 10% ethyl acetate in petroleum ether and loaded directly onto silica for purification using 10% ethyl acetate in petroleum ether as the eluent to give the title compound **1.210b** as a colourless oil (918 mg, 3.0 mmol, quant. Yield).

^1H NMR (500 MHz, CDCl_3) δ = 6.66 (dt, J = 18.0 Hz, 3.5 Hz, 1H, $\text{C}=\text{CH}$), 5.74 (dt, J = 18.0 Hz, 2.1 Hz, 1H, $\text{C}=\text{CH}$), 4.23 (dd, J = 3.5 Hz, 2.1 Hz, 2H, OCH_2), 1.26 (s, 12H, 4 \times CH_3), 0.90 (s, 9H, 3 \times CH_3), 0.05 (s, 6H, 2 \times SiCH_3)

The data recorded are consistent with the literature.²³⁰

3.2.4.6 Attempted Synthesis of Difluorocyclopropanes 1.211a and 1.211b



Shown below is a representative procedure for **Table 7**, entry **1**

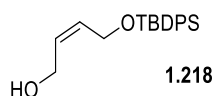
Vinyl Bpin **1.210a** (100 mg, 0.44 mmol) was taken up in dry diglyme (2.2 mL, 5 mL/mmol **1.210a**) in an oven dried two-necked flask, fitted with a reflux condenser, under a stream of argon. The mixture was heated to 150 $^{\circ}$ C and NaBDFA (693 mg, 3.52 mmol) was added dropwise as a solution in dry diglyme (4.4 mL, 10 mL/mmol of alkene) over 10 minutes. The reaction was stirred for 21 hours, then cooled to room temperature and quenched with water. The mixture was partitioned with DCM and the organic layer washed with brine, dried with magnesium sulfate and concentrated *in vacuo*. The residue was analysed by ^1H NMR and ^{19}F NMR.

All reactions attempted failed to produce the title compounds.

Table 7: Reaction Conditions of Difluorocyclopropanation

Entry	Substrate	:CF ₂	Equiv.	Temperature	Addition	Reaction
	1.211a or 1.221b	Source	of :CF ₂	(°C)	Time (h)	Time (h)
1	1.211a	NaBDFA	8	150	10 min	21
2	1.211a	NaBDFA	8	180	3.5	15
3	1.211a	NaBDFA	8	150	3	19
4	1.221b	NaCDFA	10	180	8	18.5

3.2.4.7 Synthesis of TBDPS protected Butene Diol 1.218



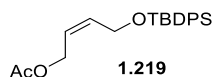
Sodium hydride (60% dispersion in mineral oil, 1.10 g, 27.6 mmol) was suspended in dry THF (40 mL, 1.4 mL/mmol of TBDPS chloride) in an oven dried round bottomed flask under an atmosphere of argon, vented to a balloon. *cis*-Butene-1,4-diol (2.28 mL, 27.7 mmol) was added dropwise over five minutes (hydrogen evolution) and stirred at room temperature for 1 hour. TBDPS chloride (7.2 mL, 27.6 mmol) as a solution in dry THF (40 mL, 1.4 mL/mmol) was added *via* cannula and the reaction stirred for 2 hours. The reaction was quenched with saturated ammonium chloride (20 mL) and the THF removed *in vacuo*. The residue was partitioned between diethyl ether and water and the aqueous layer extracted with two portions of diethyl ether. The combined organics were dried with magnesium sulfate, filtered and concentrated *in vacuo*. The residue was purified with silica chromatography using a gradient of 0-40% ethyl acetate in petroleum ether to give the title compound **1.218** as a colourless oil (8.18 g, 25 mmol, 91% yield).

¹H NMR (500 MHz, CDCl₃) δ = 7.70 (dd, *J* = 7.9 Hz, 1.4 Hz, 4H, 4 x ArH), 7.47 - 7.37 (m, 6H, 6 x ArH), 5.75 - 5.60 (m, 2H, 2 x C=CH), 4.27 (d, *J* = 5.6 Hz, 2H, OCH₂), 4.02 (br d, *J* = 5.3 Hz, 2H, OCH₂), 1.66 - 1.62 (m, 1H, OH), 1.09 - 1.04 (m, 9H, 3 x CH₃)

^{13}C NMR (126 MHz, CDCl_3) δ = 135.7, 133.6, 131.0, 130.1, 129.9, 127.8, 60.4, 58.8, 26.9, 19.2

The data recorded is consistent with the literature.²³¹

3.2.4.8 Synthesis of TBDPS and Acetate Protected Butene Diol **1.219**



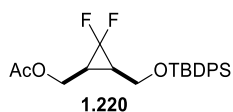
TBDPS protected butene diol **1.218** (8.18 g, 25 mmol), and DMAP (305 mg, 2.5 mmol) were taken up in dry DCM (100 mL, 4 mL/mmol of **1.218**) in an oven dried three-necked flask under an atmosphere of argon. Triethylamine (7 mL, 50 mmol) was added followed by the dropwise addition of acetic anhydride (2.6 mL, 27.5 mmol) over 10 minutes. The reaction was stirred at room temperature for 2.5 hours and quenched with water (80 mL). The layers were separated, and the aqueous layer extracted with three portions of DCM. The combined organics were washed with water and brine, dried with magnesium sulfate, filtered and concentrated *in vacuo*. The residue was purified with silica chromatography using a gradient of 0-20% ethyl acetate in petroleum ether to give the title compound **1.219** as a colourless oil (9.04 g, 24.5 mmol, 98% yield).

^1H NMR (400 MHz, CDCl_3) δ = 7.72 - 7.66 (m, 4H, 4 x ArH), 7.47 - 7.35 (m, 6H, 6 x ArH), 5.86 - 5.77 (m, 1H, C=CH), 5.60 - 5.51 (m, 1H, C=CH), 4.49 (dd, J = 6.8 Hz, 1.3 Hz, 2H, OCH_2), 4.31-4.29 (m, 2H, OCH_2), 2.02 (s, 3H, COCH_3), 1.07 - 1.05 (m, 9H, 3 x CH_3)

^{13}C NMR (101 MHz, CDCl_3) δ = 170.8, 135.7, 133.6, 133.6, 129.8, 127.9, 124.5, 60.6, 60.4, 26.9, 21.0, 19.2

The data recorded are consistent with the literature.²³²

3.2.4.9 Synthesis of Difluorocyclopropane **1.220**



Small scale procedure

TBDPS and acetate protected butene diol **1.219** (1 g, 2.84 mmol) was taken up in dry diglyme (1.5 mL, 0.54 mL/mmol of **1.219**) in an oven dried two-necked flask, fitted with a reflux condenser, under a stream of argon. The solution was heated to 180 °C and NaCDFA (4.76 g, 31.24 mmol) was added dropwise over 2 hours as a solution in dry diglyme (10.3 mL, 0.33 mL/mmol NaCDFA) using a syringe pump. Once addition was complete the reaction was stirred for 1.5 hours then cooled to room temperature. The mixture was diluted with diethyl ether and filtered through a plug of silica. The plug was washed with diethyl ether until the washings were colourless and the filtrate washed with three portions of water and three portions of brine to remove the diglyme. The combined organics were dried with magnesium sulfate, filtered and concentrated *in vacuo*. The residue was purified by silica chromatography using a gradient of 0-10% diethyl ether in petroleum ether to give the title compound **1.220** as a colourless oil (1.12 g, 2.7 mmol, 94% yield)

Large scale procedure

TBDPS and acetate protected butene diol **1.219** (6 g, 17 mmol) was taken up in dry diglyme (9 mL, 0.54 mL/mmol of **219**) in an oven dried three-necked flask, fitted with a reflux condenser, under a stream of nitrogen. The solution was heated to 180 °C and NaCDFA (28.6 g, 187 mmol) was added dropwise over 5 hours as a solution in dry diglyme (62 mL, 0.33 mL/mmol NaCDFA) using a peristaltic pump. Once addition was complete the reaction was stirred for 1.5 hours then cooled to room temperature. The mixture was diluted with diethyl ether and filtered through a plug of silica. The plug was washed with diethyl ether until the washings were colourless and the filtrate was divided into three portions to aid with work up. Each portion was washed with three portions of water and three portions of brine to remove diglyme. The organic layers were combined, dried with magnesium sulfate, filtered and concentrated *in vacuo*. The residue was purified by silica chromatography using a gradient of 0-10% diethyl ether in petroleum ether to give the title compound **1.220** as a colourless oil (7 g, 16.7 mmol, 98% yield)

^1H NMR (500 MHz, CDCl_3) δ = 7.68-7.66 (m, 4H, 4 x ArH), 7.47 - 7.37 (m, 6H, 6 x ArH), 4.31 - 4.10 (m, 2H, OCH_2), 3.89 - 3.74 (m, 2H, OCH_2), 2.08 - 1.93 (m, 5H, 2 x CH + COCH_3), 1.07 (s, 9H, 3 x CH_3)

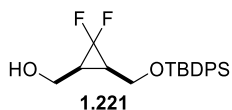
^{13}C NMR (126 MHz, CDCl_3) δ = 170.9, 135.7, 133.2, 130.0, 127.9 (d, $J = 3.2$ Hz), 113.3 (dd, $^1J_{\text{CF}} = 290.5$ Hz, 283.3 Hz), 58.2 (d, $^3J_{\text{CF}} = 6.2$ Hz), 57.3 (d, $^3J_{\text{CF}} = 5.5$ Hz), 27.5 (t, $^2J_{\text{CF}} = 9.9$ Hz), 26.9, 23.9 (t, $^2J_{\text{CF}} = 10.5$ Hz), 21.0, 19.3

^{19}F NMR (471 MHz, CDCl_3) δ = -125.1 (dt, $J = 164.3$ Hz, 12.4 Hz, 1F), -151.8 (br,d, $J = 163.0$ Hz, 1F)

HRMS: ($\text{C}_{23}\text{H}_{29}\text{F}_2\text{O}_3\text{Si}$) $[\text{M}+\text{H}]^+$ required 419.1854, found $[\text{M}+\text{H}]^+$ 419.1852

IR (neat): 3071, 2963, 2932, 1742, 1474, 1389, 1105, 700 cm^{-1}

3.2.4.10 Synthesis of Difluorocyclopropane 1.221



Small Scale Procedure

Difluorocyclopropane **1.220** (3.81 g, 9.1 mmol), was taken up in a 3:1 mixture of methanol and water (95.6 mL, 10.5 mL/mmol of **1.220**) and potassium carbonate (1.89 g, 13.6 mmol) added. The reaction was stirred at room temperature for 1 hour, then neutralised with 1M hydrochloric acid and the methanol removed *in vacuo*. The residue was partitioned between diethyl ether and water and the aqueous layer extracted with three portions of diethyl ether. The combined organics were dried with magnesium sulfate, filtered and concentrated *in vacuo*. The residue was purified with silica chromatography using a gradient of 0-15% diethyl ether in petroleum ether to give the title compound **1.221** as a colourless viscous oil (2.92 g, 7.8 mmol, 85%)

Large Scale Procedure

Difluorocyclopropane **1.220** (14 g, 33 mmol), was taken up in methanol (343 mL, 10.5 mL/mmol of **1.220**), cooled to 0 °C and potassium carbonate (2.3 g, 16 mmol) added. The reaction was stirred at room temperature for 1 hour, then the methanol removed

in vacuo and the residue neutralised with 1M hydrochloric acid. The residue was partitioned between diethyl ether and water and the aqueous layer extracted with three portions of diethyl ether. The combined organics were dried with magnesium sulfate, filtered and concentrated *in vacuo*. The residue was purified with silica chromatography using a gradient of 0-15% diethyl ether in petroleum ether to give the title compound **1.221** as a colourless viscous oil (2.92 g, 7.8 mmol, 85%)

^1H NMR (500 MHz, CDCl_3) δ = 7.71 - 7.65 (m, 4H, 4 x ArH), 7.50 - 7.39 (m, 6H, 6 x ArH), 4.03 - 3.90 (m, 2H, OCH_2), 3.83 - 3.75 (m, 2H, OCH_2), 3.07 (dd, J = 10.5 Hz, 2.4 Hz, 1H, OH), 2.23 - 2.12 (m, 1H, CH), 1.99-1.92 (m, 1H, CH), 1.07 (s, 9H, 3 x CH_3)

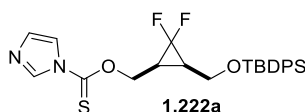
^{13}C NMR (126 MHz, CDCl_3) δ = 135.6 (d, J = 9.1 Hz), 132.5 (d, J = 6.4 Hz), 130.3 (d, J = 6.4 Hz), 128.1 (d, J = 1.8 Hz), 113.9 (dd, $^1J_{\text{CF}}$ = 290.2, 284.7 Hz), 57.6 (d, $^3J_{\text{CF}}$ = 3.6 Hz), 56.0 (d, $^3J_{\text{CF}}$ = 3.6 Hz), 28.6 (t, $^2J_{\text{CF}}$ = 10.0 Hz), 27.4 (t, $^2J_{\text{CF}}$ = 10.0 Hz), 26.9, 19.2

^{19}F NMR (471 MHz, CDCl_3) δ = -122.5 (dt, J = 164.7 Hz, 13.9 Hz, 1F), -148.4 (br d, J = 164.7 Hz, 1F)

HRMS: $\text{C}_{21}\text{H}_{27}\text{F}_2\text{O}_2\text{Si}$ $[\text{M}+\text{H}]^+$ required 377.1748, found $[\text{M}+\text{H}]^+$ 377.1745

IR (neat): 3439, 3071, 2961, 1589, 1427, 1391, 1105, 700 cm^{-1}

3.2.4.11 Synthesis of Thiocarbonylimidazolide **1.222a**



Difluorocyclopropane **1.221** (200 mg, 0.5 mmol) was taken up in dry DCM (20 mL, 38 mL/mmol **1.221**) in an oven dried round bottomed flask fitted with a reflux condenser. TCDI (566 mg, 3.18 mmol) was added and the reaction heated to reflux for 2 hours. The reaction was cooled to room temperature, diluted with DCM and washed twice with 1M hydrochloric acid, twice with saturated aqueous sodium bicarbonate, twice with water and twice with brine. The organics were then dried with magnesium sulfate, filtered and concentrated *in vacuo*. The residue was then purified by silica chromatography using a gradient of 0-75% diethyl ether in

petroleum ether to give the title compound **1.222a** as a pale-yellow sticky gum (0.23 g, 0.5 mmol, 89% yield).

1.222a is either, light, air or temperature sensitive (or a combination of the three) and was stored in a foil wrapped flask under argon at -18 °C.

^1H NMR (500 MHz, CDCl_3) δ = 8.32 (s, 1H, 1m CH), 7.66 (dt, J = 1.5, 8.0 Hz, 4H, 4 x ArH), 7.58 (d, J = 1.2 Hz, 1H, 1m CH), 7.48 - 7.38 (m, 6H, 6 x ArH), 7.02 (d, J = 0.8 Hz, 1H, 1m CH), 4.97 (ddd, J = 12.0, Hz, 7.1 Hz, 2.7 Hz, 1H, OCH), 4.70 (dd, J = 11.9 Hz, 9.2 Hz, 1H, OCH), 3.94 (ddd, J = 11.7 Hz, 7.2 Hz, 1.5 Hz, 1H, OCH), 3.78 (dd, J = 10.8 Hz, 9.3 Hz, 1H, OCH), 2.31 - 2.21 (m, 1H, CH), 2.17 - 2.07 (m, 1H, CH), 1.05 (s, 9H, 3 x CH_3)

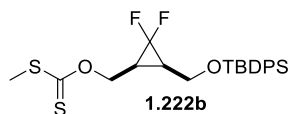
^{13}C NMR (126 MHz, CDCl_3) δ = 183.9, 137.1, 135.6, 132.9 (d, J = 6.4 Hz), 131.1, 130.1, 128.0 (d, J = 4.5 Hz), 117.9, 112.9 (dd, $^1J_{\text{CF}}$ = 290.2, 283.8 Hz), 67.4 (d, $^3J_{\text{CF}}$ = 6.4 Hz), 57.2 (d, $^3J_{\text{CF}}$ = 4.5 Hz), 27.9 (t, $^2J_{\text{CF}}$ = 10.0 Hz), 26.9, 23.1 (t, $^2J_{\text{CF}}$ = 10.9 Hz), 19.2

^{19}F NMR (471 MHz, CDCl_3) δ = -124.8 (dt, J = 164.7 Hz, 12.1 Hz, 1F), -150.6 (br d, J = 164.7 Hz, 1F)

HRMS: ($\text{C}_{25}\text{H}_{29}\text{F}_2\text{N}_2\text{O}_2\text{SSi}$) $[\text{M}+\text{H}]^+$ required 487.1687, found $[\text{M}+\text{H}]^+$ 487.1689

IR (neat): 3045, 2954, 2854, 1472, 1390, 1284, 1229, 740, 702 cm^{-1}

3.2.4.12 Synthesis of Xanthate **1.222b**



Sodium hydride (60% dispersion in mineral oil, 80 mg, 2.0 mmol) was suspended in dry THF (11 mL, 8.3 mL/mmol of **1.221**) in an oven dried round-bottomed flask under an atmosphere of argon and cooled to 0 °C using an ice bath. Difluorocyclopropane **1.221** (500 mg, 1.3 mmol) was added dropwise as a solution in dry THF (2 mL, 1.5 mL/mmol **1.221**) and the reaction stirred at 0 °C for 30 minutes. Carbon disulfide (80 μL , 1.3 mmol) was added and the reaction stirred for a further 30 minutes at 0 °C. Iodomethane (90 μL , 1.46 mmol) was then added and the reaction warmed to room temperature and stirred for 16.5 hours. The reaction was then diluted with diethyl ether (10 mL) and quenched with saturated ammonium chloride (20 mL). The layers

were then separated and the aqueous extracted with three portions of diethyl ether. The combined organics were dried with magnesium sulfate, filtered and concentrated *in vacuo*. The residue was purified by silica chromatography using a gradient of 0-9% diethyl ether in petroleum ether to give a mixture of title product and unknown by-product. The mixture was purified using silica chromatography using a gradient of 0-20% DCM in petroleum ether to give the title product **1.222b** as a colourless oil (310 mg, 0.7 mmol, 50%)

^1H NMR (500 MHz, CDCl_3) δ = 7.69 - 7.65 (m, 4H, 4 x ArH), 7.47 - 7.37 (m, 6H, 6 x ArH), 4.89 - 4.82 (m, 1H, OCH), 4.70 - 4.64 (m, 1H, OCH), 3.90 - 3.84 (m, 1H, OCH), 3.82 - 3.76 (m, 1H, OCH), 2.55 - 2.53 (m, 3H, SCH_3), 2.25 - 2.16 (m, 1H, CH), 2.11 - 2.01 (m, 1H, CH), 1.09 - 1.04 (m, 9H, 3 x CH_3)

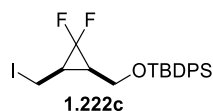
^{13}C NMR (126 MHz, CDCl_3) δ = 215.8, 135.7, 133.2 (d, J = 5.4 Hz), 130.0, 128.0 (d, J = 4.5 Hz), 113.2 (dd, $^1J_{\text{CF}}$ = 290.2, 283.8 Hz), 67.4 (d, $^3J_{\text{CF}}$ = 6.4 Hz), 57.3 (d, $^3J_{\text{CF}}$ = 4.5 Hz), 27.7 (t, $^2J_{\text{CF}}$ = 10.0 Hz), 26.9, 23.5 (t, $^2J_{\text{CF}}$ = 10.4 Hz), 19.3, 19.3

^{19}F NMR (471 MHz, CDCl_3) δ = -124.9 (dt, J = 164.3 Hz, 12.4 Hz, 1F), -150.9 (br d, J = 164.7 Hz, 1F)

HRMS: ($\text{C}_{23}\text{H}_{32}\text{F}_2\text{NO}_2\text{S}_2\text{Si}$) $[\text{M}+\text{NH}_4]^+$ 484.1612 required, found $[\text{M}+\text{NH}_4]^+$ 484.1614

IR (neat): 2959, 2857, 1472, 1391, 1207, 1059, 700 cm^{-1}

3.2.4.13 Synthesis of Iodo Difluorocyclopropane 1.222c



Triphenylphosphine (523mg, 2.0 mmol) and difluorocyclopropane **1.221** (500 mg, 1.3 mmol) were taken up dry THF (6 mL, 4.5 mL/mmol of **1.221**) in an oven dried round bottomed flask under an atmosphere of argon. The mixture was cooled to 0 °C and pyridine (200 μL , 2.7 mmol) followed by iodine (506 mg, 2.0 mmol) as a solution in dry THF (1 mL, 0.5 mL/mmol iodine) were added dropwise. The mixture was warmed to room temperature and stirred for 68 hours. The reaction was quenched with water, partitioned with diethyl ether and the aqueous layer extracted with two

portions of diethyl ether. The combined organics were washed twice with 1M hydrochloric acid, water and brine, dried with magnesium sulfate, filtered and concentrated *in vacuo*. The residue was purified using silica chromatography with a gradient of 0-8% diethyl ether in petroleum ether to give the title compound **1.222c** as a colourless oil (329.9 mg, 0.7 mmol, 51%)

^1H NMR (500 MHz, CDCl_3) δ = 7.66 (d, J = 6.6 Hz, 4H, 4 x ArH), 7.48 - 7.38 (m, 6H, 5 x ArH), 3.84 (d, J = 7.5 Hz, 2H, OCH_2), 3.23 - 3.11 (m, 2H, ICH_2), 2.26 - 2.15 (m, 1H, CH), 2.00 - 1.90 (m, 1H, CH), 1.06 (s, 9H, 3 x CH_3)

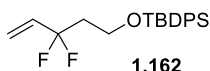
^{13}C NMR (126 MHz, CDCl_3) δ = 135.7, 133.2 (d, J = 5.4 Hz), 130.1, 128.0 (d, J = 3.6 Hz), 114.0 (dd, $^1J_{\text{CF}}$ = 293.8, 284.7 Hz), 56.3 (d, $^3J_{\text{CF}}$ = 5.4 Hz), 30.1 (t, $^2J_{\text{CF}}$ = 9.5 Hz), 29.0 (t, $^2J_{\text{CF}}$ = 10.9 Hz), 26.9, 19.3, -6.0 (d, $^3J_{\text{CF}}$ = 6.4 Hz)

^{19}F NMR (471 MHz, CDCl_3) δ = -124.9 (dt, J = 162.6 Hz, 12.4 Hz, 1F), -154.4 (br d, J = 161.3 Hz, 1F)

HRMS: ($\text{C}_{21}\text{H}_{26}\text{F}_2\text{IOSi}$) $[\text{M}+\text{H}]^+$ required 487.0766, found $[\text{M}+\text{H}]^+$ 487.0766

IR (neat): 3071, 2959, 2930, 1464, 1427, 1109, 700 cm^{-1}

3.2.4.14 Synthesis of TBDPS Protected Alcohol 1.162



This is the general procedure used in the scale up. Screening reactions were run with 50 mg of substrate **1.222a**, **1.222b** or **1.222c** as outlined in **Table 8**.

Iodo difluorocyclopropane **1.222c** (250 mg, 0.5 mmol), AIBN (8 mg, 0.05 mmol) and $(\text{TMS})_3\text{SiH}$ (200 μL , 0.55 mmol) were taken up in an oven dried microwave vial under an atmosphere of argon/ N_2 . Dry benzene, (10 mL, 20 mL/mmol of **1.222c**) was added and the reaction vial de-gassed by sonication under a balloon of argon/ N_2 for 30 minutes. The reaction was then heated to reflux for 16 hours, cooled to room temperature and concentrated *in vacuo*. The residue was then purified with silica chromatography using a gradient of 0-3% diethyl ether in petroleum ether to give the

title compound **1.162** as a mixture with unknown silyl by-products (190 mg, 0.53 mmol, quant. yield).

Table 8: Screening Conditions for Deoxygenation/Dehalogenation

Entry	Substrate	Hydrogen Donor
1	1.222a	Bu ₃ SnH
2	1.222a	(TMS) ₃ SiH
3	1.222b	Bu ₃ SnH
4	1.222b	(TMS) ₃ SiH
5	1.222c	Bu ₃ SnH
6	1.222c	(TMS) ₃ SiH

¹H NMR (500 MHz, CDCl₃) δ = 7.68 - 7.64 (m, 5H, 4 x ArH + impurity), 7.46 - 7.37 (m, 7H, 6 x ArH + impurity), 5.93 (dq, *J* = 17.4 Hz, 11.1 Hz, 1H, C=CH), 5.58 (dt, *J* = 2.5, 17.4 Hz, 1H, C=CH), 5.36 (d, *J* = 11.0 Hz, 1H, C=CH), 3.84 (t, *J* = 6.8 Hz, 2H, OCH₂), 2.23 (tt, *J* = 15.6 Hz, 6.8 Hz, 2H, CF₂CH₂), 1.05 (s, 11H, 3 x CH₃ + impurity)

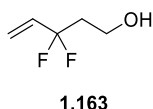
¹³C NMR (101 MHz, CDCl₃) δ = 135.7, 133.6, 133.3 (t, ²*J*_{CF} = 26.9 Hz), 129.9, 127.9, 120.6 (t, ¹*J*_{CF} = 238.9 Hz), 118.9 (t, ³*J*_{CF} = 9.6 Hz), 58.3 (t, ³*J*_{CF} = 6.2 Hz), 40.3 (t, ²*J*_{CF} = 25.8 Hz), 26.9, 19.3

¹⁹F NMR (471 MHz, CDCl₃) δ = -96.1 - -96.2 (m)

HRMS: (C₂₁H₃₀F₂NOSi) [M+NH₄]⁺ expected 378.2065, found [M+NH₄]⁺ 378.2062

IR (neat): 3071, 2963, 2830, 1589, 1427, 1391, 1105, 700 cm⁻¹

3.2.4.15 Synthesis of 3,3-difluoropent-4-en-1-ol (1.163)



Solid Supported TBAF Procedure

Resin bound TBAF (0.33g/mol of **1.162**, 45 mg) was weighed into a 5 mL Falcon tube and compound **1.162** (137 mg, 0.41 mmol) was added as a solution in diethyl ether

(0.2 M, 2 mL) and the reaction shaken for 24 hours. Upon reaction monitoring by TLC, there was no observable product upon development with vanillin or potassium permanganate. The starting material was recovered and used in subsequent reactions.

Methanolic HCl Procedure

Compound **1.162** (0.3 mmol, 100 mg) was taken up in dry methanol. Acetyl chloride (15 mol%, 3 μ L) was added at room temperature and the reaction stirred at this temperature overnight. TLC of the reaction mixture after 21 hours indicated complete consumption of the starting material with the formation of two new spots, one which was not UV active and stained in vanillin which was product. The solvent was then removed by distillation (60 °C, atmospheric pressure) and the residue isolated either by flash column chromatography or by distillation.

By flash column chromatography, the product was lost upon concentration of the clean sample.

By distillation, the product started to degrade at temperatures greater than 100 °C, atmospheric pressure.

TBAF Deprotection - Overnight Conditions

Compound **1.162** (5.5 mmol, 2 g) was taken up in dry THF (0.38 mL/mmol of **1.162**, 2.1 mL) and cooled to 0 °C. TBAF (1M THF, 16.5 mmol, 16.5 mL) was added dropwise and the reaction allowed to slowly warm to room temperature overnight with stirring. Upon addition of the TBAF solution, the reaction mixture foamed violently. TLC after 17 hours indicated the reaction had gone to completion and the reaction was quenched with 10 mL of saturated ammonium chloride and diluted with diethyl ether. The layers were partitioned, and the aqueous layers extracted three times with diethyl ether. The combined organics were dried with magnesium sulfate, filtered and concentrated at 0 °C under vacuum. The residue was then purified by column chromatography using a gradient of 0-45% diethyl ether in *n*-pentane and the fractions containing clean product collected and concentrated *in vacuo* (850 mbar,

35 °C) to give the title compound as a pale yellow oil (657 mg, >100% yield, 61% purity by ^1H NMR – impurities were *n*-pentane and diethyl ether)

TBAF Deprotection – 1-hour reaction

The same reaction conditions were employed as above with the reaction time being limited to 1 hour. The work up and purification was as above to give the title compound as a pale-yellow oil (1.39 g, >100% yield, 31 % purity by ^1H NMR – impurities were diethyl ether and *n*-pentane

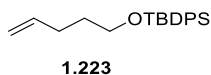
^1H NMR (500 MHz, CDCl_3) δ = 5.95 (dq, 1H, J = 17.4 Hz, 11.0 Hz, $\text{HC}=\text{C}$), 5.64 (dt, 1H, J = 17.4 Hz, 2.6 Hz, $\text{HC}=\text{C}$), 5.43 (d, 1H, J = 11.1 Hz, $\text{HC}=\text{C}$), 3.84 (t, 1H, J = 6.3 Hz, CH_2OH), 2.21 (tt, 1H, J = 16.4 Hz, 6.2 Hz, CF_2CH_2)

^{19}F NMR (470 MHz, CDCl_3) δ = -96.8 - -96.9 (m)

HRMS: too volatile to detect

IR (CDCl_3): 3361 (b), 2868, 2919, 1654, 1420, 734 cm^{-1}

3.2.4.16 Synthesis of TBDPS Protected Pentenol 1.223



Sodium hydride (11.6 mmol, 464 mg of 60% dispersion in mineral oil) was placed in an oven dried two-necked flask under an atmosphere of nitrogen. The flask was evacuated and purged three times with nitrogen then dry THF (1.5 mL/mmol, 16.5 mL) was added. Pentenol (11.6 mmol, 1.2 mL) was added dropwise to the solution with immediate hydrogen gas evolution observed. The reaction was stirred at room temperature for one hour then TBDPSCI (11.6 mmol, 3 mL) was added dropwise as a solution in dry THF (1.5 mL/mmol, 16.5 mL). The reaction was stirred for 65 hours then quenched with 20 mL of saturated ammonium chloride solution. The THF was removed under vacuum and the residue partitioned between water and diethyl ether. The aqueous layer was extracted with three portions of diethyl ether and the combined organics dried with magnesium sulfate and concentrated *in vacuo*. The residue was purified using flash column chromatography utilising a gradient of 0-10%

ethyl acetate and petroleum ether to give the title compound as a colourless oil (2.14 g, 57% yield).

^1H NMR (500 MHz, CDCl_3) δ = 7.69-7.67 (m, 4H, ArH), 7.44-7.37 (m, 6H, ArH), 5.85-5.77 (m, 1H, HC=C), 5.01 (dd, 1H, J = 17.1 Hz, 1.4 Hz, HC=C), 4.95 (dd, 1H, J = 10.2 Hz, 0.6 Hz, HC=C), 3.69 (t, 2H, J = 6.4 Hz, CH_2OSi), 2.16 (q, 2H, J = 7.0 Hz, $\text{C}=\text{CHCH}_2\text{CH}_2$), 1.67 (m, 2H, $\text{CH}_2\text{CH}_2\text{CH}_2$), 1.06 (s, 9H, 3 x CH_3)

^{13}C NMR (126 MHz, CDCl_3) δ = 138.7, 135.7, 134.2, 129.6, 127.7, 114.6, 63.4, 32.0, 30.2, 27.0, 19.4

The data recorded are consistent with the literature.²³³

3.2.4.17 Attempted Optimisation of the Acid Deprotection of 1.223

1.223 (0.28 mmol, 100 mg) was placed in a 5 mL microwave vial and taken up in diethyl ether (volume specified in **Table 9**). The vial was sealed using a rubber septum and methanol (volume specified in **Table 9**) was added followed by 2M HCl in diethyl ether (volume specified in **Table 9**). The vials were then run at 25 °C for 19 hours before analysis by TLC.

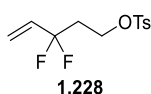
Unfortunately, complete conversion to the desired alcohol was not observed in any case and as the end product was a commercially available feedstock, it was not isolated.

Table 9: Reaction conditions deprotection optimisation using the model substrate

Entry	Acid Loading (mol%, μL)	MeOH (equiv., μL)	Et ₂ O (μL)	Total Volume (μL)
1	40, 62	0, 0	938	1000
2	40, 62	1, 12	926	1000
3	40, 62	2, 25	913	1000
4	40, 62	3, 37	901	1000
5	40, 62	4, 50	888	1000
6	40, 62	5, 62	876	1000
7	60, 92	0, 0	908	1000
8	60, 92	1, 12	895	1000

9	60, 92	2, 25	883	1000
10	60, 92	3, 37	870	1000
11	60, 92	4, 50	858	1000
12	60, 92	5, 62	845	1000
13	80, 123	0, 0	877	1000
14	80, 123	1, 12	864	1000
15	80, 123	2, 25	852	1000
16	80, 123	3, 37	839	1000
17	80, 123	4, 50	827	1000
18	80, 123	5, 62	814	1000
19	100, 154	0, 0	846	1000
20	100, 154	1, 12	833	1000
21	100, 154	2, 25	821	1000
22	100, 154	3, 37	808	1000
23	100, 154	4, 50	796	1000
24	100, 154	5, 62	784	1000

3.2.4.18 Synthesis of Tosylate 1.228



Single Purification Method

Compound **1.162** (TBDPS alcohol) (1.39 mmol, 500 mg) was taken up in dry THF (0.38 mL/ mmol **1.162**, 0.53 mL) under a nitrogen atmosphere and cooled to 0 °C. TBAF (1M THF, 4.17 mmol, 4.2 mL) was added dropwise (reaction started bubbling), and the reaction allowed to warm to room temperature and stirred for 18 hours. TLC indicated full conversion of the starting material. The reaction was quenched with saturated ammonium chloride and partitioned with diethyl ether. The aqueous layer was extracted with a further three portions of diethyl ether and the combined organic layers dried with magnesium sulfate and concentrated *in vacuo* at 0 °C.

The residue was taken up in DCM (2.3 mL/mmol of **1.162**, 3.2 mL) and DMAP (0.72 mmol, 88 mg), TsCl (1.67 mmol, 318 mg) and NEt₃ (2.78 mmol, 387 μ L) added in that order. The reaction was then stirred at room temperature for 18 hours where TLC indicated partial conversion of alcohol **1.163**. The reaction was diluted with DCM, and the reaction extracted with two portions of saturated copper(II) sulfate solution, two portions of saturated sodium bicarbonate solution and two portions of brine. The organics were dried with magnesium sulfate and concentrated under reduced pressure. The residue was purified by flash column chromatography eluting with a gradient of 0-20% diethyl ether in petroleum ether to give the title compound as a colourless oil (100 mg, 26% yield).

From alcohol **1.163**

1.163 (409 mg, 3.6 mmol) was taken up in dry DCM (8.4 mL, 2.3 mL/mmol of **1.163**) and cooled to 0 °C. DMAP (267 mg, 2.2 mmol) followed by TsCl (835 mg, 4.4 mmol) then triethylamine (1 mL, 7.3 mmol). The reaction was then warmed to room temperature and stirred for 19 hours. The reaction was then diluted with DCM and the reaction extracted with two portions of 2 M HCl, two portions of saturated sodium bicarbonate and two portions of brine. The organics were dried with magnesium sulfate and concentrated under reduced pressure. The residue was purified by flash column chromatography using a gradient of 0-20% diethyl ether in petroleum ether to give the title compound as a pale-yellow oil (1.05 g, 3.6 mmol, quant. yield).

¹H NMR (500 MHz, CDCl₃) δ = 7.78 (d, 2H, J = 8.3 Hz, ArH), 7.35 (d, 2H, J = 8.0 Hz, ArH), 5.85 (dq, 1H, J = 17.3 Hz, 11 Hz, C=CH), 5.59 (dt, 1H, J = 17.3 Hz, 2.6 Hz, C=CH), 5.43 (d, 1H, J = 11.0 Hz, C=CH), 4.19 (t, 2H, J = 6.9 Hz, CH₂O), 2.45 (s, 3H, ArCH₃), 2.33 (tt, 2H, J = 15.3 Hz, 6.9 Hz, CF₂CH₂)

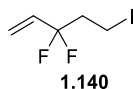
¹³C NMR (126 MHz, CDCl₃) δ = 145.2, 132.8, 132.1 (t, $^2J_{CF}$ = 26.7 Hz), 130.0, 128.0, 120.2 (t, $^3J_{CF}$ = 9.4 Hz), 119.4 (t, $^1J_{CF}$ = 240.2 Hz), 64.0 (t, $^3J_{CF}$ = 5.6 Hz), 36.7 (t, $^2J_{CF}$ = 27.4 Hz), 21.8

¹⁹F NMR (470 MHz, CDCl₃) δ = -97.3 - -97.4 (m)

HRMS (C₁₂H₁₅F₂O₃S) [M+H]⁺ expected 276.0632, found [M+H]⁺ 276.0633

IR (Et₂O): 2922, 1599, 1422, 1359, 1175, 773, 663 cm⁻¹

3.2.4.19 Synthesis of Key Building Block (1.140)



Tosylate **1.228** (1.05 g, 3.8 mmol) was taken up in acetone (2.28 mL, 0.6 mL/mmol **1.228**) and sodium iodide (1.14 g, 7.6 mmol). The reaction was then heated to reflux for 19 hours. The reaction was then cooled to room temperature and diluted with pentane and the organics washed three times with water, and brine. The aqueous washings were backwashed with pentane and the combined organics dried with magnesium sulfate and concentrated under reduced pressure. The residue was filtered through a plug of silica, eluting with pentane, and the fractions containing clean product were concentrated under reduced pressure. The residue was then submitted to Kugelrohr distillation (40 °C, atmospheric) to give the title compound as a colourless oil (513 mg, 58% yield).

¹H NMR (500 MHz, CDCl₃) δ = 5.89 (dq, 1H, *J* = 17.4 Hz, 10.9 Hz, C=CH), 5.66 (dt, 1H, *J* = 17.3 Hz, 2.5 Hz, C=CH), 5.49 (d, 1H, *J* = 11.0 Hz, C=CH), 3.19-3.15 (m, 2H, CH₂I), 2.59-2.49 (m, 2H, CF₂CH₂)

¹³C NMR (126 MHz, CDCl₃) δ = 132.1 (t, ²*J*_{CF} = 27.2 Hz), 120.4 (¹*J*_{CF} = 240.7 Hz), 120.3 (t, ³*J*_{CF} = 9.6 Hz), 42.4 (t, ²*J*_{CF} = 27.3 Hz), -7.3 (t, ³*J*_{CF} = 5.0 Hz)

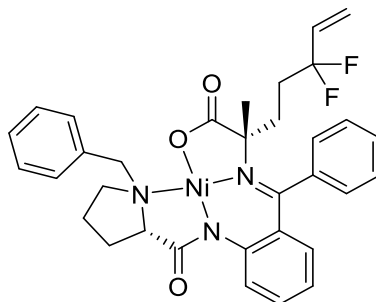
¹⁹F NMR (470 MHz, CDCl₃) δ = -99.1 - -99.2 (m)

HRMS (C₅H₇F₂I) [M]⁺ required 231.9561, found [M]⁺ 231.9565

IR (neat): 2969, 1654, 1418, 1116, 983, 953, 901, 794 cm⁻¹

3.2.5 Synthesis of Fmoc Amino Acid (1.139)

3.2.5.1 Synthesis of alkylated nickel complex (1.157)



1.157

Ni-Ala-BPB **1.144** (128 mg, 0.25 mmol), was taken up in dry THF (2.5 mL, 10 mL/mmol **1.144**) in an oven dried round bottomed flask under an atmosphere on nitrogen. The solution was then cooled to 0 °C using an ice bath and *tert*-butylammonium iodide (9 mg, 0.025 mmol), followed by freshly sublimed potassium *tert*-butoxide (70 mg, 0.625 mmol) were added. The mixture was stirred at 0 °C for 5 minutes before **1.140** (145 mg, 0.625 mmol) was added dropwise over 5 minutes. The reaction was then allowed to warm to room temperature and stirred for 24 hours. The reaction was quenched with 0.1 M hydrochloric acid and stirred for 1 hour. The reaction was diluted with DCM, stirred for 1 hour, then the phases separated. The aqueous layer was then extracted with two portions of DCM and the combined organics dried using a phase separator and concentrated *in vacuo* to give red oil. The residue was then purified using silica chromatography with a gradient of 0-5% methanol in ethyl acetate to give the title compound **1.146** as a red solid (8.8 mg, 5.7% yield).

¹H NMR (400 MHz, CDCl₃) δ = 8.06 (d, 2H, *J* = 7.2 Hz, ArH), 8.00 (d, 1H, *J* = 8.5 Hz, ArH), 7.50-7.45 (m, 2H, ArH), 7.02 (d, 1H, *J* = 7.8 Hz, ArH), 6.67-6.60 (m, 2H, ArH), 5.91 (dq, 1H, *J* = 17.2 Hz, 11.0 Hz, C=CH), 5.65 (dt, 1H, *J* = 17.3 Hz, 2.4 Hz, C=CH), 5.45 (d, 1H, *J* = 11.1 Hz, C=CH), 4.46 (d, 1H, *J* = 12.7 Hz, ArCH₂), 3.67 (d, 1H, *J* = 12.7 Hz, ArCH₂), 3.64-3.60 (m, 1H, ProH), 3.44-3.42 (m, 1H, ProH), 3.29-3.18 (m, 1H, ProH), 2.97-2.83 (m, 1H, Alkyl CH), 2.71-2.64 (m, 1H, ProH), 2.54-2.32 (m, 2H, ProH and Alkyl CH), 2.18 (td, 1H, *J* = 13.9 Hz, 3.4 Hz, Alkyl CH), 2.12-2.02 (m, 2H, ProH), 1.89 (td, 1H, *J* = 13.5 Hz, 4.3 Hz, Alkyl CH), 1.19 (s, 3H, CH₃)

¹³C NMR (100 MHz, CDCl₃) δ = 181.5, 180.7, 173.1, 141.7, 136.2, 133.6, 133.4, 132.6 (t, ²J_{CF} = 27.5 Hz), 131.9, 131.8, 130.4, 129.7, 129.2, 129.1, 128.3, 127.5, 127.1, 124.1, 121.0, 120.8 (t, ¹J_{CF} = 238 Hz), 120.0 (t, ³J_{CF} = 9.4 Hz), 70.2, 63.6, 57.2, 53.5, 50.9, 33.6 (t, ²J_{CF} = 26.2 Hz), 30.7, 29.8, 28.9

¹⁹F NMR (376 MHz, CDCl₃) δ = -95.0 - -95.7 (m, 1F), -99.5 - -100.3 (m, 1F)

HRMS (C₃₃H₃₄F₂N₃NiO₃) [M+H]⁺ required 616.1922 (⁵⁸Ni), found [M+H]⁺ 616.1930 (⁵⁸Ni)

IR (neat): 3025, 2948, 2922, 1671, 1638, 1439, 1357, 1253, 1167, 753, 704 cm⁻¹

3.2.5.2 Attempted Optimisation of the Alkylation Conditions

The alterations to the procedure described for the synthesis of **1.157** were altered as per table.

Table 10: Changes employed to attempt to optimise the alkylation conditions

Entry	Reaction Time (hr)	Concentration (M)	Temperature (°C)	Base (equiv.)	Average Conversion ^a (%)
1	72	0.1	0-RT	KO ^t Bu (2.5)	5.8 ± 0.4
2	24	0.1	0-40	KO ^t Bu (2.5)	16.9 ± 0.5
3	24	1	0-RT	KO ^t Bu (2.5)	3.3 ± 0.3
4	24	0.1	0-RT	KO ^t Bu (1.1)	21.5 ± 0.4
5	24	0.1	0-RT	NaHMDS (2.5)	0.9 ± 0.05
6	24	0.1	0-RT	DBU (2.5)	0
7	24	0.1	0-RT	BEMP (2.5)	0

Entry **1** was run on the same scale as the procedure described above in **section 3.2.5.1**

Entries **2-7** were run using: **1.144** (41 mg, 0.08 mmol) and all other reagents were scaled accordingly.

All reactions described above were worked up and submitted for HPLC analysis as described in the protocol below. Entries **1, 2, and 4** were combined and purified to give compound **1.157** as a red solid (20 mg, 0.03 mmol).

Characterisation was as above section **3.2.5.1**

HPLC Assay Conditions

Stock solutions of Caffeine, **1.144** and **1.157**, were made to a concentration of 0.01 M in methanol. Three samples of a 1:1 caffeine and **1.144** mixture were prepared by mixing 200 µL of the stock caffeine solution and 200 µL of the stock solution of **1.144** and diluting the resulting mixture with 600 µL of acetonitrile and 500 µL of water. The same procedure was used to make up three samples of a 1:1 mixture of caffeine and **1.157**. Each set of samples was used to calculate a conversion factor for both starting material **1.144** and product **1.157**. Each analyte was run in triplicate and the standard deviation calculated. The conversion factors (CF) were 7.23 ± 0.15 for **1.144** and 4.1 ± 0.1 for **1.157** as calculated using **Equation 12** below.

$$CF = \frac{\text{peak area analyte}}{\text{peak area caffeine}}$$

Equation 12: Formula used to work out the conversion factor

Each reaction was quenched and worked up as in **Section 3.2.5.1** before analysis and the residue left after the solvent was removed was diluted to a concentration of 0.04 M, with respect to starting material **1.144**, with methanol. Equal volumes of the 0.01 M caffeine stock solution and reaction mixture were mixed (giving a 1:4 ratio of caffeine to reaction mixture) the ratio (χ) of product to caffeine was calculated using **Equation 13**.

$$\chi = \frac{\text{peak area analyte}}{\text{peak area caffeine} \times 4}$$

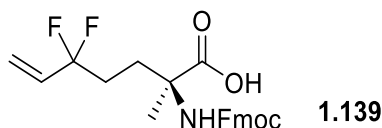
Equation 13: Calculation of the peak ratio of analyte to caffeine

This was then transformed to the conversion by dividing χ by the conversion factor as outlined in **Equation 14**.

$$\text{conversion} = \frac{\chi}{\text{conversion factor of analyte}} \times 100$$

Equation 14: Calculation of the percentage conversion from the peak ratio

3.2.5.3 Synthesis of Fmoc Amino Acid (**1.139**)



Compound **1.157** (20 mg, 0.03 mmol) was taken up in methanol (0.39 mL, 13 mL/mmol **1.157**) and heated to reflux. 2M HCl (0.54 mL, 18 mL/mmol **1.157**) was added dropwise to the refluxing solution and stirred for 2 hours. The reaction was then cooled to room temperature and the methanol removed *in vacuo*. The aqueous residue was then extracted three times with DCM. The organic layers were discarded. The aqueous layer was concentrated *in vacuo* and the pH of the residue adjusted to pH 9 using 6% (w/w) sodium carbonate solution in water. Na₂EDTA (11 mg, 0.03 mmol) was then added to the flask and stirred at room temperature for 10 minutes and the flask then cooled to -10 °C. Fmoc-OSu (11 mg, 0.033 mmol) was then added dropwise as a solution in acetonitrile (equal volume to the sodium carbonate solution) and the reaction allowed to return to room temperature and stirred for 48 hours. The acetonitrile was then removed *in vacuo* and the residue acidified with 2M HCl. The aqueous solution was then extracted 3 times with ethyl acetate and the combined organics were dried with magnesium sulfate and concentrated under reduced pressure. The residue was then purified by preparative TLC (2% MeOH/DCM) to give the title compound (9 mg, 69% yield).

¹H NMR (500 MHz, d₆-DMSO) δ = 7.89 (d, 2H, J = 7.3 Hz, ArH), 7.68 (d, 2H, J = 7.3 Hz, ArH), 7.41 (t, 2H, J = 7.3 Hz, ArH), 7.32 (t, 2H, J = 7.3 Hz, ArH), 6.04-5.94 (m, 1H, C=CH), 5.58-5.54 (m, 1H, C=CH), 5.49-5.47 (m, 1H, C=CH), 4.29-4.19 (m, 3H, Fmoc CH and Fmoc CH₂), 1.90-1.78 (m, 4H, CH₂CH₂), 1.31 (s, 3H, CH₃)

^{13}C NMR (126 MHz, d_6 -DMSO) δ = 174.7, 172.7, 143.9, 140.7, 132.8 (t, $^2J_{\text{CF}}$ = 26.7 Hz), 127.6, 127.0, 125.1, 121.8 (t, $^1J_{\text{CF}}$ = 237 Hz), 120.1, 119.7 (t, $^3J_{\text{CF}}$ = 8.9 Hz), 65.3, 65.1, 57.7, 46.7, 31.4 (t, $^2J_{\text{CF}}$ = 23.7 Hz) 29.0, 28.7, 28.5, 25.2, 23.0

^{19}F NMR (470 MHz, d_6 -DMSO) δ = -95.5 (s)

LCMS: R_t = 7.146 mins; m/z = 414.1 $[\text{M}-\text{H}^+]$

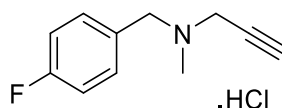
3.3 Chapter 2 – Experimental

3.3.1 General Procedure A: alkylation with DIPEA

Bromide (0.25 mmol) and amine (0.275 mmol) were taken up in acetonitrile (0.3 mL) in a conical vial. Diisopropylethylamine (DIPEA, 0.375 mmol) was added and the vial sealed with a screwcap and the reaction stirred at room temperature until TLC indicated complete consumption of the amine. A precipitate had formed which was removed by filtration and the filtrate concentrated under reduced pressure. The residue was purified by flash chromatography and sent to NKI for biological testing.

The following compounds were synthesised using this procedure.

3.3.1.1 *N*-(4-fluorobenzyl)-*N*-methylprop-2-yn-1-amine (2.02)



2.02

Synthesized using *N*-methylpropargylamine and 4-fluorobenzyl bromide to give the title which was isolated as the HCl salt (20 mg, 44% yield).

^1H NMR (500 MHz, d_6 -DMSO) δ = 11.89 (br, 1H, $[\text{NH}]^+$), 7.69 (dd, J = 8.4, 5.6 Hz, 2H, ArH), 7.31-7.27 (m, 2H, ArH), 4.30 (br s, 2H, ArCH_2), 3.99-3.88 (m, 3H, $\text{C}\equiv\text{CH}$ and $\text{HC}\equiv\text{CCH}_2$), 2.67 (s, 3H, NCH_3)

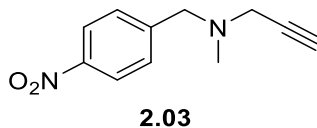
^{19}F NMR (470 MHz, d_6 -DMSO) δ = -111.9 (s)

^{13}C NMR (125 MHz, d_6 -DMSO) δ = 162.7 (d, $^1J_{\text{CF}}$ = 247.2 Hz), 133.6 (d, $^3J_{\text{CF}}$ = 8.5 Hz), 126.1, 115.6 (d, $^2J_{\text{CF}}$ = 22.1 Hz), 81.6, 73.0, 56.2, 43.3, 38.4

HRMS ($\text{C}_{11}\text{H}_{13}\text{FN}$) $[\text{M}+\text{H}]^+$ required 178.1027; found $[\text{M}+\text{H}]^+$ 178.1023

IR (neat): 3194, 2990, 2501, 2123, 1600, 1512, 1469, 1124, 725 cm⁻¹

3.3.1.2 *N*-methyl-*N*-(4-nitrobenzyl)prop-2-yn-1-amine (2.03)



Synthesized using using *N*-methylpropargylamine and 4-nitrobenzyl bromide to give the title compound (67 mg, quant. yield).

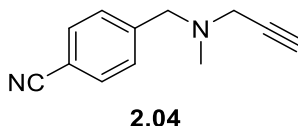
¹H NMR (400 MHz, CDCl₃) δ = 8.20-8.16 (m, 2H, ArH), 7.54-7.51 (m, 2H, ArH), 3.67 (s, 2H, ArCH₂), 3.32 (d, *J* = 2.3 Hz, 2H, C≡CCH₂), 2.34 (s, 3H, NCH₃), 2.29 (t, *J* = 2.3 Hz, 1H, C≡CH)

¹³C NMR (100 MHz, CDCl₃) δ = 147.4, 146.5, 129.7, 123.7, 78.1, 73.9, 59.3, 45.4, 41.9

HRMS (C₁₁H₁₃N₂O₂) [M+H]⁺ required 205.0972; found [M+H]⁺ 205.0970

IR (neat): 3292, 2980, 2790, 2360, 1604, 1516, 1458, 1342, 738 cm⁻¹

3.3.1.3 4-((methyl(prop-2-yn-1-yl)amino)methyl)benzonitrile (2.04)



Synthesized using *N*-methylpropargylamine and 4-(bromomethyl)benzonitrile to give the title compound (51 mg, quant. yield).

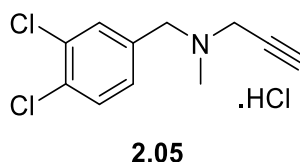
¹H NMR (500 MHz, CDCl₃) δ = 7.61 (d, *J* = 8.3 Hz, 2H, ArH), 7.46 (d, *J* = 8.3 Hz, 2H, ArH), 3.62 (s, 2H, ArCH₂), 3.30 (d, *J* = 2.4 Hz, 2H, C≡CCH₂), 2.33 (s, 3H, NCH₃), 2.28 (t, *J* = 2.4 Hz, 1H, C≡CH)

¹³C NMR (125 MHz, CDCl₃) δ = 144.3, 132.2, 129.6, 118.9, 111.1, 78.0, 73.7, 59.5, 45.2, 41.8

HRMS: (C₁₂H₁₃N₂) [M+H]⁺ required 185.1073; found [M+H]⁺ 185.1070

IR (neat): 3292, 2980, 2794, 2358, 2227, 1608, 1504, 1456, 1363 cm⁻¹

3.3.1.4 *N*-(3,4-dichlorobenzyl)-*N*-methylprop-2-yn-1-amine (2.05)



Synthesized using *N*-methylpropargylamine and 3,4-dichlorobenzyl bromide to give the title compound which was isolated as the HCl salt (13 mg, 22% yield).

^1H NMR (500 MHz, $\text{d}_4\text{-MeOH}$) δ = 7.82 (d, J = 2.0 Hz, 1H, ArH), 7.66 (d, J = 8.3 Hz, 1H, ArH), 7.54 (dd, J = 8.3 Hz, 2.0 Hz, 1H, ArH), 4.47 (s, br, 2H, ArCH₂), 4.11 (s, br, 2H, C \equiv CCH₂), 3.47 (t, J = 2.5 Hz, C \equiv CH), 2.95 (s, 3H, NCH₃)

^{13}C NMR: (125 MHz, $\text{d}_4\text{-MeOH}$) δ = 135.6, 134.3, 134.2, 132.5, 132.1, 131.0, 82.1, 72.6, 58.2, 45.7, 40.2

HRMS: (C₁₁H₁₂Cl₂N) [M+H]⁺ required 228.0341 (^{35}Cl , ^{35}Cl) found [M+H]⁺ 228.0343 (^{35}Cl , ^{35}Cl)

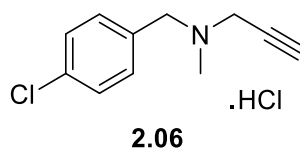
IR (neat): 3180, 2980, 2891, 2472, 2121, 1469, 1355, 731, 721 cm⁻¹

3.3.2 General Procedure B: alkylation with potassium carbonate

Amine (0.25 mmol), and bromide (0.25 mmol) were taken up in acetonitrile (0.3 mL) in a conical vial equipped with a stirrer bar. Potassium carbonate (0.5 mmol) was added followed by potassium iodide (10 mol%) if required. The vial was sealed with a screwcap and the reaction was stirred at 40 °C until thin layer chromatography (TLC) indicated complete consumption of the starting materials. A precipitate was formed during the reaction which was removed by filtration and the filtrate concentrated under reduced pressure. The residue was purified by flash column chromatography and sent to the Netherlands Cancer Institute (NKI) for biological testing.

The following compounds were synthesised using this procedure.

3.3.2.1 *N*-(4-chlorobenzyl)-*N*-methylprop-2-yn-1-amine (2.06)



Synthesized using *N*-methylpropargylamine and 4-chlorobenzyl bromide to give the title compound which was isolated as the HCl salt (11.3 mg, 23% yield).

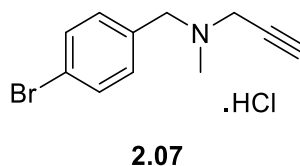
^1H NMR (500 MHz, $\text{d}_6\text{-DMSO}$) δ = 11.66 (br, 1H, $[\text{NH}]^+$), 7.63 (d, J = 8.4 Hz, 2H, *ArH*), 7.53 (d, J = 8.4 Hz, 2H, *ArH*), 4.29 (s, br, 2H, ArCH_2), 3.94-3.89 (m, 3H, $\text{C}\equiv\text{CH}$ and $\text{C}\equiv\text{CCH}_2$), 2.68 (s, 3H, NCH_3)

^{13}C NMR (100 MHz, $\text{d}_6\text{-DMSO}$) δ = 134.4, 133.1, 128.8, 81.6, 73.1, 56.4, 43.5, 38.6, *signal for one quaternary aromatic not observed.

HRMS ($\text{C}_{11}\text{H}_{13}\text{ClN}$) $[\text{M}+\text{H}]^+$ required 194.0731 (^{35}Cl), found $[\text{M}+\text{H}]^+$ 194.0729 (^{35}Cl)

IR (neat): 3192, 2800, 2488, 2123, 1598, 1492, 1460, 1350, 725 cm^{-1}

3.3.2.2 *N*-(4-bromobenzyl)-*N*-methylprop-2-yn-1-amine (2.07)



Synthesized using general procedure A using *N*-methylpropargylamine and 4-bromobenzyl bromide and the title compound isolated as the HCl salt (29 mg, 48% yield).

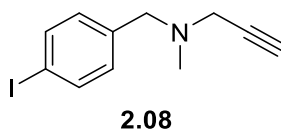
^1H NMR (500 MHz, $\text{d}_6\text{-DMSO}$) δ = 11.61 (br, 1H, $[\text{NH}]^+$), 7.67 (d, J = 8.7 Hz, 2H, *ArH*), 7.55 (d, J = 8.7 Hz, 2H, *ArH*), 4.27 (s, br, 2H, ArCH_2), 4.01-3.89 (m, 3H, $\text{C}\equiv\text{CH}$ and $\text{C}\equiv\text{CCH}_2$), 2.68 (s, 3H, NCH_3)

^{13}C NMR (100 MHz, $\text{d}_6\text{-DMSO}$) δ = 160.1, 132.7, 121.5, 114.1, 81.5, 73.1, 56.7, 55.2, 43.2

HRMS ($\text{C}_{11}\text{H}_{13}\text{BrN}$) $[\text{M}+\text{H}]^+$ required 238.0227 (^{79}Br); found $[\text{M}+\text{H}]^+$ 238.0226 (^{79}Br)

IR (neat): 3194, 2800, 2490, 2123, 1593, 1490, 1469, 725 cm^{-1}

3.3.2.3 *N*-(4-iodobenzyl)-*N*-methylprop-2-yn-1-amine (2.08)



Synthesized on a 0.5 mmol scale using using *N*-methylpropargylamine and 4-iodobenzyl bromide to give the title compound (104 mg, 73% yield).

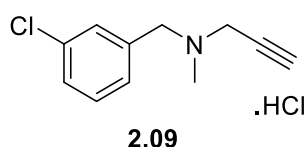
^1H NMR (400 MHz, CDCl_3) δ = 7.66-7.63 (m, 2H, ArH), 7.11-7.08 (m, 2H, ArH), 3.51 (s, 2H, ArCH₂), 3.29 (d, J = 2.4 Hz, 2H, C \equiv CCH₂), 2.32 (s, 3H, NCH₃), 2.27 (t, J = 2.4 Hz, 1H, C \equiv CH)

^{13}C NMR (100 MHz, CDCl_3) δ = 138.2, 137.5, 131.2, 92.7, 78.4, 73.6, 59.4, 45.0, 41.8

HRMS ($\text{C}_{11}\text{H}_{13}\text{IN}$) $[\text{M}+\text{H}]^+$ required 286.0014; found $[\text{M}+\text{H}]^+$ 286.0081

IR (neat): 3190, 2800, 2484, 2123, 1589, 1487, 727 cm^{-1}

3.3.2.4 *N*-(3-chlorobenzyl)-*N*-methylprop-2-yn-1-amine (2.09)



Synthesized using using *N*-methylpropargylamine and 3-chlorobenzyl bromide to give the title compound which was isolated as the HCl salt (21 mg, 43% yield).

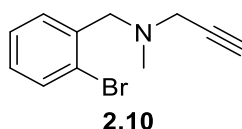
^1H NMR (500 MHz, $\text{d}_6\text{-DMSO}$) δ = 11.57 (br, 1H, $[\text{NH}]^+$), 7.73 (s, 1H, ArH), 7.57-7.47 (m, 3H, ArH), 4.29 (br,s, 2H, ArCH₂), 4.03-3.89 (m, 3H, C \equiv CH, and C \equiv CCH₂), 2.69 (s, 3H, NCH₃)

^{13}C NMR (100 MHz, $\text{d}_6\text{-DMSO}$) δ = 133.3, 132.2, 131.0, 130.6, 129.8, 129.5, 81.7, 73.1, 56.6, 43.8, 38.7

HRMS ($\text{C}_{11}\text{H}_{13}\text{ClN}$) $[\text{M}+\text{H}]^+$ required 194.0731 (^{35}Cl); found $[\text{M}+\text{H}]^+$ 194.0729 (^{35}Cl)

IR (neat): 3180, 2800, 2499, 2121, 1600, 1575, 1462, 790, 732 cm^{-1}

3.3.2.5 *N*-(2-bromobenzyl)-*N*-methylprop-2-yn-1-amine (2.10)



Synthesized on a 0.5 mmol scale using using *N*-methylpropargylamine and 2-bromobenzyl bromide to give the title compound (57 mg, 47% yield).

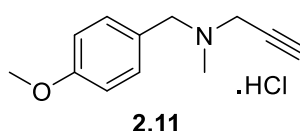
^1H NMR (500 MHz, CDCl_3) δ = 7.55 (d, J = 7.5 Hz, 1H, ArH), 7.44 (d, J = 7.5 Hz, 1H, ArH), 7.28 (t, J = 7.5 Hz, 1H, ArH), 7.12 (td, J = 7.5 Hz, 1.5 Hz, 1H, ArH), 3.68 (s, 2H, ArCH_2), 3.38 (d, J = 2.2 Hz, 2H, $\text{C}\equiv\text{CCH}_2$), 2.38 (s, 3H, NCH_3), 2.29 (t, J = 2.2 Hz, 1H, $\text{C}\equiv\text{CH}$)

^{13}C NMR (125 MHz, CDCl_3) δ = 137.8, 133.0, 131.1, 128.8, 127.4, 125.1, 78.8, 73.6, 59.4, 45.4, 41.8

HRMS: ($\text{C}_{11}\text{H}_{13}\text{BrN}$) $[\text{M}+\text{H}]^+$ required 238.0226 (^{79}Br); found $[\text{M}+\text{H}]^+$ 238.0229 (^{79}Br)

IR (neat): 3296, 2922, 2792, 2360, 1612, 1566, 1460, 1360, 749 cm^{-1}

3.3.2.6 *N*-(4-methoxybenzyl)-*N*-methylprop-2-yn-1-amine (2.11)



Synthesized using *N*-methylpropargylamine and 4-methoxybenzyl chloride to give the title compound which was isolated as the HCl salt (19 mg, 41%).

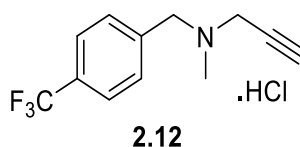
^1H NMR (500 MHz, $\text{d}_6\text{-DMSO}$) δ = 11.46 (br, 1H, $[\text{NH}]^+$), 7.51 (d, J = 8.6 Hz, 2H, ArH), 7.00 (d, J = 8.6 Hz, 2H, ArH), 4.25-4.22 (m, 2H, ArCH_2), 3.98-3.89 (m 3H, $\text{C}\equiv\text{CH}$ and $\text{C}\equiv\text{CCH}_2$), 3.78 (s, 3H, ArOCH_3), 2.67 (s, 3H, NCH_3)

^{13}C NMR (100 MHz, d_6 DMSO) δ = 160.1, 132.7, 121.5, 114.1, 81.5, 73.1, 56.7, 55.2, 43.2, 38.3

HRMS ($\text{C}_{12}\text{H}_{16}\text{NO}$) $[\text{M}+\text{H}]^+$ required 190.1226; found $[\text{M}+\text{H}]^+$ 190.1224

IR (neat): 3190, 2800, 2505, 2123, 1612, 1514, 1460, 1357, 725 cm^{-1}

3.3.2.7 *N*-methyl-*N*-(4-(trifluoromethyl)benzyl)prop-2-yn-1-amine (2.12)



Synthesized using *N*-methylpropargylamine and 4-(trifluoromethyl)benzyl bromide to give the title compound which was isolated as the HCl salt (48 mg, 85% yield).

^1H NMR (500 MHz, $\text{d}_4\text{-MeOH}$) δ = 7.83-7.79 (m, 4H, ArH), 4.55 (s, br, 2H, ArCH₂), 4.12 (s, br, 2H, C \equiv CCH₂), 3.49 (t, J = 2.4 Hz, 1H, C \equiv CH), 2.95 (s, 3H, NCH₃)

^{19}F NMR (376 MHz, $\text{d}_4\text{-MeOH}$) δ = -64.4 (s)

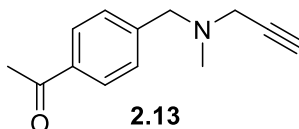
^{13}C NMR: (125 MHz, $\text{d}_4\text{-MeOH}$) δ = 134.7, 133.2 (q, $^2J_{\text{CF}}$ = 32.8 Hz), 133.1, 127.3 (q, $^3J_{\text{CF}}$ = 3.7 Hz), 125.2 (q, $^1J_{\text{CF}}$ = 273.1 Hz), 82.1, 72.7, 58.9, 45.8, 40.3

$^{13}\text{C}\{^{19}\text{F}\}$ NMR (100 MHz, $\text{d}_4\text{-MeOH}$) δ = 134.7 (t, J = 8 Hz), 133.1 (dd, J = 164.4, 4.8 Hz), 133.3 (t, J = 6.5 Hz), 127.3 (dd, J = 165.2, 5.0 Hz), 125.3 (s), 82.1 (d, J = 256 Hz), 72.7 (d, J = 51.1 Hz), 58.9 (t, J = 149.5 Hz), 45.8 (t, J = 147.5 Hz), 40.3 (q, J = 144.9 Hz)

HRMS: ($\text{C}_{12}\text{H}_{13}\text{F}_3\text{N}$) $[\text{M}+\text{H}]^+$ required 228.0995; found $[\text{M}+\text{H}]^+$ 228.0997

IR (neat): 3188, 2800, 2493, 2362, 2123, 1612, 1514, 1460, 1327, 727 cm^{-1}

3.3.2.8 1-(4-((methyl(prop-2-yn-1-yl)amino)methyl)phenyl)ethan-1-one (2.13)



Synthesized on a 0.5 mmol scale using *N*-methylpropargylamine and 1-(4-(bromomethyl)phenyl)ethan-1-one to give the title compound (153 mg, quant. yield).

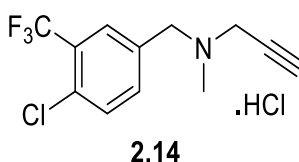
^1H NMR (400 MHz, CDCl_3) δ = 7.91 (d, J = 8.4 Hz, 2H, ArH), 7.44 (d, J = 8.4 Hz, 2H, ArH), 3.62 (s, 2H, ArCH₂), 3.31 (d, J = 2.3 Hz, 2H, C \equiv CCH₂), 2.59 (s, 3H, ArC(O)CH₃), 2.34 (s, 3H, NCH₃), 2.28 (t, J = 2.3 Hz, 1H, C \equiv CH)

^{13}C NMR (100 MHz, CDCl_3) δ = 197.9, 144.2, 136.3, 129.2, 128.5, 78.3, 73.6, 59.6, 45.2, 41.9, 26.7

HRMS: ($\text{C}_{13}\text{H}_{16}\text{NO}$) $[\text{M}+\text{H}]^+$ required 202.1226; found $[\text{M}+\text{H}]^+$ 202.1226

IR (neat): 3196, 2980, 2503, 2125, 1688, 1608, 1462, 1352, 723 cm^{-1}

3.3.2.9 *N*-(4-chloro-3-(trifluoromethyl)benzyl)-*N*-methylprop-2-yn-1-amine (2.14)



Synthesized on a 0.5 mmol scale using *N*-methylpropargylamine and 4-chloro-3-(trifluoromethyl)benzyl bromide to give the title compound which was isolated as the HCl salt (66 mg, 50% yield).

^1H NMR (500 MHz, $\text{d}_4\text{-MeOH}$) δ = 8.06-8.05 (m, 1H, ArH), 7.86-7.84 (m, 1H, ArH), 7.78-7.76 (m, 1H, ArH), 4.55 (s, br, 2H, ArCH₂), 4.13 (s, br, 2H, C \equiv CCH₂), 3.49 (t, J = 2.5 Hz, 1H, C \equiv CH), 2.96 (s, 3H, NCH₃),

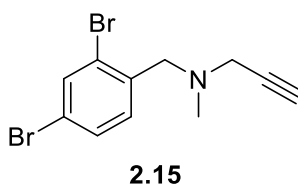
^{19}F NMR (470 MHz, $\text{d}_4\text{-MeOH}$) δ = -64.1 (s)

^{13}C NMR (125 MHz, $\text{d}_4\text{-MeOH}$) δ = 137.5, 135.4, 133.8, 131.7 (q, $^3J_{\text{CF}}$ = 5.4 Hz), 130.1, 130.1 (q, $^2J_{\text{CF}}$ = 31.8 Hz), 124.0 (q, $^1J_{\text{CF}}$ = 272.5 Hz), 82.2, 72.6, 58.3, 45.8, 40.2

HRMS ($\text{C}_{12}\text{H}_{12}\text{ClF}_3\text{N}$) $[\text{M}+\text{H}]^+$ required 262.0605 (^{35}Cl); found $[\text{M}+\text{H}]^+$ 262.0604 (^{35}Cl)

IR (neat): 3184, 2980, 2484, 2123, 1614, 1433, 1321, 731, 661 cm^{-1}

3.3.2.10 *N*-(2,4-dibromobenzyl)-*N*-methylprop-2-yn-1-amine (2.15)



Synthesized on a 0.5 mmol scale using *N*-methylpropargylamine and 2,4-dibromo-1-(bromomethyl)benzene (**2.33**) to give the title compound (130 mg, 82% yield).

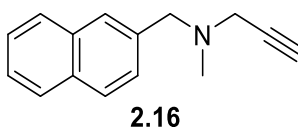
^1H NMR (500 MHz, CDCl_3) δ = 7.71 (d, J = 1.9 Hz, 1H, ArH), 7.41 (dd, J = 8.2, 1.9 Hz, 1H, ArH), 7.33 (d, J = 8.2 Hz, 1H, ArH), 3.61 (d, J = 8.3 Hz, 2H, ArCH₂), 3.36 (d, J = 2.3 Hz, 2H, C \equiv CCH₂), 2.36 (s, 3H, NCH₃), 2.29 (t, J = 2.3 Hz, 1H, C \equiv CH)

^{13}C NMR (101 MHz, CDCl_3) δ = 137.1, 135.3, 132.1, 130.6, 125.5, 121.4, 78.6, 73.7, 58.9, 45.5, 41.8

HRMS: ($\text{C}_{11}\text{H}_{12}\text{Br}_2\text{N}$) $[\text{M}+\text{H}]^+$ required 315.9331 (^{79}Br , ^{79}Br); found $[\text{M}+\text{H}]^+$ 315.9329 (^{79}Br)

IR (neat): 3294, 3082, 2971, 2939, 2915, 2842, 2789, 1463, 807 cm^{-1}

3.3.2.11 *N*-methyl-*N*-(naphthalen-2-ylmethyl)prop-2-yn-1-amine (2.16)



Synthesized on a 0.5 mmol scale using *N*-methylpropargylamine and 2-(bromomethyl)naphthalene to give the title compound (82 mg, 78% yield).

^1H NMR (500 MHz, CDCl_3) δ = 7.84-7.81 (m, 3H, ArH), 7.78 (s, 1H, ArH), 7.50 (dd, J = 8.3, 1.5 Hz, 1H, ArH), 7.48-7.44 (m, 2H, ArH), 3.74 (s, 2H, ArCH₂), 3.36 (d, J = 2.4 Hz, 2H, C \equiv CCH₂), 2.40 (s, 3H, NCH₃), 2.31 (t, J = 2.4 Hz, 1H, C \equiv CH)

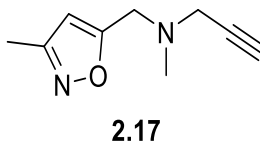
^{13}C NMR (100 MHz, CDCl_3) δ = 136.1, 133.4, 132.9, 128.1, 127.8, 127.8, 127.7, 127.4, 126.0, 125.7, 78.6, 73.5, 60.2, 45.1, 41.9

HRMS: (C₁₅H₁₆N) [M+H]⁺ required 210.1227; found [M+H]⁺ 210.1227

IR (neat): 3180, 2980, 2891, 2484, 2121, 1602, 1512, 1469, 1357, 731 cm⁻¹

Data are consistent with literature values.²³⁴

3.3.2.12 *N*-methyl-*N*-((3-methylisoxazol-5-yl)methyl)prop-2-yn-1-amine (2.17)



Synthesized on a 0.5 mmol scale using *N*-methylpropargylamine and 5-(bromomethyl)-3-methylisoxazole to give the title compound (77 mg, 93% yield).

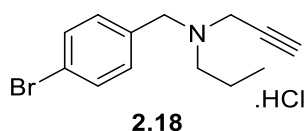
^1H NMR (500 MHz, CDCl_3) δ = 6.03 (s, 1H, HetH), 3.71 (s, 2H, HetCH₂), 3.36 (d, J = 2.4 Hz, 2H, C \equiv CCH₂), 2.37 (s, 3H, NCH₃), 2.28-2.27 (m, 4H, HetCH₃ and C \equiv CH)

^{13}C NMR (100 MHz, CDCl_3) δ = 169.3, 159.8, 104.0, 77.9, 73.9, 50.6, 45.4, 41.8, 11.5

HRMS: (C₉H₁₃N₂O) [M+H]⁺ required 165.1022; found [M+H]⁺ 165.1019

IR (neat): 3196, 2980, 2891, 2457, 2360, 2125, 1620, 1462, 1361, 7221 cm⁻¹

3.3.2.13 *N*-(4-bromobenzyl)-*N*-propylprop-2-yn-1-amine (2.18)



Synthesized on a 0.5 mmol scale using compound **2.52** and 1-bromopropane with the presence of 10 mol% potassium iodide to give the title compound which was isolated as the HCl salt (60 mg, 45% yield).

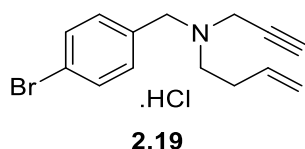
^1H NMR (500 MHz, d_6 -DMSO) δ = 11.87 (b, 1H, $[\text{NH}]^+$), 7.67-7.61 (m, 4H, ArH), 4.32 (d, J = 47.1 Hz, 2H ArCH₂) 4.04-3.82 (m, 3H, C \equiv CCH₂ and C \equiv CH), 2.50-2.46 (m, 2H, NCH₂), 3.00 (b, 2H, NCH₂), 1.76-1.75 (m, 2H, NCH₂CH₂), 0.87 (t, J = 7.5 Hz, 3H, NCH₂CH₂CH₃)

^{13}C NMR (125 MHz, d_6 -DMSO) δ = 133.5, 131.7, 128.9, 123.1, 81.8, 72.5, 55.1, 53.5, 40.7, 16.7, 10.9

HRMS: (C₁₃H₁₇BrN) $[\text{M}+\text{H}]^+$ required 266.0539 (^{79}Br); found $[\text{M}+\text{H}]^+$ 266.0542 (^{79}Br)

IR (neat): 3176, 2980, 2875, 2499, 2121, 1595, 1450, 1367, 758, 727 cm⁻¹

3.3.2.14 *N*-(4-bromobenzyl)-*N*-(prop-2-yn-1-yl)but-3-en-1-amine (2.19)



Synthesized on a 0.5 mmol scale using compound **2.52** and 4-bromobut-1-ene with the presence of 10 mol% potassium iodide to give the title compound which was isolated as the HCl salt (82 mg, 59% yield).

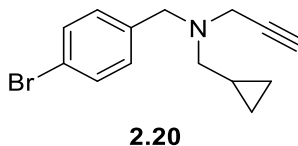
^1H NMR (500 MHz, d_4 -MeOH) δ = 7.68 (d, J = 8.4 Hz, 2H, ArH), 7.52 (d, J = 8.4 Hz, 2H, ArH), 5.85-5.77 (m, 1H, C=CH), 5.26 (dd, J = 17.2, 1.4 Hz, 1H, C=CH₂), 5.20 (dd, J = 10.3, 1.1 Hz, 1H, C=CH₂), 4.49-4.46 (m, b, 2H, ArCH₂), 4.04 (d, b, J = 44.5 Hz, C \equiv CCH₂), 3.49 (t, J = 2.4 Hz, 1H, C \equiv CH), 3.36 (t, J = 8.0 Hz, 2H, NCH₂), 2.61-2.59 (m, 2H, NCH₂CH₂)

^{13}C NMR (125 MHz, d_4 -MeOH) δ = 134.3, 133.7, 133.4, 129.3, 125.8, 119.5, 82.3, 72.3, 57.4, 53.5, 42.6, 29.5

HRMS: (C₁₄H₁₇BrN) $[\text{M}+\text{H}]^+$ required 278.0539 (^{79}Br); found $[\text{M}+\text{H}]^+$ 278.0542 (^{79}Br)

IR (neat): 3165, 2980, 2331, 2115, 1637, 1593, 1487, 1436, 723, 759 cm^{-1}

3.3.2.15 *N*-(4-bromobenzyl)-*N*-(cyclopropylmethyl)prop-2-yn-1-amine (2.20)



Synthesized on a 0.5 mmol scale using compound **2.52** and (bromomethyl)cyclopropane with the presence of 10 mol% potassium iodide to give the title compound (94 mg, 67% yield).

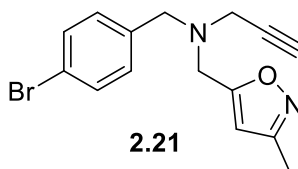
^1H NMR (400 MHz, CDCl_3) δ = 7.45-7.42 (m, 2H, ArH), 7.26-7.23 (m, 2H, ArH), 3.61 (s, 2H, ArCH), 3.46 (d, J = 2.4 Hz, 2H, $\text{C}\equiv\text{CCH}_2$), 2.40 (d, J = 6.6 Hz, 2H, NCH_2), 2.21 (t, J = 2.4 Hz, 1H, $\text{C}\equiv\text{CH}$), 0.89-0.81 (m, 1H, cPrCH), 0.53-0.48 (m, 2H, cPrCH₂), 0.19-0.15 (m, 2H, cPrCH₂)

^{13}C NMR (100 MHz, CDCl_3) δ = 138.1, 131.5, 130.9, 121.0, 78.6, 73.4, 58.1, 57.4, 41.4, 9.3, 3.8

HRMS: ($\text{C}_{14}\text{H}_{17}\text{BrN}$) $[\text{M}+\text{H}]^+$ required 278.0539 (^{79}Br); found $[\text{M}+\text{H}]^+$ 278.0543 (^{79}Br)

IR (neat): 3298, 2966, 2358, 1591, 1485, 1458, 1382, 624 cm^{-1}

3.3.2.16 *N*-(4-bromobenzyl)-*N*-((3-methylisoxazol-5-yl)methyl)prop-2-yn-1-amine (2.21)



Synthesized on a 0.5 mmol scale using compound **2.52** and 5-(bromomethyl)-3-methylisoxazole in the presence of 10 mol% potassium iodide to give the title compound (143 mg, 89% yield).

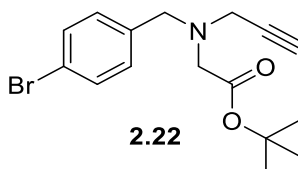
^1H NMR (400 MHz, CDCl_3) δ = 7.47-7.43 (m, 2H, ArH), 7.27-7.24 (m, 2H, ArH), 6.05 (s, 1H, HetH), 3.80 (s, 2H, HetCH₂), 3.65 (s, 2H, ArCH₂), 3.31 (d, J = 2.4 Hz, 2H, $\text{C}\equiv\text{CCH}_2$), 2.30-2.29 (m, 4H, $\text{C}\equiv\text{CH}$ and HetCH₃)

^{13}C NMR (100 MHz, CDCl_3) δ = 169.5, 159.9, 137.0, 131.7, 130.8, 121.4, 104.1, 77.8, 74.1, 56.9, 48.5, 42.0, 11.6

HRMS: ($\text{C}_{15}\text{H}_{16}\text{BrN}_2\text{O}$) $[\text{M}+\text{H}]^+$ required 319.0441, (^{79}Br); found $[\text{M}+\text{H}]^+$ 319.0438 (^{79}Br)

IR (neat): 3163, 2893, 2500, 2119, 1608, 1489, 1438, 1373, 729, 711 cm^{-1}

3.3.2.17 *tert*-Butyl *N*-(4-bromobenzyl)-*N*-(prop-2-yn-1-yl)glycinate (2.22)



Synthesized on a 1 mmol scale using compound **2.52** and *tert*-butyl 2-bromoacetate with the presence of 10 mol% potassium iodide to give the title compound (237 mg, 70% yield).

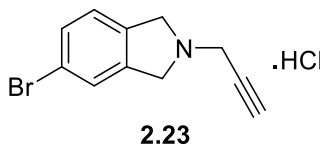
^1H NMR (400 MHz, CDCl_3) δ = 7.45-7.43 (m, 2H, ArH), 7.29-7.27 (m, 2H, ArH), 3.69 (s, 2H, ArCH₂), 3.43 (d, J = 2.2 Hz, 2H, C \equiv CCH₂), 3.29 (s, 2H, NCH₂), 2.25 (t, J = 2.2 Hz, C \equiv CH), 1.47 (s, 9H, 3x CH₃)

^{13}C NMR (100 MHz, CDCl_3) δ = 170.1, 137.3, 131.6, 131.0, 121.3, 81.3, 78.5, 73.6, 56.8, 55.2, 42.3, 28.3

HRMS: ($\text{C}_{16}\text{H}_{21}\text{BrNO}_2$) $[\text{M}+\text{H}]^+$ required 338.0750 (^{79}Br); found $[\text{M}+\text{H}]^+$ 338.0749 (^{79}Br)

IR (neat): 3296, 2978, 2833, 1735, 1591, 1487, 1367, 628 cm^{-1}

3.3.2.18 5-bromo-2-(prop-2-yn-1-yl)isoindoline (2.23)



Synthesized on a 0.5 mmol scale using 5-bromoisindoline hydrochloride and propargyl bromide (60% solution in toluene) to give the title compound which was isolated as the HCl salt (66 mg, 55% yield).

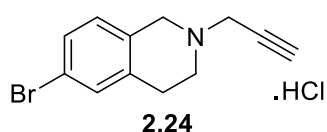
^1H NMR (500 MHz, $\text{d}_6\text{-DMSO}$) δ = 12.95 (b, 1H, $[\text{NH}]^+$), 7.67 (s, 1H, ArH), 7.56 (d, J = 8.2 Hz, 1H, ArH), 7.38 (d, J = 8.2 Hz, 1H, ArH), 4.63 (s, 2H, ArCH_2), 4.60 (s, 2H, ArCH_2), 4.33 (d, J = 2.4 Hz, 2H, $\text{C}\equiv\text{CCH}_2$), 3.81 (t, J = 2.4 Hz, 1H, $\text{C}\equiv\text{CH}$)

^{13}C NMR (125 MHz, $\text{d}_6\text{-DMSO}$) δ = 137.0, 133.8, 131.3, 126.0, 125.0, 121.3, 80.5, 74.1, 56.7, 56.6, 42.4

HRMS: ($\text{C}_{11}\text{H}_{11}\text{BrN}$) $[\text{M}+\text{H}]^+$ required 236.0069 (^{79}Br); found 236.0071 (^{79}Br)

IR (neat): 3205, 2980, 2931, 2466, 2341, 2127, 1604, 1577, 1462, 1344, 709, 661 cm^{-1}

3.3.2.19 6-bromo-2-(prop-2-yn-1-yl)-1,2,3,4-tetrahydroisoquinoline (2.24)



Synthesized on a 0.5 mmol scale using 6-bromo-1,2,3,4-tetrahydroisoquinoline and propargyl bromide (60% solution in toluene) to give the title compound which was isolated as the HCl salt (146 mg, quant. yield).

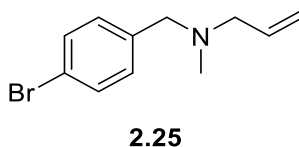
^1H NMR (500 MHz, $\text{d}_4\text{-MeOH}$) δ = 7.50 (s, 1H, ArH), 7.46 (d, J = 8.3 Hz, 1H, ArH), 7.18 (d, J = 8.3 Hz, 1H, ArH), 4.62-4.45 (m, 2H, ArCH_2N), 4.30 (d, J = 2.4 Hz, 2H, $\text{C}\equiv\text{CCH}_2$), 3.89-3.53 (m, 2H, ArCH_2), 3.45 (t, J = 2.4 Hz, 1H, $\text{C}\equiv\text{CH}$), 3.23 (b, 2H, NCH_2),

^{13}C NMR (125 MHz, $\text{d}_4\text{-MeOH}$) δ = 134.4, 132.8, 131.5, 129.8, 127.9, 123.2, 81.6, 72.8, 53.2, 50.2, 46.2, 26.3

HRMS: ($\text{C}_{12}\text{H}_{13}\text{BrN}$) $[\text{M}+\text{H}]^+$ required 250.0226 (^{79}Br); found $[\text{M}+\text{H}]^+$ 250.0226 (^{79}Br)

IR (neat): 3205, 2980, 2324, 2123, 1595, 1485, 1458, 1352, 713, 675 cm^{-1}

3.3.2.20 *N*-(4-bromobenzyl)-*N*-methylprop-2-en-1-amine (2.25)



Synthesized on a 0.5 mmol scale using 1-(4-bromophenyl)-*N*-methylmethanamine and allyl bromide to give the title compound (100 mg, 83% yield).

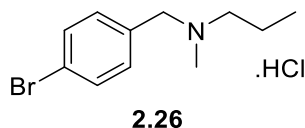
^1H NMR (400 MHz, CDCl_3) δ = 7.45-7.41 (m, 2H, ArH), 7.21-7.18 (m, 2H, ArH), 5.94-5.84 (m, 1H, C=CH), 5.22-5.19 (m, 2H, C=CH₂), 3.44 (s, 2H, ArCH₂), 3.01 (dt, J = 6.5 Hz, 1.3 Hz, 2H, CH₂CH=CH₂), 2.17 (s, 3H, NCH₃)

^{13}C NMR (100 MHz, CDCl_3) δ = 138.3, 135.8, 131.4, 130.8, 120.8, 117.7, 61.1, 60.6, 42.2

HRMS ($\text{C}_{11}\text{H}_{15}\text{BrN}$) $[\text{M}+\text{H}]^+$ required 240.0382 (^{79}Br); found $[\text{M}+\text{H}]^+$ 240.0386 (^{79}Br)

IR (neat) 2980, 2891, 2474, 1593, 1490, 1460, 1390, 999, 916, 715, 655 cm^{-1}

3.3.2.21 *N*-(4-bromobenzyl)-*N*-methylpropan-1-amine (2.26)



Synthesized on a 0.5 mmol scale using 1-(4-bromophenyl)-*N*-methylmethanamine and bromopropane to give the title compound which was isolated as the HCl salt (161 mg, quant. yield).

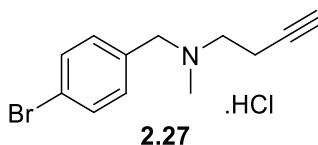
^1H NMR (500 MHz, $\text{d}_4\text{-MeOH}$) δ = 7.66 (d, J = 8.4 Hz, 2H, ArH), 7.48 (d, J = 8.4 Hz, 2H, ArH), 4.41 (b, 1H, ArCH₂), 4.26 (b, 1H, ArCH₂), 3.11 (b, 2H, NCH₂), 2.79 (s, 3H, NCH₃), 1.82 (s, 2H, NCH₂CH₂), 1.01 (t, J = 7.4 Hz, 3H, NCH₂CH₂CH₃)

^{13}C NMR (125 MHz, $\text{d}_4\text{-MeOD}$) δ = 134.2, 133.6, 130.0, 125.5, 60.0, 58.7, 40.0, 18.7, 11.1

HRMS: ($\text{C}_{13}\text{H}_{17}\text{BrN}$) $[\text{M}+\text{H}]^+$ required 242.0539 (^{79}Br); found $[\text{M}+\text{H}]^+$ 242.0542 (^{79}Br)

IR (neat): 2978, 2877, 2578, 2493, 1595, 1489, 1467, 1382

3.3.2.22 *N*-(4-bromobenzyl)-*N*-methylbut-3-yn-1-amine (2.27)



Synthesized on a 0.5 mmol scale using 1-(4-bromophenyl)-*N*-methylethanamine and 4-bromobut-1-yne with the presence of 10 mol% potassium iodide to give the title compound which was isolated as the HCl salt (39 mg, 30% yield).

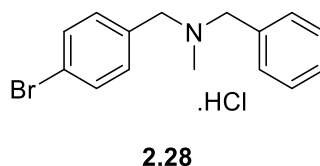
^1H NMR (500 MHz, $\text{d}_6\text{-DMSO}$) δ = 11.21 (b, 1H, $[\text{NH}]^+$), 7.67 (d, J = 8.3 Hz, 2H, ArH), 7.57 (d, J = 8.3 Hz, 2H, ArH), 4.41-4.20 (m, 2H, ArCH_2), 3.25-3.12 (m, 2H, $\text{CH}_2\text{C}\equiv\text{C}$), 3.06 (s, 1H, $\text{C}\equiv\text{CH}$) 2.81-2.79 (m, 2H, NCH_2), 2.63 (s, 3H, NCH_3),

^{13}C NMR (125 MHz, $\text{d}_6\text{-DMSO}$) δ = 133.4, 131.7, 129.3, 123.1, 79.8, 73.7, 57.4, 52.6, 38.4, 13.7

HRMS: ($\text{C}_{12}\text{H}_{15}\text{BrN}$) $[\text{M}+\text{H}]^+$ required 252.0382 (^{79}Br); found $[\text{M}+\text{H}]^+$ 252.0386 (^{79}Br)

IR (neat): 3309, 2980, 2528, 2125, 1597, 1499, 1460, 1332, 659 cm^{-1}

3.3.2.23 N-benzyl-1-(4-bromophenyl)-*N*-methylethanamine (2.28)



Synthesized on a 0.5 mmol scale using 1-(4-bromophenyl)-*N*-methylethanamine and benzyl bromide to give the title compound which was isolated as the HCl salt (222 mg, quant. yield).

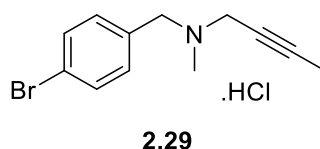
^1H NMR (500 MHz, $\text{d}_6\text{-DMSO}$) δ = 11.53 (b, 1H, $[\text{NH}]^+$) 7.66-7.62 (m, 6H, ArH), 7.45-7.44 (m, 3H, ArH), 4.39-4.34 (m, 2H, ArCH_2), 4.23-4.18 (m, 2H, ArCH_2), 2.47 (d, J = 4.7 Hz, 3H, NCH_3)

^{13}C NMR (125 MHz, $\text{d}_6\text{-DMSO}$) δ = 133.7, 131.6, 131.4, 130.0, 129.4, 128.7, 123.0, 58.0, 57.2, 37.8

HRMS ($\text{C}_{15}\text{H}_{17}\text{BrN}$) $[\text{M}+\text{H}]^+$ required 290.0539 (^{79}Br); found $[\text{M}+\text{H}]^+$ 290.0543 (^{79}Br)

IR (neat): 2980, 2889, 2490, 1595, 1489, 1465, 1377, 711, 646 cm^{-1}

3.3.2.24 *N*-(4-bromobenzyl)-*N*-methylbut-2-yn-1-amine (2.29)



Synthesized on 0.5 mmol scale using 1-(4-bromophenyl)-*N*-methylmethanamine and 1-bromobut-2-yne to give the title compound which was isolated as the HCl salt (141 mg, quant. yield).

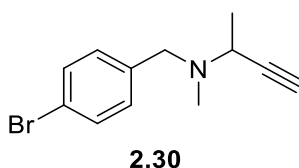
^1H NMR (500 MHz, $\text{d}_6\text{-DMSO}$) δ = 11.68 (b, 1H, $[\text{NH}]^+$), 7.66 (d, J = 8.4 Hz, 2H, ArH), 7.59 (d, J = 8.4 Hz, 2H, ArH), 4.29 (d, J = 19.7 Hz, 2H, ArCH_2), 3.96-3.82 (m, 2H, $\text{C}\equiv\text{CCH}_2$), 2.66 (s, 3H, NCH_3), 1.93 (t, J = 2.3 Hz, 3H, $\text{C}\equiv\text{CCH}_3$)

^{13}C NMR (125 MHz, $\text{d}_6\text{-DMSO}$) δ = 133.4, 131.7, 129.3, 123.1, 87.2, 68.2, 56.1, 44.0, 38.5, 3.3

HRMS: ($\text{C}_{12}\text{H}_{15}\text{BrN}$) $[\text{M}+\text{H}]^+$ required 252.0382 (^{79}Br); found $[\text{M}+\text{H}]^+$ 252.0386 (^{79}Br)

IR (neat): 2980, 2870, 2470, 2241, 1593, 1489, 1456, 1373, 713, 640 cm^{-1}

3.3.2.25 *N*-(4-bromobenzyl)-*N*-methylbut-3-yn-2-amine (2.30)



Synthesized on a 0.5 mmol scale using 1-(4-bromophenyl)-*N*-methylmethanamine and but-3-yn-2-yl 4-methylbenzenesulfonate (**2.37**) to give the title compound (64 mg, 50% yield).

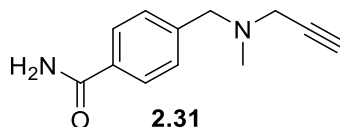
^1H NMR (500 MHz, CDCl_3) δ = 7.43 (d, J = 8.3 Hz, 2H, ArH), 7.23 (d, J = 8.3 Hz, 2H, ArH), 3.60 (d, J = 13.4 Hz, 1H, ArCH_2), 3.54 (qd, J = 7.1 Hz, 2.2 Hz, 1H, NCH), 3.42 (d, J = 13.4 Hz, 1H, ArCH_2), 2.30 (d, J = 2.2 Hz, 1H, $\text{C}\equiv\text{CH}$), 2.21 (s, 3H, NCH_3), 1.35 (d, J = 7.1 Hz, 3H, CHCH_3)

^{13}C NMR (125 MHz, CDCl_3) δ = 138.3, 131.5, 130.8, 120.9, 82.1, 72.8, 58.3, 50.1, 37.4, 20.0

HRMS: (C₁₂H₁₅BrN) [M+H]⁺ required 252.0382 (⁷⁹Br); found [M+H]⁺ 252.0386 (⁷⁹Br)

IR (neat): 3296, 2980, 2846, 1591, 1487, 1460, 1369, 630 cm⁻¹

3.3.2.26 4-((methyl(prop-2-yn-1-yl)amino)methyl)benzamide (2.31)



Synthesised on a 0.5 mmol scale using *N*-methylpropargylamine and 4-(bromomethyl)benzamide (**2.39**) to give the title compound (70 mg, 69% yield).

¹H NMR (500 MHz, CDCl₃) δ = 7.77 (d, 2H, *J* = 8.3 Hz, Ar*H*), 7.43 (d, 2H, *J* = 8.3 Hz, Ar*H*), 6.03 (b, 1H, NH), 5.60 (b, 1H, NH), 3.62 (s, 2H, ArCH₂), 3.31 (d, 2H, *J* = 2.3 Hz, C≡CCH₂), 2.34 (s, 3H, NCH₃), 2.28 (t, 1H, *J* = 2.3 Hz, C≡CH)

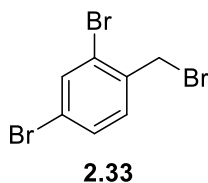
¹³C NMR (126 MHz, CDCl₃) δ = 169.1, 143.1, 132.4, 129.4, 127.6, 78.4, 73.6, 59.7, 45.2, 41.9

HRMS (C₁₂H₁₅N₂O) [M+H]⁺ required 203.1179, found [M+H]⁺ 203.1178

IR (neat): 3382, 3279, 3158, 1649, 1617, 1569, 1394, 1033, 663 cm⁻¹

3.3.3 Bespoke Alkylating Agent Synthesis

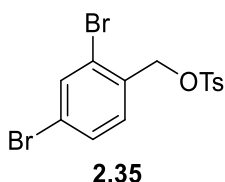
3.3.3.1 Attempted Synthesis of 2,4-dibromo-1-(bromomethyl)benzene (2.33)



Triphenylphosphine (197 mg, 0.75 mmol) was taken up in dry DCM (13 mL) and cooled to -5 °C. Carbon tetrabromide (373 mg, 1.125 mmol) was then added dropwise as a solution in dry DCM (5 mL). Upon addition, the colourless solution turned bright yellow and the reaction was stirred at -5 °C for 10 minutes. (2,4-dibromophenyl)methanol (200 mg, 0.75 mmol) was then added to the reaction dropwise as a solution in dry DCM (9 mL). The reaction was stirred for a further hour at -5 °C then warmed to room temperature and stirred for 17 hours. the reaction was

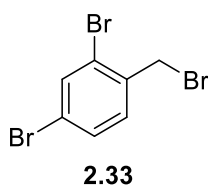
then quenched with water (20 mL) and the layers partitioned. The aqueous layer was washed with three portions of DCM and the organics combined, dried with magnesium sulfate and concentrated under reduced pressure. The residue was purified by flash column chromatography and eluted with a gradient of 0-20% diethyl ether and petroleum ether to give a yellow oil which was a mixture of the title compound **2.33** and ether **2.34**

3.3.3.2 Attempted Synthesis of 2,4-dibromobenzyl 4-methylbenzenesulfonate (2.35)



(2,4-dibromophenyl)methanol (300 mg, 1.1 mmol) was taken up in dry DCM and cooled to 0 °C. DMAP (78 mg, 0.7 mmol), tosyl chloride (244 mg, 1.3 mmol) and triethylamine (306 μ L, 2.2 mmol) were added in that order and the reaction allowed to warm to room temperature and stirred for 17 hours. The reaction was then filtered through a pad of Celite and the organic layers washed twice with saturated copper(II) sulfate, twice with saturated sodium bicarbonate and twice with brine, dried with magnesium sulfate and concentrated under reduced pressure. The crude residue was then purified using flash chromatography eluting with a gradient of 0-12.5% ethyl acetate and petroleum ether. The title compound was not isolated.

3.3.3.3 Synthesis of 2,4-dibromo-1-(bromomethyl)benzene (2.33)

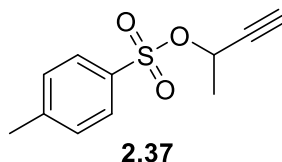


(2,4-dibromophenyl)methanol (266 mg, 1 mmol) was taken up in acetic acid (2 mL, 1mL/mmol). 40% w.v. solution of hydrobromic acid in water (1.3 mL, 10 mmol) was added dropwise at room temperature and the reaction stirred for 5 minutes then heated to reflux for 3 hours. The reaction was quenched with 33% sodium hydroxide solution (pH 10) then the aqueous was washed three times with ethyl acetate. The

combined organics were dried with magnesium sulfate and concentrated to give the title compound as a brown oil (328 mg, quant. yield) which was used without further purification in the synthesis of compound **2.15**.

^1H NMR (500 MHz, CDCl_3) δ = 7.75 (d, 1H, J = 1.9 Hz, ArH), 7.44 (dd, 1H, J = 8.2 Hz, 1.9 Hz, ArH), 7.32 (d, 1H, J = 8.2 Hz, ArH), 4.54 (s, 2H, ArCH₂)

3.3.3.4 But-3-yn-2-yl 4-methylbenzenesulfonate (**2.37**)



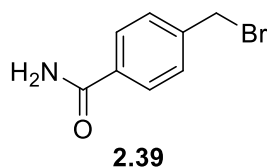
But-3-yn-2-ol (7.1 mmol) was taken up in dry dichloromethane (16.5 mL) in an oven dried round bottomed flask under an atmosphere of nitrogen and cooled to 0 °C using an ice bath. *N,N*-dimethylpyridin-4-amine (4.3 mmol), tosyl chloride (8.5 mmol) and triethylamine (14.2 mmol) were added and the reaction stirred at 0 °C for 30 minutes then cooling was removed and the reaction stirred until TLC indicated complete consumption of starting material. The reaction was then filtered through a pad of celite and the organics washed with two portions of saturated aqueous copper(II) sulfate, two portions of saturated aqueous sodium bicarbonate solution and two portions of brine, then dried with magnesium sulfate, filtered and concentrated *in vacuo*. The crude residue was purified by flash chromatography to give the title compound which was used in further reactions (403 mg, 25% yield)

^1H NMR (500 MHz, CDCl_3) δ = 7.82 (d, J = 7.8 Hz, 2H, ArH), 7.33 (d, J = 8.1 Hz, 2H, ArH), 5.1 (qd, J = 6.7 Hz, 2.1 Hz, 1H, OCH), 2.45 (s, 3H, ArCH₃), 2.41 (d, J = 2.0 Hz, 1H, C \equiv CH), 1.57 (d, J = 6.8 Hz, 3H, CHCH₃)

^{13}C NMR (125 MHz, CDCl_3) δ = 145.0, 134.0, 129.8, 128.2, 80.0, 75.7, 67.5, 22.7, 21.8

The data are consistent with literature values.²³⁵

3.3.3.5 Synthesis of 4-(bromomethyl)benzamide (2.39)



4-(bromomethyl)benzoic acid (1 g, 4.65 mmol) was suspended in ethyl acetate (19 mL), Thionyl chloride (0.51 mL, 7 mmol) was then added dropwise and the reaction heated to 75 °C for 17 hours. The reaction was cooled to room temperature and the solvent was removed *in vacuo* to give the crude acid chloride. The residue was then taken up in dry DCM (19 mL) and cooled to 0 °C. Aqueous ammonia (0.51 mL, 9.3 mmol), was then added dropwise to the solution and the reaction allowed to warm to room temperature. During addition, the product began precipitating out of the reaction. The reaction was quenched with water and DCM removed *in vacuo*. The precipitate was collected by filtration and recrystallized from 40 mL of hot ethyl acetate to give the title compound as colourless crystals (505 mg, 51% yield).

^1H NMR (400 MHz, $\text{d}_6\text{-DMSO}$) δ = 7.97 (b, 1H, NH), 7.85 (d, J = 8.1 Hz, 2H, ArH), 7.51 (d, J = 8.1 Hz, 2H, ArH), 7.38 (b, 1H, NH), 4.73 (s, 2H, ArCH_2)

^{13}C NMR (100 MHz, $\text{d}_6\text{-DMSO}$) δ = 167.4, 141.1, 134.1, 129.1, 127.8, 33.5

The data are consistent with literature values.²⁰⁴

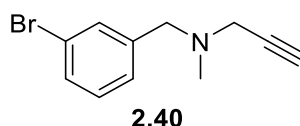
3.3.4 General Procedure C: reductive amination

Aldehyde (3 mmol) was taken up in dry DCM (10 mL) in an oven dried round bottomed flask under an atmosphere of nitrogen. Acetic acid (1 mmol) was added and the reaction stirred at room temperature for 5 minutes. Amine (1 mmol) was then added and the reaction stirred at room temperature for 1 hour. The reaction was cooled to 0 °C using an ice bath, then sodium triacetoxyborohydride (3 mmol) was added and the reaction warmed to room temperature and stirred until TLC indicated complete consumption of the amine. The reaction was quenched with saturated aqueous sodium bicarbonate solution. The organic layer was washed with three portions of saturated sodium bicarbonate, then acidified with concentrated hydrochloric acid. The organic layer was then washed with three portions of 2 M

aqueous hydrochloric acid. The pH of the acidic washes was then adjusted to pH 10 using 4 M aqueous sodium hydroxide and the aqueous extracted with three portions of diethyl ether. The combined ether washes were dried with magnesium sulfate, filtered and concentrated to give crude product. The residue was then purified by flash column chromatography or by preparative TLC (as stated) and sent to NKI for biological testing.

The following compounds were synthesised using this procedure.

3.3.4.1 *N*-(3-bromobenzyl)-*N*-methylprop-2-yn-1-amine (2.40)



Synthesized on a 0.5 mmol scale using *N*-methylpropargylamine and 3-bromobenzaldehyde to give the title compound (62 mg, 52% yield).

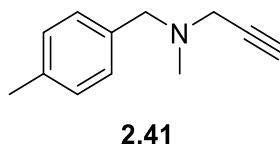
^1H NMR (500 MHz, CDCl_3) δ = 7.51 (s, 1H, ArH), 7.39 (d, J = 7.8 Hz, 1H, ArH), 7.26 (d, J = 7.8 Hz, 1H, ArH), 7.18 (t, J = 7.8 Hz, 1H, ArH), 3.54 (s, 2H, ArCH₂), 3.31 (d, J = 2.2 Hz, 2H, C \equiv CCH₂), 2.33 (s, 3H, NCH₃), 2.28 (t, J = 2.2 Hz, 1H, C \equiv CH)

^{13}C NMR (125 MHz, CDCl_3) δ = 141.0, 132.2, 130.5, 130.0, 127.8, 122.6, 78.4, 73.7, 59.4, 45.1, 41.8

HRMS: (C₁₁H₁₃BrN) [M+H]⁺ required 238.0226 (^{79}Br); found [M+H]⁺ 238.0228 (^{79}Br)

IR (neat): 3296, 2922, 2791, 2362, 1612, 1570, 1471, 1360, 775 cm⁻¹

3.3.4.2 *N*-methyl-*N*-(4-methylbenzyl)prop-2-yn-1-amine (2.41)



Synthesized using *N*-methylpropargylamine and 4-methylbenzaldehyde to give the title compound (264 mg, quant. yield).

^1H NMR (400 MHz, CDCl_3) δ = 7.23 (d, J = 7.9 Hz, 2H, ArH), 7.14 (d, J = 7.9 Hz, 2H, ArH), 3.54 (s, 2H, ArCH_2), 3.30 (d, J = 2.4 Hz, 2H, $\text{C}\equiv\text{CCH}_2$), 2.34 (s, 6H, Ar-CH_3 and NCH_3), 2.27 (t, J = 2.4 Hz, 1H, $\text{C}\equiv\text{CH}$)

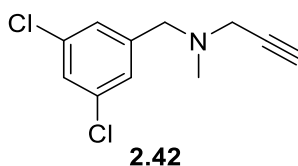
^{13}C NMR (100 MHz, CDCl_3) δ = 136.8, 135.2, 129.1, 129.0, 78.6, 73.2, 59.6, 44.7, 41.7, 21.1

HRMS: ($\text{C}_{12}\text{H}_{16}\text{N}$) $[\text{M}+\text{H}]^+$ required 174.1277; found $[\text{M}+\text{H}]^+$ 174.1275

IR (neat): 3192, 2800, 2493, 2123, 1618, 1516, 1471, 1359, 727 cm^{-1}

Data are consistent with literature values.²³⁴

3.3.4.3 *N*-(3,5-dichlorobenzyl)-*N*-methylprop-2-yn-1-amine (2.42)



Synthesized on a 0.5 mmol scale using *N*-methylpropargylamine and 3,5-dichlorobenzaldehyde to give the title compound (40 mg, 35% yield).

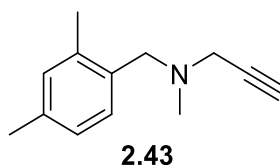
^1H NMR (400 MHz, CDCl_3) δ = 7.25 -7.24 (m, 3H, ArH), 3.52 (s, 2H, ArCH_2), 3.31 (d, J = 2.4 Hz, 2H, $\text{C}\equiv\text{CCH}_2$), 2.32 (s, 3H, NCH_3), 2.28 (t, J = 2.4 Hz, 1H, $\text{C}\equiv\text{CH}$)

^{13}C NMR (100 MHz, CDCl_3) δ = 142.3, 135.0, 127.6, 127.5, 78.1, 73.8, 59.0, 45.2, 41.8

HRMS ($\text{C}_{11}\text{H}_{12}\text{Cl}_2\text{N}$) $[\text{M}+\text{H}]^+$ required 228.0341 (^{35}Cl , ^{35}Cl); found $[\text{M}+\text{H}]^+$ 228.0342 (^{35}Cl , ^{35}Cl)

IR (neat): 3300, 2980, 2792, 2341, 1591, 1560, 1431, 1359, 794 cm^{-1}

3.3.4.4 *N*-(2,4-dimethylbenzyl)-*N*-methylprop-2-yn-1-amine (2.43)



Synthesized on a 0.5 mmol scale using *N*-methylpropargylamine and 2,4-dimethyl benzaldehyde to give the title compound (68 mg, 72% yield).

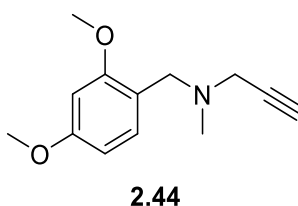
^1H NMR (400 MHz, CDCl_3) δ = 7.17 (d, J = 7.4 Hz, 1H, ArH), 6.99-6.96 (m, 2H, ArH), 3.53 (s, 3H, ArCH_2), 3.31 (d, J = 2.3 Hz, 2H, $\text{C}\equiv\text{CCH}_2$), 2.35 (s, 3H, ArCH_3), 2.34 (s, 3H, ArCH_3), 2.31 (s, 3H, NCH_3), 2.28 (t, J = 2.3 Hz, 1H, $\text{C}\equiv\text{CH}$)

^{13}C NMR (100 MHz, CDCl_3) δ = 137.6, 136.9, 133.4, 131.3, 130.1, 126.3, 78.9, 73.4, 57.5, 44.9, 41.7, 21.1, 19.1

HRMS ($\text{C}_{13}\text{H}_{18}\text{N}$) $[\text{M}+\text{H}]^+$ required 188.1434; found $[\text{M}+\text{H}]^+$ 188.1433

IR (neat): 3294, 2970, 2791, 1616, 1502, 1458, 1361 cm^{-1}

3.3.4.5 *N*-(2,4-dimethoxybenzyl)-*N*-methylprop-2-yn-1-amine (2.44)



Synthesized on a 0.5 mmol scale using *N*-methylpropargylamine and 2,4-dimethoxybenzaldehyde to give the title compound (216 mg, quant. yield).

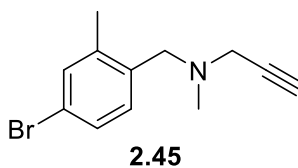
^1H NMR (400 MHz, CDCl_3) δ = 7.21-7.19 (m, 1H, ArH), 6.45-6.43 (m, 2H, ArH), 3.80 (s, 3H, ArOCH_3), 3.80 (s, 3H, ArOCH_3), 3.53 (s, 2H, ArCH_2), 3.33 (d, J = 2.4 Hz, 2H, $\text{C}\equiv\text{CCH}_2$), 2.35 (s, 3H, NCH_3), 2.26 (t, J = 2.4 Hz, 1H, $\text{C}\equiv\text{CH}$)

^{13}C NMR (100 MHz, CDCl_3) δ = 160.4, 159.2, 131.8, 118.9, 103.9, 98.7, 79.1, 73.2, 55.7, 55.5, 53.6, 44.9, 41.8

HRMS ($\text{C}_{13}\text{H}_{18}\text{NO}_2$) $[\text{M}+\text{H}]^+$ required 220.1332; found $[\text{M}+\text{H}]^+$ 220.1333

IR (neat): 3286, 2933, 2835, 2360, 1610, 1587, 1506, 1456 cm^{-1}

3.3.4.6 *N*-(4-bromo-2-methylbenzyl)-*N*-methylprop-2-yn-1-amine (2.45)



Synthesized on a 0.5 mmol scale using *N*-methylpropargylamine and 4-bromo-2-methylbenzaldehyde to give the title compound (107 mg, 85% yield).

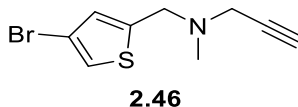
^1H NMR (500 MHz, CDCl_3) δ = 7.23-7.19 (m, 2H, ArH), 7.08 (d, J = 8.1 Hz, 1H, ArH), 3.42 (s, 2H, ArCH₂), 3.21 (d, J = 2.2 Hz, 2H, C \equiv CCH₂), 2.27 (s, 3H, ArCH₃), 2.24 (s, 3H, NCH₃), 2.20 (t, J = 2.2 Hz, 1H, C \equiv CH)

^{13}C NMR (125 MHz, CDCl_3) δ = 140.0, 135.5, 133.1, 131.5, 128.6, 121.0, 78.5, 73.5, 57.0, 44.9, 41.7, 18.9

HRMS ($\text{C}_{12}\text{H}_{15}\text{BrN}$) $[\text{M}+\text{H}]^+$ required 252.0382 (^{79}Br); found $[\text{M}+\text{H}]^+$ 252.0386 (^{79}Br)

IR (neat): 3294, 2980, 2789, 2358, 1591, 1491, 1456, 1361, 628 cm^{-1}

3.3.4.7 *N*-((4-bromothiophen-2-yl)methyl)-*N*-methylprop-2-yn-1-amine (2.46)



Synthesized on a 0.5 mmol scale using *N*-methylpropargylamine and 4-bromothiophene-2-carbaldehyde to give the title compound (115 mg, 94% yield).

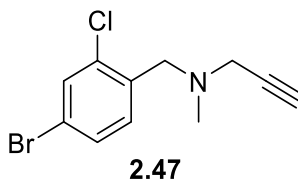
^1H NMR (400 MHz, CDCl_3) δ = 7.14 (d, J = 1.5 Hz, ArH), 6.88-6.87 (m, 1H, ArH), 3.74 (d, J = 0.6 Hz, 2H, ArCH₂), 3.36 (d, J = 2.4 Hz, 2H, C \equiv CCH₂), 2.37 (s, 3H, NCH₃), 2.27 (t, J = 2.4 Hz, 1H, C \equiv CH)

^{13}C NMR (100 MHz, CDCl_3) δ = 143.7, 128.7, 122.6, 108.9, 78.0, 73.9, 54.0, 44.9, 41.7

HRMS ($\text{C}_9\text{H}_{11}\text{BrNS}$) $[\text{M}+\text{H}]^+$ required 243.9790 (^{79}Br); $[\text{M}+\text{H}]^+$ found 243.9793 (^{79}Br)

IR (neat): 3294, 3109, 2980, 2792, 2360, 1529, 1462, 1361, 628 cm^{-1}

3.3.4.8 *N*-(4-bromo-2-chlorobenzyl)-*N*-methylprop-2-yn-1-amine (2.47)



Synthesized on a 0.5 mmol scale using *N*-methylpropargylamine and 4-bromo-2-chlorobenzaldehyde and purified by preparative TLC (10% Et₂O in hexane) to give the title compound (27 mg, 20% yield).

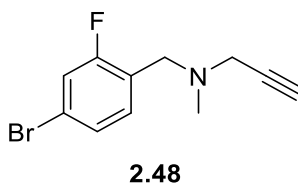
¹H NMR (500 MHz, CDCl₃) δ = 7.53 (d, *J* = 1.9 Hz, 1H, Ar*H*), 7.37 (dd, *J* = 8.2, 1.9 Hz, 1H, Ar*H*), 7.33 (d, *J* = 8.2 Hz, 1H, Ar*H*), 3.63 (s, 2H, ArCH₂), 3.35 (d, *J* = 2.3 Hz, 2H, C≡CCH₂), 2.36 (s, 3H, NCH₃), 2.29 (t, *J* = 2.3 Hz, 1H, C≡CH)

¹³C NMR (125 MHz, CDCl₃) δ = 135.5, 135.4, 132.2, 132.1, 130.0, 121.2, 78.6, 73.7, 56.4, 45.5, 41.8

HRMS: (C₁₁H₁₂BrClN) [M+H]⁺ required 271.9836 (³⁵Cl, ⁷⁹Br); found [M+H]⁺ 271.9840 (³⁵Cl, ⁷⁹Br)

IR (neat): 3296, 3076, 2979, 2943, 2852, 2787, 1586, 1465, 1033, 792 cm⁻¹

3.3.4.9 *N*-(4-bromo-2-fluorobenzyl)-*N*-methylprop-2-yn-1-amine (2.48)



Synthesized on a 0.5 mmol scale using *N*-methylpropargylamine and 4-bromo-2-fluorobenzaldehyde and purified by preparative TLC (10% Et₂O in hexane) to give the title compound (21 mg, 17% yield).

¹H NMR (500 MHz, CDCl₃) δ = 7.30-7.21 (m, 3H, Ar*H*), 3.59 (s, 2H, ArCH₂), 3.32 (d, *J* = 2.0 Hz, 2H, C≡CCH₂), 2.33 (s, 3H, NCH₃), 2.28 (t, *J* = 2.0 Hz, 1H, C≡CH)

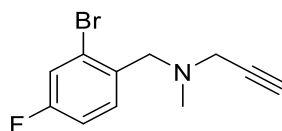
¹⁹F NMR (470 MHz, CDCl₃) δ = -115.1 - -115.2 (m)

¹³C NMR (125 MHz, CDCl₃) δ = 161.2 (d, ¹*J*_{CF} = 251.8 Hz), 132.6 (d, ³*J*_{CF} = 5.3 Hz), 127.4 (d, ⁴*J*_{CF} = 3.5 Hz), 124.5 (d, ²*J*_{CF} = 14.3 Hz), 121.3 (d, ³*J*_{CF} = 9.6 Hz), 119.2 (d, ²*J*_{CF} = 25.5 Hz), 78.4, 73.7, 52.4, 45.3, 41.7

HRMS: (C₁₁H₁₂BrFN) [M+H]⁺ required 256.0137 (⁷⁹Br); found [M+H]⁺ 256.0137 (⁷⁹Br)

IR (neat): 3296, 3067, 2919, 2944, 2794, 1606, 1578, 1485, 1403, 879 cm⁻¹

3.3.4.10 *N*-(2-bromo-4-fluorobenzyl)-*N*-methylprop-2-yn-1-amine (2.49)



2.49

Synthesized on a 0.27 mmol scale using *N*-methylpropargylamine and 2-bromo-4-fluorobenzaldehyde and purified by preparative TLC (10% Et₂O in hexane) to give the title compound (20 mg, 16% yield).

¹H NMR (500 MHz, d₄-MeOH) δ = 7.82 (dd, *J* = 8.6, 5.9 Hz, 1H, Ar*H*), 7.60 (dd, *J* = 8.3, 2.6 Hz, 1H, Ar*H*), 7.31 (td, *J* = 8.3, 2.6 Hz, 1H, Ar*H*), 4.67 (d, *b*, *J* = 55.4 Hz, 2H, ArCH₂), 4.25 (d, *J* = 2.2 Hz, 2H, C≡CCH₂), 3.49 (t, *J* = 2.5 Hz, 1H, C≡CH), 2.97 (s, 3H, NCH₃)

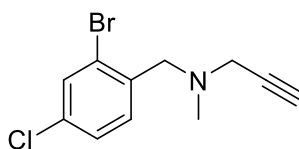
¹⁹F NMR (470 MHz, d₄-MeOH) δ = -109 - -109.3 (m)

¹³C NMR (125 MHz, d₄-MeOH) δ = 164.7 (d, ¹*J*_{CF} = 255.2 Hz), 136.3 (d, ³*J*_{CF} = 9.8 Hz), 127.7 (d, ³*J*_{CF} = 9.8 Hz), 126.8 (d, ⁴*J*_{CF} = 3.7 Hz), 122.0 (d, ²*J*_{CF} = 25.1 Hz), 116.9 (d, ²*J*_{CF} = 21.5 Hz), 82.1, 72.8, 58.5, 46.6, 40.2

HRMS: (C₁₁H₁₂BrFN) [M+H]⁺ required 256.0137 (⁷⁹Br); found [M+H]⁺ 256.0136 (⁷⁹Br)

IR (neat): 3300, 3064, 2921, 2852, 2792, 1599, 1485, 861 cm⁻¹

3.3.4.11 *N*-(2-bromo-4-chlorobenzyl)-*N*-methylprop-2-yn-1-amine (2.50)



2.50

Synthesized on a 0.5 mmol scale using *N*-methylpropargylamine and 2-bromo-4-chlorobenzaldehyde and purified by preparative TLC (10% Et₂O in hexane) to give the title compound (36 mg, 27% yield).

¹H NMR (500 MHz, CDCl₃) δ = 7.56 (d, *J* = 2.1 Hz, 1H, Ar*H*), 7.38 (d, *J* = 8.2 Hz, 1H, Ar*H*), 7.26 (dd, *J* = 8.2, 2.1 Hz, 1H, Ar*H*), 3.63 (s, 2H, ArCH₂), 3.36 (d, *J* = 2.3 Hz, 2H, C≡CCH₂), 2.36 (s, 3H, NCH₃), 2.29 (t, *J* = 2.3 Hz, 1H, C≡CH)

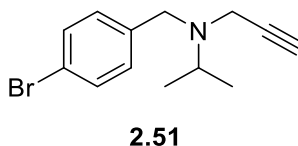
^{13}C NMR (125 MHz, CDCl_3) δ = 136.5, 133.6, 131.7, 127.6, 125.1, 78.6, 73.7, 58.8, 45.5, 41.8, * one signal for a quaternary carbon not observed

HRMS: ($\text{C}_{11}\text{H}_{12}\text{BrClN}$) $[\text{M}+\text{H}]^+$ required 271.9842 (^{35}Cl , ^{79}Br); found $[\text{M}+\text{H}]^+$ 271.9838 (^{35}Cl , ^{79}Br)

IR (neat): 3298, 3082, 2971, 2941, 2915, 2842, 2790, 1586, 1467, 1030, 808 cm^{-1}

3.3.5 Compounds Synthesised Using Modified Reductive Amination Conditions

3.3.5.1 *N*-(4-bromobenzyl)-*N*-isopropylprop-2-yn-1-amine (2.51)



Dry acetone (5 mL) and acetic acid (1 mmol) were placed in an oven-dried round-bottomed flask under an atmosphere of argon and the mixture stirred at room temperature for 5 minutes. Compound **2.52** (1 mmol) was then added and the reaction stirred at room temperature for 3 days. Sodium triacetoxyborohydride (5 mmol) was added and the reaction stirred at room temperature for 5 days. The reaction was diluted with acetone and transferred to a 100 mL conical flask equipped with a magnetic stirring bar. Saturated aqueous sodium bicarbonate was added slowly to the flask and the mixture stirred at room temperature for 1 hour. The acetone was then removed *in vacuo* and the residue extracted with three portions of dichloromethane. The combined organics were then washed with saturated aqueous sodium bicarbonate, water and brine, then dried with magnesium sulfate, filtered and concentrated under vacuum. The residue was purified by flash chromatography (0-7% diethyl ether in petroleum ether) to give the title compound (185 mg, 69% yield).

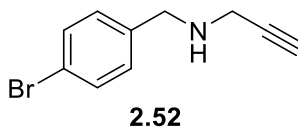
^1H NMR (500 MHz, CDCl_3) δ = 7.42 (d, J = 8.2 Hz, 2H, ArH), 7.24 (d, J = 8.2 Hz, 2H, ArH), 3.65 (s, 2H, ArCH₂), 3.27 (d, J = 2.4 Hz, 2H, C \equiv CCH₂), 3.02 (sept, J = 6.5 Hz, 1H, NCH), 2.18 (t, J = 2.4 Hz, 1H, C \equiv CH), 1.14 (d, J = 6.5 Hz, 6H, 2 x CH₃)

^{13}C NMR (125 MHz, CDCl_3) δ = 139.0, 131.5, 130.6, 120.7, 80.7, 72.6, 52.8, 51.7, 38.8, 20.0

HRMS: (C₁₃H₁₇BrN) [M+H]⁺ required 266.0539 (⁷⁹Br); found [M+H]⁺ 266.0545 (⁷⁹Br)

IR (neat): 3298, 2966, 2331, 1591, 1485, 1458, 1382, 624 cm⁻¹

3.3.5.2 *N*-(4-bromobenzyl)prop-2-yn-1-amine (2.52)



4-bromobenzaldehyde (9 mmol) was taken up in dry DCM (45 mL) in an oven dried flask under an atmosphere of argon. Acetic acid (9 mmol) was added and the mixture stirred for 5 minutes, then propargyl amine (10.8 mmol) and 3 Å molecular sieves were added and the mixture warmed to 40 °C until TLC indicated complete consumption of the aldehyde. The reaction was slowly cooled to 0 °C and sodium triacetoxyborohydride (13.5 mmol) was added and the reaction stirred until TLC indicated complete consumption of the imine. The reaction was quenched with saturated aqueous sodium bicarbonate (75 mL) and the layers partitioned. The aqueous layer was extracted with 3 portions of dichloromethane. The combined organics were washed with saturated aqueous sodium bicarbonate, water and brine, then dried with magnesium sulfate, filtered and concentrated under reduced pressure. The crude residue was purified by flash chromatography (0-70% diethyl ether in petroleum ether) to give the title compound (1.05 g, 51% yield).

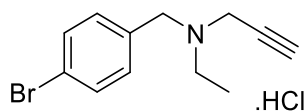
¹H NMR (400 MHz, CDCl₃) δ = 7.46-7.43 (m, 2H, ArH), 7.24-7.22 (m, 2H, ArH), 3.83 (s, 2H, ArCH₂), 3.40 (d, *J* = 2.4 Hz, 2H, C≡CCH₂), 2.26 (t, *J* = 2.4 Hz, 1H, C≡CH), 1.45 (b, 1H, NH)

¹³C NMR (100 MHz, CDCl₃) δ = 138.5, 131.6, 130.2, 121.1, 82.0, 71.8, 51.6, 37.4

HRMS: (C₁₀H₁₁BrN) [M+H]⁺ required 224.0069 (⁷⁹Br); found [M+H]⁺ 224.0064 (⁷⁹Br)

IR (neat): 3234, 2922, 2763, 2615, 2133, 1595, 1583, 1489, 1450, 1384, 705, 634 cm⁻¹

3.3.5.3 *N*-(4-bromobenzyl)-*N*-ethylprop-2-yn-1-amine (2.53)



Isolated as a by-product in the synthesis of compound **2.52** and converted to the HCl salt (200 mg, 8% yield)

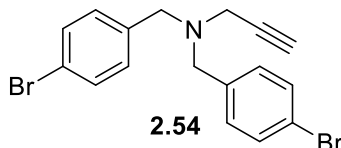
^1H NMR (500 MHz, $\text{d}_4\text{-MeOH}$) δ = 7.57 (d, J = 8.4 Hz, 2H, ArH), 7.41 (d, J = 8.4 Hz, 2H, ArH), 4.35 (d, b, J = 24.3 Hz, 2H, ArCH₂), 3.92 (d, J = 52.4 Hz, 2H, C \equiv CCH₂), 3.36 (t, J = 2.5 Hz, 1H, C \equiv CH), 3.27 (b, 2H, NCH₂CH₃), 1.31 (t, J = 7.4 Hz, 3H, NCH₂CH₃)

^{13}C NMR (125 MHz, $\text{d}_4\text{-MeOH}$) δ = 134.2, 133.7, 129.4, 125.7, 82.0, 72.3, 56.9, 49.6, 41.8, 9.6

HRMS: ($\text{C}_{12}\text{H}_{15}\text{BrN}$) $[\text{M}+\text{H}]^+$ required 252.0382 (^{79}Br); found $[\text{M}+\text{H}]^+$ 252.0386 (^{79}Br)

IR (neat): 3190, 2980, 2503, 2123, 1593, 1492, 1446, 1369, 709, 646 cm^{-1}

3.3.5.4 *N,N*-bis(4-bromobenzyl)prop-2-yn-1-amine (2.54)



Isolated as a by-product in the synthesis of compound **40** (640 mg, 18% yield).

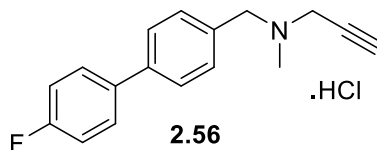
^1H NMR (400 MHz, CDCl_3) δ = 7.46-7.44 (m, 4H, ArH), 7.27-7.25 (m, 4H, ArH), 3.61 (s, 4H, 2 x ArCH₂), 3.22 (d, J = 2.4 Hz, 2H, C \equiv CCH₂), 2.28 (t, J = 2.4 Hz, 1H, C \equiv CH)

^{13}C NMR (100 MHz, CDCl_3) δ = 137.7, 131.6, 130.8, 121.2, 78.1, 73.9, 56.9, 41.3

HRMS: ($\text{C}_{17}\text{H}_{16}\text{Br}_2\text{N}$) $[\text{M}+\text{H}]^+$ required 391.9644 (^{79}Br , ^{79}Br), found $[\text{M}+\text{H}]^+$ 391.9641 (^{79}Br , ^{79}Br)

IR (neat): 3180, 2980, 2320, 2115, 1595, 1489, 1450, 715, 694 cm^{-1}

3.3.6 Synthesis of *N*-((4'-fluoro-[1,1'-biphenyl]-4-yl)methyl)-*N*-methylprop-2-yn-1-amine (2.56)



Compound **2.07** (35 mg, 0.25 mmol), 4-fluorophenylboronic acid (60 mg, 0.25 mmol), potassium phosphate (159 mg, 0.75 mmol) and Pd(dppf)₂Cl₂. DCM (8.2 mg, 4 mol%) were weighed into a dry 5 mL microwave vial under an atmosphere of argon. The vial was capped and evacuated and purged three times with argon and THF (1 mL) and distilled water (22 μL, 1.25 mmol) added. The reaction was then stirred at 70 °C for 4 hours, then cooled to room temperature and diluted with dichloromethane. The organics were then extracted with 2 portions of saturated aqueous ammonium chloride, followed by two portions of brine, and filtered through a phase separator and concentrated. The crude residue was then purified by flash chromatography, eluting with a gradient of 0-35% diethyl ether and petroleum ether to give the title compound which was converted to the HCl salt (6 mg, 8% yield) and sent to NKI for testing.

¹H NMR (500 MHz, d₄-MeOH) δ = 7.74 (d, *J* = 8.2 Hz, 2H, Ar*H*), 7.68 (dd, *J* = 8.6, 5.5 Hz, 2H, Ar*H*), 7.63 (d, *J* = 8.2 Hz, 2H, Ar*H*), 7.22-7.18 (m, 2H, Ar*H*), 4.48 (d, b, *J* = 42.1 Hz, 2H, ArCH₂), 4.10 (d, b, *J* = 26.6 Hz, 2H, C≡CCH₂), 3.48 (t, *J* = 2.4 Hz, 1H, C≡CH), 2.96 (s, 3H, NCH₃)

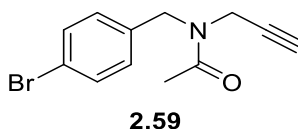
¹⁹F NMR (470 MHz, d₄-MeOH) δ = -116.8 - -116.9 (m)

¹³C NMR (125 MHz, d₄-MeOH) δ = 164.3 (d, ¹*J*_{CF} = 246.0 Hz), 143.5, 137.4 (d, ⁴*J*_{CF} = 3.1 Hz), 132.8, 130.0 (d, ³*J*_{CF} = 8.2 Hz), 129.2, 128.9, 116.8 (d, ²*J*_{CF} = 21.9 Hz), 81.9, 72.8, 59.5, 45.4, 40.1

HRMS (C₁₇H₁₇FN) [M+H]⁺ required 254.1340; found [M+H]⁺ 254.1341

IR (neat): 3199, 2980, 2902, 2462, 2123, 1604, 1460, 1359, 1240, 721 cm⁻¹

3.3.7 Synthesis of *N*-(4-bromobenzyl)-*N*-(prop-2-yn-1-yl)acetamide (2.59)



Compound **2.52** (0.5 mmol) was taken up in dry dichloromethane (2 mL) in an oven dried round bottomed flask under an atmosphere of nitrogen. Pyridine (1.5 mmol) and acetyl chloride (0.6 mmol) were added and the reaction stirred at room temperature until TLC indicated complete consumption of the starting material. The reaction was diluted with diethyl ether then quenched with 1M aqueous hydrochloric acid. The layers were partitioned, and the organic layer washed with water, saturated aqueous sodium bicarbonate solution and brine, then dried with magnesium sulfate, filtered and concentrated *in vacuo*. The crude residue was then purified by flash chromatography (100 % diethyl ether) to give the title compound (153 mg, quant. yield).

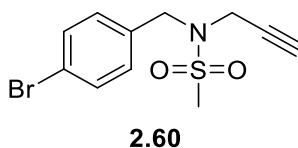
^1H NMR (400 MHz, CDCl_3) δ = 7.50-7.43 (m, 2H, ArH, rotomer), 7.16-7.09 (m, 2H, ArH, rotomer), 4.62 (s, 2H, ArCH₂), 4.20 (d, J = 2.3 Hz, 1H, C \equiv CCH₂ rotomer), 3.90 (d, J = 2.3 Hz, 1H, C \equiv CH₂, rotomer), 2.29 (t, J = 2.3 Hz, 0.5H, C \equiv CH, rotomer), 2.23 (s, 1.5H, C(O)CH₃, rotomer), 2.20 (t, J = 2.3 Hz, 0.5H, C \equiv CH, rotomer), 2.15 (s, 1.5H, C(O)CH₃, rotomer) *isolated as a mixture of rotomers.

^{13}C NMR (100 MHz, CDCl_3) δ = 170.7, 136.1, 135.3, 132.3, 131.9, 130.3, 128.5, 121.9, 121.7, 78.7, 78.1, 73.1, 72.4, 50.6, 47.8, 37.4, 34.2, 21.8 *isolated as a mixture of rotomers

HRMS: ($\text{C}_{12}\text{H}_{13}\text{BrNO}$) [$\text{M}+\text{H}$]⁺ required 266.0175 (^{79}Br); found [$\text{M}+\text{H}$]⁺ 266.0178 (^{79}Br)

IR (neat): 3655, 3292, 3226, 2980, 2117, 1647, 1487, 1463, 1354, 711, 640 cm^{-1}

3.3.8 *N*-(4-bromobenzyl)-*N*-(prop-2-yn-1-yl)methanesulfonamide (2.60)



Compound **2.52** (0.5 mmol), was taken up in dry DCM (5 mL) in an oven dried round bottomed flask under an atmosphere of argon and cooled to -20 °C using an ice/acetone bath. Triethylamine (0.5 mmol) was added followed by addition of mesyl chloride (0.75 mmol) dropwise *via* syringe. The reaction was warmed to room temperature and stirred until TLC indicated complete consumption of the starting material. The reaction was then quenched with saturated aqueous ammonium chloride solution and the resulting biphasic mixture partitioned. The aqueous layer was extracted with three portions of dichloromethane and the combined organics washed with water and brine, then dried with magnesium sulfate, filtered and concentrated *in vacuo*. The crude residue was then purified by flash chromatography (100% diethyl ether) to give the title compound (109 mg, 72% yield).

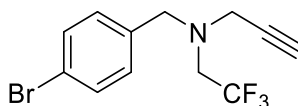
^1H NMR (400 MHz, CDCl_3) δ = 7.52-7.48 (m, 2H, ArH), 7.29-7.27 (m, 2H, ArH), 4.39 (s, 2H, ArCH₂), 3.91 (d, J = 2.4 Hz, 2H, C \equiv CCH₂), 3.02 (s, 3H, SO₂CH₃), 2.42 (t, J = 2.4 Hz, 1H, C \equiv CH)

^{13}C NMR (100 MHz, CDCl_3) δ = 134.0, 132.1, 130.5, 122.5, 77.0, 74.9, 49.4, 38.5, 35.6

HRMS: (C₁₁H₁₃BrNO₂S) [M+H]⁺ required 301.9845 (^{79}Br); found [M+H]⁺ 301.9851 (^{79}Br)

IR (neat): 3242, 2980, 2981, 2113, 1487, 1433, 1367, 1321, 1141, 698 cm⁻¹

3.3.9 Synthesis of *N*-(4-bromobenzyl)-*N*-(2,2,2-trifluoroethyl)prop-2-yn-1-amine (2.61)



2.61

Compound **2.52** (448 mg, 2 mmol) was taken up in dry THF (2 mL, 1 mL/mmol **2.52**). trifluoroacetic acid (268 μL , 3.5 mmol) was added followed by the dropwise addition of phenylsilane (492 μL , 4 mmol). The reaction was then heated and stirred at reflux for 4 hours (gas evolution). The reaction was then cooled to room temperature and concentrated onto silica. The crude material was then subjected to flash chromatography, eluting with a gradient of 0-20% DCM and petroleum and fractions

containing product were collected and concentrated to give the title compound (185 mg, 30% yield). **2.61** was not sufficiently pure for biological testing.

^1H NMR (400 MHz, CDCl_3) δ = 7.48-7.44 (m, 2H, ArH), 7.26-7.23 (m, 2H, ArH), 3.77 (s, 2H, ArCH₂), 3.41 (d, 2H, J = 2.4 Hz, C \equiv CCH₂), 3.16 (q, 2H, $^3J_{\text{HF}}$ = 9.3 Hz, NCH₂CF₃), 2.28 (t, 1H, J = 2.4 Hz, C \equiv CH)

^{13}C NMR (100 MHz, CDCl_3) δ = 136.7, 131.7, 130.7, 125.5 (q, $^1J_{\text{CF}}$ = 277 Hz), 121.6, 77.7, 73.9, 58.2, 53.9 (q, $^2J_{\text{CF}}$ = 31.3 Hz), 42.8

^{19}F NMR (376 Hz, CDCl_3) δ = -70.1 (t, $^3J_{\text{HF}}$ = 9.3 Hz)

4 References

- (1) Blanco, A.; Blanco, G. In *Medical Biochemistry*; Academic Press, 2017; pp 21–71.
- (2) IUPAC. *J. Biol. Chem.* **1970**, 245 (24), 6489.
- (3) Dunitz, J. D. *Angew. Chemie - Int. Ed.* **2001**, 40 (22), 4167.
- (4) Nick Pace, C.; Martin Scholtz, J. *Biophys. J.* **1998**, 75 (1), 422.
- (5) Bollati, M.; Barbiroli, A.; Favalli, V.; Arbustini, E.; Charron, P.; Bolognesi, M. *Biochem. Biophys. Res. Commun.* **2012**, 418 (2), 217.
- (6) AppliedPhotophysics. Circular Dichroism (CD) and Higher Order Structure (HOS) of biomolecules <https://www.photophysics.com/circular-dichroism/chirascan-technology/cd-and-hos-of-biomolecules/> (accessed May 27, 2019).
- (7) AppliedPhotophysics. Chirality and Circular Dichroism Spectroscopy <https://www.photophysics.com/circular-dichroism/chirascan-technology/chirality-and-cd/> (accessed May 27, 2019).
- (8) Coleska, A.; Wang, S.; Yang, C.-Y.; Ran, X.; Yi, H.; Kawamoto, S. A. *J. Med. Chem.* **2011**, 55 (3), 1137.
- (9) Luo, P.; Baldwin, R. L. *Biochemistry* **1997**, 36 (27), 8413.
- (10) AppliedPhotophysics. Units and Conversions <https://www.photophysics.com/circular-dichroism/chirascan-technology/circular-dichroism-spectroscopy-units-conversions/> (accessed May 28, 2019).
- (11) Jochim, A. L.; Arora, P. S. *Mol. Biosyst.* **2009**, 5 (9), 924.
- (12) Ko, S.; Kang, G. B.; Song, S. M.; Lee, J. G.; Shin, D. Y.; Yun, J. H.; Sheng, Y.; Cheong, C.; Jeon, Y. H.; Jung, Y. K.; Arrowsmith, C. H.; Avvakumov, G. V.; Dhe-Paganon, S.; Yoo, Y. J.; Eom, S. H.; Lee, W. *J. Biol. Chem.* **2010**, 285 (46), 36070.

- (13) Bullock, B. N.; Jochim, A. L.; Arora, P. S. *J. Am. Chem. Soc.* **2011**, *133* (36), 14220.
- (14) Scholtz, J. M.; Baldwin, R. L. *Annu. Rev. Biophys. Biomol. Struct.* **1992**, *21* (1), 95.
- (15) Marqusee, S.; Baldwin, R. L. *Proc. Natl. Acad. Sci. U. S. A.* **1987**, *84* (24), 8898.
- (16) Chorev, M.; Roubini, E.; McKee, R. L.; Gibbons, S. W.; Goldman, M. E.; Caulfield, M. P.; Rosenblatt, M. *Biochemistry* **1991**, *30* (24), 5968.
- (17) Phelan, J. C.; Skelton, N. J.; Braisted, A. C.; McDowell, R. S. *J. Am. Chem. Soc.* **1997**, *119* (3), 455.
- (18) Koval', I. V. *Russ. J. Org. Chem.* **2007**, *43* (3), 319.
- (19) Zhang, F.; Sadovski, O.; Xin, S. J.; Woolley, G. A. *J. Am. Chem. Soc.* **2007**, *129* (46), 14154.
- (20) Spokoyny, A. M.; Zou, Y.; Ling, J. J.; Yu, H.; Lin, Y. S.; Pentelute, B. L. *J. Am. Chem. Soc.* **2013**, *135* (16), 5946.
- (21) Blackwell, H. E.; Grubbs, R. H. *Angew. Chemie Int. Ed.* **1998**, *37* (23), 3281.
- (22) Schafmeister, C. E.; Po, J.; Verdine, G. L. *J. Am. Chem. Soc.* **2000**, *122* (24), 5891.
- (23) Schöllkopf, U.; Groth, U.; Deng, C. *Angew. Chemie Int. Ed. English* **1981**, *20* (9), 798.
- (24) Schöllkopf, U. *Tetrahedron* **1983**, *39* (12), 2085.
- (25) Sigma Aldrich. (S)-2,5-Dihydro-3,6-dimethoxy-2-isopropylpyrazine
<https://www.sigmaaldrich.com/catalog/product/sial/37289?lang=en®ion=GB> (accessed Jun 4, 2019).
- (26) Sigma Aldrich. (R)-2,5-Dihydro-3,6-dimethoxy-2-isopropylpyrazine
https://www.sigmaaldrich.com/catalog/product/aldrich/37286?lang=en®ion=GB&cm_sp=Insite-_-prodRecCold_xviews-_-prodRecCold3-3 (accessed Jun 4, 2019).
- (27) Sigma Aldrich. (S)-3-Isopropyl-2,5-piperazinedione

<https://www.sigmaaldrich.com/catalog/product/aldrich/59732?lang=en®ion=GB> (accessed Jun 4, 2019).

- (28) Sigma Aldrich. (R)-(-)-3-Isopropyl-2,5-piperazinedione
<https://www.sigmaaldrich.com/catalog/product/aldrich/448362?lang=en®ion=GB> (accessed Jun 4, 2019).
- (29) Belokon, Y. N.; Chernoglazova, N. I.; Kochetkov, C. A.; Garbalinskaya, N. S.; Belikov, V. M. *J. Chem. Soc. Chem. Commun.* **1985**, No. 3, 171.
- (30) Belokon, Y. N.; Bulychev, A. G.; Vitt, S. V.; Struchkov, Y. T.; Batsanov, A. S.; Timofeeva, T. V.; Tsyryapkin, V. A.; Ryzhov, M. G.; Lysova, L. A.; Bakhmutov, V. I.; Belikov, V. M. *J. Am. Chem. Soc.* **1985**, *107* (14), 4252.
- (31) O'Donnell, M. J. *Tetrahedron* **2019**.
- (32) Nian, Y.; Wang, J.; Moriwaki, H.; Soloshonok, V. A.; Liu, H.; Li, R.; Dalton, /; Vadim, S.; Soloshonok, A.; Nian, Y.; Wang, J.; Moriwaki, H.; Soloshonok, V. A.; Liu, H. *Dalt. Trans.* **2017**, *46* (13), 4191.
- (33) Watson, M. The Design and Synthesis of Molecular Tools for the Ubiquitin Proteasome System, University of Strathclyde, 2015.
- (34) Li, B.; Zhang, J.; Xu, Y.; Yang, X.; Li, L. *Tetrahedron Lett.* **2017**, *58* (24), 2374.
- (35) Wang, Y.; Wang, J.; Moriwaki, H.; Soloshonok, V. A.; Liu, H.; Song, X. *Amino Acids* **2017**, *49* (9), 1487.
- (36) Tanaka, M. *Chem. Pharm. Bull. (Tokyo)*. **2007**, *55* (3), 349.
- (37) Kato, K.; Suemune, H.; Sakai, K. *Tetrahedron* **1994**, *50* (11), 3315.
- (38) Sakai, K.; Suemune, H. *Tetrahedron: Asymmetry* **1993**, *4* (10), 2109.
- (39) Strecker, A. *Justus Liebigs Ann. Chem.* **1850**, *75* (1), 27.
- (40) Wang, J.; Liu, X.; Feng, X. *Chem. Rev* **2011**, *111* (11), 6947.
- (41) Ma, D.; Ding, K. *Org. Lett.* **2000**, *2* (16), 2515.
- (42) Ooi, T.; Takeuchi, M.; Kameda, M.; Maruoka, K. *J. Am. Chem. Soc.* **2000**, *122*

(21), 5228.

- (43) Sigma Aldrich. (11bS)-(+)-4,4-Dibutyl-4,5-dihydro-2,6-bis(3,4,5-trifluorophenyl)-3H-dinaphth[2,1-c:1',2'-e]azepinium bromide
<https://www.sigmaaldrich.com/catalog/product/ALDRICH/677086?lang=en®ion=GB>.
- (44) Wang, J.; Sánchez-Roselló, M.; Aceña, J. L.; Del Pozo, C.; Sorochinsky, A. E.; Fustero, S.; Soloshonok, V. A.; Liu, H. *Chem. Rev.* **2014**, *114* (4), 2432.
- (45) Purser, S.; Moore, P. R.; Swallow, S.; Gouverneur, V. *Chem Soc Rev* **2008**, *37* (2), 237.
- (46) Lipinski, C. A.; Lombardo, F.; Dominy, B. W.; Feeney, P. J. *Adv. Drug Deliv. Rev.* **2001**, *23* (1–3), 3.
- (47) Smart, B. E. *J. Fluor. Chem.* **2001**, *109* (1), 3.
- (48) Rowley, M.; Hallett, D. J.; Goodacre, S.; Moyes, C.; Crawforth, J.; Sparey, T. J.; Patel, S.; Marwood, R.; Patel, S.; Thomas, S.; Hitzel, L.; O'Connor, D.; Szeto, N.; Castro, J. L.; Hutson, P. H.; MacLeod, A. M. *J. Med. Chem.* **2001**, *44* (10), 1603.
- (49) Fera, M. T.; Giannone, M.; Pallio, S.; Tortora, A.; Blandino, G.; Carbone, M. *Int. J. Antimicrob. Agents* **2001**, *17* (2), 151.
- (50) Reddy, V. P. In *Organofluorine Compounds in Biology and Medicine*; Elsevier, 2015; pp 133–178.
- (51) Molloy, J. J.; Clohessy, T. A.; Irving, C.; Anderson, N. A.; Lloyd-Jones, G. C.; Watson, A. J. B. *Chem. Sci.* **2017**, *8* (2), 1551.
- (52) Cobb, S. L.; Murphy, C. D. *J. Fluor. Chem.* **2009**, *130* (2), 132.
- (53) Dalvit, C.; Fagerness, P. E.; Hadden, D. T. A. A.; Sarver, R. W.; Stockman, B. J. *J. Am. Chem. Soc.* **2003**, *125* (25), 7696.
- (54) Liang, T.; Neumann, C. N.; Ritter, T. *Angew. Chemie - Int. Ed.* **2013**, *52* (32), 8214.

- (55) Sigma Aldrich. selectfluor
<https://www.sigmaaldrich.com/catalog/product/aldrich/439479?lang=en®ion=GB> (accessed Mar 27, 2019).
- (56) Sigma Aldrich. NFSI
<https://www.sigmaaldrich.com/catalog/product/aldrich/392715?lang=en®ion=GB> (accessed Mar 27, 2019).
- (57) Sigma Aldrich. xenon difluoride
<https://www.sigmaaldrich.com/catalog/product/aldrich/394505?lang=en®ion=GB> (accessed Mar 27, 2019).
- (58) Yamada, S.; Gavryushin, A.; Knochel, P. *Angew. Chemie - Int. Ed.* **2010**, *49* (12), 2215.
- (59) Shibata, N.; Suzuki, E.; Takeuchi, Y. *J. Am. Chem. Soc.* **2000**, *122* (43), 10728.
- (60) Deyoung, J.; Kawa, H.; Lagow, R. J. *J. Chem. Soc. Chem. Commun.* **1992**, *0* (11), 811.
- (61) Zhou, Y.; Wang, J.; Gu, Z.; Wang, S.; Zhu, W.; Aceña, J. L.; Soloshonok, V. A.; Izawa, K.; Liu, H.; Acenã, J. L.; Soloshonok, V. A.; Izawa, K.; Liu, H. *Chem. Rev.* **2016**, *116* (2), 422.
- (62) Sznajdman, M. L.; Almond, M. R.; Pesyan, A. *Nucleosides, Nucleotides and Nucleic Acids* **2002**, *21* (2), 155.
- (63) Sigma Aldrich. DAST
<https://www.sigmaaldrich.com/catalog/product/aldrich/235253?lang=en®ion=GB> (accessed Mar 27, 2019).
- (64) Sigma Aldrich. xtalfluor-e
<https://www.sigmaaldrich.com/catalog/product/aldrich/719439?lang=en®ion=GB> (accessed Mar 27, 2019).
- (65) Sigma Aldrich. KF
<https://www.sigmaaldrich.com/catalog/product/aldrich/449148?lang=en®ion=GB>

gion=GB (accessed Mar 27, 2019).

- (66) Finger, G. C.; Kruse, C. W. *J. Am. Chem. Soc.* **1956**, 78 (23), 6034.
- (67) Middleton, W. J. *J. Org. Chem.* **1975**, 40 (5), 574.
- (68) Beaulieu, F.; Beauregard, L. P.; Courchesne, G.; Couturier, M.; Laflamme, F.; L'Heureux, A. *Org. Lett.* **2009**, 11 (21), 5050.
- (69) Gauthier, J. Y.; Chauret, N.; Cromlish, W.; Desmarais, S.; Duong, L. T.; Falgoutret, J. P.; Kimmel, D. B.; Lamontagne, S.; Léger, S.; LeRiche, T.; Li, C. S.; Massé, F.; McKay, D. J.; Nicoll-Griffith, D. A.; Oballa, R. M.; Palmer, J. T.; Percival, M. D.; Riendeau, D.; Robichaud, J.; Rodan, G. A.; Rodan, S. B.; Seto, C.; Thérien, M.; Truong, V. L.; Venuti, M. C.; Wesolowski, G.; Young, R. N.; Zamboni, R.; Black, W. C. *Bioorganic Med. Chem. Lett.* **2008**, 18 (3), 923.
- (70) Price, D. A.; Gayton, S.; Selby, M. D.; Ahman, J.; Haycock-Lewandowski, S.; Stammen, B. L.; Warren, A. *Tetrahedron Lett.* **2005**, 46 (30), 5005.
- (71) Haycock-Lewandowski, S. J.; Wilder, A.; Åhman, J. *Org. Process Res. Dev.* **2008**, 12 (6), 1094.
- (72) Patel, S. T.; Percy, J. M.; Wilkes, R. D. *Tetrahedron* **1995**, 51 (33), 9201.
- (73) Sigma Aldrich. TFE
<https://www.sigmaaldrich.com/catalog/product/sigald/t63002?lang=en®ion=GB> (accessed Mar 27, 2019).
- (74) Percy, J. M.; McCarter, A. W.; Sewell, A. L.; Sloan, N.; Kennedy, A. R.; Hirst, D. *J. Chem. - A Eur. J.* **2015**, 21 (52), 19119.
- (75) Sigma Aldrich. 3-Cl-4FAniline
<https://www.sigmaaldrich.com/catalog/product/aldrich/228583?lang=en®ion=GB> (accessed Mar 27, 2019).
- (76) Wang, J. Q.; Gao, M.; Miller, K. D.; Sledge, G. W.; Zheng, Q. H. *Bioorganic Med. Chem. Lett.* **2006**, 16 (15), 4102.
- (77) Olah, G. A.; Welch, J. T.; Vankar, Y. D.; Nojima, M.; Kerekes, I.; Olah, J. A. *J. Org.*

Chem. **1979**, *44* (22), 3872.

- (78) Prakash, G. K. S.; Mathew, T.; Martinez, E. R.; Esteves, P. M.; Rasul, G.; Olah, G. A. *J. Org. Chem.* **2006**, *71* (10), 3952.
- (79) Suryadevara, P. K.; Racherla, K. K.; Olepu, S.; Norcross, N. R.; Tatipaka, H. B.; Arif, J. A.; Planer, J. D.; Lepesheva, G. I.; Verlinde, C. L. M. J.; Buckner, F. S.; Gelb, M. H. *Bioorg. Med. Chem. Lett.* **2013**, *23* (23), 6492.
- (80) Sigma Aldrich. ethyl trifluoroacetate
<https://www.sigmaaldrich.com/catalog/product/aldrich/e50000?lang=en®ion=GB> (accessed Mar 27, 2019).
- (81) Penning, T. D.; Talley, J. J.; Bertenshaw, S. R.; Carter, J. S.; Collins, P. W.; Docter, S.; Graneto, M. J.; Lee, L. F.; Malecha, J. W.; Miyashiro, J. M.; Rogers, R. S.; Rogier, D. J.; Yu, S. S.; Anderson, G. D.; Burton, E. G.; Cogburn, J. N.; Gregory, S. A.; Koboldt, C. M.; Perkins, W. E.; Seibert, K.; Veenhuizen, A. W.; Zhang, Y. Y.; Isakson, P. C. *J. Med. Chem.* **1997**, *40* (9), 1347.
- (82) Gao, X.; Ohtsuka, Y.; Ishimura, K.; Nagase, S. *J. Phys. Chem. A* **2009**, *113* (36), 9852.
- (83) Sigma Aldrich. Ruppert-Prakash
<https://www.sigmaaldrich.com/catalog/product/aldrich/488712?lang=en®ion=GB> (accessed May 8, 2019).
- (84) Sigma Aldrich. MDFA
<https://www.sigmaaldrich.com/catalog/product/aldrich/390755?lang=en®ion=GB> (accessed May 8, 2019).
- (85) Sigma Aldrich. TFDA
<https://www.sigmaaldrich.com/catalog/product/aldrich/531421?lang=en®ion=GB> (accessed May 8, 2019).
- (86) Sigma Aldrich. NaCDFA
<http://www.fluorochem.co.uk/Products/Product?code=001061> (accessed Mar 27, 2019).

- (87) Apollo Scientific. Sodium bromo(difluoro)acetate 97% - PC3374 - 84349-27-9 from Apollo Scientific http://www.apolloscientific.co.uk/display_item.php?id=8363 (accessed May 8, 2019).
- (88) Enamine. Seyferth Reagent <https://www.enaminestore.com/catalog/EN300-25440> (accessed May 27, 2019).
- (89) Xe. XE Currency Converter: 1 USD to GBP = 0.767608 British Pounds <https://www.xe.com/currencyconverter/convert/?Amount=1&From=USD&To=GBP> (accessed May 8, 2019).
- (90) Birchall, J. M.; Cross, G. W.; Haszeldine, R. N. *Proc. Chem. Soc.* **1960**, 81.
- (91) Oshiro, K.; Morimoto, Y.; Amii, H. *Synthesis (Stuttg.)*. **2010**, 2010 (12), 2080.
- (92) Orr, D.; Percy, J. M.; Tuttle, T.; Kennedy, A. R.; Harrison, Z. A. *Chem. - A Eur. J.* **2014**, 20 (44), 14305.
- (93) Masuhara, Y.; Tanaka, T.; Takenaka, H.; Hayase, S.; Nokami, T.; Itoh, T. *J. Org. Chem.* **2019**, 84 (9), 5440.
- (94) Greene, T. W.; Wuts, P. G. M. In *Protective Groups in Organic Synthesis*; John Wiley & Sons, Inc.: Hoboken, NJ, USA, 2007; pp 16–366.
- (95) Sigma Aldrich. ethylene glycol <https://www.sigmaaldrich.com/catalog/product/sigald/102466?lang=en®ion=GB> (accessed Mar 27, 2019).
- (96) Yanai, H.; Okada, H.; Sato, A.; Okada, M.; Taguchi, T. *Tetrahedron Lett.* **2011**, 52 (23), 2997.
- (97) Yang, X.; Wu, T.; Phipps, R. J.; Toste, F. D. *Chemical Reviews*. January 28, 2015, pp 826–870.
- (98) JINMING, W.; SIQING, W. Flame-retardant type refrigerant and preparation method thereof. CN104592942 (A); CN104592942 (B), 2015.
- (99) Srikrishna, A.; Babu, R. R. *Tetrahedron* **2008**, 64 (46), 10501.

- (100) McCombie, S. W.; Quiclet-Sire, B.; Zard, S. Z. *Tetrahedron* **2018**, 74 (38), 4969.
- (101) Wackerly, J. W.; Dunne, J. F. *J. Chem. Educ.* **2017**, 94 (11), 1790.
- (102) Allevi, P.; Paroni, R.; Ragusa, A.; Anastasia, M. *Tetrahedron: Asymmetry* **2004**, 15 (19), 3139.
- (103) Velusamy, S.; Borpuzari, S.; Punniyamurthy, T. *Tetrahedron* **2005**, 61 (8), 2011.
- (104) Murphy, J. A.; Mahesh, M.; McPheators, G.; Vijaya Anand, R.; McGuire, T. M.; Carlinga, R.; Kennedy, A. R. *Org. Lett.* **2007**, 9 (17), 3233.
- (105) Morikawa, T.; Uejima, M.; Kobayashi, Y. *Chem. Lett.* **2006**, 17 (8), 1407.
- (106) Pietruszka, J.; Witt, A. *J. Chem. Soc. Perkin Trans. 1* **2000**, No. 24, 4293.
- (107) Sadhu, K. M.; Matteson, D. S. *Organometallics* **1985**, 4 (9), 1687.
- (108) Pereira, S.; Srebnik, M. *Organometallics* **1995**, 14 (7), 3127.
- (109) Orr, D. Utilisation of Rearrangement Chemistry in the Synthesis of Novel Fluorinated Ring Systems: A Computational and Experimental Study, University of Strathclyde, 2015.
- (110) Li, H.; Yoo, J. C.; Kim, E.; Hong, J. H. *Nucleosides, Nucleotides and Nucleic Acids* **2011**, 30 (11), 945.
- (111) Gerber, A. B.; Leumann, C. J. *Chem. - A Eur. J.* **2013**, 19 (22), 6990.
- (112) Sizun, G.; Dukhan, D.; Griffon, J. F.; Griffe, L.; Meillon, J. C.; Leroy, F.; Storer, R.; Sommadossi, J. P.; Gosselin, G. *Carbohydr. Res.* **2009**, 344 (4), 448.
- (113) Singh, I.; Seitz, O. *Org. Lett.* **2006**, 8 (19), 4319.
- (114) Odedra, A.; Geyer, K.; Gustafsson, T.; Gilmour, R.; Seeberger, P. H. *Chem. Commun.* **2008**, 0 (26), 3025.
- (115) Chatgililoglu, C. *Acc. Chem. Res.* **1992**, 25 (4), 188.
- (116) Luo, Y. R. *Comprehensive handbook of chemical bond energies*; CRC Press, 2007.

- (117) Khan, A. T.; Mondal, E. *Synlett* **2003**, 2003 (5), 0694.
- (118) Archambeau, A.; Rovis, T. *Angew. Chemie - Int. Ed.* **2015**, 54 (45), 13337.
- (119) El-Maiss, J.; Darmanin, T.; Guittard, F. *RSC Adv.* **2015**, 5 (47), 37196.
- (120) Henderson, R. K.; Hill, A. P.; Redman, A. M.; Sneddon, H. F. *Green Chem.* **2015**, 17 (2), 945.
- (121) Terekhova, M. I.; Belokon', Y. N.; Maleev, V. I.; Chernoglazova, N. I.; Kochetkov, K. A.; Belikov, V. M.; Petrov, E. S. *Bull. Acad. Sci. USSR Div. Chem. Sci.* **1986**, 35 (4), 824.
- (122) Obkircher, M.; Stähelin, C.; Dick, F. J. *Pept. Sci.* **2008**, 14 (6), 763.
- (123) Lendrem, D.; Owen, M.; Godbert, S. *Org. Process Res. Dev.* **2001**, 5 (3), 324.
- (124) Andrei, M.; Römmeing, C.; Undheim, K. *Tetrahedron Asymmetry* **2004**, 15 (17), 2711.
- (125) Kumar, A.; Sharma, A.; Haimov, E.; El-Faham, A.; De La Torre, B. G.; Albericio, F. *Org. Process Res. Dev.* **2017**, 21 (10), 1533.
- (126) Balmain, A. *Nat. Rev. Cancer* **2001**, 1 (1), 77.
- (127) Danaei, G.; Vander Hoorn, S.; Lopez, A. D.; Murray, C. J. L.; Ezzati, M. *Lancet* **2005**, 366 (9499), 1784.
- (128) Lodish H, Berk A, Zipursky SL, et al. In *Molecular Cell Biology*; W. H. Freeman: New York, 2000.
- (129) De Zio, D.; Cianfanelli, V.; Cecconi, F. *Antioxid. Redox Signal.* **2012**, 19 (6), 559.
- (130) Hanahan, D.; Weinberg, R. A. *Cell* **2000**, 100 (1), 57.
- (131) Weinstein, I. B.; Joe, A. K. *Nature Clinical Practice Oncology*. Nature Publishing Group August 2006, pp 448–457.
- (132) Rosen, E. M.; Fan, S.; Pestell, R. G.; Goldberg, I. D. *Journal of Cellular Physiology*. John Wiley & Sons, Ltd July 1, 2003, pp 19–41.

- (133) Mitri, Z.; Constantine, T.; O'Regan, R. *Chemother. Res. Pract.* **2012**, 2012, 1.
- (134) Moasser, M. M. *Oncogene*. NIH Public Access 2007, pp 6469–6487.
- (135) Arruebo, M.; Vilaboa, N.; Sáez-Gutierrez, B.; Lambea, J.; Tres, A.; Valladares, M.; González-Fernández, Á. *Cancers (Basel)*. **2011**, 3 (3), 3279.
- (136) Gale, R. P. Cancer Treatment Principles - Cancer - MSD Manual Consumer Version <https://www.msdmanuals.com/en-gb/home/cancer/prevention-and-treatment-of-cancer/cancer-treatment-principles> (accessed Jul 4, 2019).
- (137) MacMillan. Statistics Fact Sheet https://www.macmillan.org.uk/_images/cancer-statistics-factsheet_tcm9-260514.pdf (accessed Jun 11, 2019).
- (138) Featherstone, H.; Whitham, L. *The Cost of Cancer*; 2010.
- (139) CancerResearch. Cancer statistics for the UK <https://www.cancerresearchuk.org/health-professional/cancer-statistics-for-the-uk#heading-Three> (accessed Jun 11, 2019).
- (140) Medical Research Council, E. M. C. (eMC). Mercaptopurine 50 mg tablets - Summary of Product Characteristics (SPC) - (eMC) <https://www.medicines.org.uk/emc/product/4655/smpc> (accessed Jun 17, 2019).
- (141) Cisplatin SmPC. Cisplatin 1 mg/ml Sterile Concentrate for Solution for Infusion: Summary of Product Characteristics <https://www.medicines.org.uk/emc/product/6111/smpc> (accessed Jun 17, 2019).
- (142) Hospira, U. Paclitaxel 6 mg/ml concentrate for solution for infusion - Summary of Product Characteristics (SPC) - (eMC) <https://www.medicines.org.uk/emc/product/6076/smpc> (accessed Jun 17, 2019).
- (143) European Medicines Agency. Iressa 250mg film-coated tablets - Summary of

Product Characteristics (SmPC) - (eMC)

<https://www.medicines.org.uk/emc/product/6602> (accessed Jun 17, 2019).

- (144) Morgan, J. A.; Lynch, J.; Panetta, J. C.; Wang, Y.; Frase, S.; Bao, J.; Zheng, J.; Opferman, J. T.; Janke, L.; Green, D. M.; Chemaitilly, W.; Schuetz, J. D. *Sci. Rep.* **2015**, 5 (1), 16488.
- (145) Zaza, G.; Cheok, M.; Krynetskaia, N.; Thorn, C.; Stocco, G.; Hebert, J. M.; McLeod, H.; Weinshilboum, R. M.; Relling, M. V.; Evans, W. E.; Klein, T. E.; Altman, R. B. *Pharmacogenet. Genomics* **2010**, 20 (9), 573.
- (146) 6-Mercaptopurine ribonucleotide | C10H13N4O7PS - PubChem
<https://pubchem.ncbi.nlm.nih.gov/compound/5184161> (accessed Oct 9, 2019).
- (147) Broekman, M. M. T. J.; Coenen, M. J. H.; Van Marrewijk, C. J.; Wanten, G. J. A.; Wong, D. R.; Verbeek, A. L. M.; Klungel, O. H.; Hooymans, P. M.; Guchelaar, H. J.; Scheffer, H.; Derijks, L. J. J.; De Jong, D. J. *Inflamm. Bowel Dis.* **2017**, 23 (10), 1873.
- (148) Johnstone, T. C.; Suntharalingam, K.; Lippard, S. J. *Chem. Rev.* **2016**, 116 (5), 3436.
- (149) Siddik, Z. H. *Oncogene* **2003**, 22 (47), 7265.
- (150) Wang, D.; Lippard, S. J. *Nat. Rev. Drug Discov.* **2005**, 4 (4), 307.
- (151) Astolfi, L.; Ghiselli, S.; Guaran, V.; Chicca, M.; Simoni, E.; Olivetto, E.; Lelli, G.; Martini, A. *Oncol. Rep.* **2013**, 29 (4), 1285.
- (152) Weaver, B. A. *Mol. Biol. Cell* **2014**, 25 (18), 2677.
- (153) Alushin, G. M.; Lander, G. C.; Kellogg, E. H.; Zhang, R.; Baker, D.; Nogales, E. *Cell* **2014**, 157 (5), 1117.
- (154) Sibaud, V.; Leboeuf, N. R.; Roche, H.; Belum, V. R.; Gladieff, L.; Deslandres, M.; Montastruc, M.; Eche, A.; Vigarios, E.; Dalenc, F.; Lacouture, M. E. *Eur. J. Dermatology* **2016**, 26 (5), 427.

- (155) Aggarwal, S. *Nat. Rev. Drug Discov.* **2010**, 9 (6), 427.
- (156) Iqbal, N.; Iqbal, N. *Chemother. Res. Pract.* **2014**, 2014, 1.
- (157) Winger, J. A.; Hantschel, O.; Superti-Furga, G.; Kuriyan, J. *BMC Struct. Biol.* **2009**, 9 (1), 7.
- (158) Armour, A. A.; Watkins, C. L. *Eur. Respir. Rev.* **2010**, 19 (117), 186.
- (159) Dowell, J.; Minna, J. D.; Kirkpatrick, P. *Nat. Rev. Drug Discov.* **2005**, 4 (1), 13.
- (160) Gajiwala, K. S.; Feng, J.; Ferre, R.; Ryan, K.; Brodsky, O.; Weinrich, S.; Kath, J. C.; Stewart, A. *Structure* **2013**, 21 (2), 209.
- (161) Scott, A. M.; Allison, J. P.; Wolchok, J. D. *Cancer Immun.* **2012**, 12, 14.
- (162) Findlay, V. J.; Scholar, E. In *xPharm: The Comprehensive Pharmacology Reference*; AlphaMed Press, 2011; Vol. 16, pp 1–5.
- (163) Hudis, C. A. *N. Engl. J. Med.* **2007**, 357 (1), 39.
- (164) Pohlmann, P. R.; Mayer, I. A.; Mernaugh, R. *Clin. Cancer Res.* **2009**, 15 (24), 7479.
- (165) Morgillo, F.; Della Corte, C. M.; Fasano, M.; Ciardiello, F. *ESMO Open*. BMJ Publishing Group 2016, p e000060.
- (166) Housman, G.; Byler, S.; Heerboth, S.; Lapinska, K.; Longacre, M.; Snyder, N.; Sarkar, S. *Cancers (Basel)*. **2014**, 6 (3), 1769.
- (167) Loayza-Puch, F.; Rooijers, K.; Zijlstra, J.; Moumbeini, B.; Zaal, E. A.; Oude Vrielink, J. F.; Lopes, R.; Ugalde, A. P.; Berkers, C. R.; Agami, R. *EMBO Rep.* **2017**, 18 (4), 549.
- (168) Loayza-Puch, F.; Rooijers, K.; Buil, L. C. M.; Zijlstra, J.; Oude Vrielink, J. F.; Lopes, R.; Ugalde, A. P.; Van Breugel, P.; Hofland, I.; Wesseling, J.; Van Tellingen, O.; Bex, A.; Agami, R. *Nature* **2016**, 530 (7591), 490.
- (169) Rabinovich, S.; Adler, L.; Yizhak, K.; Sarver, A.; Silberman, A.; Agron, S.; Stettner, N.; Sun, Q.; Brandis, A.; Helbling, D.; Korman, S.; Itzkovitz, S.;

- Dimmock, D.; Ulitsky, I.; Nagamani, S. C.; Ruppin, E.; Erez, A. *Nature* **2015**, 527 (7578), 379.
- (170) Egler, R.; Ahuja, S.; Matloub, Y. *J. Pharmacol. Pharmacother.* **2016**, 7 (2), 62.
- (171) Loayza-Puch, F.; Agami, R. *Cell Cycle* **2016**, 15 (17), 2229.
- (172) Christensen, E. M.; Patel, S. M.; Korasick, D. A.; Campbell, A. C.; Krause, K. L.; Becker, D. F.; Tanner, J. J. *J. Biol. Chem.* **2017**, 292 (17), 7233.
- (173) Deber, C. M.; Brodsky, B.; Rath, A. In *Encyclopedia of Life Sciences*; John Wiley & Sons, Ltd: Chichester, UK, 2010.
- (174) Liang, X.; Zhang, L.; Natarajan, S. K.; Becker, D. F. *Antioxid. Redox Signal.* **2013**, 19 (9), 998.
- (175) Phang, J. M.; Donald, S. P.; Pandhare, J.; Liu, Y. *Amino Acids* **2008**, 35 (4), 681.
- (176) Berg, J.; Tymoczko, J.; Stryer, L. In *Biochemistry. 5th Edition*; W H Freeman, 2002.
- (177) Tanner, J. J.; Fendt, S. M.; Becker, D. F. *Biochemistry* **2018**, 57 (25), 3433.
- (178) Zeng, T.; Zhu, L.; Liao, M.; Zhuo, W.; Yang, S.; Wu, W.; Wang, D. *Med. Oncol.* **2017**, 34 (2), 27.
- (179) de Ingeniis, J.; Ratnikov, B.; Richardson, A. D.; Scott, D. A.; Aza-Blanc, P.; De, S. K.; Kazanov, M.; Pellicchia, M.; Ronai, Z.; Osterman, A. L.; Smith, J. W. *PLoS One* **2012**, 7 (9), e45190.
- (180) Ding, J.; Kuo, M. L.; Su, L.; Xue, L.; Luh, F.; Zhang, H.; Wang, J.; Lin, T. G.; Zhang, K.; Chu, P.; Zheng, S.; Liu, X.; Yen, Y. *Carcinogenesis* **2017**, 38 (5), 519.
- (181) Cai, F.; Miao, Y.; Liu, C.; Wu, T.; Shen, S.; Su, X.; Shi, Y. *Oncol. Lett.* **2018**, 15 (1), 731.
- (182) Riss, T. L.; Moravec, R. A.; Niles, A. L.; Duellman, S.; Benink, H. A.; Worzella, T. J.; Minor, L. *Cell Viability Assays*; Eli Lilly & Company and the National Center for Advancing Translational Sciences, 2004.

- (183) Dojindo. *Measuring Cell Viability / Cytotoxicity*; 2012.
- (184) *Nature* **2019**, 570 (7760), 137.
- (185) Cyranoski, D.; Ledford, H. *Nature* **2018**, 563 (7733), 607.
- (186) Reversade, B.; Escande-Beillard, N.; Dimopoulou, A.; Fischer, B.; Chng, S. C.; Li, Y.; Shboul, M.; Tham, P. Y.; Kayserili, H.; Al-Gazali, L.; Shahwan, M.; Brancati, F.; Lee, H.; O'Connor, B. D.; Kegler, M. S. Von; Merriman, B.; Nelson, S. F.; Masri, A.; Alkazaleh, F.; Guerra, D.; Ferrari, P.; Nanda, A.; Rajab, A.; Markie, D.; Gray, M.; Nelson, J.; Grix, A.; Sommer, A.; Savarirayan, R.; Janecke, A. R.; Steichen, E.; Sillence, D.; Haußer, I.; Budde, B.; Nürnberg, G.; Nürnberg, P.; Seemann, P.; Kunkel, D.; Zambruno, G.; Dallapiccola, B.; Schuelke, M.; Robertson, S.; Hamamy, H.; Wollnik, B.; Van Maldergem, L.; Mundlos, S.; Kornak, U. *Nat. Genet.* **2009**, 41 (9), 1016.
- (187) Workman, P.; Collins, I. *Chem. Biol.* **2010**, 17 (6), 561.
- (188) Arrowsmith, C. H.; Audia, J. E.; Austin, C.; Baell, J.; Bennett, J.; Blagg, J.; Bountra, C.; Brennan, P. E.; Brown, P. J.; Bunnage, M. E.; Buser-Doepner, C.; Campbell, R. M.; Carter, A. J.; Cohen, P.; Copeland, R. A.; Cravatt, B.; Dahlin, J. L.; Dhanak, D.; Edwards, A. M.; Frye, S. V.; Gray, N.; Grimshaw, C. E.; Hepworth, D.; Howe, T.; Huber, K. V. M.; Jin, J.; Knapp, S.; Kotz, J. D.; Kruger, R. G.; Lowe, D.; Mader, M. M.; Marsden, B.; Mueller-Fahrnow, A.; Müller, S.; O'Hagan, R. C.; Overington, J. P.; Owen, D. R.; Rosenberg, S. H.; Roth, B.; Ross, R.; Schapira, M.; Schreiber, S. L.; Shoichet, B.; Sundström, M.; Superti-Furga, G.; Taunton, J.; Toledo-Sherman, L.; Walpole, C.; Walters, M. A.; Willson, T. M.; Workman, P.; Young, R. N.; Zuercher, W. J. *Nat. Chem. Biol.* **2015**, 11 (8), 536.
- (189) Schreiber, S. L.; Kotz, J. D.; Li, M.; Aubé, J.; Austin, C. P.; Reed, J. C.; Rosen, H.; White, E. L.; Sklar, L. A.; Lindsley, C. W.; Alexander, B. R.; Bittker, J. A.; Clemons, P. A.; de Souza, A.; Foley, M. A.; Palmer, M.; Shamji, A. F.; Wawer, M. J.; McManus, O.; Wu, M.; Zou, B.; Yu, H.; Golden, J. E.; Schoenen, F. J.; Simeonov, A.; Jadhav, A.; Jackson, M. R.; Pinkerton, A. B.; Chung, T. D. Y.; Griffin, P. R.; Cravatt, B. F.; Hodder, P. S.; Roush, W. R.; Roberts, E.; Chung, D.-H.; Jonsson,

- C. B.; Noah, J. W.; Severson, W. E.; Ananthan, S.; Edwards, B.; Oprea, T. I.; Conn, P. J.; Hopkins, C. R.; Wood, M. R.; Stauffer, S. R.; Emmitte, K. A.; Brady, L. S.; Driscoll, J.; Li, I. Y.; Loomis, C. R.; Margolis, R. N.; Michelotti, E.; Perry, M. E.; Pillai, A.; Yao, Y. *Cell* **2015**, *161* (6), 1252.
- (190) Gierse, J.; Thorarensen, A.; Beltey, K.; Bradshaw-Pierce, E.; Cortes-Burgos, L.; Hall, T.; Johnston, A.; Murphy, M.; Nemirovskiy, O.; Ogawa, S.; Pegg, L.; Pelc, M.; Prinsen, M.; Schnute, M.; Wendling, J.; Wene, S.; Weinberg, R.; Wittwer, A.; Zweifel, B.; Masferrer, J. *J. Pharmacol. Exp. Ther.* **2010**, *334* (1), 310.
- (191) LOPAC®1280 (International Version) | Sigma-Aldrich
<https://www.sigmaaldrich.com/catalog/product/sigma/lo3300?lang=en®ion=GB> (accessed Oct 5, 2018).
- (192) Erlanson, D. A. In *Topics in Current Chemistry*; Springer, Berlin, Heidelberg, 2012; Vol. 317, pp 1–32.
- (193) Congreve, M.; Carr, R.; Murray, C.; Jhoti, H. *Drug Discov. Today* **2003**, *8* (19), 876.
- (194) the Royal Society of Chemistry. Pargyline.
- (195) Lamoree, B.; Hubbard, R. E. *Essays Biochem.* **2017**, *61* (5), 453.
- (196) Chen, H.; Engkvist, O.; Kogej, T. In *The Practice of Medicinal Chemistry*; 2015; pp 379–393.
- (197) Swett, L. R.; Martin, W. B.; Taylor, J. D.; Everett, G. M.; Wykes, A. A.; Gladish, Y. C. *Ann. N. Y. Acad. Sci.* **2006**, *107* (3), 891.
- (198) Yang, H. L.; Cai, P.; Liu, Q. H.; Yang, X. L.; Li, F.; Wang, J.; Wu, J. J.; Wang, X. B.; Kong, L. Y. *Eur. J. Med. Chem.* **2017**, *138*, 715.
- (199) Binda, C.; Newton-Vinson, P.; Hubálek, F.; Edmondson, D. E.; Mattevi, A. *Nat. Struct. Biol.* **2002**, *9* (1), 22.
- (200) Juaristi, E.; Moore, J. L.; Taylor, S. M.; Soloshonok, V. A. *Arkivoc* **2005**, No. 6, 287.

- (201) Chaumontet, M.; Piccardi, R.; Audic, N.; Hitce, J.; Peglion, J. L.; Clot, E.; Baudoin, O. *J. Am. Chem. Soc.* **2008**, *130* (45), 15157.
- (202) Sigma Aldrich. 4-(Bromomethyl)benzamide
<https://www.sigmaaldrich.com/catalog/buildingblock/product/combiblocksinc/com448646160?lang=en®ion=GB> (accessed Jul 30, 2019).
- (203) Sigma Aldrich. 4-(Bromomethyl)benzoic acid
<https://www.sigmaaldrich.com/catalog/product/aldrich/159549?lang=en®ion=GB> (accessed Jul 30, 2019).
- (204) Cao, R.; Müller, P.; Lippard, S. J. *J. Am. Chem. Soc.* **2010**, *132* (49), 17366.
- (205) Burfield, D. R.; Smithers, R. H. *J. Org. Chem.* **1978**, *43* (20), 3966.
- (206) Fyfe, J. W. B.; Fazakerley, N. J.; Watson, A. J. B. *Angew. Chemie - Int. Ed.* **2017**, *56* (5), 1249.
- (207) Blakemore, D. In *Synthetic Methods in Drug Discovery: Volume 1*; Blakemore, D. C., Doyle, P. M., Fobian, Y. M., Eds.; Royal Society of Chemistry, 2016; Vol. 2016-Janua, pp 1–69.
- (208) Andrews, K. G.; Faizova, R.; Denton, R. M. *Nat. Commun.* **2017**, *8* (1), 15913.
- (209) Mowat, J. PYCR1 Enzyme: A Novel Therapeutic Target in Cancer Treatment, University of Strathclyde, 2018.
- (210) Ford, M. C.; Ho, P. S. *J. Med. Chem.* **2016**, *59* (5), 1655.
- (211) Gross, G. In *The Practice of Medicinal Chemistry*; 2015; pp 631–655.
- (212) Bazzini, P.; Wermuth, C. G. In *The Practice of Medicinal Chemistry*; 2008; pp 319–357.
- (213) Wilcken, R.; Zimmermann, M. O.; Lange, A.; Joerger, A. C.; Boeckler, F. M. *Journal of Medicinal Chemistry*. American Chemical Society February 28, 2013, pp 1363–1388.
- (214) Hernandez, M.; Cavalcanti, S. M.; Moreira, D. R.; de Azevedo Junior, W.; Leite,

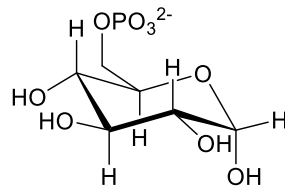
A. C. *Curr. Drug Targets* **2010**, *11* (3), 303.

- (215) Griffen, E.; Leach, A. G.; Robb, G. R.; Warner, D. J. *J. Med. Chem.* **2011**, *54* (22), 7739.
- (216) Clementi, E.; Raimondi, D. L.; Reinhardt, W. P. *J. Chem. Phys.* **1967**, *47* (4), 1300.
- (217) Stepan, A. F.; Subramanyam, C.; Efremov, I. V.; Dutra, J. K.; O'Sullivan, T. J.; Dirico, K. J.; McDonald, W. S.; Won, A.; Dorff, P. H.; Nolan, C. E.; Becker, S. L.; Pustilnik, L. R.; Riddell, D. R.; Kauffman, G. W.; Kormos, B. L.; Zhang, L.; Lu, Y.; Capetta, S. H.; Green, M. E.; Karki, K.; Sibley, E.; Atchison, K. P.; Hallgren, A. J.; Oborski, C. E.; Robshaw, A. E.; Sneed, B.; O'Donnell, C. J. *J. Med. Chem.* **2012**, *55* (7), 3414.
- (218) Topliss, J. G. *J. Med. Chem.* **1972**, *15* (10), 1006.
- (219) Kilbourn, M. R. *Int. J. Rad. Appl. Instrum. B.* **1989**, *16* (7), 681.
- (220) Weli, A. M.; Lindere, B. *Biochem. Pharmacol.* **1985**, *34* (11), 1991.
- (221) Kanie, K.; Mizuno, K.; Kuroboshi, M.; Hiyama, T. *Bull. Chem. Soc. Jpn.* **1998**, *71* (8), 1973.
- (222) Giuffredi, G.; Bobbio, C.; Gouverneur, V. *J. Org. Chem.* **2006**, *71* (14), 5361.
- (223) Yasujima, J.; Fukunishi, K.; Nomura, M.; Yamanaka, H. *Nippon Kagaku Kaishi* **1981**, *1981* (11), 1744.
- (224) Ellwood, A. R.; Porter, M. J. *J. Org. Chem.* **2009**, *74* (20), 7982.
- (225) Lang, S. B.; Wiles, R. J.; Kelly, C. B.; Molander, G. A. *Angew. Chemie - Int. Ed.* **2017**, *56* (47), 15073.
- (226) Qiu, R.; Zhang, G.; Ren, X.; Xu, X.; Yang, R.; Luo, S.; Yin, S. *J. Organomet. Chem.* **2010**, *695* (8), 1182.
- (227) Sun, S.; Wu, P. *J. Phys. Chem. A* **2010**, *114* (32), 8331.
- (228) Shirakawa, K.; Arase, A.; Hoshi, M. *Synthesis (Stuttg.)* **2004**, *2004* (11), 1814.
- (229) Karjalainen, O. K.; Passiniemi, M.; Koskinen, A. M. P. *Org. Lett.* **2010**, *12* (6),

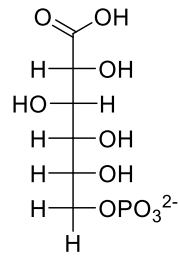
1145.

- (230) Taniguchi, T.; Zaimoku, H.; Ishibashi, H. *J. Org. Chem.* **2009**, 74 (6), 2624.
- (231) Trost, B. M.; Waser, J.; Meyer, A. *J. Am. Chem. Soc.* **2008**, 130 (48), 16424.
- (232) Zawisza, A. M.; Muzart, J. *J. Organomet. Chem.* **2010**, 695 (1), 62.
- (233) Dakin, L. A.; Langille, N. F.; Panek, J. S. *J. Org. Chem.* **2002**, 67 (19), 6812.
- (234) Willand, N.; Desroses, M.; Toto, P.; Dirié, B.; Lens, Z.; Villeret, V.; Rucktooa, P.; Loch, C.; Baulard, A.; Deprez, B. *ACS Chem. Biol.* **2010**, 5 (11), 1007.
- (235) Lehane, K. N.; Moynihan, E. J. A.; Brondel, N.; Lawrence, S. E.; Maguire, A. R. *CrystEngComm* **2007**, 9 (11), 1041.

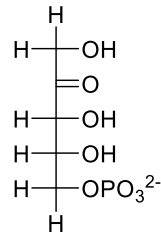
Appendix 1: Structures Names and Abbreviations of Sugars Involved in the Pentose Phosphate Pathway



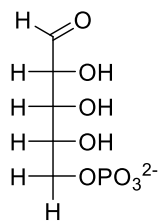
G-6-P
Glucose-6-Phosphate



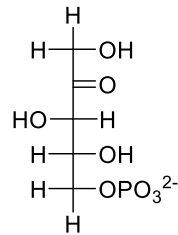
6-PG
6-Phosphogluconate



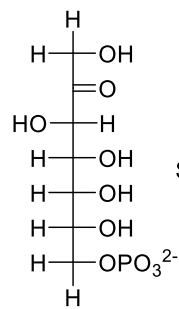
Ru-5-P
Ribulose-5-Phosphate



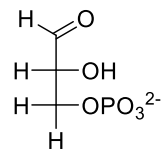
R-5-P
Ribose-5-Phosphate



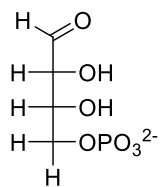
X-5-P
Xylulose-5-phosphate



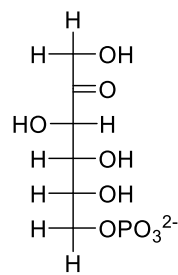
S-7-P
Sedoheptulose-7-phosphate



G-3-P
glyceraldehyde-3-phosphate



E-4-P
Erythrose-4-Phosphate



F-6-P
Fructose-6-Phosphate

Appendix 2: Topliss Decision Tree for Aromatic Systems (adapted from reference 218)

